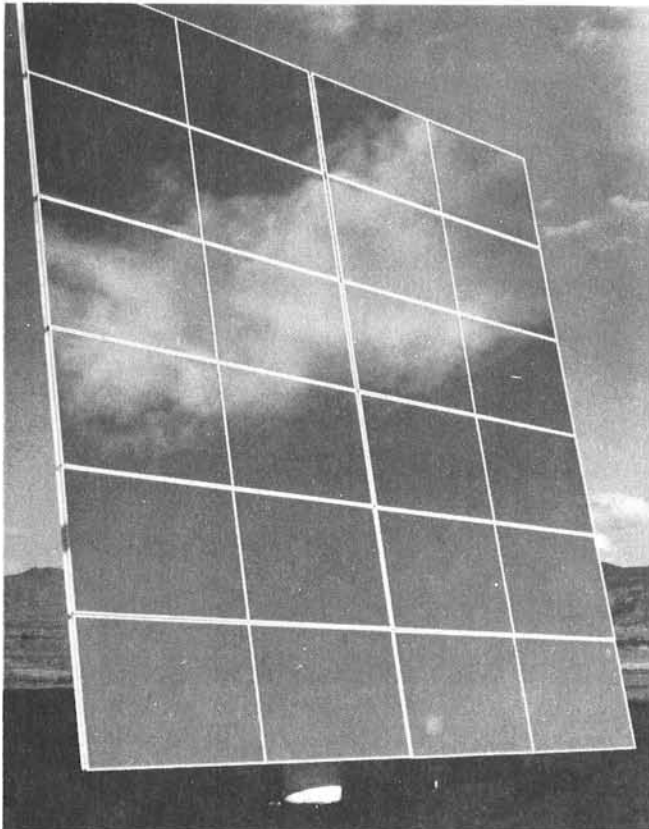


MARCH 1981

SAND 81-8178
SANDIA CONTRACT
83-2729E

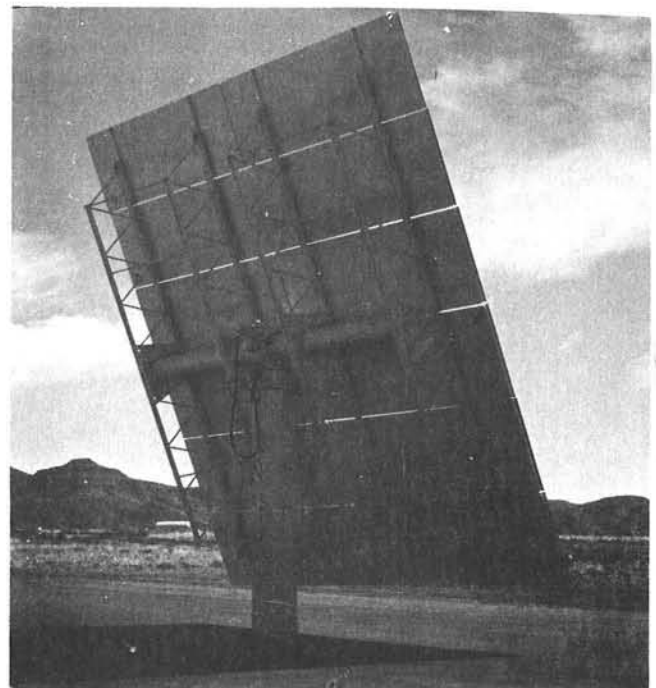
**SECOND GENERATION HELIOSTAT DEVELOPMENT
FOR
SOLAR CENTRAL RECEIVER SYSTEMS**



FINAL REPORT
VOLUME III
APPENDICES A-E
BILL OF MATERIALS
DRAWINGS
TRADE STUDIES
SYSTEM STUDIES

PREPARED BY
NORTHROP, INCORPORATED
A SUBSIDIARY OF
ATLANTIC RICHFIELD CO.

AND



BECHTEL NATIONAL, INC. AND BOOZ-ALLEN AND HAMILTON, INC.

***When printing a copy of any digitized SAND
Report, you are required to update the
markings to current standards.***

SECOND GENERATION HELIOSTAT DEVELOPMENT

FINAL REPORT

VOLUME III

Appendices A - E

Sandia Contract No. 83-2729E
Sandia Requestor - C. L. Mavis/8451
Contracting Representative - R. C. Christman

Work performed during the period
July 16, 1979 through March 31, 1981

by

Northrup, Incorporated
302 Nichols Drive
Hutchins, Tx. 75141

and Subcontractors:

Bechtel National, Inc.
50 Beale St.
San Francisco, California 94119
and
Booz-Allen and Hamilton, Inc.
8801 E. Pleasant Valley Rd.
Cleveland, Ohio 44131

This report is presented in 4 Volumes. The content of these volumes is as follows:

Volume I - Sections 1.0 - 3.0

- 1.0 Introduction
- 2.0 Summary of Results
- 3.0 Northrup Heliostat Description

Volume II - Sections 4.0 - 8.0

- 4.0 Manufacturing
- 5.0 Transportation
- 6.0 Field Assembly and Installation
- 7.0 Maintenance
- 8.0 Cost Estimates

Volume III - Appendices A - E

- A. Bill of Materials
- B. Part Drawings (Subassemblies)
- C. Assembly Drawings
- D. Trade Studies
- E. System Studies

This volume →

Volume IV - Appendices F - J

- F. Control Software
- G. Test Results
- H. Manufacturing
- I. Specification S-101
- J. Specification S-102

LEGAL NOTICE

This report was prepared as an account of Government sponsored work. Neither the United States, nor the DOE, nor any person acting on behalf of the DOE:

a. Makes any warranty or representation, express or implied, with respect to the accuracy, completeness, or usefulness of the information contained in this report, nor that the use of any information, apparatus, method, or process disclosed in this report may not infringe privately owned rights; or

b. Assumes any liabilities with respect to the use of, or for damages resulting from the use of any information, apparatus, method, or process disclosed in this report.

9.1 BILL OF MATERIALS (APPENDIX A)

The following series of tables provide the bill of material for the Northrup heliostat. Specifically, the table numbers and material lists are as follows:

Table A-1	Northrup II Heliostat Assembly Bill of Materials
Table A-2	Mirror Module Bill of Materials
Table A-3	Rack Truss Bill of Materials
Table A-4	Drive Unit Bill of Materials
Table A-5	Electronics Rack Bill of Materials
Table A-6	Pedestal Bill of Materials
Table A-7	Limit Switch Bill of Materials
Table A-8	Heliostat Electronics Bill of Materials

TABLE A-1

12-010

NORTHROP II HELIOSTAT ASSEMBLY BILL OF MATERIALS

PART NUMBER	DESCRIPTION	QUANTITY PER HELIOSTAT
12-010	NORTHROP II HELIOSTAT ASSEMBLY	1
12-100	MIRROR MODULE ASSEMBLY	12
12-200	RACK TRUSS ASSEMBLY	2
12-300	DRIVE UNIT ASSEMBLY	1
12-400	ELECTRONICS RACK ASSEMBLY	1
12-500	PEDESTAL ASSEMBLY	1
12-600	HELIOSTAT LIMIT SWITCH ASSEMBLY	1
12-700	HELIOSTAT ELECTRONICS	1
0011	STEPPER MOTOR; P/N M112-FJ327 SUPERIOR ELEC CO. BRISTOL CONN.	2
0012	FLEXIBLE COUPLING; P/N L-070 LOVEJOY INC., DOWNERS GROVE, ILL.	2
0013	KEYWAY STOCK; .1875" SQUARE X 1.25" LONG CARBON STEEL	2
0014	BOLT, HEX HEAD; 1/4-20 UNC-2A x 1 1/4" LG ZINC PLATED CARBON STEEL	8
0015	LOCKWASHER; 1/4" BOLT SIZE, ZINC PLATED CARBON STEEL	8
0016	NUT, HEX; 1/4 - 20 UNC -2B ZINC PLATED CARBON STEEL	8
0017	STUD - DRIVE TO PEDESTAL; 5/8 - 11 UNC - 2A x 3.5" LG ZINC PLATED CARBON STEEL	12
0018	LOCKWASHER; 5/8" BOLT SIZE ZINC PLATED CARBON STEEL	12
0019	NUT, HEX; 5/8 - 11 UNC 2B ZINC PLATED CARBON STEEL	12
0021	STUD, MIRROR MOUNT; 3/8-24 UNF-2A x 4.0" LG ASTM A 307, ZINC PLATED CARBON STEEL	36

TABLE A-1 (Continued)

12-010

NORTHROP II HELIOSTAT ASSEMBLY BILL OF MATERIALS

<u>PART NUMBER</u>	<u>DESCRIPTION</u>	<u>QUANTITY PER HELIOSTAT</u>
0022	FLAT WASHER; 3/8" BOLT SIZE, ZINC PLATED CARBON STEEL	72
0023	JAM NUT, HEX; 3/8-24 UNF-2B ZINC PLATED CARBON STEEL	36
0024	SPHERICAL NUT-WASHER; 3/8-24 UNF-2B PART #H19300-6 KAYNAR CORP, FULLERTON, CALIF.	72
0025	BOLT HEX HEAD; 5/16-24 UNF - 2A x 1.0" LONG, ZINC PLATED CARBON STEEL	16
0026	FLATWASHER; 5/16" BOLT SIZE, ZINC PLATED CARBON STEEL	16
0027	GASKET, LONG; 5/32" x 1" WIDE x 26" LG SPONGE RUBBER ADHESIVE BACK, MCMASTER-CARR #1117A13	2
0028	GASKET, SHORT; 5/32" x 1" WIDE X 10.8" LG SPONGE RUBBER ADHESIVE BACK, MCMASTER-CARR #1117A13	2
0029	NUT, HEX; #10-32 UNF-2B ZINC PLATED CARBON STEEL	4
0031	CLAMP-LOOP, CUSHIONED; 1/2", P/N S370-8 UMPCO INC., GARDEN GROVE, CALIF.	3
0032	CLAMP-LOOP CUSHIONED; 3/8", P/N S370-6 UMPCO INC., GARDEN GROVE, CALIF	2
0033	CLAMP-LOOP, CUSHIONED; 3/4" P/N S370-12 UMPCO INC., GARDEN GROVE, CALIF	1
0034	BOLT, HEX HEAD; NO 10-32 UNF -2A x 3/4" LG ZINC PLATED CARBON STEEL	1
0035	FLAT WASHER; #10 BOLT SIZE ZINC PLATED CARBON STEEL	1
0036	CONNECTOR, STRAIN RELIEF; P/N TB 2521 RYALL ELECTRIC, DENVER, COLO.	3
0037	NUT, CONNECTOR; P/N BL 50 RYALL ELECTRIC, DENVER, COLO.	2
0038	CONNECTOR, STRAIN RELIEF; P/N TB2523 RYALL ELECTRIC, DENVER, COLO.	1

Table A-1 (Continued)

12-010

NORTHROP II HELIOSTAT ASSEMBLY BILL OF MATERIALS

PART NUMBER	DESCRIPTION	QUANTITY PER HELIOSTAT
0039	CONNECTOR, STRAIN RELIEF; P/N TB 2535 RYALL ELECTRIC, DENVER, COLO.	2
0041	NUT, CONNECTOR; P/N BL75 RYALL ELECTRIC, DENVER, COLO.	2
0043	ACCELERATOR #TS-3108-37 HUGHSON CHEMICALS, ERIE PA.	.1 oz
0044	STRUCTURAL ADHESIVE; VERSILOK 204 HUGHSON CHEMICALS, ERIE, PA.	2 oz
0045	PRIMER; #9924, HUGHSON CHEMICALS ERIE, PA.	1 Pint
0046	PAINT; WHITE POLYURETHANE CHEMGLAZ #A276 HUGHSON CHEMICALS, ERIE, PA.	1 Pint
0047	CONNECTOR, ½" - 90° SQUEEZE TYPE BOX; P/N TB268 RYALL ELECTRIC, DENVER, CO.	1
0048	CONNECTOR, ½" - TWO SCREW BOX; P/N TR3312 RYALL ELECTRIC, DENVER, CO.	1
0049	CABLE TIE; P/N PLT 2M-CP RYALL ELECTRIC, DENVER, COLO OR EQUAL	12
0051	#8 x 3/4" LG HEX HEAD THREAD FORMING SCREW; P/N 90060A197 MCMaster-CARR CHICAGO, ILL.	1

Table A-2

12-100

MIRROR MODULE BILL OF MATERIALS

<u>PART NUMBER</u>	<u>DESCRIPTION</u>	<u>QUANTITY PER MODULE</u>	<u>QUANTITY PER HELIOSTAT</u>
0100	MIRROR MODULE		12
0103	CENTER MOULDING; DIE NO. 1111-EPDM COMPOUND BC-0-630, LAUREN MFG. CO., NEW PHILADELPHIA, OHIO	4 ft	48 ft
0105	EDGE MOULDING, LONG; SH. .022" x .75" x 72.25" GALVANNEALED STEEL, ASTM A527	4	48
0106	EDGE MOULDING, SHORT; SH .022" x .75" x 47.50" GALVANNEALED STEEL, ASTM A527	2	24
0107	EDGE MOULDING CORNER; SH .022" x .75" x 1.8" GALVANNEALED STEEL ASTM A527	4	48
0108	CENTER MOULDING COVER; SH .022" x .75" x 49.75" GALVANNEALED STEEL, ASTM A527	1	12
0110	MIRROR-SUPPORT STRUCTURE ASSEMBLY	1	12
0115	MIRROR FACET; .094" THK x 48.0" x 72.0" GARDNER MIRROR CORP. NORTH WILKESBORO, N.C.	2	24
0116	MIRROR BACKING SHEET; .028" x 48.0" x 144.32" GALVANNEALED STEEL ASTM A527	1	12
0120	OUTER FRAME ASSEMBLY	1	12
0121	OUTER FRAME WEB; .022" x 4.0" x 32 ft GALVANNEALED STEEL PER ASTM A527	1	12
0130	WEB ASSEMBLY	5	60
0131	WEB; GALVANNEALED SHEET .022" x 4.0" x 144.16" PER ASTM A527	5	60
0132	STIFFENER; GALVANNEALED STEEL .078" x 2.0" x 3.12" PER ASTM A527	14	168
0140	STUD MOUNT ASSEMBLY	2	24
0141	RECTANGULAR STRUCTURAL TUBING; CARBON STEEL .120" w x 1.5" x 2.0" x 48.0" PER ASTM A500	2	24

Table A-2 (Continued)

12-100

MIRROR MODULE BILL OF MATERIALS

<u>PART NUMBER</u>	<u>DESCRIPTION</u>	<u>QUANTITY PER MODULE</u>	<u>QUANTITY PER HELIOSTAT</u>
0142	FLOATING NUT PLATE; PART #F5001-6 KAYNAR MFG. CO. INC., FULLERTON, CALIF.	4	48
0151	RIVET; 1/8" DIA x 1/4" GRIP TYPE MD-BS USM CORP. POP RIVET DIV. SHELTON, CONN.	14	168
0152	STRUCTURAL ADHESIVE; VERSILOK 204 HUGHSON CHEMICALS, ERIE PA.	.5 lb	6 lb
0153	ACCELERATOR #TS-3108-37; HUGHSON CHEMICALS LORD CORP., ERIE, PA.	1 oz	12 oz
0154	DIMETHYL SILICONE; #4 COMPOUND DOW CORNING CORP. MIDLAND, MICH.	14 oz	10.5 lb
0156	RUBBER ADHESIVE; #15160A ST CLAIR RUBBER CO., DETROIT, MICH.	1/2 oz	6 oz
0158	RTV SILICONE, WHITE; P/N 102 GENERAL ELECTRIC CO. INC.	6 oz	4.5
0161	PRIMER; #9924, HUGHSON CHEMICALS ERIE, PA.	1 Qt	3 Gal
0162	PAINT; WHITE POLYURETHANE CHEMGLAZ #A276 HUGHSON CHEMICALS, ERIE, PA	1 Qt	3 Gal
0170	SUB-STRATE ASSEMBLY	1	12
0171	SUB-STRATE BACKING SHEET; .022 x 48.0 x 144.32 GALVANNEALED STEEL ASTM A527	1	12

Table A-3

12-200

RACK STRUCTURE BILL OF MATERIALS

PART NUMBER	DESCRIPTION	QUANTITY PER TRUSS ASSY	QUANTITY PER HELIOSTAT
0200	RACK ASSEMBLY		2
0201	TRUSS CROSS BRACE; ANGLE 1" x 1" x ½" x 91.0" LONG ASTM A 36 STEEL	4	8
0202	TRUSS LOWER BRACE; ANGLE 1" x 1" x ½" x 90.0" LONG ASTM A 36 STEEL	2	4
0210	TRUSS ASSEMBLY; PART #D-272624 BUTLER MFG. CO., KANSAS CITY, MO.	2	4
0220	TORQUE TUBE ASSEMBLY	1	2
0221	TORQUE TUBE FLANGE; PLATE 3/4" x 16.0" x 16.0" ASTM A36 STEEL	1	2
0222	TORQUE TUBE SUPPORT BRACKET; .090" x 28.0" x 39.0" ASTM A366 STEEL	2	4
0223	RIVET; ½" DIA X 5/8" GRIP TYPE MD-BS USM CORP., POP RIVET DIV., SHELTON, CONN.	2	4
0224	PIPE - TORQUE TUBE; 12 3/4" OD x .250" WALL X 111.0" LG ASTM A53 GRB	1	2
0225	RIVET; ½" DIA X 3/8" GRIP TYPE MD-BS USM CORP., POP RIVET DIV., SHELTON, CONN	16	32
0226	PRIMER; #9922 HUGHSON CHEMICALS, ERIE, PA.	1/2 Gal	1 Gal
0227	PAINT, POLYURETHANE WHITE; CHEMGLAZE # A276 HUGHSON CHEMICALS, ERIE, PA	1/2 Gal	1 Gal

Table A-4

12-300

DRIVE UNIT BILL OF MATERIALS

<u>PART NUMBER</u>	<u>DESCRIPTION</u>	<u>QUANTITY PER DRIVE UNIT</u>
PS12-301	PROCUREMENT SPEC-DRIVE UNIT, SOLAR HELIOSTAT	-
D-651137-2	AZIMUTH & ELEVATION DRIVE ASSEMBLY	1
D-651137-16	ELEVATION DRIVE ASSEMBLY	1
651137-83	MOTOR ADAPTER	1
651137-80	PLANETARY PINION SHAFT	1
651137-85	GITS EXPANSION CHAMBER #LO - 1487	1
15118	KEY - 3/16 x 3/16 x 1" LG	1
13336	1/4 LOCKWASHER - ZINC PLATED	8
11870	1/4 x 20 x 3/4 LG. HEX HD. BOLT - ZINC	8
651137-84	MOUNTING PLATE - EXPANSION CHAMBER	1
651137 -86	1/8 COPPER TUBE 18" LONG	1
11109	1/8 WEATHERHEAD ELBOW #69 x 4	2
651137-58	CLAMPING DISC	1
15710	KEY - 1/2 x 1/2 x 7/8 LG	1
11210	1/2 PIPE PLUG - ZINC PLATED	4
11208	1/4 PIPE PLUG - ZINC PLATED	3
10548	1/4 x 1" LG. SPIROL PIN	12
20314	TORRINGTON NEEDLE BEARING - J-1012	4
11868	3/8 - 16 x 1 1/4 LG. HEX HD. BOLT - ZINC	6
12281	3/8 - 16 x 1" LG. SOCKET HD. CAP SCREW	8
12242	1/4 - 20 x 3/4 LG. SOCKET HD. CAP SCREW	12
5908	OIL SEAL C/R 13650	2
10241	SPIROLOX RETAINING RING - RRN - 212	1
10240	SPIROLOX RETAINING RING - RSN - 112	1
20313	MRC BALL BEARING R - 18	1
651137-67	GASKET PLANETARY	1
651137-63	GASKET PLANETARY	1
20311	TIMKEN CONE HM 911245	2
20312	TIMKEN CUP HM 911210	2
651137-56	JOURNAL PIN	2
651137-55	PLANET GEAR	2
651137-54	PLANETARY PINION	1
651137-72	SECONDARY RING GEAR	1

Table A-4 (Continued)
12-300

DRIVE UNIT BILL OF MATERIALS

<u>PART NUMBER</u>	<u>DESCRIPTION</u>	<u>QUANTITY PER DRIVE UNIT</u>
651137-71	PRIMARY RING GEAR	1
651137-52	PLANETARY FRAME	1
651137-57	PLANETARY GEAR WEB	1
651137-51	PLANETARY COVER	1
651137-50	PLANETARY HOUSING	1
651137-59	HIGH SPEED WORM	1
30178	NATIONAL OIL SEAL 509756 SIR	4
30177	DOWTY "O" RING ARP 568 -920	2
651137-70	SPACER	24
13339	5/8 LOCKWASHER - ZINC PLATED	24
13338	1/2 LOCKWASHER - ZINC PLATED	12
13337	3/8 LOCKWASHER - ZINC PLATED	11
11878	5/8 - 11 x 2 1/2 LG. HEX HD. BOLT-ZINC	24
11879	1/2-13 x 1 3/4 LG. HEX HD. BOLT - ZINC	12
11871	3/8 - 16 x 1" LG. HEX HD. BOLT - ZINC	5
651137-66	GASKET - ELEVATION - INNER RING	1
651137-65	GASKET - ELEVATION - OUTER RING	1
651137-64	GASKET - ELEVATION - OUTER RING	1
20315	KAYDON BALL BEARING - KG 160 XPO	1
651137-60	WORM SUPPORT - ELEVATION	1
651137-41	S.S. GEAR - ELEVATION	1
651137-44	S.S. BEARING - INNER CLAMP RING	1
651137-43	S.S. BEARING - OUTER CLAMP RING	1
651137-42	S.S. BEARING - RETAINING RING	1
651137-40	ELEVATION HOUSING	1

Table A-4 (Continued)
12-300

DRIVE UNIT BILL OF MATERIALS

<u>PART NUMBER</u>	<u>DESCRIPTION</u>	<u>QUANTITY PER DRIVE</u>
D-651137-17	AZIMUTH DRIVE ASSEMBLY	1
651137-87	DUST SHIELD	1
651137-83	MOTOR ADAPTER	1
651137-80	PLANETARY PINION SHAFT	1
15118	KEY 3/16 x 3/16 x 1"LG	1
13336	1/4 LOCKWASHER - ZINC PLATED	4
11870	1/4 - 20 x 3/4 LG. - ZINC PLATED	4
651137-73	PLUG - AZIMUTH GEAR	1
651137-58	CLAMPING DISC	1
11208	1/4 PIPE PLUG - ZINC PLATED	3
11868	3/8 - 16 x 1 1/4 LG HEX HD. BOLT - ZINC	6
12281	3/8 - 16 x 1" LG. SOC. HD. CAP SCREW	8
12242	1/4 - 20 x 3/4 LG. SOC. HD. CAP SCREW	12
10548	1/4 x 1" LG. SPIROL PIN	12
20314	TORRINGTON NEEDLE BEARING J-1012	4
10241	SPIROLOX RETAINING RING RRN - 212	1
10240	SPIROLOX RETAINING RING RSN - 112	1
20313	MRC BALL BEARING R-18	1
20311	TIMKEN CONE HM 911245	2
20312	TIMKEN CUP HM 911210	2
651137- 56	JOURNAL PIN	2
651137-63	GASKET - PLANETARY	1
651137-67	GASKET - PLANETARY	1
5908	OIL SEAL - C/R 13650	2
15710	KEY 1/2 x 1/2 x 7/8 LG.	1
651137-54	PLANETARY PINION	1
651137-72	SECONDARY RING GEAR	1
651137-71	PRIMARY RING GEAR	2
651137-55	PLANET GEAR	2
651137-52	PLANETARY FRAME	1
651137-57	PLANETARY GEAR WEB	1
651137-51	PLANETARY COVER	1
651137-50	PLANETARY HOUSING	1
561137-59	HIGH SPEED WORM	1

Table A-4 (Continued)
12-300

DRIVE UNIT BILL OF MATERIALS

<u>PART NUMBER</u>	<u>DESCRIPTION</u>	<u>QUANTITY PER DRIVE UNIT</u>
11210	1/2 PIPE PLUG - ZINC PLATED	1
11209	3/8 PIPE PLUG - ZINC PLATED	1
30177	DOWTY "O" RING ARP 568-920	1
30176	OIL SEAL - C/R 1550540	2
651137-69	3/4 - 10 x 4" LG. STUD - ZINC PLATED	6
13338	1/2 LOCKWASHER - ZINC PLATED	12
13337	3/8 LOCKWASHER - ZINC PLATED	27
11869	1/2 - 13 x 1 3/8 LG. HEX BOLT - ZINC	12
11871	3/8 - 16 x 1" LG. HEX HD. BOLT - ZINC	21
651137-62	GASKET AZIMUTH HOUSING	1
20315	KAYDON BALL BEARING - KG 160 x PO	1
651137-61	WORM SUPPORT - AZIMUTH	1
651137-46	S.S. GEAR - AZIMUTH	1
651137-49	S.S. BEARING RETAINING RING	1
651137-48	S.S. BEARING CLAMPING RING	1
651137-47	S.S. COVER - AZIMUTH	1
651137-45	AZIMUTH HOUSING	1

Table A-5

12-400

ELECTRONICS RACK ASSEMBLY BILL OF MATERIALS

PART NUMBER	DESCRIPTION	QUANTITY PER SUB-ASSEMBLY	QUANTITY P' HELIOSTAT
0400	ELECTRONICS RACK ASSEMBLY		1
0401	FLANGE; .120" THK x 10.84" x 26.00" COLD ROLLED STEEL PER ASTM- A366	1	1
0402	SIDE PLATE; .090" THK x 24.0" x 24.0" COLD ROLLED STEEL PER ASTM-A366	2	2
0403	TOP PLATE; RYERSON P/N 3/4" NO 13-15 7.29" x 11.62" EXPANDED METAL-FLATTENED	1	1
0404	RACK BRACKET: .090 THK x .75" x 2.0" COLD ROLLED STEEL PER ASTM-A366	2	2
0406	CLOSURE PLATE; .030" THK x 1.32" x 7.28" COLD ROLLED STEEL PER ASTM-A366	2	2
0407	EDGE MOULDING; DIE NO. 1113-EPDM COMPOUND BC-0-610 OR BC-0-630 LAURN MFG. CO. NEW PHILADELPHIA, OHIO	2 FT	2 FT
0410	LOWER SHELF ASSEMBLY	1	1
0411	LOWER SHELF; RYERSON P/N 3/4" No. 13-15 7.28" x 24.0" EXPANDED METAL-FLATTENED	1	1
0412	TOP GUIDE, SHORT; .120" THK x 1.0" x 4.0" COLD ROLLED STEEL PER ASTM-A366	4	8
0413	BOTTOM GUIDE, LONG; 120" THK x .75" x 22.0" COLD ROLLED STEEL PER ASTM A366	2	4
0414	REAR STOP; .120" THK x 1.0" x 5.5" COLD ROLLED STEEL PER ASTM-A366	1	2
0420	CENTER SHELF ASSEMBLY	1	1
0421	CENTER SHELF; RYERSON P/N 3/4" NO. 13-15 7.28" x 22.5" EXPANDED METAL-FLATTENED	1	1
0430	UPPER SHELF ASSEMBLY	1	1
0431	UPPER SHELF; RYERSON P/N 3/4" No 13-15 7.28" x 22.5" EXPANDED METAL-FLATTENED	1	1
0432	TOP GUIDE; .120" THK x 1.0" x 7.25" COLD ROLLED STEEL PER ASTM A366	1	1
0433	BOTTOM GUIDE; .120" THK x .75" x 7.25" COLD ROLLED STEEL PER ASTM-A 366	1	1
0440	DOOR ASSEMBLY	1	1

Table 4-5 (Continued)

12-400

ELECTRONICS RACK ASSEMBLY BILL OF MATERIALS

<u>PART NUMBER</u>	<u>DESCRIPTION</u>	<u>QUANTITY PER SUB-ASSEMBLY</u>	<u>QUANTITY PER HELIOSTAT</u>
0441	DOOR; .090" THK x 9.5" x 25.5" COLD ROLLED STEEL PER ASTM-A366	1	1
0442	HINGE; #1577A27 CONTINUOUS, PLAIN TYPE STEEL .062" THK x 1½" WIDE X 3/16" DIA PIN X 24.0" LONG	1	1
0443	RACK BRACKET; .090" THK x 1.0" x 2.0" COLD ROLLED STEEL PER ASTM A 366	2	2
0444	DOOR GASKET; #1117A11 SPONGE RUBBER ADHESIVE BACK WEATHERSTRIP 1/2" WIDE X 5/32" THK X 6 FEET LONG	1	1
0450	BREATHER ASSEMBLY	1	1
0451	BREATHER; 3" DIA ALUM MINI PORT MCMASTER-CARR P/N 2016K5	1	1
0452	BREATHER COVER; .022" x 4.0" GALVANNEALED STEEL ASTM-A-527	1	1
0462	CAPTIVE THUMB SCREW; 1/4-20 UNC X 1 1/8" LG, BRASS NICKEL PLATE STOCK DRIVE PRODUCTS 55 S. DENTON AVE NEW HYDE PARK, N.Y. 11040	2	2
0463	SPEED NUT; 1/4 - 20 UNC. MCMASTER-CARR P/N 90528A115 OR EQUAL	2	2
0464	CAGE NUT, TYPE J; 1/4-20 UNC, MCMASTER-CARR P/N 90679A029 Or EQUAL	2	2
0465	FLAT HEAD MACHINE SCREW; #10-32 UNF X 3/4" LG ZINC PLATED STEEL	9	9
0466	LOCKWASHER; #10 BOLT SIZE ZINC PLATED STEEL	9	9
0467	JAMB NUT, HEX; #10-32 UNF ZINC PLATED STEEL	9	9
0468	STRUCTURAL ADHESIVE-VERSILOK 201 HUGHSON CHEMICALS, ERIE, PA.	2 OZ	2 OZ
0469	ACCELERATOR NO. TS-3108-37 HUGHSON CHEMICALS, ERIE PA.	.2 OZ	.2 OZ
0471	PRIMER; #9924 HUGHSON CHEMICALS, ERIE PA.	1 QT	1 QT
0472	PAINT; WHITE POLYURETHANE CHEMGLAZ #A276 HUGHSON CHEMICALS, ERIE, PA.	1 QT	1 QT

Table A-6

12-500

PEDESTAL ASSEMBLY BILL OF MATERIALS

<u>PART NUMBER</u>	<u>DESCRIPTION</u>	<u>QUANTITY PER SUB-ASSEMBLY</u>	<u>QUANTITY PER HELIOSTAT</u>
M-101	HELIOSTAT PILE ASSEMBLY		1
M-101-1	FLANGE; ½" x 29.0" x 29.0" CARBON STEEL PER AISI 1020		1
M-101-5	SPIRAL WOUND PIPE PER ASTM A 252, GRADE 2 24.00" OD x .250" WALL X 25 FT LG.		1
M-103	TAPERED LEVELING SHIM; 5/8" x 29.0" x 29.0" CARBON STEEL PER AISI 1020, NORMALIZED AT 1100° F MIN FOR 1 HOUR MIN		2
M-104-1	DRIVING STUB ASSY FLANGE; ½" x 23.0" I.D. x 28.5" O.D. CARBON STEEL AISI 1020	1	1 per 10 Heliostats
	PIPE; 24.0" O.D. x .25" WALL x 12.0" LG SPIRAL WOUND PIPE PER ASTM A252 GR 2	1	
M-104-3	FLANGE COVER; EXTERIOR GRADE C/D PLYWOOD 3/4" x 23.0" ID x 28.5" OD		1
M-104-5	COVER PLATE; 3/8" x 10.81" x 26.0" CARBON STEEL PER AISI 1020		1 per 10 Heliostats
M-105	FLANGE; ELECTRONIC OPENING; 5/8" x 10.81" x 26.0" CARBON STEEL PER AISI 1020		1

SPECIFICATIONS

M-102	HELIOSTAT PILE INSTALLATION	-
S-101	INSTALLATION OF OPEN END PIPE PILES	-
S-102	SURFACE PREPARATION, APPLICATION AND INSPECTION OF PROTECTIVE COATINGS FOR CARBON STEEL HELIOSTAT PILES	-

Table A-7
12-600

HELIOSTAT LIMIT SWITCH BILL OF MATERIALS

PART NUMBER	DESCRIPTION	QUANTITY PER SUB-ASSEMBLY	QUANTITY PER HELIOSTAT
0600	ELEVATION LIMIT SWITCH ASSEMBLY		1
0601	ELEVATION LIMIT SWITCH BRACKET 1.0" x 2.0" x 6.5" FLAT CRS 1018 ASTM-A-108	1	1
0610	CW ACTUATOR ASSEMBLY	1	2
0611	CW ACTUATOR BRACKET; .120" x 2.5" x 3.75" CRS PER ASTM-A366	1	2
0620	CCW ACTUATOR ASSEMBLY		2
0621	CCW ACTUATOR BRACKET; .120" x 2.5" x 3.75" CRS PER ASTM-A366	1	2
0630	WEST AZIMUTH SWITCH ASSEMBLY		1
0631	WEST AZIMUTH LIMIT SWITCH BRACKET; .120" x 2.5" x 7.2" CRS PER ASTM-A366	1	1
0640	EAST AZIMUTH SWITCH ASSEMBLY		1
0641	EAST AZIMUTH LIMIT SWITCH BRACKET; .120" x 2.5" x 7.2" CRS PER ASTM-A366	1	1
0661	LIMIT SWITCH SPACER; 1/8" THICK HIGH IMPACT STYRENE OR EQUAL	2	4
0662	FLAT HEAD MACHINE SCREW; #6-32 UNF-2A x 3.0" LG-ZINC CHROMATE PLATED	4	4
0663	NUT, HEX; #6-32-UNF-2B ZINC CHROMATE PLATED	4	8
0664	LOCKWASHER, SPLIT; #6 SCREW SIZE-ZINC PLATED	4	8
0665	FLAT HEAD MACHINE SCREW; #6-32 UNF-2A x 2.0" LG-ZINC CHROMATE PLATED	2	4
0666	PLAIN THUMB SCREW; PART #7137S1 R.A.F. ELECTRONIC HWP, INC., STRATFORD, CONN	2	8
0667	NUT HEX; #10-32 UNF-2B ZINC CHROMATE PLATED	4	8
0668	MICRO SWITCH; P/N BZ-2RDS725551-A2 MINNEAPOLIS-HONEYWELL, FREEPORT, ILL	2	6

Table A-7 (Continued)

12-600 HELIOSTAT LIMIT SWITCH BILL OF MATERIALS (Continued)			
PART NUMBER	DESCRIPTION	QUANTITY PER SUB-ASSEMBLY	QUANTITY PER HELIOSTAT
0669	MICRO SWITCH; P/N BZ-2RDS5551-A2 MINNEAPOLIS-HONEYWELL, FREEPORT, ILLINOIS	2	8
0671	PRIMER; #9924- HUGHSON CHEMICALS, ERIE PA	AS REQUIRED	1 PINT
0672	PAINT: POLYURETHANE WHITE CHEM GLAZE #A276- HUGHSON CHEMICALS, ERIE, PA	AS REQUIRED	1 PINT

Table A-8

12-700

HELIOSTAT ELECTRONICS BILL OF MATERIAL

<u>PART NUMBER</u>	<u>DESCRIPTION</u>	<u>QUANTITY PER HELIOSTAT</u>
12-710	HELIOSTAT CONTROL ELECTRONICS	1
12-720	HELIOSTAT MANUAL CONTROL BOX	1 per 10 Heliostats
12-730	HELIOSTAT WIRE HARNESS	1
12-740	HELIOSTAT WIRING DIAGRAM	AS REQD.
12-750	HELIOSTAT CONTROLLER SOFTWARE	AS REQD.
12-760	DRIVER CONTROLLER ASSEMBLY	1

12-710

HELIOSTAT CONTROL ELECTRONICS BILL OF MATERIAL

<u>QUAN</u>	<u>DESCRIPTION</u>	<u>MFG.</u>	<u>PART NO.</u>
1	Processor	Syn.	6502
1	I/O Timer	Syn.	6532
1	ACIA	Mot.	6850
1	EROM	Intel	2716
1	Baud Gen	Mot	14411
1	Line Driver	TI	75110
2	Line Rovr	TI	75108
1	Inverter	TI	5404
1	Timer	Nat.	LM 555
3	Capacitors		10uf 10v
1	Capacitor		22pf 50v
10	Capacitors		.1uf 50v
1	Crystal		1Mhz
1	Crystal		1.843 Mhz.
1	Resistor Pk		2.2k
6	Resistors		220 ohm 1/4w
2	Resistors		100 ohn 1/4w
2	Resistors		1k 1/4w
2	Resistors		470 ohm 1/4w
1	Resistor		100k 1/4w
1	Resistor		15m 1/2w
1	Power Supply	Northrup	
2	Translators	Superior	TBM 105-1218
1	Housing	Hoffman	A1008HAL

Table A-8 (Continued)

12-710

HELIOSTAT CONTROL ELECTRONICS BILL OF MATERIAL

(Continued)

<u>QUAN</u>	<u>DESCRIPTION</u>	<u>MFG.</u>	<u>PART NO.</u>
1	PC board	Augat	12-0701
3	Isolators	Mot.	4n33
1	Fan	Pam Motor	4666XP
CONNECTORS			
ITT Cannon			
2	ss3 boot		317-1398-000
2	ss3 grommet		351-1641-000
2	ss3p plug		120-1808-000
2	ss3s recpt.		120-1805-000
1	ss4p plug		120-1809-000
1	ss4s recpt.		120-1806-000
1	ss7p plug		120-1873-000
1	ss7s recpt.		120-1874-000
2	ss8p plug		120-1865-000
2	ss8s recpt.		120-1866-000
1	ss9p plug		120-1867-000
1	ss9s recpt.		120-1868-000
2	ss10p plug		120-1869-000
2	ss10s recpt.		120-1870-000
56	pins		030-2196-001
56	sockets		030-1267-001

Table A-8 (Continued)

12-720

HELIOSTAT MANUAL CONTROL BOX BILL OF MATERIALS

PART NUMBER	DESCRIPTION	QUANTITY PER BOX
7404	IC1	1
555	IC2	1
6502	IC3	1
2716 OR 2758	IC4	1
6532	IC5	1
75110	IC6	1
C1	CAPACITOR, 80 Pf	1
C2	CAPACITOR, 180 Pf,	1
C3, C4	CAPACITOR, 10 uf,	2
C5, C6	CAPACITOR, 3 uf	2
C7, C8	CAPACITOR, 2200	2
R1, R2	RESISTOR, 470 Ω	2
R3	RESISTOR, 4.7k	1
R4	RESISTOR, 10 k	1
R5,R6,R7,R8,R12	RESISTOR, 2.2 k	5
R9, R11	RESISTOR, 220 Ω	2
S1,S2,S3,S4,S5	SWITCH	5
CRI	DIODE BRIDGE	1
T1	TRANSFORMER	1
LM340T	VOLTAGE REGULATOR, VR1	1
LM320T	VOLTAGE REGULATOR, VR2	1
X1	CRYSTAL, 1 MHZ	1

Table A-8 (Continued)

12-730

HELIOSTAT WIRE HARNESS BILL OF MATERIAL

PART NUMBER	DESCRIPTION	QUANTITY PER HELIOSTAT
14 GAUGE	STRANDED WIRE; INTRA-RACK	22 FT

Table A-8 (Continued)

12-740

HELIOSTAT WIRING DIAGRAM

PART NUMBER	DESCRIPTION	QUANTITY PER HELIOSTAT
14-7	CABLE, TYPE SO NEOPRENE; ELEVATION MOTOR	20 FT
14-7	CABLE, TYPE SO NEOPRENE; AZIMUTH MOTOR	15 FT
18-8	CABLE, TYPE SO NEOPRENE; SAFETY LIMIT SWITCH	22 FT
22-8	CABLE, TYPE SO NEOPRENE; LIMIT SWITCH	22 FT
16-3	CABLE, TYPE SO NEOPRENE; POWER SUPPLY	10 FT
22-4	CABLE, 2 TWISTED SHIELDED PAIR TYPE SO NEOPRENE; DATA BUS	10 FT

Table A-8 (Continued)

12-750

HELIOSTAT SYSTEM CONTROLLER EQUIPMENT

PART NUMBER	DESCRIPTION	QUANTITY PER FIELD
0750	HELIOSTAT CONTROLLER EQUIPMENT	AS REQD
0751	PLOTTER; P/N 9872B HEWLETT PACKARD, FORT COLLINS, CO	1
0751a	INTERFACE CABLE; P/N 98034A HEWLETT PACKARD, FORT COLLINS, CO	1
0752	TERMINAL/PRINTER; P/N 2621P HEWLETT PACKARD, FORT COLLINS, CO.	1
0753	EXPANDER; P/N 9878 I/O HEWLETT PACKARD, FORT COLLINS, CO.	1
0753a	INTERFACE CABLE; P/N 98036A OPTION 001 HEWLETT PACKARD, FORT COLLINS, CO.	1
0753b	TIME CLOCK; P/N 98035A HEWLETT PACKARD, FORT COLLINS, CO.	1
0754	CALCULATOR; P/N 9825 HEWLETT PACKARD, FORT COLLINS, CO	1
0754a	INTERFACE CABLE; P/N 98036A (STD) HEWLETT PACKARD, FORT COLLINS, CO.	1
0755	DISK DRIVE; P/N 9885 HEWLETT PACKARD, FORT COLLINS, CO.	1
0756	LINE VOLTAGE REGULATOR; P/N 70303 TOPAZ ELECTRONICS, SAN DIEGO, CA.	1

Table A-8 (Continued)

12-760

DRIVER CONTROLLER ASSEMBLY

PART NUMBER	DESCRIPTION	QUANTITY PER FIELD
1488	IC1	1
1489	IC2	1
4N33	ISOLATOR IC3, IC4	2
75108	IC5	1
75110	IC6	1
C1,C3,C5,C7	CAPACITOR 3 uf	4
C2,C4,C6,C8	CAPACITOR, 2200	4
R1, R4	RESISTOR, 220 Ω	2
R2,R3	RESISTOR, 470 Ω	2
R5	RESISTOR, 1K	1
R6,R7,R8,R9	RESISTOR, 200	4
LM340T	VOLTAGE REGULATOR, VR2, VR3	2
LM320T	VOLTAGE REGULATOR, VR1	1
CR1, CR2	DIODE BRIDGES	2
TRIAD F-112x	TRANSFORMER 14vct, T1, T2	2

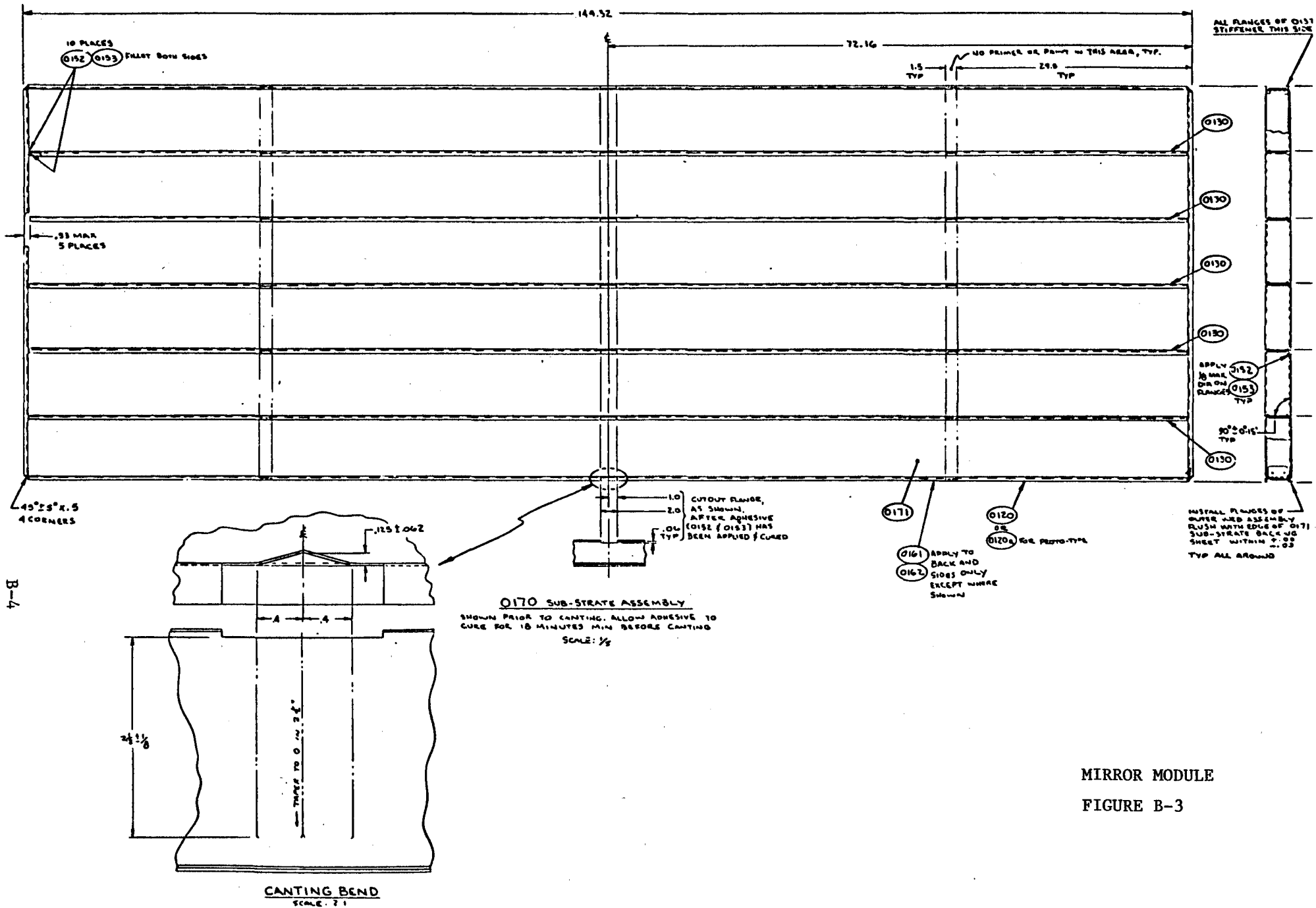
9.2 Part Drawings (Subassemblies) (Appendix B)

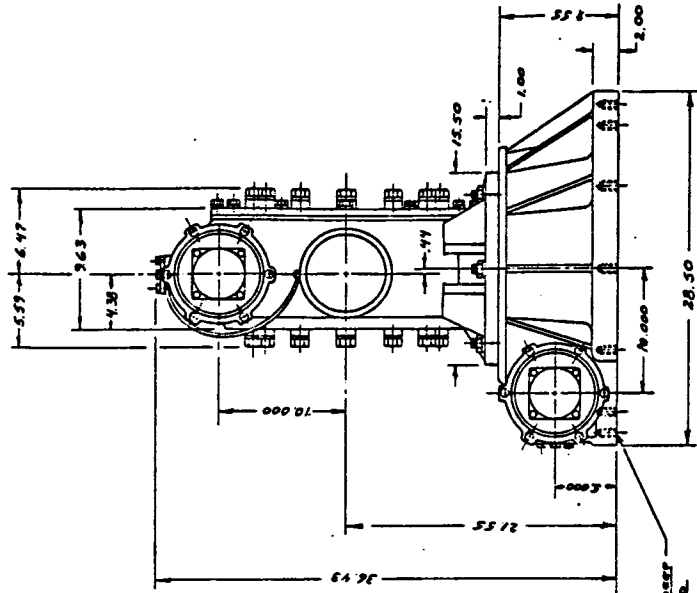
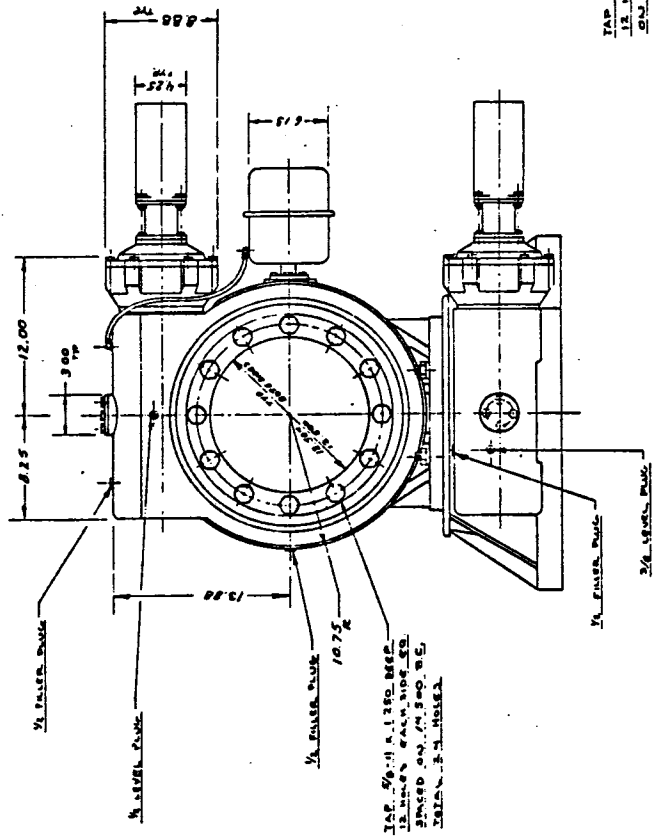
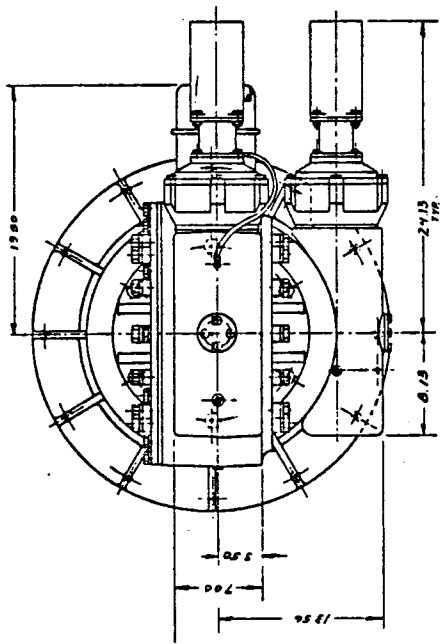
Major subassemblies of the Northrup II heliostat include:

- a. Northrup P/N 12-100 Mirror Module
- b. Northrup P/N 12-200 Rack Truss
- c. Winsmith P/N D-651137-2 Drive Unit
- d. Bechtel P/N M-102 Pedestal
- e. Northrup P/N 12-710 Control Electronics
- f. Northrup P/N 12-750 System Controller Equipment

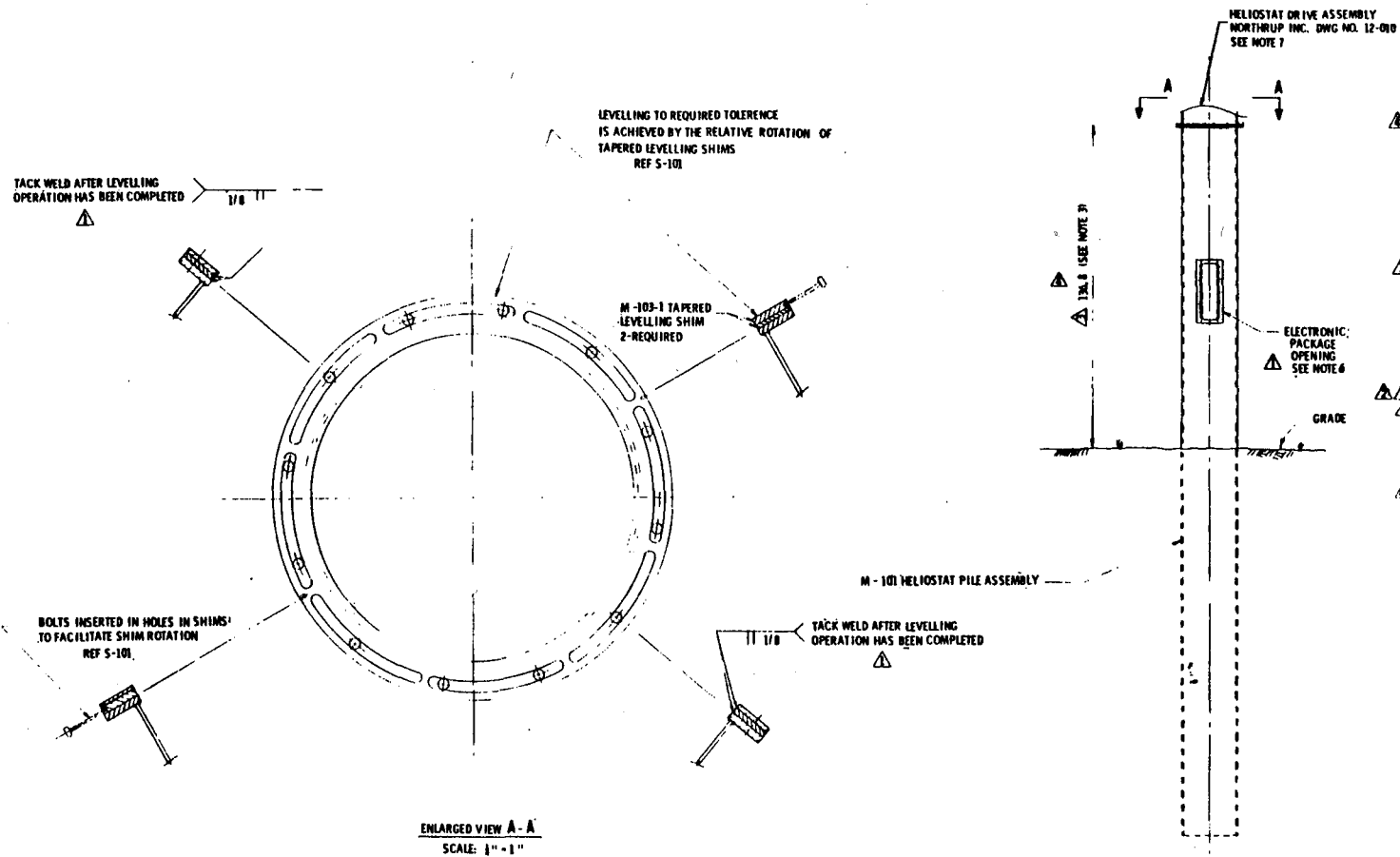
Portions of the drawings defining these subassemblies are included in this section in the following order.

	<u>Figure</u>
a. Mirror Module P/N 12-100	B1,B2,B3
b. Rack Structure P/N 12/200	B4
c. Drive Unit P/N D2	B5
d. Pedestal Pile Installation P/N M 102	B6
e. Control Electronics P/N 12-710	B7
f. System Controller Equipment P/N 12-750	B8





DRIVE UNIT
FIGURE B-5



- NOTES:
1. LEVEL SHIMS PER INSTRUCTIONS IN PILE DRIVING SPECIFICATION S-101
 2. PILE MUST BE PLUMB WITHIN 2% (2.73" IN 136.5")
 3. ELEVATION OF FLANGE SHALL NOT DEVIATE FROM DIMENSION SHOWN BY MORE THAN 2"
 4. ELECTRONIC PACKAGE OPENING SHALL BE ORIENTED TO FACE AWAY FROM TOWER
 5. PILE SHALL BE DRIVEN PER PILE DRIVING SPECIFICATION S-101
 6. ELECTRONIC PACKAGE COVER DWG. M-104-5 SHALL BE INSTALLED WITH ALL BOLTS TIGHTENED WHEN PILE IS DRIVEN
 7. HELIOSTAT DRIVE ASSEMBLY FLANGE TO BE SECURED WITH 12, 5/8 - 11 UNC CL2 SELF LOCKING NUTS AND FLAT WASHERS SUBSEQUENT TO PILE PLACEMENT. ELECTRONIC PACKAGE (NORTHROP INC. DWG NO. 12-001) SHALL BE INSTALLED WITH 16, 5/16 - 24 UNF x 1" CL2B BOLTS WITH FLAT WASHERS SUBSEQUENT TO DRIVING PILE.
 9. DIMENSIONS ARE IN INCHES
 10. WELD PER AWS D.1.1 STRUCTURAL WELDING CODE
 11. REMOVE M-104-3 PLYWOOD FLANGE COVER AND ATTACH M-104-1 DRIVING STUB PRIOR TO DRIVING PILE.

△ HOLDS REMOVED
TACK WELDS WERE ON O.D. OF SHIMS

FIGURE B-6
Pedestal Pile Installation

REVISION 4
 CHANGED: (a) NOTE 2. ...2% (2.58" IN 129") TO (2.73" IN 136.5")
 (b) NOTE 7. ...FLAT WASHER. TO ...FLAT WASHER SUBSEQUENT TO DRIVING PILE.
 (c) PILE HEIGHT FROM 135 TO 136.8
 DELETED: NOTE 8. (TOLERANCE, X. .100)
 ADDED: NOTE 11.

INSTALLED PILE
 SCALE: 1"=2'-0"

NO.	DATE	DESCRIPTION	BY	CHKD	APP'D
1	12/10/88	REVISIONS NOTED			
2	12/10/88	PILE HEIGHT WAS 129			
3	12/10/88	24 UNF x 1 WAS 18 UNF x 1 1/2			
4	12/10/88	REVISIONS NOTED			
5	12/10/88	ISSUED FOR FABRICATION			

NOTED: [Signature] CD

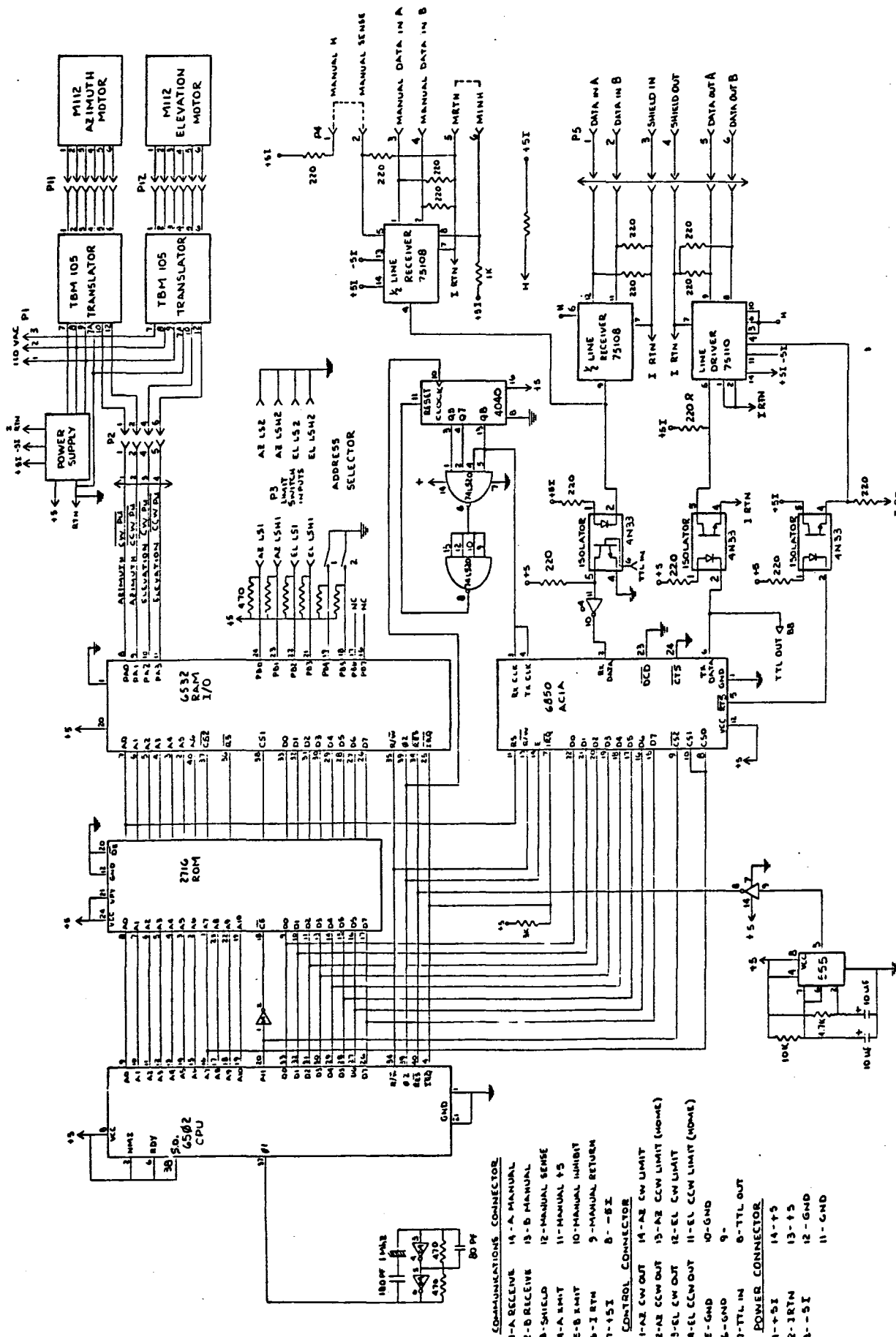
BECHTEL
SAN FRANCISCO

SECOND GENERATION HELIOSTAT DEVELOPMENT

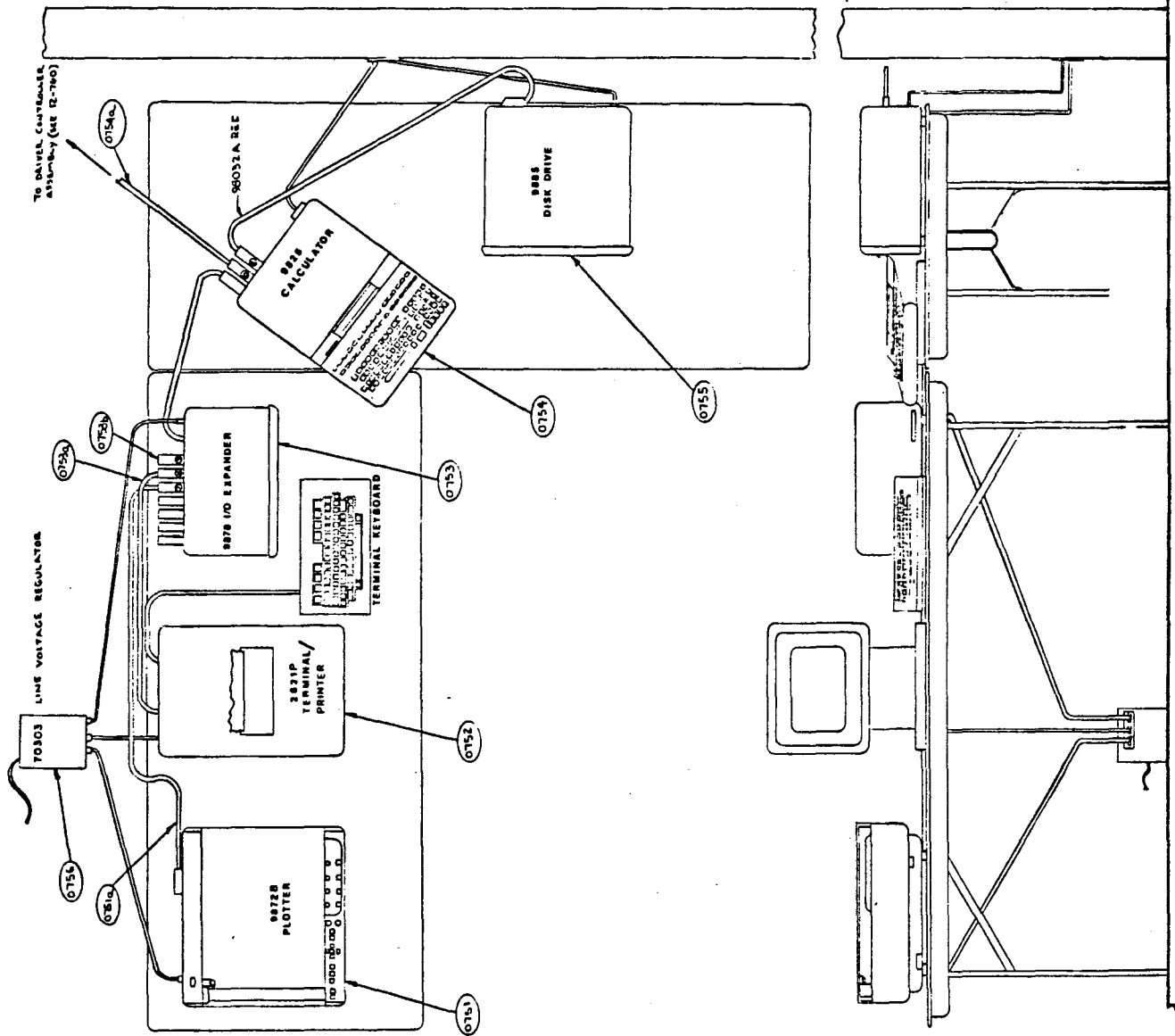
HELIOSTAT PILE INSTALLATION

JOB NO.	DESCRIPTION NO.	REV.
13393	M-102	4

CONTROL ELECTRONICS
FIGURE B-7



NOTE: ALL RESISTORS $\frac{1}{4}$ W $\pm 10\%$.



SYSTEM CONTROLLER
EQUIPMENT
FIGURE B-8

9.3 ASSEMBLY DRAWINGS, HELIOSTAT (APPENDIX C)

Table C-1 provides a complete list of the drawings required for the Northrup II heliostat. Figure C-1 presents the Northrup II heliostat top-level assembly drawing.

Figure C-2 presents a perspective rendering of the frontside view of the Northrup heliostat. Even though the heliostat only contains 12 mirror modules, the frontal view gives a 24 module appearance because each mirror module contains two mirror facets.

The design goal was to provide a near-continuous mirrored surface with minimal void or blockage area. The total envelope area is 590.7 ft². The mirror module edge seal, center seal; and between-mirror spaces reduce this to a net reflective area of 568 ft². Hence, the area-usage efficiency is 96%.

9.3.2 Heliostat Backside View

Figure C-3 presents a perspective view of the backside of the Northrup heliostat. Key features include the 4 relatively deep Butler truss members, the Winsmith 2-axis drive unit, and the two interconnecting torque tubes. Each mirror module is attached to the top chord of the trusses using a 3-point attachment pattern. The mirror modules are cantilevered out-board from the truss envelope on the top, bottom, and sides to reduce the truss and torque tube lengths. Twelve cross-brace members are installed in 8 places to rigidize the assembly (a pair of criss-cross braces are used in 4 of these places). These braces also serve as an added measure of protection to resist the tendency of the truss compression chord to deflect laterally sideways under load.

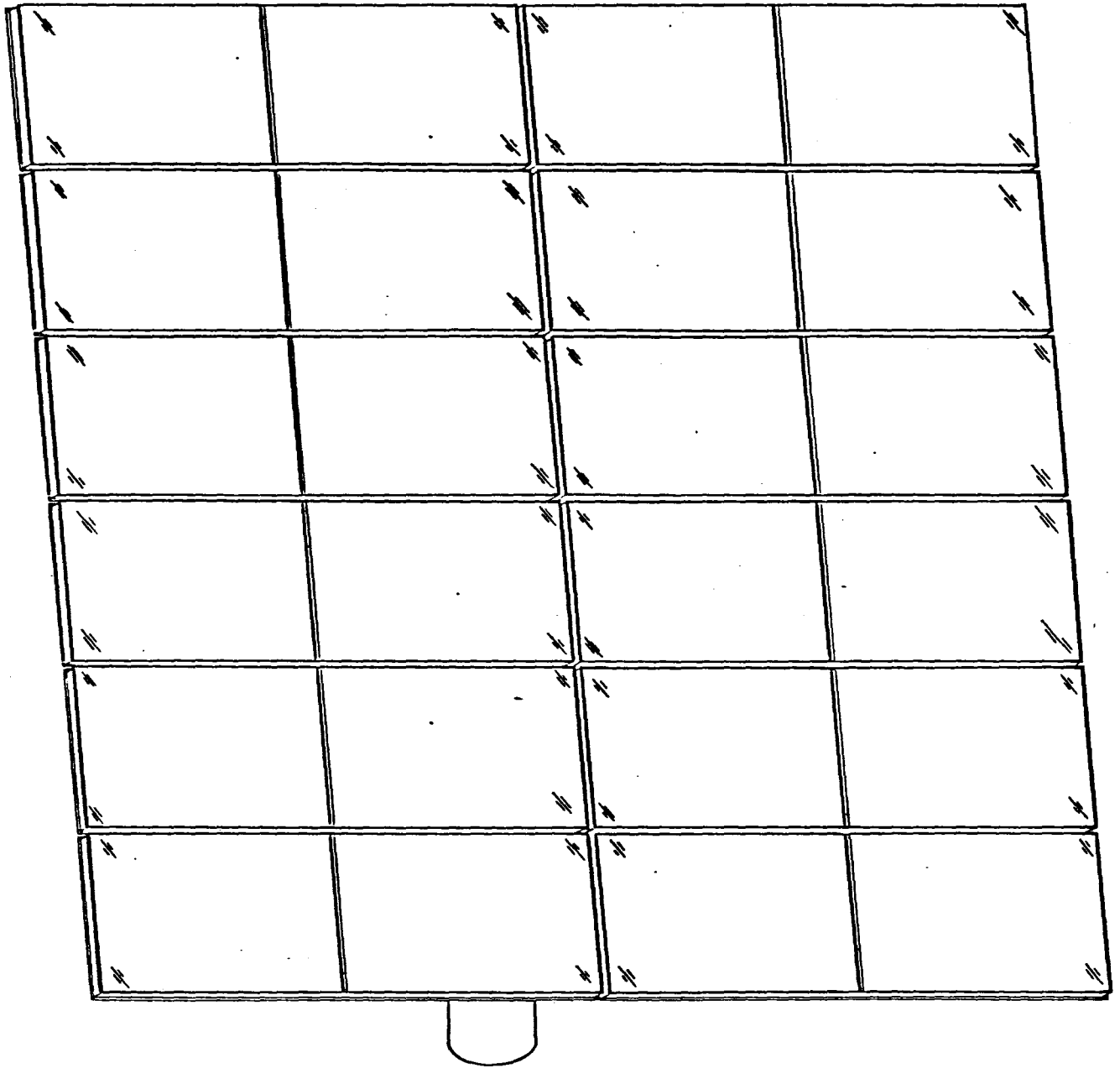
The pedestal is actually a one-piece pile which is driven in place by a vibratory hammer. A flange at the top of the pedestal serves as the drive interface. A pair of tapered, gasket-like shims are used on the pedestal flange to correct for any pile or flange misalignment. By selectively rotating these shims, a true-horizontal mounting plane can be established.

TABLE C-1

DRAWING LIST

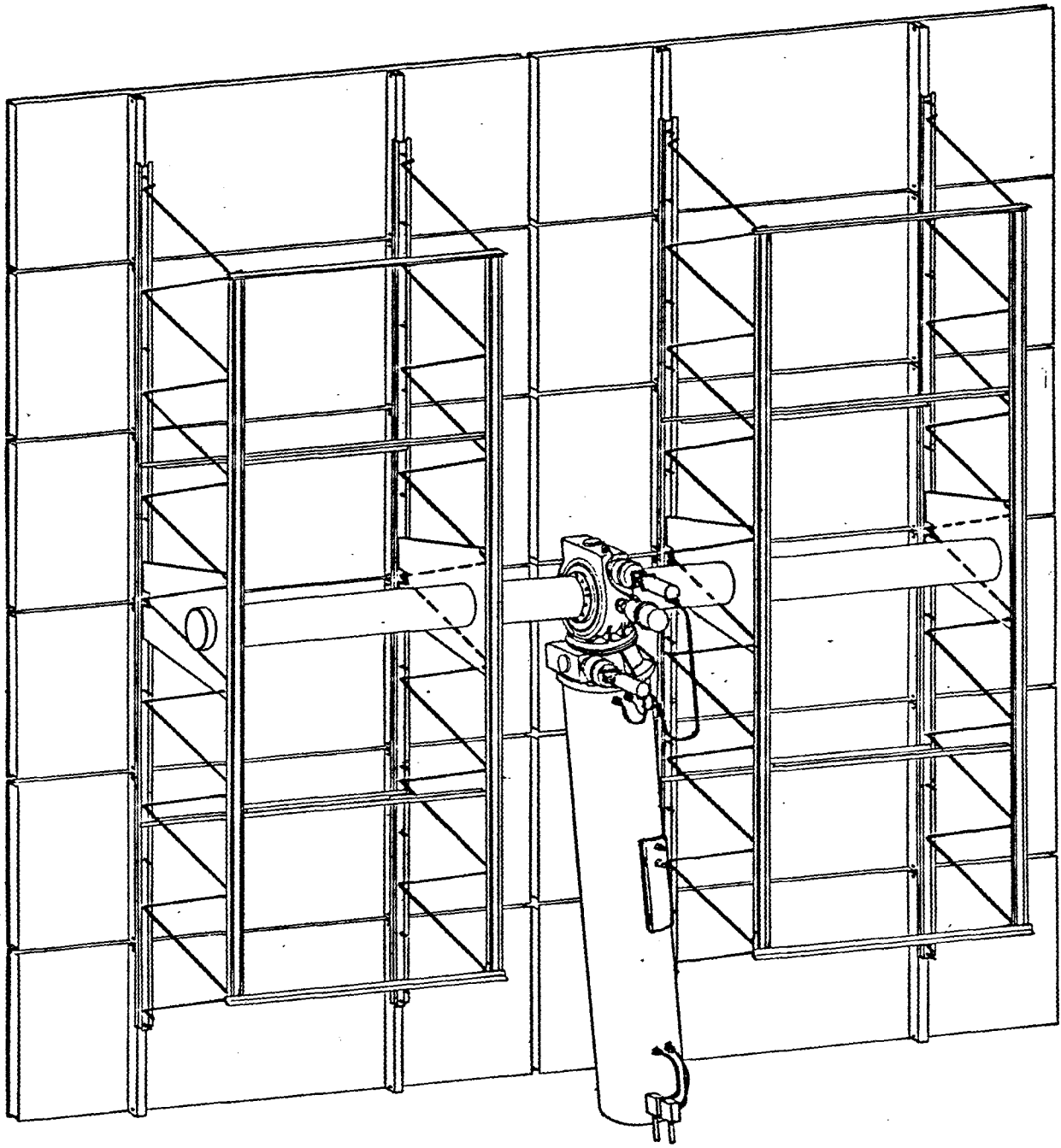
NORTHROP II SECOND GENERATION HELIOSTAT

DRAWING NUMBER	TITLE
12-010	NORTHROP II HELIOSTAT ASSEMBLY
12-100	MIRROR MODULE ASSEMBLY
12-200	RACK TRUSS ASSEMBLY
12-300	DRIVE UNIT ASSEMBLY
PS12-301	PROCUREMENT SPEC-DRIVE UNIT, SOLAR HELIOSTAT
D-651137-2	AZIMUTH & ELEVATION DRIVE ASSEMBLY
12-400	ELECTRONICS RACK ASSEMBLY
12-500	PEDESTAL ASSEMBLY
M-101	HELIOSTAT PILE ASSEMBLY
M-102	HELIOSTAT PILE INSTALLATION
M-103	TAPERED LEVELING SHIM
M-104	PILE DRIVING ATTACHMENTS
M-105	ELECTRONIC PACKAGE OPENING FLANGE
12-600	HELIOSTAT LIMIT SWITCH
12-700	HELIOSTAT ELECTRONICS
12-710	HELIOSTAT CONTROL ELECTRONICS
12-720	HELIOSTAT MANUAL CONTROL BOX
12-730	HELIOSTAT ELECTRICAL CABLING
12-740	HELIOSTAT WIRING DIAGRAM
12-750	HELIOSTAT SYSTEM CONTROLLER EQUIPMENT
12-760	DRIVER CONTROLLER ASSEMBLY



Northrup II Hellostast Front View

FIGURE C-2



Northrup II Heliostat Back View

FIGURE C-3

9.3.3 Heliostat Assembly and Installation

Paragraphs 6.2 and 6.3 provide a detailed discussion of the on-site heliostat assembly and installation. The following is a brief synopsis of that discussion:

a. The heliostat field site is cleared, grubbed, and graded. A spiral-welded steel pipe serves as an integral foundation and pedestal. Vibratory hammers are used to drive the piles in place. The vibratory technique can drive the low displacement piles extremely rapidly into silty sand or gravel soils.

b. After pile driving, the top flange of the pedestal is corrected to a true-horizontal plane by the installation of a pair of tapered shims. The shims are tack-welded to the flange after alignment to fix the relative rotational position while awaiting the heliostat installation.

c. The heliostat piece parts are delivered by truck to the site assembly building. The site assembly building would likely consist of a permanent section (which would become a maintenance shop after completion of the heliostat assemblies), and a temporary section which could be disassembled and moved to another construction site.

d. The heliostat rack structure is assembled in 2 identical half-sections. Two truss units and a torque tube are set-up in a mechanical fixture which controls truss spacing and the relative alignment between the trusses and with the torque tube. The torque tube contains two factory-welded plates which interface with the trusses. These plates are then welded to the top and bottom truss chords, and tack-welded to the web tubing.

e. The next step in the rack half-section assembly is to install the 6 cross-brace members, 2 of which are laterals between adjacent truss bottom chords, and 4 of which are criss-crossed from the top chord of one truss to the bottom chord of the adjacent truss. These cross-brace angles are installed by riveting.

f. Two rack half-section assemblies are brought together and assembled to a drive unit. The connection is made by bolting the torque tube flanges to the drive unit.

g. The twelve mirror modules are installed on the assembled racks. The desired canting is accomplished at this time. This operation completes the heliostat subassembly.

h. The assembled heliostat is transported to the pedestal and installed by bolting the mating flanges together.

9.4 TRADE STUDIES (APPENDIX D)

The following discussion presents the trade studies that were performed in the course of the design progression which lead to the current configuration.

9.4.1. Mirror Module Trade Study

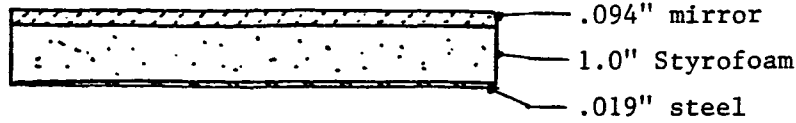
The mirror module configuration initially proposed consisted of an adhesively bonded 2.39 mm (0.094 inch) thick glass mirror, a 25.4 mm (1.0 inch) thick layer of Styrofoam, and a 0.48 mm (0.019 inch) thick backing sheet of galvanized steel formed into a pan-shape to completely enclose the styrofoam core. A thermal deflection analysis of this configuration was performed using the tri-composite analysis described in para 9.5.3.2. The deflection and curvature equations from this analysis have been combined with the appropriate stress equations, and with a thermal analyzer model into the computer model named "MMOD". This program is used to evaluate mirror module candidates. Output includes the temperatures through the composite, stress levels for each layer of the composite, and the resultant concave or convex radius of curvature. Pre-curvatures can be input, material thicknesses and properties can be varied, and the effects of dirty glass and wind convection can be evaluated.

Table D-1 presents the results of a "MMOD" analysis for the originally proposed mirror module configuration described above. It should be noted that the radius of curvature results are independent of facet size or shape, but the maximum deflection values are for a 1.22 x 1.22 m (4.0 x 4.0 ft) mirror module.

The curvature is a function of the glass absorptivity, the heat flux on the mirror ($Q \times \cos \theta$), and the wind convection coefficient. The clean glass reflectivity was assumed to be 87% with the 13% reflectivity loss being attributed to diffuse scattering (5%) and mirror absorption (8%). For the dirty glass cases, the absorption was increased to 12%. Temperature limits were 32°F to 122°F, wind convection coefficients from 1.0 to 2.5 BTU/ft²-hr-°F (0-27 mph wind),

TABLE D-1

MIRROR MODULE ALTERNATE - THERMAL CURVATURE



Environmental Condition	Initial Shape	Initial Shape
	$\delta = 0.0''$ $R = \infty$	$\delta = .0414''$ $R = 580'$
1. $T_{amb} = 32^\circ F$, $V_{wind} = 0$ mph, Clean Glass, $Q \cos \theta = 340$	$\delta = .0358''$ $R = 670'$ Convex	$\delta = .0006''$ $R = 4297'$ Concave
2. $T_{amb} = 122^\circ F$, $V_{wind} = 0$ mph, Clean Glass, $Q \cos \theta = 340$	$\delta = .0243''$ $R = 988'$ Concave	$\delta = .0657''$ $R = 365'$ Concave
3. $T_{amb} = 32^\circ F$, $V_{wind} = 27$ mph, Clean Glass, $Q \cos \theta = 100$	$\delta = .0267''$ $R = 899'$ Convex	$\delta = .0147''$ $R = 1631'$ Concave
4. $T_{amb} = 122^\circ F$, $V_{wind} = 27$ mph, Clean Glass, $Q \cos \theta = 100$	$\delta = .0315''$ $R = 763'$ Concave	$\delta = .0729''$ $R = 329'$ Concave
5. $T_{amb} = 32^\circ F$, $V_{wind} = 0$ mph, Dirty Glass, $Q \cos \theta = 340$	$\delta = .0414''$ $R = 580'$ Convex	$\delta = 0''$ $R = \infty$ Flat
6. $T_{amb} = 122^\circ F$, $V_{wind} = 0$ mph, Dirty Glass, $Q \cos \theta = 340$	$\delta = .0198''$ $R = 1212'$ Concave	$\delta = .0612''$ $R = 392'$ Concave
7. $T_{amb} = 32^\circ F$, $V_{wind} = 27$ mph, Dirty Glass, $Q \cos \theta = 100$	$\delta = .0278''$ $R = 863'$ Convex	$\delta = .0136''$ $R = 1765'$ Concave
8. $T_{amb} = 122^\circ F$, $V_{wind} = 27$ mph, Dirty Glass, $Q \cos \theta = 100$	$\delta = .0305''$ $R = 788'$ Concave	$\delta = .0719''$ $R = 334'$ Concave

and heliostat-normal solar flux from 100-340 BTU/ft²-hr. Two cases are presented; the first shows the glass curvature resulting from an initially flat shape, and the second case incorporates an initial curvature which precludes any subsequent convex shaping.

Paragraph 9.5.3.1 provides a derivation of the optical effect of both convex and concave curvature radii in terms of a milliradian fringe. For a 1.22 x 1.22 m (4.0 x 4.0 ft) mirror module at a slant range of 762 m (2500 ft), the worst-case convex and concave curvatures shown in Table D-1 for the originally proposed mirror module correspond to the following fringe angles:

$$R = 763 \text{ ft concave, fringe} = 3.64 \text{ mrad}$$

$$R = 580 \text{ ft convex, fringe} = 6.90 \text{ mrad}$$

With a pre-deflection formed into the mirror module during fabrication, the convex curvature can be avoided. For this case the resultant worst concave curvature is:

$R = 329 \text{ ft concave, fringe} = 10.56 \text{ mrad}$. In either case, the fringe error was excessive, and a mirror module configuration change was necessary.

Table D-2 presents the results of a 'MMOD' analysis for the same basic concept, except the Styrofoam thickness is increased to 76.2 mm (3.0 inches). The worst case convex and concave curvatures and fringe angles with no pre-deflection are:

$$R = 2113' \text{ ft concave, fringe} = 0.29 \text{ mrad}$$

$$R = 1473 \text{ ft convex, fringe} = 2.72 \text{ mrad}$$

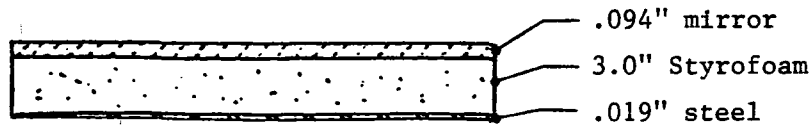
The convex cases can be precluded by pre-curving the module during fabrication. For this case the worst concave curvature is:

$$R = 868 \text{ ft concave, fringe} = 3.01 \text{ mrad}$$

Again, this curvature is considered unacceptable even though the thicker Styrofoam does improve the performance. It should be noted that the fringe angle error is a function of slant range. The values computed above are for the maximum range of 762 m (2500 ft). If this range were reduced to 265 m (870 ft), the 3.01 mrad fringe error would be reduced to zero. So, the concept is not unacceptable in

TABLE D-2

MIRROR MODULE ALTERNATE - THERMAL CURVATURE



Environmental Condition	Initial Shape	Initial Shape
	$\delta = 0.0''$ $R = \infty$	$\delta = .0163''$ $R = 1473'$
1. $T_{amb} = 32^\circ F$, $V_{wind} = 0$ mph, Clean Glass, $Q \cos \theta = 340$	$\delta = .0139''$ $R = 1732'$ Convex	$\delta = .0024''$ $R = 9809'$ Concave
2. $T_{amb} = 122^\circ F$, $V_{wind} = 0$ mph, Clean Glass, $Q \cos \theta = 340$	$\delta = .0081''$ $R = 2953'$ Concave	$\delta = .0244''$ $R = 493'$ Concave
3. $T_{amb} = 32^\circ F$, $V_{wind} = 27$ mph, Clean Glass, $Q \cos \theta = 100$	$\delta = .0037''$ $R = 3476'$ Convex	$\delta = .0062''$ $R = 3300'$ Concave
4. $T_{amb} = 122^\circ F$, $V_{wind} = 27$ mph, Clean Glass, $Q \cos \theta = 100$	$\delta = .0114''$ $R = 2113'$ Concave	$\delta = .0277''$ $R = 368'$ Concave
5. $T_{amb} = 32^\circ F$, $V_{wind} = 0$ mph, Dirty Glass, $Q \cos \theta = 340$	$\delta = .0163''$ $R = 1473'$ Convex	$\delta = 0''$ $R = \infty$ Flat
6. $T_{amb} = 122^\circ F$, $V_{wind} = 0$ mph, Dirty Glass, $Q \cos \theta = 340$	$\delta = .0062''$ $R = 3882'$ Concave	$\delta = .0225''$ $R = 1069'$ Concave
7. $T_{amb} = 32^\circ F$, $V_{wind} = 27$ mph, Dirty Glass, $Q \cos \theta = 100$	$\delta = .0101''$ $R = 2367'$ Convex	$\delta = .0062''$ $R = 3896'$ Concave
8. $T_{amb} = 122^\circ F$, $V_{wind} = 27$ mph, Dirty Glass, $Q \cos \theta = 100$	$\delta = .0110''$ $R = 2186'$ Concave	$\delta = .0273''$ $R = 380'$ Concave

the general sense, but is application-dependent. However, the cost of this configuration is also quite high at \$24.86/m² (2.31/ft²). Hence, this configuration was abandoned.

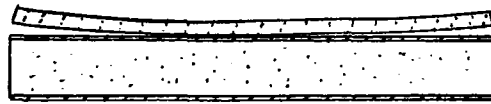
To reduce the thermal curvature effect, a thermally-stabilized configuration was next examined. This concept again utilized the Styrofoam core, but identical facing sheets of steel, aluminum, or fiberglass are employed to maintain "thermal flatness". The mirror is not continuously bonded to this resultant substrate, but instead is only bonded in a small central zone and at the edges using a soft compliant adhesive. This permits the mirror to expand or contract freely and independent of the stabilized substrate. Table D-3 shows the curvature performance for 2" Styrofoam with steel facing sheets for a 1.83 x 1.83 m (6.0 x 6.0 ft) mirror module at temperatures from 32 to 122°F, heat fluxes from 100 to 340 BTU/ft²-hr, and wind speeds from 0 to 27 mph. Both clear glass and dirty glass cases are examined, as are flat-fabrication and pre-curved configurations. It will be noted that a considerable improvement in performance accompanies the stabilized steel configuration versus the unstabilized steel configuration discussed earlier. The worst thermally induced fringe angle is only 1.56 mrad for the low flux, high wind case, and 0.36 mrad for the high flux, no wind case.

In addition to the steel-foam-steel substrate configuration described above, similar thermally stabilized configurations were examined using 0.64 mm (.025 inch) thick aluminum sheets, and 0.94 mm (0.37 inch) thick fiberglass sheets. The goal of this trade-off study was to lower the weight. In addition, the Styrofoam thickness was reduced to 38.1 mm (1.5 inches) to reduce cost, and the mirror module size was increased to 1.83 x 1.83 m (6.0 ft x 6.0 ft) to reduce the number of modules required per heliostat. Table D-4 presents the performance comparison for the steel, aluminum, and fiberglass alternates with this new size and thickness.

Even though the steel alternate offered the lowest cost and best performance, the aluminum alternate was very close and provided a 223kg (490 lb) weight advantage. Hence, at this point in

TABLE D-3

ENVIRONMENTAL PERFORMANCE
STEEL - FOAM - STEEL SUBSTRATE FOR MIRROR SUPPORT



.094" Glass
.019" Steel
2" Styrofoam
.019" Steel

Environmental Condition	Initial Shape	Initial Shape
	$\delta = 0.0''$	$\delta = 0.0397''$
	$R = \infty$	$R = 1360'$
1. $T_{amb} = 32^\circ F$, $V_{wind} = 0$ mph, Clean Glass, $Q \cos \theta = 340$	$\delta = .0267''$ $R = 2021'$ Convex	$\delta = .0130''$ $R = 4158'$ Concave
2. $T_{amb} = 122^\circ F$, $V_{wind} = 0$ mph, Clean Glass, $Q \cos \theta = 340$	$\delta = .0213''$ $R = 2532'$ Convex	$\delta = .0184''$ $R = 2939'$ Concave
3. $T_{amb} = 32^\circ F$, $V_{wind} = 27$ mph, Clean Glass, $Q \cos \theta = 100$	$\delta = .0046''$ $R = 11800'$ Convex	$\delta = .0351''$ $R = 1537'$ Concave
4. $T_{amb} = 122^\circ F$, $V_{wind} = 27$ mph, Clean Glass, $Q \cos \theta = 100$	$\delta = .0046''$ $R = 13461'$ Convex	$\delta = .0357''$ $R = 1513'$ Concave
5. $T_{amb} = 32^\circ F$, $V_{wind} = 0$ mph, Dirty Glass, $Q \cos \theta = 340$	$\delta = .0397''$ $R = 1360'$ Convex	$\delta = 0$ $R = \infty$ Flat
6. $T_{amb} = 122^\circ F$, $V_{wind} = 0$ mph, Dirty Glass, $Q \cos \theta = 340$	$\delta = .0317''$ $R = 1701'$ Convex	$\delta = .0080''$ $R = 6786'$ Concave
7. $T_{amb} = 32^\circ F$, $V_{wind} = 27$ mph, Dirty Glass, $Q \cos \theta = 100$	$\delta = .0068''$ $R = 7889'$ Convex	$\delta = .0329''$ $R = 1644'$ Concave
8. $T_{amb} = 122^\circ F$, $V_{wind} = 27$ mph, Dirty Glass, $Q \cos \theta = 100$	$\delta = .0060''$ $R = 8982'$ Convex	$\delta = .0337''$ $R = 1603'$ Concave

TABLE D-4

MIRROR MODULES, OPTIONS & PERFORMANCE

PARAMETER	.094" GLASS .019" STEEL 1.5" STYROFOAM .019" STEEL	.094" GLASS .025" ALUMINUM 1.5" STYROFOAM .025" ALUMINUM	.094" GLASS .037" FIBERGLASS 1.5" STYROFOAM .037" FIBERGLASS
1. COST OF MATERIALS	\$ 1409	\$ 1489	\$ 1631
2. TOTAL WEIGHT	1851 LB	1361 LB	1222 LB
3. GRAVITY MOMENT	7224 FT-LB	5591 FT-LB	5127 FT-LB
4. RADIUS OF CURVATURE*	+2880' $\rightarrow \infty$	+1441' $\rightarrow \infty$	+1195' $\rightarrow \infty$
5. WIND & WEIGHT DEFLEC. A. FACET, AVG B. BEAM, AVG C. TORQUE TUBE, AVG D. TOTAL, AVG	0.133 MRAD .114 .746 <u>0.993 MRAD</u>	0.302 MRAD .096 .647 <u>1.045 MRAD</u>	1.434 MRAD .090 .620 <u>2.144 MRAD</u>
6. WIND & WEIGHT DEFLEC. A. FACET, MAX B. BEAM, MAX C. TORQUE TUBE, MAX D. TOTAL, MAX	0.276 MRAD .167 <u>1.053</u> 1.496 MRAD	0.625 MRAD .144 <u>.913</u> 1.682 MRAD	2.968 MRAD .137 <u>.875</u> 3.980 MRAD
RATING	# 2	# 1	# 3

* AT WINDSPEED = 0 MPH, CLEAN GLASS, $T_{AMB} = 32-122^{\circ}F$, $Q \cos \theta = 150-300 \text{ BTU/ft}^2\text{-hr}$

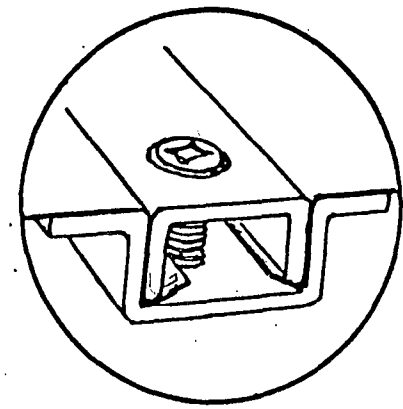
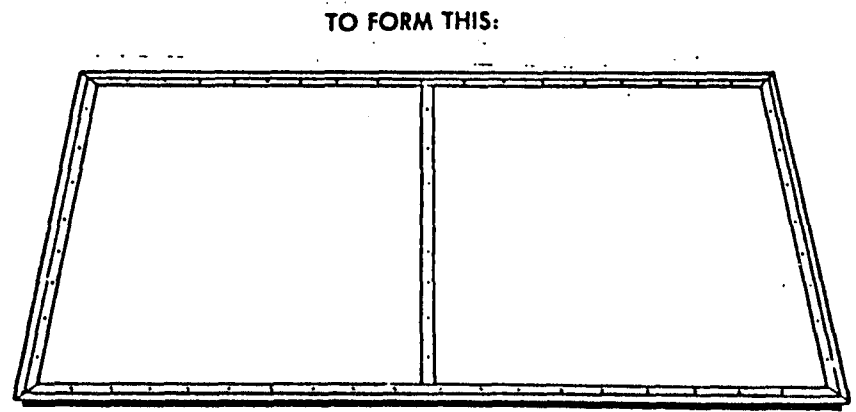
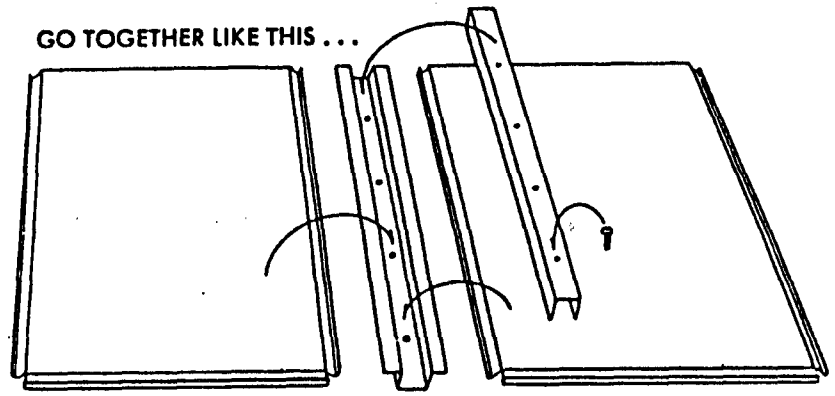
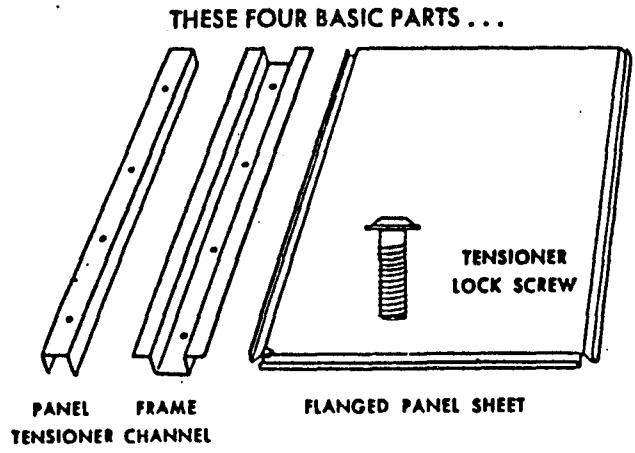
time the aluminum-Styrofoam-aluminum configuration was selected. However, the alternate-candidate search was continued primarily due to the relatively high cost of the basic Styrofoam-based composites. The favored configuration at this point exhibited a unit cost of \$27.77/m² (\$2.58/ft²), and a goal was established to lower this to \$20/m² (\$1.86 ft²) or less.

At this point the concept of using a thin layer of silicone grease as a mirror "adhesive" was introduced. This concept is a general one, and a wide range of substrates may be used with it, including those based on intermittent supports such as the longitudinal stringer approach. The reason for this is that the grease permits shearing motion for slow-acting phenomenon such as thermal expansion or contraction and flexural bending. However, for fast-acting phenomenon such as hail impact, the viscous grease permits the load to be transferred to the steel facing sheet. Therefore, continuous support, such as that offered by a Styrofoam core, is no longer required. However, to establish an economic-optimum design, a variety of substrates were examined. These included a tensioned, single-sheet panel (Figure D-1), an expanded high-impact polystyrene core (Figure D-2), a polystyrene bead board core (Figure D-3), and the steel stringer approach (Figure D-4).

A detailed weight and material cost analysis was performed for each of these candidate substrates in a 1.22 x 1.22 m (4.0 x 12.0 ft) module size. The larger module size was selected to minimize installation and alignment cost. Tables D-5 through D-8 present the results of this weight and material cost analysis. The conclusion is that the stringer approach results in a minimum material cost. The reason that this design is low cost is best explained by Table D-9. It shows that the major cost difference lies between the two sheets of the substrates. The "C-stringers" used in this core are less than one-half the cost of the nearest competitor.

FIGURE D-1

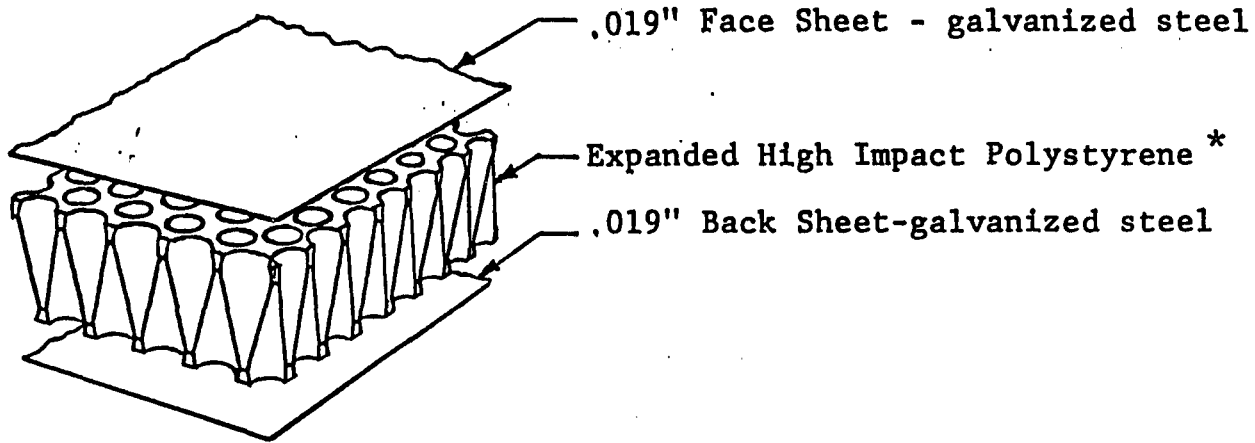
TENSIONED PANELS - LINDSAY DIVISION
INTERNATIONAL STEEL CO.



D-9

FIGURE D-2

NOR-CORE MIRROR MODULE ALTERNATE

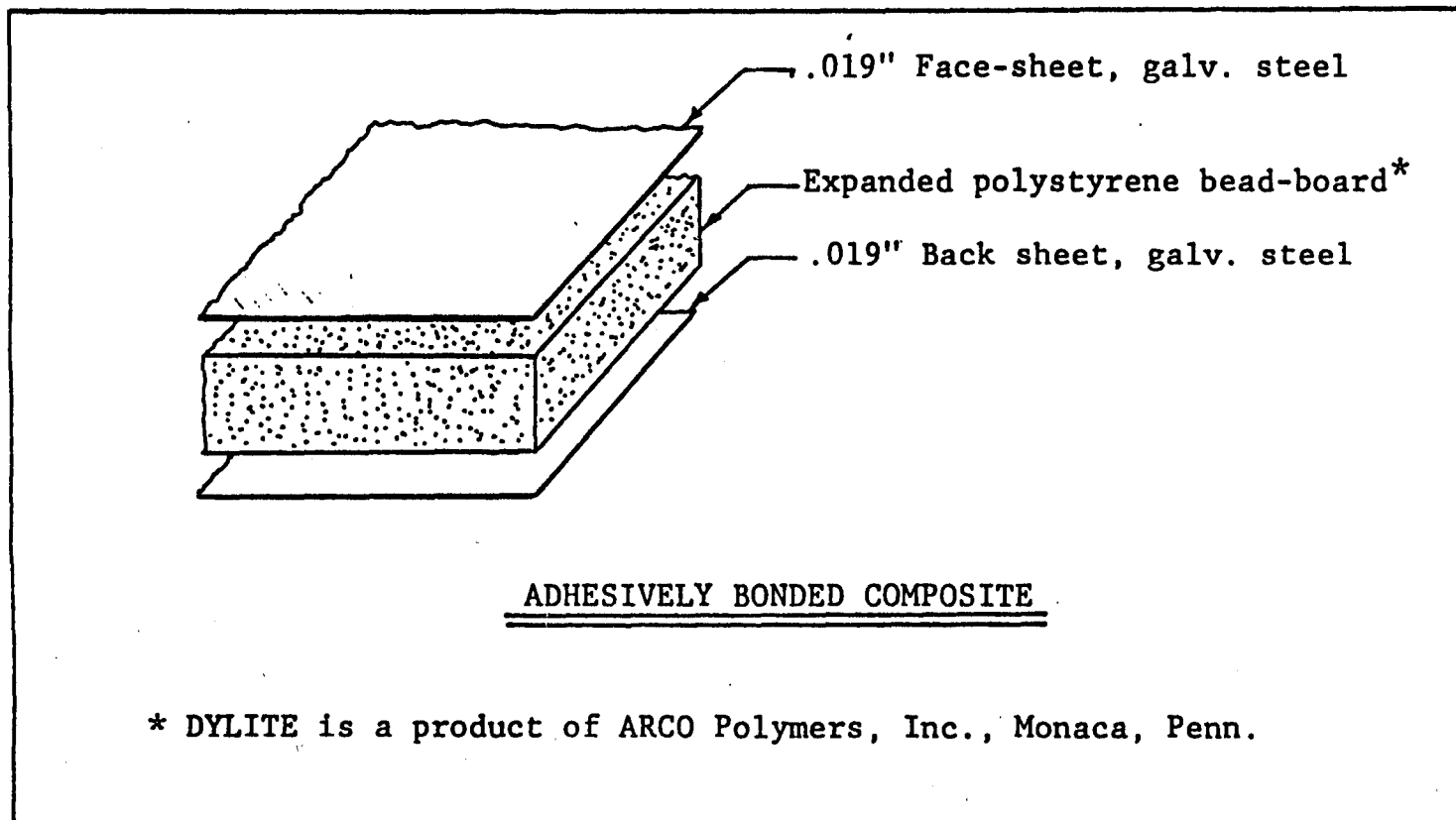


ADHESIVELY BONDED COMPOSITE

* NOR-CORE is a product of the Norfield Mfg. Co., Danbury, Conn

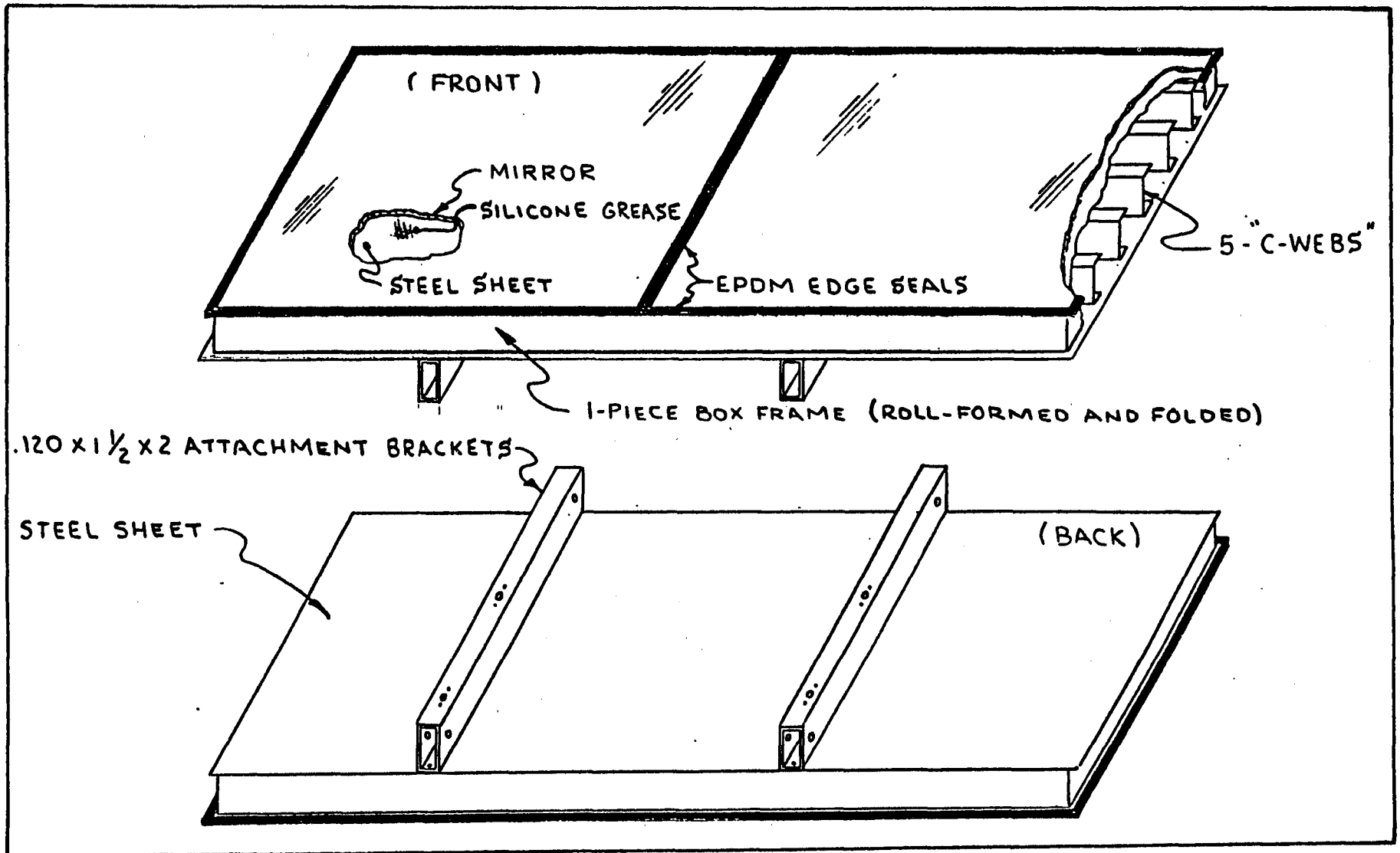
FIGURE D-3

ARCO DYLITE BEAD-BOARD MIRROR MODULE



D-11

D-12



NORTHROP MIRROR MODULE CONSTRUCTION

FIGURE D-4

TABLE D-5

4' x 12': TENSIONED PANEL ALTERNATE

MIRROR MODULE MATERIAL WEIGHT & COST

Piece Part Description	Size or Quantity Per Module	Weight, lb		Cost, \$	
		Module	Heliostat	Module	Heliostat
Face Sheet - galv. steel	1-.019 x 48x142.5"	37.10	445.2	13.96	167.53
U - Channel, horizontal	2-1/8x7/8x23/4x144.3"	38.48	461.8	12.39	148.70
U - Channel, vertical	2-1/8x7/8x23/4x48"	12.80	153.6	4.12	49.46
U - Tensioner, horizontal	2-1/8x3/4x13/16x144.3	24.05	288.6	7.74	92.92
U - Tensioner, Vertical	2-1/8x3/4x13/16x48"	8.00	96.0	2.58	30.91
U - Channel Spreaders	3-1/8x7/8x23/4x453/4"	18.30	219.6	5.89	70.71
Support bracket T-fitting	6-0.26lb each	1.55	18.56	0.50	5.98
Corner fittings	4-0.23 lb each	0.92	11.04	0.30	3.55
Cap Screws	82-3/8-16NCx11/8"	3.28	39.36	5.74	68.88
Center Seal - EPDM	(Assume same cost & weight	1.82	21.9	6.54	78.32
Edge Seal - EPDM					
Center Brace					
Contact Adhesive					
Mirror Facets	2 -44"x70"	52.67	632.0	24.38	292.60
Silicone Grease	10.7 oz	0.66	8.0	6.35	76.25
Rivets for Nut Plates	8-1/8Dx3/16 G.L.	0.02	0.2	0.05	0.58
Screws for Center Seal	24-(6-32)	0.75	9.0	0.36	4.32
Nut Plates	4-3/8"nut	0.06	0.7	3.56	42.70
TOTALS		200.46	2405.6	\$94.46	\$1133.51
MIRROR AREA				42.8	513.4ft²
MATERIAL COST PER FT²					\$2.21

TABLE D-6

4' x 12': NOR-CORE ALTERNATE
MIRROR MODULE MATERIAL WEIGHT & COST

Piece Part Description	Size or Quantity Per Module	Weight, lb		Cost, \$	
		Module	Heliostat	Module	Heliostat
Face Sheet-galv. steel	1-.019 x 48x1441/4"	37.55	450.6	\$14.13	\$169.56
Back Sheet-galv. steel	1-.019x48x1441/4"	37.55	450.6	14.13	169.56
Nor-Core Honeycomb*	1-3"x47x1431/4	57.60	691.2	23.04	276.48
Adhesive (400ft ² /gal)	2 layers-0.12gal/layer	2.0	24.0	8.40	100.80
Side Frame - "C"	2-.019x4x47"	2.04	24.5	0.77	9.21
Edge Frame - "C"	2-.019x4x143.3"	6.22	74.6	2.34	28.05
Attachment Angles	4-1/8x1x1x42"	11.20	134.4	3.61	43.32
Handling Angle	1-1/8x1x1x34"	2.27	27.2	0.73	8.77
Center Brace	1-1/8x3/4x49.5"	1.32	15.8	0.43	5.09
Center Seal - EPDM	1-48"	0.06	0.7	0.47	5.62
Edge Seal- EPDM	1-383"	0.38	4.6	5.57	66.82
Contact Adhesive	1 oz	0.06	0.8	0.07	0.79
Rivets	29-1/8Dx3/16 GL.	0.09	1.11	0.17	2.07
Screws	24-(6-32)	0.75	9.0	0.36	4.32
Nut Plates	4-3/8"nut	0.06	0.7	3.56	42.70
Mirror Facets	2-48" x 72"	59.1	709.2	27.36	328.32
Silicone Grease	12 oz	0.75	9.0	7.13	85.56
TOTAL		219.01b	26281b	\$112.27	\$1347.24
MIRROR AREA				48 ft²	576ft²
MATERIAL COST/ft²					\$2.34

* 3" thick, 1.21b/ft², \$0.48/ft²

TABLE D-7

4' x 12': POLYSTYRENE BEAD BOARD (ARCO "DYLITE") ALTERNATEMIRROR MODULE MATERIAL WEIGHT & COST

Piece Part Description	Size or Quantity Per Module	Weight, lb		Cost, \$	
		Module	Heliostat	Module	Heliostat
Face sheet-galv. steel	1-.019x48x1441/4"	37.55	450.6	\$14.13	\$169.56
Back Sheet-galv. steel	1-.019x48x1441/4"	37.55	450.6	14.13	169.56
Polystyrene Bead Board	1-3"x47x143 $\frac{1}{2}$	23.38	280.5	11.22	134.66
Adhesive (400 ft ² /gal)	2 layers-0.12 gal/layer	2.0	24.0	8.40	100.80
Side Frame - "C"	2-.019 x 4 x 47"	2.04	24.5	0.77	9.21
Edge Frame - "C"	2-.019 x 4 x 143.3"	6.22	74.6	2.34	28.05
Attachment Angles	4-1/8x1x1x42"	11.20	134.4	3.61	43.32
Handling Angle	1-1/8x1x1x34"	2.27	27.2	0.73	8.77
Center Brace	1-1/8x3/4x49.5"	1.32	15.8	0.43	5.09
Center Seal EPDM	1-48"	0.06	0.7	0.47	5.62
Edge Seal - EPDM	1-383"	0.38	4.6	5.57	66.82
Contact Adhesive	1 oz	0.06	0.8	0.07	0.79
Rivets	29-1/8D x 3/16 G.L	0.09	1.1	0.17	2.07
Screws	24 -(6-32)	0.75	9.0	0.36	4.32
Nut Plates	4- 3/8"Nut	0.06	0.7	3.56	42.70
Mirror Facets	2-48"x72"	59.1	709.2	27.36	328.32
Silicone Grease	12 oz	0.75	9.0	7.13	85.56
TOTALS		184.78	2217.3	\$100.45	\$1205.40
MIRROR AREA				48ft²	576ft²
MATERIAL COST PER FT²					\$2.09

TABLE D-8

4' X 12' INTERMITTANT STRINGER ALTERNATE
MIRROR MODULE MATERIAL WEIGHT & COST

Piece Part Description	Size or Quantity Per Module	Weight, lb		Cost, \$	
		Module	Heliostat	Module	Heliostat
Face Sheet - galv. steel	1 - .019 x 48 x 144.25"	37.55	450.6	14.13	169.56
Back Sheet - galv. steel	1 - .019 x 48 x 144.25"	37.55	450.6	14.13	169.56
Horizontal Webs-galv. steel	5 - .019 x 4 x 143.25"	15.54	186.5	5.85	70.16
Structural Adhesive	6 oz	0.38	4.5	1.04	12.45
Torque Box Frame	1 - .019 x 4 x 384"	8.33	100.0	3.13	37.62
Attachment Angles	2 - 1/8 x 1 x 1x 47"	6.27	75.2	2.02	24.21
Mirror Facets	2 - 48" x 72"	59.1	709.2	27.36	328.32
Silicone Grease	12 oz	0.75	9.0	7.13	85.56
Center Brace	1 - 1/8 x 3/4 x 49.5 "	1.32	15.8	0.43	5.09
Center Seal - EPDM	1 - 48"	0.06	0.7	0.47	5.62
Edge Seal - EPDM	1-383"	0.38	4.6	5.57	66.82
Contact Adhesive	1 oz.	0.06	0.8	0.07	0.79
Rivets	8 - 1/8 D x 3/16 G. L.	0.03	0.3	0.05	0.58
Screws	2 - (6-32)	0.06	0.8	0.03	0.36
Nut Plates	4 - 3/8"	0.06	0.8	3.56	42.70
TOTAL		167.44	2009.4	\$84.97	\$1019.40
MIRROR AREA				48 ft ²	576 ft ²
MATERIAL COST PER FT. ²					\$ 1.77

TABLE D-9

"BETWEEN-THE-SHEETS" COMPARISON

D-17

<u>"C - WEB" BASELINE</u>			<u>TENSIONED PANEL</u>	
<u>Piece Part</u>	<u>Current</u>	<u>Simplified</u>	<u>Piece Part</u>	<u>Cost</u>
Vertical Webs....	\$7.29	\$3.13	U-Channels.....	\$16.51
Horizontal Webs..	2.34	5.85	U-Tensioners.....	10.32
Adhesive.....	1.56	1.04	U-Spreader	5.89
Corner Braces....	0.03	0	Brackets.....	0.80
Rivets.....	0.41	0.05	Screws.....	5.74
<u>TOTAL COST.....</u>	<u>\$11.63</u>	<u>\$10.07</u>	Back Sheet.....	-13.96
Mirror Area.....	48ft ²	48ft ²	<u>Attachment Angles.....</u>	<u>-4.34</u>
Cost/ft ²	24.2¢	<u>21.0¢</u> ←	<u>TOTAL COST.....</u>	<u>\$20.96</u>
			Mirror Area	42.8ft ²
			Cost/ft ²	<u>49.0¢</u> ←
<u>NOR-CORE PANEL</u>			<u>BEAD BOARD PANEL</u>	
<u>Piece Part</u>	<u>Cost</u>		<u>Piece Part</u>	<u>Cost</u>
Nor-Core Honeycomb.....	\$23.04		Bead Board	\$11.22
Adhesive.....	8.40		Adhesive.....	8.40
Side Frame.....	3.11		Side Frame	3.11
Rivets.....	0.17		Rivets.....	0.17
<u>TOTAL COST</u>	<u>\$34.72</u>		<u>TOTAL COST.....</u>	<u>\$22.90</u>
Mirror Area.....	48ft ²		Mirror Area.....	48ft ²
Cost/ft ²	<u>72.3¢</u> ←		Cost/ft ²	<u>47.7¢</u> ←

9.4.2. Rack Structure Alternates

Figure D-5 illustrates the original rack structure design for the Northrup II heliostat. This structure was based on the use of 6 tapered trusses, each of which was 8.5 m (28 ft) long, and weighed 80 kg (175 lb). The construction of these truss members was based on using steel angles and solid rod webbing. The chord angles were 38 x 38 x 3 mm (1.5 x 1.5 x 0.125 inch), and the rod webs were 12.7mm (0.5 inch). The truss members tapered from 0.2 m (0.67 ft) at the ends to 0.5 m (1.67 ft) at the center. The top and bottom chords were constructed from 2 angles each with the zig-zag webbing sandwiched and welded in-between. The bend-resisting inertia for this configuration varied from 783 cm⁴ (18.8 in⁴) at the shallow end to 5514 cm⁴ (132.5 in⁴) in the middle. The total weight for the 6 trusses was 477 kg (1050 lb). By way of direct comparison, the current truss configuration provides a bend-resisting inertia of 10364 cm⁴ (249 in⁴), and has the total weight for the 4 trusses of 208 kg (456 lb).

The path which led to the current Butler Manufacturing Co. truss selection, and the 4-truss configuration was governed by the following considerations:

1. The drive unit is relatively large in terms of azimuth-swing radius. To avoid an off-set torque tube-to-drive unit interface, it was considered a desirable feature to be able to contain the drive within the truss-depth envelope. This factor dictated a deep truss.

2. If the web "zig-zag" angles are maintained at a constant angle (usually 60°) as the truss depth is increased, the truss weight remains unchanged; i.e., a deep truss will weigh the same as a shallow truss. Since the beam stiffness increases with the square of the truss depth, the deeper truss is considerably less expensive per unit of stiffness.

3. As the truss depth is increased, the web rod length increases, and the tendency for column buckling increases. However, a change from a 0.5 inch diameter solid rod to a 1.0 inch

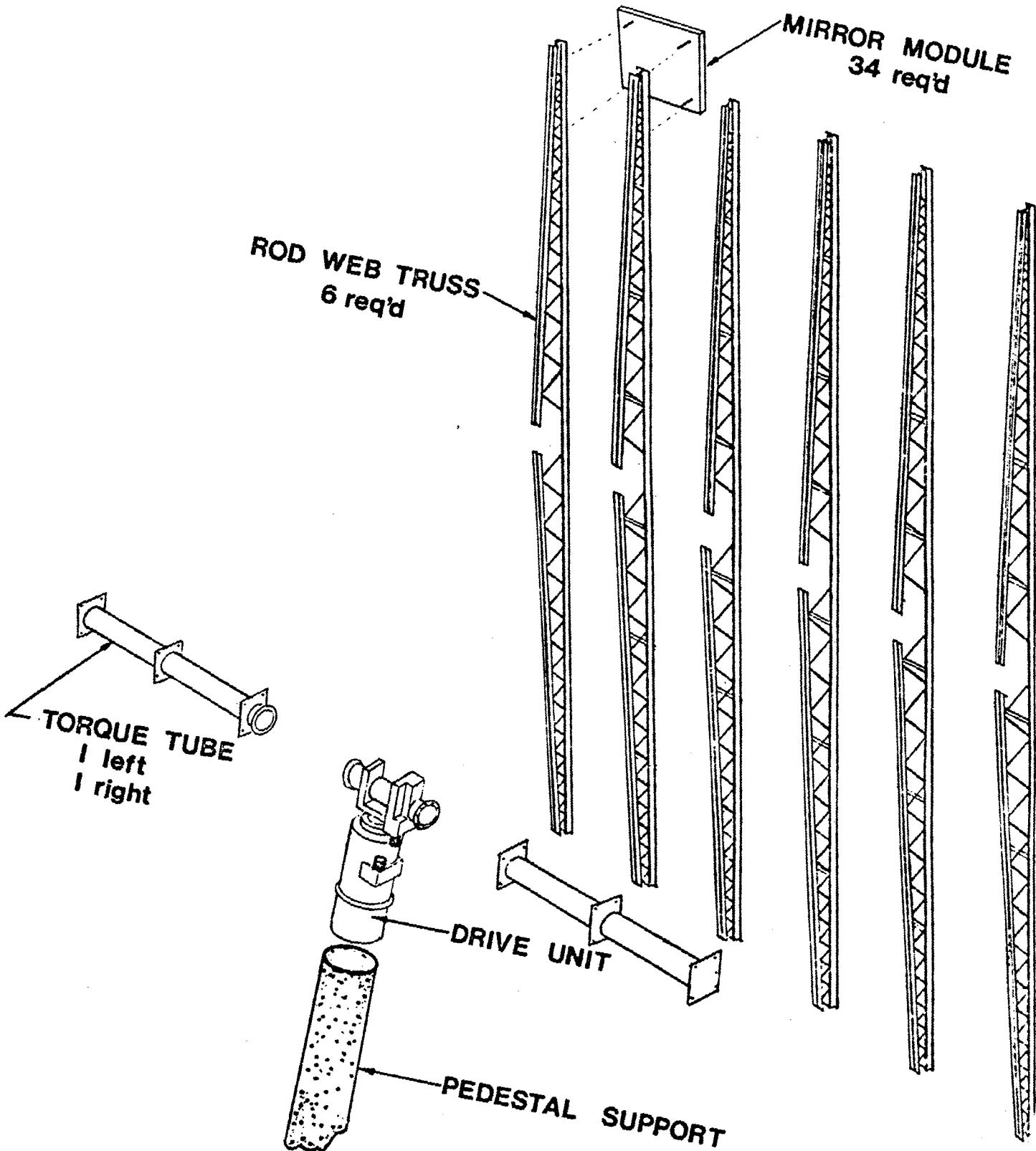


FIGURE D-5
ORIGINAL NORTHRUP
RACK STRUCTURE DESIGN

diameter hollow tube of the same weight increases the buckling resistance by a factor of 7.

4. As the truss depth is increased, the compression chord of the truss tends to buckle horizontally sideways. This phenomenon dictates the addition of cross-bracing between trusses. However, the Butler truss chord provides about 2.5 times the transverse inertia of the dual-angle chord originally planned with the expenditure of less material, so fewer cross-braces are required.

5. The change in mirror module size from 1.22 x 1.22 m (4.0 x 4.0 ft) to 1.22 x 3.66 m (4.0 x 12.0 ft) reduced the required number of mirror modules from 34 to 12, and enabled the number of truss members to be reduced from 6 to 4. The net effect of this change was a significant reduction in rack structure weight and material cost, and an even greater reduction in field labor cost due to the reduction in major piece parts from 40 to 16.

Each torque tube provides the lateral structural support by rigidly connecting a pair of trusses together and to the drive unit. A study was performed early in the program to establish the weight and inertia versus diameter and wall thickness. Table D-10 tabulates the results of this study. The "WINDBEND" computer model was utilized to evaluate the resultant bending and torsional errors as a function of the bending and polar inertia. Within the confines of the error budget and the software and alignment error-removal ability, it was established that the polar inertia should be on the order of 400 in⁴, and the bending inertia about 200 in⁴. Table D-10 shows these would most efficiently be met with a 16-inch O.D. torque tube having a wall thickness of 0.135 inches. This size was originally selected for the torque tube, and no interface problem existed with the drive unit because the drive unit had a 43-inch diameter single stage worm gear, and could, if necessary, accommodate a very large torque tube.

Subsequent optimization studies reduced the drive unit size by the introduction of the planetary input stage. The output worm gear size was reduced to a size less than one half of the original diameter. As a result of the smaller size, the torque tube diameter had

TABLE D-10
 TORQUE TUBE INERTIA AND WEIGHT

<u>Torque Tube Diameter</u>	<u>Polar Moment of Inertia, in⁴</u>				
	<u>.075" Wall</u>	<u>.105" Wall</u>	<u>.135" Wall</u>	<u>.188" Wall</u>	<u>.250" Wall</u>
12 inch	99.9	138.8	177.1	242.8	318.7
14	159.1	221.2	282.6	388.1	510.6
16	237.9	331.2	423.4	582.3	767.3
	<u>Weight for 110 inch Length, lb</u>				
12	87.5	122.1	156.7	216.6	287.3
14	102.1	142.7	183.1	253.3	336.2
16	116.8	163.2	209.5	290.0	385.1
	<u>Inertia Per Unit Weight, in⁴/lb</u>				
12	1.14	1.14	1.13	1.12	1.11
14	1.58	1.55	1.54	1.53	1.52
16	2.04	2.03	2.02	2.01	1.99

Note: The bending inertia is one-half of the polar inertia.

to be reduced to enable its flange to interface cleanly with the drive unit. Hence, a 12.75 inch diameter torque tube with a wall thickness 0.25 inch was selected. The following provides a comparison between the optimum and selected torque tubes:

	16" OD Optimum Torque Tube	12.75" OD Selected Torque Tube
1. Wall Thickness, inch	0.135	0.250
2. Polar Inertia, in ⁴	423.4	383.6
3. Bending Inertia, in ⁴	211.7	191.8
4. Total Weight (2), lb	419.0	611.2
5. Material Cost, \$	144.56	210.86

The \$66 cost differential was justified by the estimated \$115 cost of increasing the drive unit housing, bearing and seal size to accomodate the optimum torque tube.

9.4.3 Drive Unit Alternates

The drive unit originally proposed was based on a double worm and gear for each axis, a concept which was employed on the Northrup I heliostat. An 80:1 ratio was planned for each first stage, and a 52:1 ratio for each output stage. A large stepper motor and sophisticated translator (Superior Electric Co. M172-FD306 motor and TM-600 translator) was required to drive this gear combination to an ample output torque level. Since the motor and translator cost was high, an effort was undertaken to change the gearing to permit a smaller stepper motor to be used.

A drive concept was next examined in which the same two worm gear ratios were maintained, but a small 3:1 gear stage was added at the motor. This reduced the motor size to a Superior Electric Co. M112-FJ326 unit (which is \$125 less than the M172-FD306). A gear box survey was performed, and an 11.5:1 ratio unit was selected which further reduced the motor size to an M093-FD301 unit (which is \$225 less

than the original M172-FD306 motor). Since the gear box cost was under \$100, it became very evident that it was far more economical to "buy" torque with gearing than with motor size. Table D-11 provides the evaluation results for 54 different stage 1 and stage 2 gear combinations with output torque (T), output gear shear tooth stress (S), and approximate drive element cost (C) as the performance parameters. Nine of the gear combinations were then selected, and a complete drive unit material and piece part relative-cost analysis was performed.

Figure D-6 presents the double worm and gear concept with the added gear box at the motor. The tabular data on this figure shows the nine candidate gear combinations examined in detail and the resultant backlash, torque (T), output gear tooth shear stress(S), weight(W), and the relative drive unit material costs (C). The main conclusion to be drawn from this data is that over a relatively wide range of gear sizes, the costs are relatively high and no clear-cut optimum is apparent. A concept change was required to lower the cost.

An effort was initiated to simplify the drive unit and lower its cost by eliminating the first worm gear stage by employing a larger ratio gear box at the motor. A low cost, triple reduction helical gear box manufactured by Bison Gear & Engineering Corp., was selected for the input stage. It provided a 115:1 gear ratio, an output torque capacity of 2500 lb-in, and a higher efficiency than a comparable worm gear stage. The size of the output gear and its ratio increased significantly, but the overall material and piece part were reduced by about 15%. Figure D-7 presents the performance characteristics and a schematic representation of this initial single-worm-per-axis drive unit. Figure D-8 shows a perspective rendering of this drive concept which highlights the use of the azimuth gear as a turntable for the elevation drive, the sector elevation gear, and the use of a cam-follower bearings for support.

A subsequent modification to this one-worm per axis drive unit resulted in a change to the next larger motor size

TABLE D-11

WORM GEAR EVALUATION

WITH MO92-FD310 MOTOR & 11.5:1 REDUCER

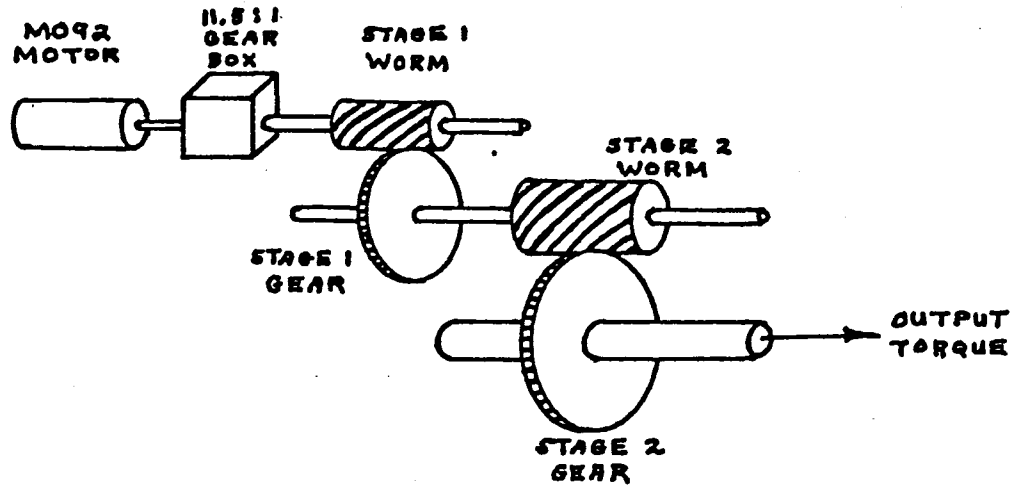
STAGE 1 AND STAGE 2 COMBINATIONS

STAGE 2 WORM-GEAR DIAMETRAL PITCH = 1.5			STAGE 2 WORM-GEAR DIAMETRAL PITCH = 2.0		
16" PD, 24:1	18" PD, 27:1	20" PD, 30:1	20" PD, 40:1	24" PD, 48:1	27" PD, 54:1
8 DP 168:1 T = 16019 S = 9220 C = \$378	8 DP 144:1 T = 12351 S = 9478 C = \$380	8 DP 144:1 T = 13723 S = 8503 C = \$390	8 DP 144:1 T = 15371 S = 7636 C = \$382	8 DP 96:1 T = 12366 S = 9554 C = \$385	8 DP 120:1 T = 17332 S = 6798 C = \$409
8 DP 144:1 T = 10979 S = 10745 C = \$370	8 DP 120:1 T = 10314 S = 11374 C = \$371	8 DP 120:1 T = 11459 S = 10204 C = \$381	8 DP 120:1 T = 12838 S = 9190 C = \$373	8 DP 80:1 T = 10339 S = 11465 C = \$379	8 DP 96:1 T = 13912 S = 8498 C = \$400
8 DP 120:1 T = 9168 S = 12895 C = \$361	8 DP 96:1 T = 8276 S = 14217 C = \$362	8 DP 96:1 T = 9196 S = 12755 C = \$372	8 DP 96:1 T = 10305 S = 11374 C = \$364	8 DP 64:1 T = 8313 S = 14331 C = \$373	8 DP 80:1 T = 11632 S = 10197 C = \$394
6 DP 144:1 T = 11592 S = 4533 C = \$414	6 DP 144:1 T = 13041 S = 3998 C = \$424	6 DP 120:1 T = 12100 S = 4304 C = \$419	6 DP 120:1 T = 13555 S = 3860 C = \$411	6 DP 84:1 T = 11452 S = 4606 C = \$409	6 DP 84:1 T = 12884 S = 4089 C = \$424
6 DP 120:1 T = 9680 S = 5440 C = \$399	6 DP 120:1 T = 10890 S = 4798 C = \$409	6 DP 96:1 T = 9709 S = 5381 C = \$404	6 DP 96:1 T = 10881 S = 4825 C = \$396	6 DP 72:1 T = 9848 S = 5374 C = \$401	6 DP 72:1 T = 11079 S = 4771 C = \$416
6 DP 96:1 T = 7767 S = 6800 C = \$384	6 DP 96:1 T = 8738 S = 5998 C = \$394	6 DP 72:1 T = 7319 S = 7174 C = \$388	6 DP 84:1 T = 9543 S = 5444 C = \$388	6 DP 60:1 T = 8243 S = 6449 C = \$393	6 DP 60:1 T = 9274 S = 5725 C = \$409
5 DP 130:1 T = 11033 S = 2505 C = \$521	5 DP 120:1 T = 11468 S = 2423 C = \$516	5 DP 120:1 T = 12742 S = 2174 C = \$526	5 DP 100:1 T = 11928 S = 2326 C = \$488	5 DP 100:1 T = 14313 S = 1941 C = \$509	5 DP 70:1 T = 11350 S = 2478 C = \$480
5 DP 120:1 T = 10194 S = 2714 C = \$506	5 DP 110:1 T = 10524 S = 2643 C = \$501	5 DP 100:1 T = 10644 S = 2609 C = \$496	5 DP 80:1 T = 9580 S = 2895 C = \$459	5 DP 80:1 T = 11497 S = 2426 C = \$479	5 DP 60:1 T = 9767 S = 2891 C = \$465
5 DP 110:1 T = 9355 S = 2961 C = \$491	5 DP 100:1 T = 9580 S = 2908 C = \$486	5 DP 80:1 T = 8547 S = 3261 C = \$467	5 DP 60:1 T = 7234 S = 3850 C = \$429	5 DP 60:1 T = 8681 S = 3235 C = \$449	5 DP 50:1 T = 8183 S = 3469 C = \$450

T = TORQUE, TOTAL TRAIN OUTPUT, FT-LB (9500 ft-lb req'd)
 S = GEAR TOOTH SHEAR STRESS, PSI (8000 psi max. for gray cast iron)
 C = COST, TOTAL MOTOR + REDUCER BOX + 2 WORM-GEAR STAGES, \$

FIGURE D-6

PERFORMANCE FOR 2 - STAGE WORM DRIVE CONCEPT

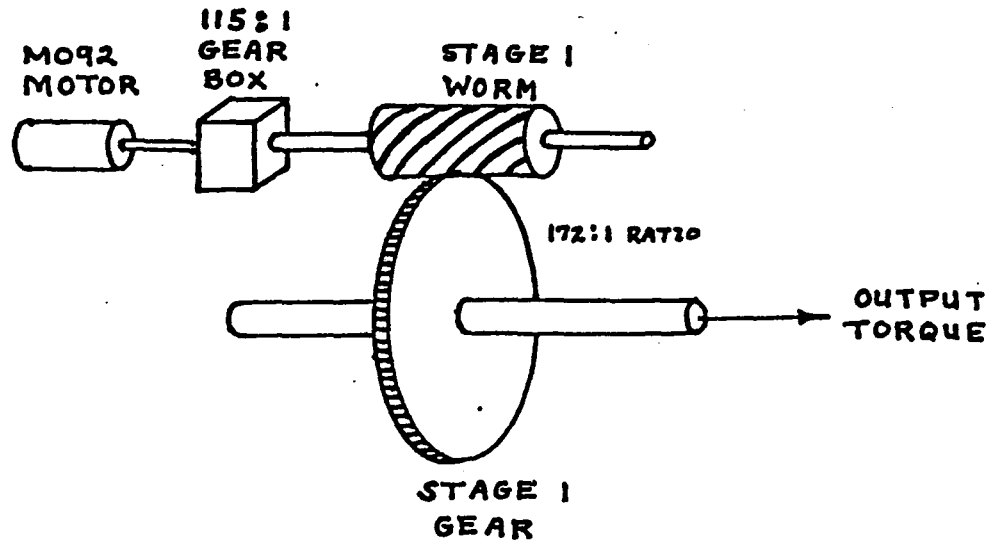


DRIVE UNIT PERFORMANCE

STAGE 2 WORM & GEAR	STAGE 1 WORM & GEAR		
D.P. = 1.5 GEAR P.D. = 16" WORM P.D. = 4" RATIO = 24:1 BACKLASH 0.63mrad	8 D.P. 144:1 GEAR P.D. = 18" T = 10979 ft-lb S = 10745 psi W = 1681 lb C = \$ 1528	6 D.P. 120:1 GEAR P.D. = 20" T = 9680 ft-lb S = 5440 psi W = 1693 lb C = \$ 1561	5 D.P. 120:1 GEAR P.D. = 22" T = 9355 ft-lb S = 2961 psi W = 1717 lb C = \$ 1660
D.P. = 2 GEAR P.D. = 20" WORM P.D. = 4" RATIO = 40:1 BACKLASH 0.50mrad	8 D.P. 96:1 GEAR P.D. = 12" T = 10305 ft-lb S = 11374 psi W = 1699 lb C = \$ 1533	6 D.P. 96:1 GEAR P.D. = 16" T = 10881 ft-lb S = 4825 psi W = 1719 lb C = \$ 1566	5 D.P. 100:1 GEAR P.D. = 20" T = 11928 ft-lb S = 2326 psi W = 1731 lb C = \$ 1665
D.P. = 2 GEAR P.D. = 27" WORM P.D. = 4" RATIO = 54:1 BACKLASH 0.37mrad	8 D.P. 80:1 GEAR P.D. = 10" T = 11632 ft-lb S = 10197 psi W = 1755 lb C = \$ 1575	6 D.P. 72:1 GEAR P.D. = 12" T = 11079 ft-lb S = 4771 psi W = 1769 lb C = \$ 1601	5 D.P. 70:1 GEAR P.D. = 14" T = 11350 ft-lb S = 2478 psi W = 1772 # C = \$ 1670

FIGURE D-7

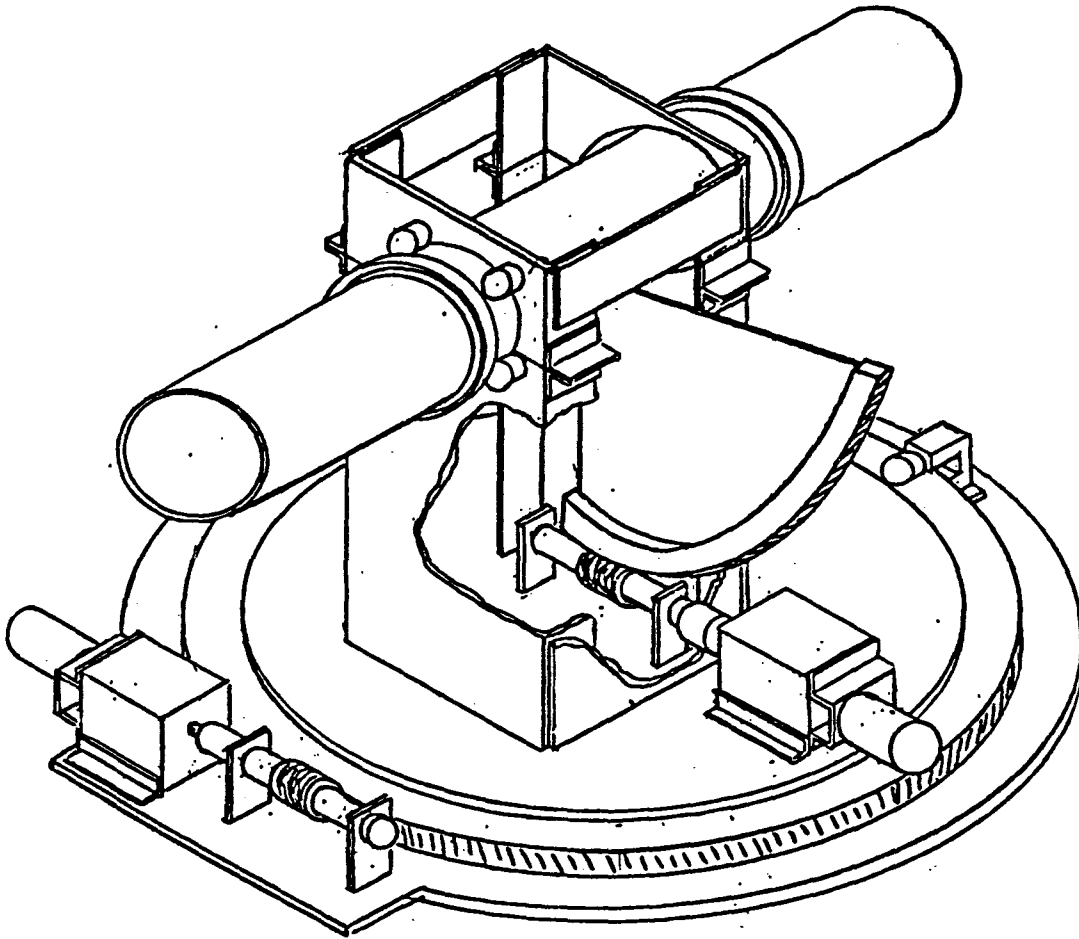
INITIAL CONFIGURATION OF A SINGLE-WORM STAGE DRIVE



CHARACTERISTICS

	<u>WORM</u>	<u>GEAR</u>
DIAMETRAL PITCH	4	4
PITCH DIAMETER	3.00"	43.00"
NO. OF THREADS/TEETH	1	172
THREAD/TOOTH STRESS	34009 psi	10769 psi
MATERIAL	STEEL	CAST IRON
WEIGHT, AZIM	6 lb	102 lb
WEIGHT, ELEV	6 lb	34 lb
FACE WIDTH	3.50"	1.50"
MAXIMUM TORQUE	-	9640 ft-lb
BACKLASH EFFECT	-	0.23 mrad

FIGURE D-8
PERSPECTIVE VIEW OF THE INITIAL
NORTHROP 1 - WORM DRIVE UNIT



(from the Superior Electric Co. MD92-FD310 to the M112-FJ326), but to a simpler, less expensive driver (translator). In addition, the azimuth gear was fixed (i.e., non-revolving). This latter change enabled the protruding azimuth and elevation motors to always maintain the same position relative to the mirrored surface plane during azimuth maneuvers (which eliminated a potential interference problem between the drive and mirror modules). An additional change was an optimization of the output worm gear in which the diametral pitch was raised from 4 to 5, and the pitch diameter reduced from 43 inches to 26.4 inches. Table D-12 presents the performance characteristics for the improved one-worm drive with the 115:1 helical gear box. Figure D-9 shows an exploded view of this drive unit.

The Winsmith Division of UMC Industries was working closely with Northrup as a potential fabricator, cost-estimator, and alternate-design consultant. Winsmith proposed a concept employing a large ratio, high torque capability planetary unit which replaces the triple reduction helical gear box. The higher ratio of the planetary stage (450.45:1) enabled the output worm gear size to be further reduced in ratio and size. The decreased gear size in turn enabled the use of ball-and-race bearings which became cost-competitive with the 19 individual cam-follower bearings used in the previous design. Only one bearing is used in each axis with this alternate Winsmith design. Table D-13 presents a comparison between the helical gear box reducer configuration (North-Win 1), and the alternate planetary input stage (North-Win 2). Table D-14 presents the worm thread bending stress and the gear tooth shear stress as a function of wind speed for the two design alternates. This tabulation shows very similar stress levels for the two alternates, but more importantly, shows that both design options can withstand a 90 mph wind in the vertical position. Hence, no latch or docking restraint is required to remove wind loads from the gearing during operation or stow.

Table D-15 presents a comparison of the mechanical performance of the two design alternates in terms of output torque, efficiency, and slew rate. Although the torque characteristics are

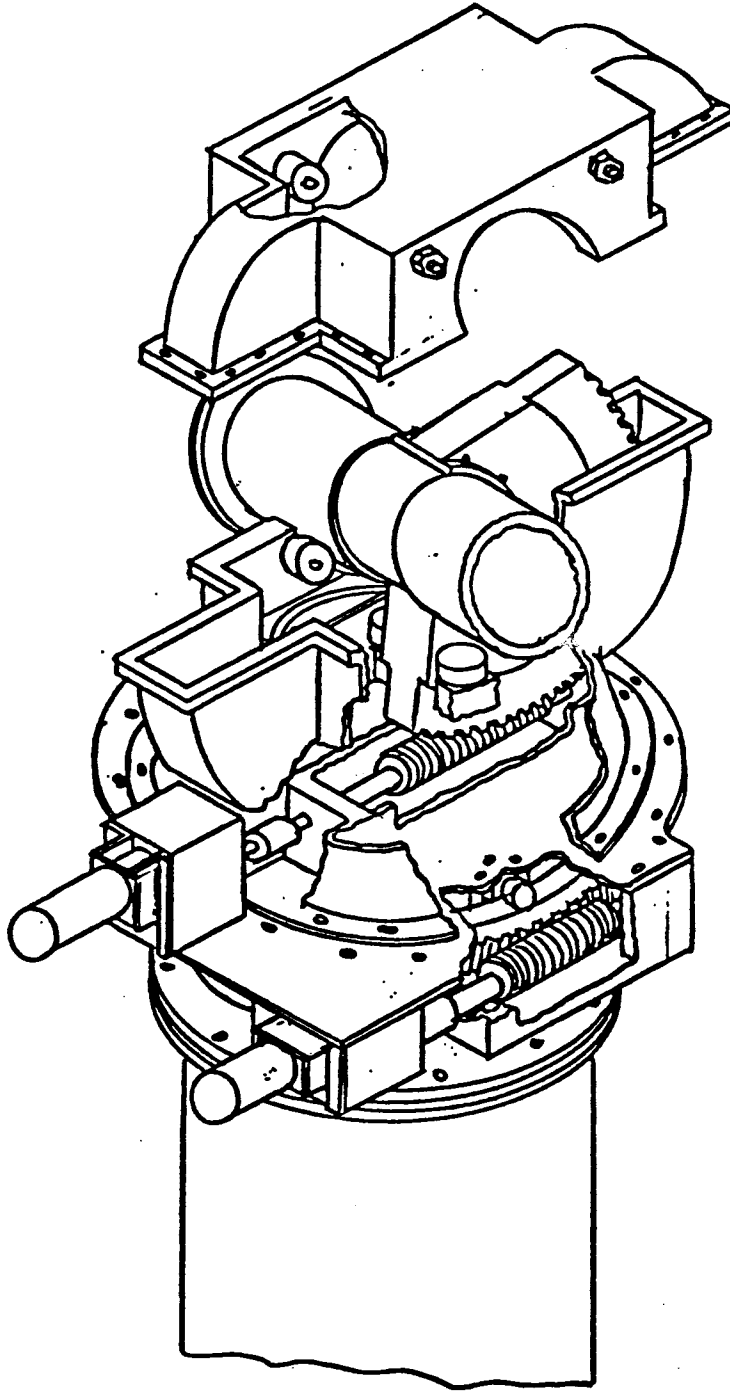


FIGURE D-9
NORTHROP FIXED-AZIMUTH DRIVE
EXPLODED VIEW

TABLE D-12

Improved One-Worm Drive Characteristics

1. M112-FJ326 stepper motor/TBM105 translator
2. Bison Model 030-415-0115 gear box, 115:1 ratio
3. Worm and gear diametral pitch = 5
4. Lead = 0.6283 inches, lead angle = 4.3986°
5. Worm pitch diameter = 2.60 inches
6. Gear pitch diameter = 26 inches
7. Gear face width = 1.5 inches
8. Number of teeth in contact = 2 (minimum)
9. Worm thread bending stress = 126,811 psi (steel) *
10. Gear tooth shear stress = 40,156 psi (cast iron) *
11. Torque output capability:

<u>Pulse Rate</u>	<u>Motor rpm</u>	<u>Output Torque</u>	<u>Drive Efficiency</u>
200/sec	60	6602 ft-lb	20.77%
600	180	9797	21.17
1000	300	10287	21.58
1400	420	8913	22.01
1800	540	7009	22.45
2000	600	6218	22.68

* Stresses are for vertical stow, 90 mph wind

TABLE D-13

COMPARISON "NORTH-WIN 1" VS "NORTH-WIN 2"

	NORTH-WIN 1	NORTH-WIN 2
A. MOTOR	M112	M112
B. STAGE 1 1. TYPE 2. RATIO 3. EFFICIENCY	PLANETARY 450.45: 1 55%	HELICAL 115: 1 80%
C. STAGE 2 1. TYPE 2. RATIO 3. GEAR DIAMETER 4. GEAR FACE WIDTH 5. DIAMETRAL PITCH 6. NUMBER OF TEETH 7. LEAD ANGLE 8. WORM PITCH DIAMETER 9. WORM THREAD 10. EFFICIENCY	WORM & GEAR 40.1 17.7" 2.36 " 2.37 40 7.7° 3.12" SINGLE 38%	WORM & GEAR 130:1 26.4 1.50" 5 130 4.4° 2.30" SINGLE 27%
OVERALL RATIO	18018	14950
D. BEARINGS, ELEVATION AZIMUTH	SINGLE BALL & RACE SINGLE BALL & RACE	10-CAMROLLS 9-CAMROLLS
E. ENCLOSURE, MATERIAL LUBRICATION CAVITY SEAL	CAST IRON SHELL OIL FILLED SEALED	CAST IRON SHELL OIL BATH VENTED

TABLE D-14
WORM & GEAR STRESSES

WINDSPEED MPH	TYPE	"NORTH-WIN 1" (PLANETARY + WORM)	"NORTH-WIN 2" (HELICAL + WORM)
10	WTB	1,650 psi	1,566 psi
27	WTB	12,039	11,413
50	WTB	41,326	39,177
90	WTB	133,769	126,811
10	GTS	523 psi	496 psi
27	GTS	3,812	3,614
50	GTS	13,086	12,406
90	GTS	42,359	40,156

WTB = worm thread bending stress, allowable (yield) = 190,000 psi
 GTS = gear tooth shear stress, allowable (yield) = 80,000 psi

CONCLUSION: Worm thread and gear teeth can withstand 90 mph wind in vertical stow position without yielding.

TABLE D-15

DRIVE COMPARISON: "NORTH-WIN 1" VS NORTH-WIN 2"

MOTOR STEPPING RATE STEPS/SEC	MOTOR INPUT TORQUE OZ-IN	OUTPUT TORQUE FT-LB		EFFICIENCY PERCENT		SLEW RATE DEG/MIN	
		#1-WORM/ PLANETARY	#2-WORM/ HELICAL	#1-WORM/ PLANETARY	#2-WORM/ HELICAL	#1-WORM/ PLANETARY	#2-WORM/ HELICAL
200	408	7914	6602	20.66	20.77	1.198	1.444
400	549	10677	8967	20.72	20.97	2.397	2.889
600	594	11588	9797	20.78	21.17	3.596	4.334
800	621	12140	10334	20.83	21.37	4.795	5.779
1000	612	12001	10287	20.89	21.58	5.994	7.224
1200	574	11295	<u>9749</u>	20.95	21.79	7.192	<u>8.668</u>
1400	520	<u>10253</u>	8913	21.01	22.01	<u>8.391</u>	10.113
1600	459	9079	7950	21.06	22.23	9.590	11.558
1800	401	7947	7009	21.12	22.45	10.789	13.003
2000	352	7000	6218	21.18	22.68	11.988	14.448
REQM'T in 50 MPH WIND		9500 ft-lb		-		6°/min	

somewhat different, both are acceptable. Likewise, both have comparable slew rates when driven at a stepping rate necessary to meet a 9500 ft-lb wind torque, and both have a very similar efficiency characteristic.

Tables D-16 and D-17 present the estimated weight and cost for the two competitive designs. Again there was very little difference between the two design concepts. In fact, in evaluating all of the stress values, the mechanical performance, weight, and cost, the trade-off study between the helical gear box/large worm gear/Camroll bearing concept and the planetary gear stage/small worm gear/ball-and-race configuration resulted in a virtual tie.

The "North-Win 2" planetary drive concept was selected based on several decisive features:

1. Possibility for future cost savings using the integral bearing concept, in which the races are machined into the castings.
2. Unit is oil-filled and sealed versus oil-bathed and vented for the alternate. The moisture condensation concern is eliminated, and the bearings are subjected to continuous lubrication.
3. The planetary gear box offers flexibility in future motor-gear ratio trade-offs. The planetary gear ratio can be varied over a very large range without changing the size of the enclosure envelope or interface. Future advances in the motor drive translator and software might enable the use of a smaller (but higher pulse rate) motor which might in turn necessitate a higher planetary gear ratio.
4. The selected drive unit is simpler and has significantly fewer parts, fewer machining operations, and fewer assembly adjustments than the alternate using discrete Camroll bearings. It is believed that the simpler unit will, therefore, be the most reliable.

TABLE D-16

DRIVE WEIGHT COMPARISON

ITEM	NORTH-WIN 1 (PLANETARY)	NORTH-WIN 2 (HELICAL)
AZIMUTH GEAR	176.6 lb	190.1 lb
ELEVATION GEAR	168.5	69.2
TORQUE ARMS	0	216.6
STAGE 1 GEAR BOX	126.0	32.0
AZIMUTH HOUSING	264.6	237.0
ELEVATION HOUSING	240.5	270.8
WORMS, SHAFTS, BEARINGS	90.2	38.4
MAIN BEARINGS	15.6	64.5
M112 MOTORS	29.0	29.0
MISCELLANEOUS	119.6	90.6
TOTAL	1230.6 lb	1238.2 lb

TABLE D-17

DRIVE COST COMPARISON-ENGINEERING ESTIMATE

<u>ITEM</u>	<u>NORTH-WIN 1 (PLANETARY)</u>	<u>NORTH-WIN 2 (HELICAL)</u>
AZIMUTH GEAR	\$150.11	\$161.59
ELEVATION GEAR	143.23	58.82
TORQUE ARMS	0.00	74.08
STAGE 1 GEARING	230.00	168.00
AZIMUTH HOUSING	158.76	142.20
ELEVATION HOUSING	144.30	162.48
WORMS, SHAFTS, BEARINGS	180.40	76.80
MAIN BEARINGS	400.00	328.04
MISCELLANEOUS	89.71	67.95
<u>SUB-TOTAL</u>	<u>1496.51</u>	<u>1229.96</u>
LABOR	224.48	606.41
M112 MOTORS	350.00	350.00
<u>TOTAL</u>	<u>\$2070.99</u>	<u>\$2186.37</u>

9.4.4 Electronics Alternates

Trade studies were performed on elimination of the 6850 ACIA (asynchronous communications interface adapter). The alternative would be to perform the serial communications with the 6532 (ram-i/o-timer) since this part is already needed to interface with the translator and provide RAM. The problem encountered in the trade study showed extreme timing complications in using the 6532. The 6850 ACIA provides double buffering of input and output data, this allows the processor to be accomplishing other tasks while receiving and sending data. The constraint of accelerating and decelerating the motor and being able to receive and send data at the same time prohibits software data handling of individual bits. The ACIA allows handing of data at the byte level. Additional studies are being considered to constrain the data communications to times where the motors are stopped but at this point it was desirable to have data at all times.

Three types of motor translators were considered and evaluated. They are the resistor, soft switching, and hard switching types. The evaluation results are summarized in figure D-10. The soft switching type (TBM 105) was selected because it met the speed-torque requirements and was less complex than the TC600. The resistor type was not considered due to its inability to perform at our required speed and torque. Evaluation of the TBM 105 translator showed moderate expense and complexity and was selected for the prototype Heliostat. Studies are under way to improve the design and simplify the translator to provide a more cost effective design readily adaptable for mass production.

TRANSLATOR EVALUATION

DC-RESISTOR STM101

SOFT SWITCHING TBM105

HARD SWITCHING TC600

TRANSLATOR TYPE	<u>ADVANTAGES</u>	<u>DISADVANTAGES</u>
DC-RESISTOR	SIMPLE/LEAST COMPLEX EASY COMPUTER CONTROL MULTIPLEXING POSSIBLE LOW POWER MODE	HIGH POWER CONSUMPTION WHEN ON LOW TORQUE/SPEED
SOFT SWITCHING	GOOD SPEED/TORQUE PERFORMANCE LOW MOTOR HEATING NO EXTERNAL POWER SUPPLIES SELF CONTAINED	MORE COMPLEX PULSE FEEDBACK NEEDED HEAVY PARTS REQUIRED UNIT TUNED FOR PARTICULAR MOTOR
HARD SWITCHING	BEST SPEED/TORQUE PERFORMANCE COMPUTER CONTROLS EASY LOW POWER MODE POSSIBLE	MOTOR HEATING SWITCHING TRANSIENTS NOISE GENERATION COMPLEX FEEDBACK MOST COMPLEX CIRCUITRY EXTERNAL POWER SUPPLIES REQUIRED

Figure D-10

Summary of Translator Trade - Offs

9.5 SYSTEM STUDIES (APPENDIX E)

In this section the system studies which were performed in support of the Northrup heliostat are presented. The following subsections and topics are included:

- 9.5.1 Wind Loads, Distribution, and Moments
- 9.5.2 Wind and Gravity Deflections
 - 9.5.2.1 Mirror Module
 - 9.5.2.2 Rack Structure
 - 9.5.2.3 Drive Unit
- 9.5.3 Thermal Curvature and Stress
 - 9.5.3.1 Beam Quality, Convex and Concave Mirrors
 - 9.5.3.2 Thermal Curvature for Tri-Composites
- 9.5.4 Stress Analysis - 90 mph Wind
 - 9.5.4.1 Mirror Module
 - 9.5.4.2 Rack Structure
 - 9.5.4.3 Drive Unit
- 9.5.5 Drive Unit Performance

The general format of each subsection is to include a topical introduction, and then to provide the original analysis with appropriate equations, assumptions, values, and computations.

9.5.1 WIND LOADS, DISTRIBUTION, AND MOMENTS

The following tabulations and figures provide the wind forces on the Northrup heliostat, the distribution of the normal forces on the surface, and the moments about each axis, and about the pedestal base at ground level. The basis for this analysis is ASCE Paper No. 3269, "Wind Forces on Structures", 1961.

Northrup Inc

Wind Force Parameter Summary

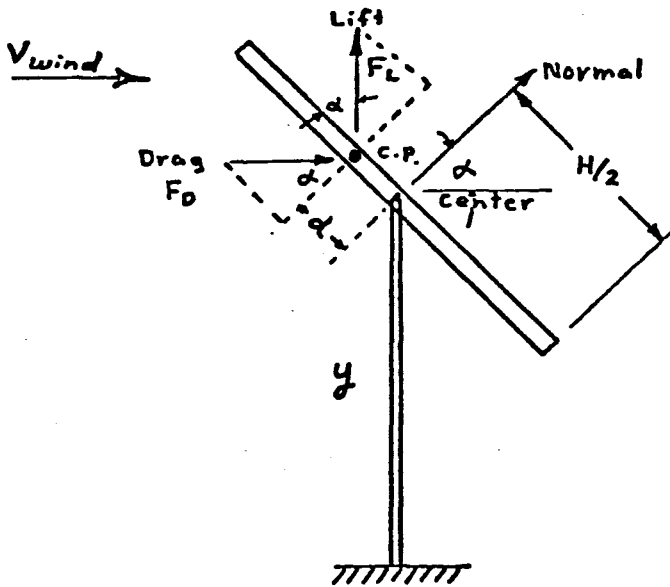


Figure 1

Backside Wind Diagram

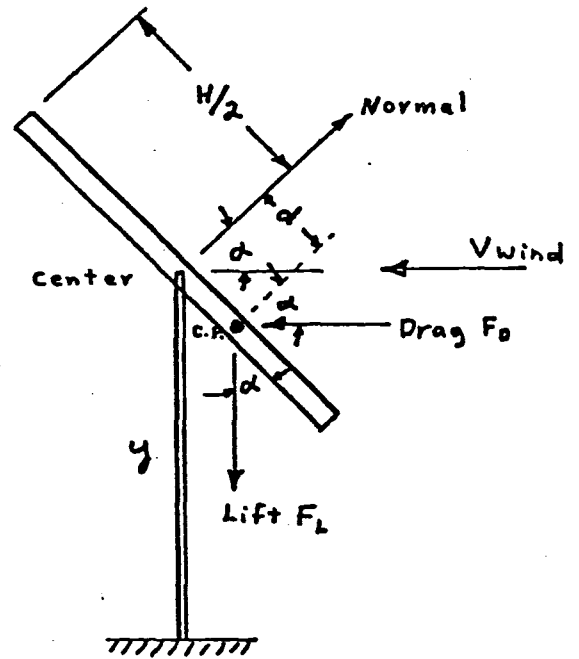


Figure 2

Frontside Wind Diagram

Equations

1. Drag: $F_D = C_D \cdot A \cdot RV^2 / 2g_c = C_D \cdot A \cdot g$

2. Lift: $F_L = C_L \cdot A \cdot RV^2 / 2g_c = C_L \cdot A \cdot g$

3. Moment Arm: $d = H \cdot (0.5 - C_{cp})$

4. Drag Moment (center): $M_{Dc} = F_D \cdot \cos \alpha \cdot d$

5. Lift Moment (center): $M_{Lc} = F_L \cdot \sin \alpha \cdot d$

6. Drag Moment (base): $M_{Db} = F_D \cdot (y \pm d \cdot \cos \alpha)$

7. Lift Moment (base): $M_{Lb} = F_L \cdot d \cdot \sin \alpha$

Wind Force Parameter Summary

<u>Angle of Attack</u>	<u>C_L</u>	<u>C_D</u>	<u>C_{CP}</u>
0	0	1.126	.500
10	.228	1.103	.470
20	.400	1.061	.451
30	.571	.989	.437
40	.730	.890	.430
50	.860	.761	.420
60	.898	.593	.398
70	.803	.274	.343
80	.361	.107	.263
90	0	0	0

Note: C_L = lift coefficient

C_D = drag coefficient

C_{CP} = center of pressure coefficient

Wind Induced Pressures and Loads

	<u>27 mph</u> <u>(reqmts)</u>	<u>35 mph</u> <u>(operating)</u>	<u>50 mph</u> <u>(stowing)</u>	<u>90 mph</u> <u>(survival)</u>
1. Windspeed corrected to 12.75 ft height	23.748 mph	30.784 mph	43.977 mph	79.159 mph
2. Dynamic pressure, q, lb/ft ²	1.413	2.374	4.845	15.698
3. Dynamic pressure x Area, lb _f	848.2	1425.1	2908.5	9423.5
4. Drag Force, F _D , lb _f				
0°	955	1605	3275	10611
10	936	1572	3208	10394
20	900	1512	3086	9998
30	839	1409	2877	9320
40	755	1268	2589	8387
50	645	1085	2213	7171
60	503	845	1725	5588
70	232	390	796	2582
80	91	152	311	1008
90	0	0	0	0
5. Lift Force, F _L , lb _f				
0°	0	0	0	0
10	193	325	663	2149
20	339	570	1163	3769
30	484	814	1661	5381
40	619	1040	2123	6879
50	729	1226	2501	8104
60	762	1280	2612	8462
70	681	1144	2336	7567
80	306	514	1050	3402
90	0	0	0	0

Elevation and Azimuth Moments

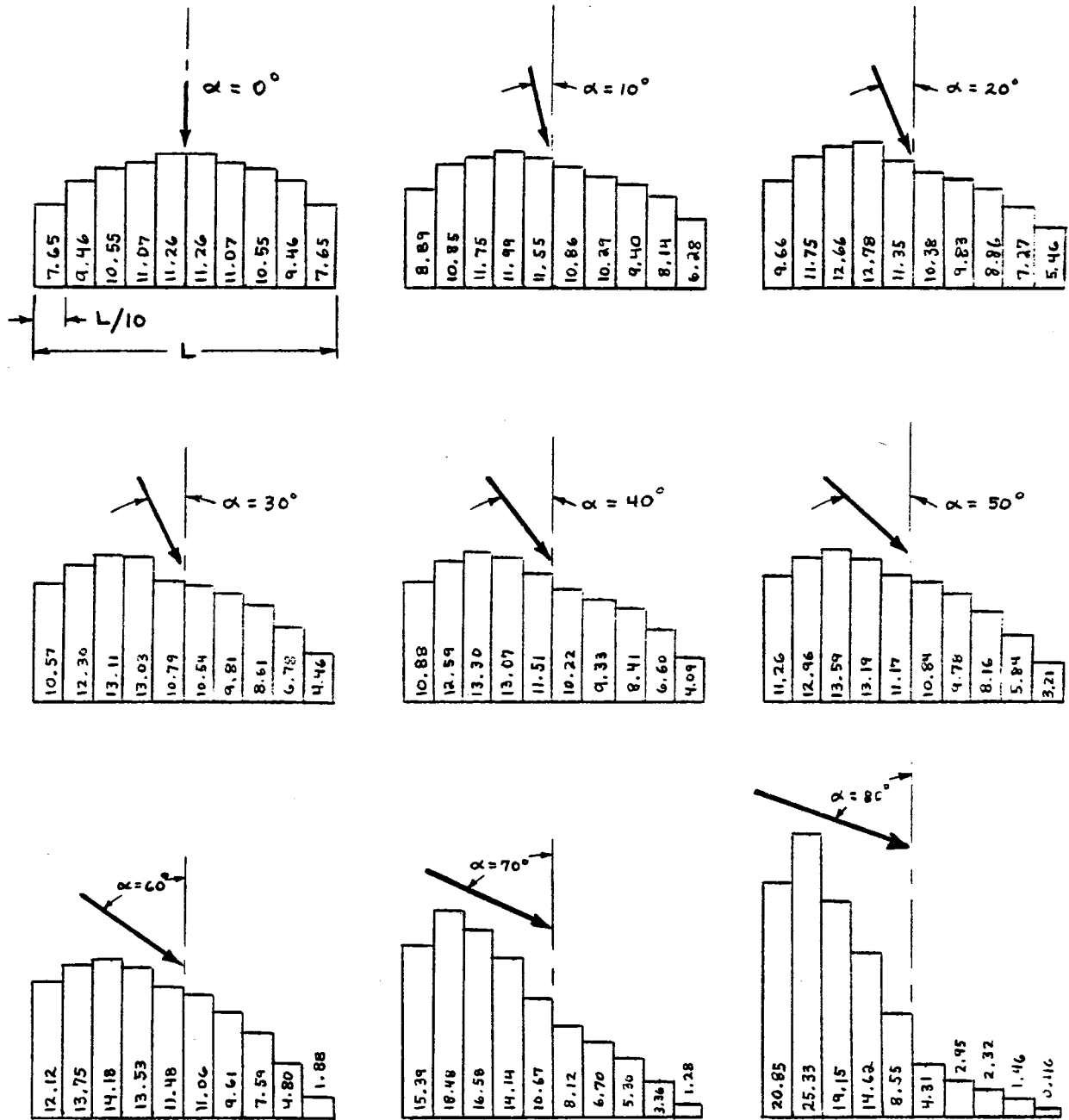
<u>Angle of Attack</u>	<u>Moment Arm d,ft</u>	<u>Windspeed at 30 ft Height</u>			
		<u>27 mph (reqmts)</u>	<u>35 mph (operating)</u>	<u>50 mph (stowing)</u>	<u>90 mph (survival)</u>
0	0	0 ft-lb	0 ft-lb	0 ft-lb	0 ft-lb
10	.735	702	1179	2407	7799
20	1.201	1155	1941	3961	12832
30	1.544	1496	2513	5130	16620
40	1.715	1674	2813	5740	18598
50	1.960	1909	3207	6546	21209
60	2.499	2277	3826	7808	25297
70	3.847	2768	4651	9497	30752
80	5.807	1843	3097	6320	20476
90	12.25	0	0	0	0

Ground-Level Column Base Moments

Angle of Attack	Windspeed at 30 ft Height			
	27 mph (reqmts)	35 mph (operate)	50 mph (stowing)	90 mph (survival)
0	12176 ft-lb	20460 ft-lb	41756 ft-lb	135290 ft-lb
10	12629	21222	43309	140323
20	12628	21219	43304	140307
30	12191	20485	41805	135450
40	11298	18985	38744	125532
50	10138	17035	34765	112639
60	8689	14601	29797	96544
70	5731	9630	19652	63673
80	3000	5040	10286	33328
90	0	0	0	0

Northrup Inc

Normal Force Distribution on Surface



Note: Angle α is the wind angle of attack relative to the heliostat normal.

The values shown in the blocks are the percentages of the total normal wind load on a heliostat having a height or width of dimension L .

9.5.2 WIND AND GRAVITY DEFLECTIONS

In this subsection the gravity and wind- induced deflections of the mirror modules, trusses, torque tubes, and drive unit are presented.

The paragraphs, topical subjects and page numbers are as follows:

9.5.2.1 Mirror Module Deflections, pg. E-9 through E-28

9.5.2.2 Rack Structure Deflections

- a. Gravity Only, pg. E-29 through E-41
- b. No Gravity, 27 mph wind, pg. E-42 through E-53
- c. Gravity plus 27 mph wind, pg. 54 through E-65

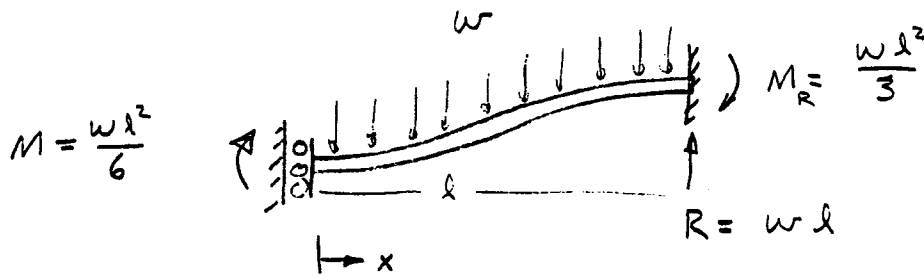
9.5.2.3 Drive Unit Deflections, pg. E-66 through E-88

In all instances the deflections have been resolved into the appropriate milliradian errors in the azimuth or elevation direction.

9.5.2.1 Mirror Module Deflections

In the following subsection the analysis of the mirror module deflections from gravity and/or a 27 mph wind are presented. The analysis method, assumptions, equations, and computations are provided. The topics covered include between-stringer sag, shear deflections, and bending deflections.

Between - Stringer Gravity Sag Analysis



$$(a) \quad EI \frac{d^2 y}{dx^2} = \frac{wx^2}{2} - \frac{wl^2}{6}$$

$$(b) \quad EI \frac{dy}{dx} = \frac{wx^3}{6} - \frac{wl^2 x}{6} + C_1 \quad \text{slope}$$

$$(c) \quad EI y = \frac{wx^4}{24} - \frac{wl^2 x^2}{12} + C_1 x + C_2 \quad \text{deflection}$$

2 Boundary Conditions exist

$$(1) \quad y = 0 \quad \text{at} \quad x = l$$

$$(2) \quad \frac{dy}{dx} = 0 \quad \text{at} \quad x = 0 \quad \text{and} \quad x = l$$

(slope)

$$(b) \quad EI(0) = \frac{wl^3}{6} - \frac{wl^3}{6} + C_1 = 0 - 0 + C_1$$

$$C_1 = 0$$

$$(c) \quad EI(0) = \frac{wl^4}{24} - \frac{wl^4}{12} + C_1 l + C_2$$
$$= -\frac{wl^4}{24} + 0 + C_2$$

$$C_2 = \frac{wl^4}{24}$$

Slope Equation

$$\begin{aligned} EI \theta &= \frac{wx^3}{6} - \frac{wl^2x}{6} \\ &= \frac{w}{6} (x^3 - l^2x) \end{aligned}$$

Find the Rms Slope (1" strip)

$$\theta_{RMS} = \sqrt{\frac{\sum_0^n \theta_i^2}{n}} = \sqrt{\frac{B}{l}} \quad \text{where } B = \int_0^l \theta^2 dx$$

$$B = \left(\frac{W}{6EI}\right)^2 \int_0^l (x^3 - l^2 x)^2 dx$$

$$= \left(\frac{W}{6EI}\right)^2 \int_0^l (x^6 - 2x^4 l^2 + l^4 x^2) dx$$

$$= \left(\frac{W}{6EI}\right)^2 \left(\frac{x^7}{7} - 2 \frac{x^5 l^2}{5} + \frac{l^4 x^3}{3} \right)_0^l$$

$$= \left(\frac{W}{6EI}\right)^2 \left(\frac{l^7}{7} - \frac{2}{5} l^7 + \frac{l^7}{3} \right) = \left(\frac{W}{6EI}\right)^2 \left(\frac{2}{105} l^7 \right)$$

$$= \frac{2}{945} \left(\frac{W}{EI}\right)^2 l^7$$

$$\theta_{RMS} = \sqrt{\frac{\frac{2}{945} \left(\frac{W}{EI}\right)^2 l^7}{l}} = \sqrt{\frac{2}{945} \left(\frac{W}{EI}\right)^2 l^6}$$

For worst wind & gravity at 60° from vertical

$$w = .0234 \text{ lbs/in} \quad \text{ref: E-25 report}$$

$$EI = 790 \text{ lbs in}^2 \quad \text{" " "}$$

$$\Theta_{\text{RMS}} = \sqrt{\frac{2}{945} \left(\frac{.0234}{790} \right)^2 (4'')^6}$$

$$= .000087 \text{ radians}$$

Check numerically

$$l = 4''$$

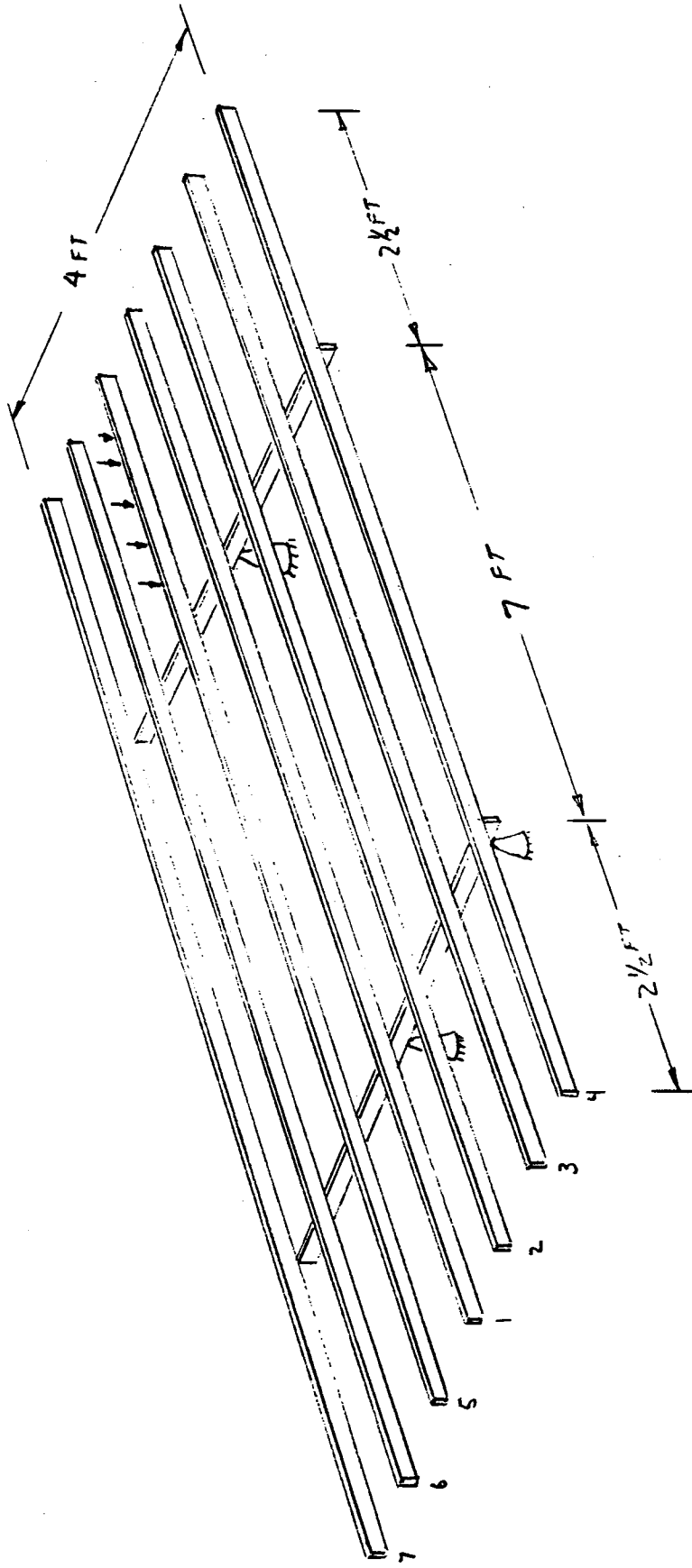
$$EI = 790 \text{ lb in}^2$$

$$w = .0234 \text{ lbs/in}$$

$$\begin{aligned} \theta &= \frac{w}{6EI} (x^3 - l^2 x) \\ &= \frac{.0234}{6(790)} (x^3 - 16x) \\ &= 4.94 \times 10^{-6} (x^3 - 16x) \end{aligned}$$

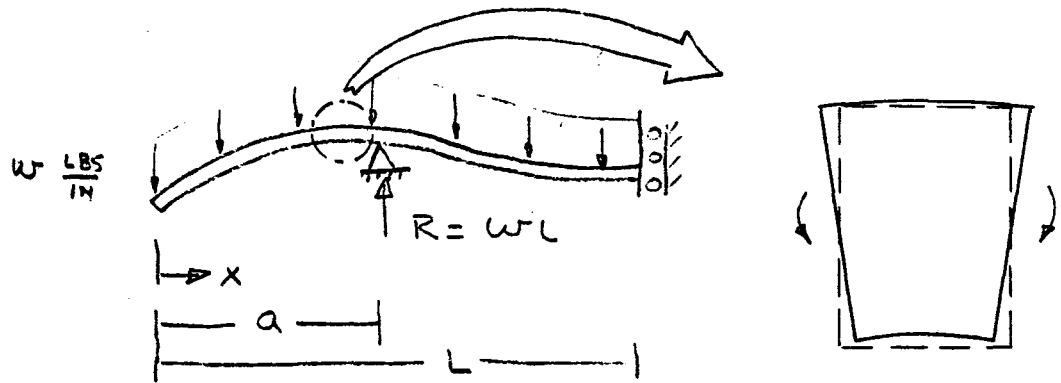
<u>x</u>	<u>x³</u>	<u>(x³ - 16x)</u>	<u>θ</u>	<u>θ²</u>
.25	.01563	3.984	19.7 × 10 ⁻⁶	388 × 10 ⁻¹²
.75	.4219	11.578	57.2 × 10 ⁻⁶	3271
1.25	1.953	18.047	89.2 × 10 ⁻⁶	7943
1.75	5.359	22.641	111.84 × 10 ⁻⁶	12509
2.25	11.391	24.609	121.57 × 10 ⁻⁶	14779
2.75	20.797	23.203	114.62 × 10 ⁻⁶	13139
3.25	34.328	17.672	87.30 × 10 ⁻⁶	7621
3.75	52.734	7.266	35.89 × 10 ⁻⁶	1288
				<hr/>
				60,943 × 10 ⁻¹²

$$\begin{aligned} \theta_{RMS} &= \sqrt{\frac{60,943 \times 10^{-12}}{8}} = 87 \times 10^{-6} \\ &= .087 \text{ mrad} \checkmark \text{ cks} \end{aligned}$$



MIRROR MODULE DEFLECTION/IMPERFECTION ANALYSIS

BENDING DEFLECTION FORMULA FOR STRINGER HALF-SPAN



$x = 0$ TO a

$$EI \frac{d^2y}{dx^2} = \frac{wx^2}{2}$$

(a) $EI \frac{dy}{dx} = \frac{wx^3}{6} + C_1$ (SLOPE)

(b) $EI y = \frac{wx^4}{24} + C_1x + C_2$ (DEFLECTION)

$x = a$ TO L

$$EI \frac{d^2y}{dx^2} = \frac{wx^2}{2} - WL(x-a) = \frac{wx^2}{2} - WLx + WLa$$

(c) $EI \frac{dy}{dx} = \frac{wx^3}{6} - \frac{WLx^2}{2} + WLa x + C_3$ (SLOPE)

(d) $EI y = \frac{wx^4}{24} - \frac{WLx^3}{6} + \frac{WLa x^2}{2} + C_3x + C_4$ (DEFLECTION)

BOUNDARY CONDITIONS

- (1) $y = 0$ at $x = a$ LEFT & RIGHT
- (2) $\frac{dy}{dx} = 0$ at $x = L$ RIGHT
- (3) $\frac{dy}{dx}$ LEFT SIDE = $\frac{dy}{dx}$ RIGHT SIDE at $x = a$

SUBSTITUTING BOUNDARY CONDITIONS

$$\text{COND(1) (b)} \quad EI(0) = \frac{w a^4}{24} + C_1 a + C_2$$

$$\begin{aligned} \text{(d)} \quad EI(0) &= \frac{w}{24} a^4 - \frac{wL}{6} a^3 + \frac{wLa}{2} a^2 + C_3 a + C_4 \\ &= \frac{w a^4}{24} + \frac{wLa^3}{3} + C_3 a + C_4 \end{aligned}$$

$$\begin{aligned} \text{COND(2) (c)} \quad EI(0) &= \frac{wL^3}{6} - \frac{wLL^2}{2} + wLaL + C_3 \\ &= -\frac{wL^3}{3} + wL^2a + C_3 \end{aligned}$$

$$C_3 = \frac{wL^3}{3} - wL^2a$$

$$\text{COND(3) (a \& c)} \quad \frac{w}{6} a^3 + C_1 = \frac{w}{6} a^3 - \frac{wL}{2} a^2 + wLa a + C_3$$

$$C_1 = \frac{wL}{2} a^2 + C_3$$

$$C_1 = \frac{wL}{2} a^2 + \frac{wL^3}{3} - wL^2a$$

SUBST C_1 INTO (b)

$$\frac{w a^4}{24} + \frac{wLa^3}{2} + \frac{wL^3a}{3} - wL^2a^2 + C_2 = 0$$

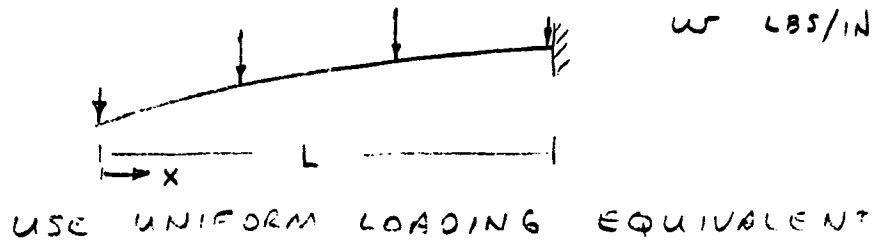
$$C_2 = -\frac{w a^4}{24} - \frac{wLa^3}{2} + wL^2a^2 - \frac{wL^3a}{3}$$

SUBST C_3 INTO (d)

$$\frac{w a^4}{24} + \frac{wLa^3}{3} + \frac{wL^3a}{3} - wL^2a^2 + C_4 = 0$$

$$C_4 = -\frac{w a^4}{24} - \frac{wLa^3}{3} + wL^2a^2 - \frac{wL^3a}{3}$$

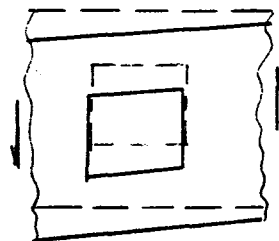
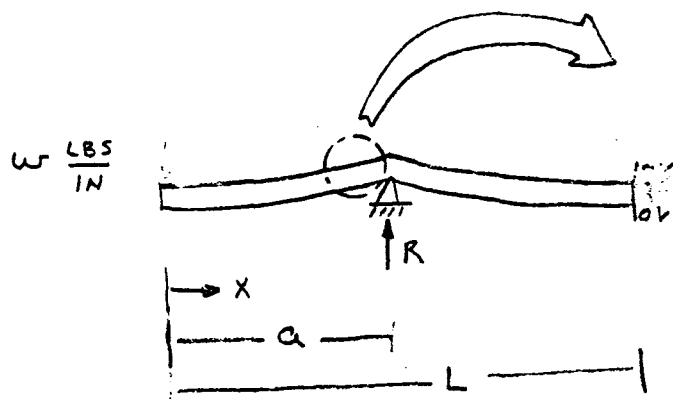
DEFLECTION FORMULA FOR CROSS MEMBER HALF SPAN



$$\text{SLOPE } EI \frac{dy}{dx} = \frac{wL^3}{6} \left(1 - \frac{x^3}{L^3} \right)$$

$$\text{DEFL. } EI y = \frac{w}{24} (x^4 - 4L^3x + 3L^4)$$

SHEAR DEFLECTION FORMULA FOR STRINGER HALF SPAN



$$k = \frac{\text{MAX STRESS}}{\text{AVG STRESS}}$$

$x = 0 \text{ TO } a$ $\frac{dy}{dx} = -\frac{kV}{A_sG} = -\frac{kwx}{A_sG}$ SLOPE

$$y = -\frac{kwx^2}{2A_sG} + C_1$$

$$y = 0 \text{ at } x = a$$

$$C_1 = \frac{kwa^2}{2A_sG}$$

$$y = \frac{kwx}{2A_sG} (a^2 - x^2)$$
DEFLECTION

$x = a \text{ TO } L$ $\frac{dy}{dx} = \frac{kx}{AG} (L-x)$ SLOPE

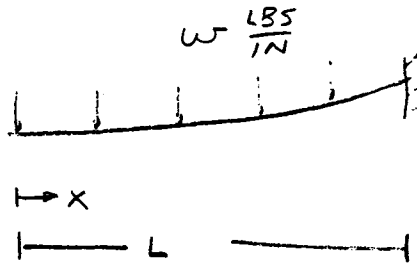
$$y = \frac{kx}{AG} Lx - \frac{kx}{AG} \frac{x^2}{2} + C_2$$

$$y = 0 \text{ at } x = a$$

$$C_2 = \frac{kx}{AG} \frac{a^2}{2} - \frac{kx}{AG} La$$

$$y = \frac{kx}{AG} \left(Lx - \frac{x^2}{2} + \frac{a^2}{2} - La \right)$$
DEFLECTION

SHEAR DEFLECTION FORMULA FOR CROSS MEMBER
HALF SPAN



$$\frac{dy}{dx} = \frac{kw-x}{AG}$$

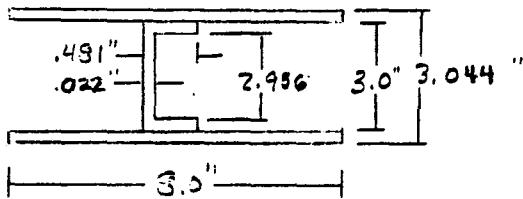
SLOPE

$$v = \frac{kw}{2AG} (L^2 - x^2)$$

DEFLECTION

SECTION PROPERTIES OF BEAMS

CENTRAL BEAMS



$$I = \frac{1}{12} (8 \times 3.044^3 - 7.519 \times 3.0^3 - .459 \times 2.956^3)$$

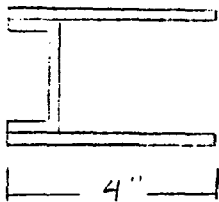
$$= \frac{1}{12} (225.644 - 203.013 - 11.856)$$

$$= .898 \text{ IN}^4$$

$$A_s = 3.0 \times .022 = .066 \text{ IN}^2$$

$$k = 1$$

EDGE BEAMS



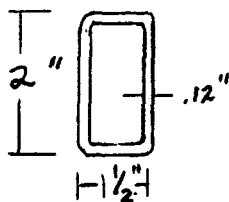
$$I = \frac{1}{12} (4 \times 3.044^3 - 3.519 \times 3.0^3 - .459 \times 2.956^3)$$

$$= \frac{1}{12} (112.822 - 95.013 - 11.856)$$

$$= .496$$

$$A_s = .066 \text{ IN}^2 \quad k = 1$$

CROSS MEMBERS



$$I = .43 \text{ IN}^4$$

$$A_s = .48 \text{ IN}^2 \quad k = 1$$

Sample Computer Print-Outs For
Mirror Module Deflection Evaluation

MIRROR MODULE BENDING AND SHEAR MRAD ERRORS - RUN #90GR

ENTER CENTRAL STRINGER BENDING INERTIA, $IN_{14} = .898$

ENTER CENTRAL STRINGER SHEAR AREA, $IN_{12} = .066$

ENTER CENTRAL STRINGER SHEAR CONSTANT = 1

ENTER EDGE STRINGER BENDING INERTIA, $IN_{14} = .496$

ENTER EDGE STRINGER SHEAR AREA, $IN_{12} = .066$

ENTER EDGE STRINGER SHEAR CONSTANT = 1

ENTER CROSS MEMBER BENDING INERTIA, $IN_{14} = .43$

ENTER CROSS MEMBER SHEAR AREA, $IN_{12} = .48$

ENTER CROSS MEMBER SHEAR CONSTANT = 1

ENTER STRINGER HALF-SPAN LENGTH, $IN = 72$

ENTER CROSS MEMBER HALF-SPAN LENGTH, $IN = 24$

ENTER STRINGER SUPPORT LOCATION, $IN = 30$

ENTER CROSS MEMBER SUPPORT LOCATION, $IN = 20$

ENTER STRINGER SPACING, $IN = 8$

ENTER LOAD, LB/SQ-FT = 4.21

MIRROR ELEMENT VECTOR-SUMMED SLOPE ERRORS - RUN #90GR

.....MICRO-RADIANS (RAD*1E-6)..... ...MRAD...

RIB #	NODE	(LONGITUDINAL)		(TRANSVERSE)			AREA-WEIGHTED VECTOR-SUM TOTAL
		STRINGER BENDING	DIRECTION SHEAR	CROSS MEMBER BENDING	DIRECTION SHEAR	ROTATION	
1	1	11	-1	0	-11	269	.28
1	2	12	-3	0	-11	269	.28
1	3	16	-5	0	-11	269	.28
1	4	25	-7	0	-11	269	.28
1	5	40	-10	0	-11	269	.282
1	6	60	14	0	-11	269	.29
1	7	72	12	0	-11	269	.292
1	8	73	10	0	-11	269	.292
1	9	65	7	0	-11	269	.289
1	10	51	5	0	-11	269	.286
1	11	33	3	0	-11	269	.282
1	12	11	1	0	-11	269	.28
2	1	11	-1	-265	-7	269	.01
2	2	12	-3	-265	-7	269	9E-03
2	3	16	-5	-265	-7	269	.011
2	4	25	-7	-265	-7	269	.017
2	5	40	-10	-265	-7	269	.03
2	6	60	14	-265	-7	269	.074
2	7	72	12	-265	-7	269	.083
2	8	73	10	-265	-7	269	.082
2	9	65	7	-265	-7	269	.073
2	10	51	5	-265	-7	269	.057
2	11	33	3	-265	-7	269	.036
2	12	11	1	-265	-7	269	.012
3	1	11	-1	-362	-4	269	.097
3	2	12	-3	-362	-4	269	.097
3	3	16	-5	-362	-4	269	.097
3	4	25	-7	-362	-4	269	.098
3	5	40	-10	-362	-4	269	.101
3	6	60	14	-362	-4	269	.121
3	7	72	12	-362	-4	269	.127
3	8	73	10	-362	-4	269	.127
3	9	65	7	-362	-4	269	.121
3	10	51	5	-362	-4	269	.112
3	11	33	3	-362	-4	269	.103
3	12	11	1	-362	-4	269	.097
4	1	10	-1	-376	0	269	.053
4	2	11	-2	-376	0	269	.053
4	3	15	-3	-376	0	269	.054
4	4	22	-4	-376	0	269	.054
4	5	36	-5	-376	0	269	.056
4	6	55	7	-376	0	269	.062
4	7	65	6	-376	0	269	.064
4	8	66	5	-376	0	269	.064
4	9	59	4	-376	0	269	.062
4	10	46	3	-376	0	269	.059
4	11	30	2	-376	0	269	.056
4	12	10	1	-376	0	269	.054

MIRROR ELEMENT VECTOR-SUMMED SLOPE ERRORS - CONTINUED - RUN #90GR

	MICRO-RADIANS (RAD*1E-6).....					...MRAD...
RIB #	NODE	(LONGITUDINAL)		(TRANSVERSE)			AREA-WEIGHTED VECTOR-SUM TOTAL
		STRINGER BENDING	DIRECTION SHEAR	CROSS BENDING	MEMBER SHEAR	DIRECTION ROTATION	
5	1	11	-1	265	7	269	.541
5	2	12	-3	265	7	269	.541
5	3	16	-5	265	7	269	.541
5	4	25	-7	265	7	269	.541
5	5	40	-10	265	7	269	.542
5	6	60	14	265	7	269	.546
5	7	72	12	265	7	269	.547
5	8	73	10	265	7	269	.547
5	9	65	7	265	7	269	.546
5	10	51	5	265	7	269	.544
5	11	33	3	265	7	269	.542
5	12	11	1	265	7	269	.541
6	1	11	-1	362	3	269	.635
6	2	12	-3	362	3	269	.635
6	3	16	-5	362	3	269	.635
6	4	25	-7	362	3	269	.635
6	5	40	-10	362	3	269	.636
6	6	60	14	362	3	269	.639
6	7	72	12	362	3	269	.64
6	8	73	10	362	3	269	.64
6	9	65	7	362	3	269	.639
6	10	51	5	362	3	269	.637
6	11	33	3	362	3	269	.636
6	12	11	1	362	3	269	.635
7	1	10	-1	376	0	269	.623
7	2	11	-2	376	0	269	.623
7	3	15	-3	376	0	269	.623
7	4	22	-4	376	0	269	.623
7	5	36	-5	376	0	269	.623
7	6	55	7	376	0	269	.624
7	7	65	6	376	0	269	.625
7	8	66	5	376	0	269	.625
7	9	59	4	376	0	269	.624
7	10	46	3	376	0	269	.624
7	11	30	2	376	0	269	.623
7	12	10	1	376	0	269	.623
RMS AVERAGE359

MIRROR MODULE BENDING AND SHEAR MRAD ERRORS - RUN #60 GR+WIND

ENTER CENTRAL STRINGER BENDING INERTIA, IN14 = .898

ENTER CENTRAL STRINGER SHEAR AREA, IN12 = .066

ENTER CENTRAL STRINGER SHEAR CONSTANT = 1

ENTER EDGE STRINGER BENDING INERTIA, IN14 = .496

ENTER EDGE STRINGER SHEAR AREA, IN12 = .066

ENTER EDGE STRINGER SHEAR CONSTANT = 1

ENTER CROSS MEMBER BENDING INERTIA, IN14 = .43

ENTER CROSS MEMBER SHEAR AREA, IN12 = .48

ENTER CROSS MEMBER SHEAR CONSTANT = 1

ENTER STRINGER HALF-SPAN LENGTH, IN = 72

ENTER CROSS MEMBER HALF-SPAN LENGTH, IN = 24

ENTER STRINGER SUPPORT LOCATION, IN = 30

ENTER CROSS MEMBER SUPPORT LOCATION, IN = 20

ENTER STRINGER SPACING, IN = 8

ENTER LOAD, LB/SQ-FT = 5.164

MIRROR ELEMENT VECTOR-SUMMED SLOPE ERRORS - RUN #60 GR+WIND

	MICRO-RADIANS (RAD*1E-6).....					...MRAD...
RIB #	NODE	(LONGITUDINAL)		(TRANSVERSE)			AREA-WEIGHTE VECTOR-SUM TOTAL
		STRINGER DIRECTION BENDING	SHEAR	CROSS MEMBER DIRECTION BENDING	SHEAR	ROTATION	
1	1	14	-1	0	-13	330	.344
1	2	15	-4	0	-13	330	.344
1	3	20	-7	0	-13	330	.344
1	4	30	-9	0	-13	330	.344
1	5	49	-12	0	-13	330	.345
1	6	74	17	0	-13	330	.355
1	7	88	14	0	-13	330	.358
1	8	89	12	0	-13	330	.358
1	9	80	9	0	-13	330	.355
1	10	63	7	0	-13	330	.35
1	11	40	4	0	-13	330	.346
1	12	14	1	0	-13	330	.344
2	1	14	-1	-325	-9	330	.013
2	2	15	-4	-325	-9	330	.011
2	3	20	-7	-325	-9	330	.014
2	4	30	-9	-325	-9	330	.021
2	5	49	-12	-325	-9	330	.037
2	6	74	17	-325	-9	330	.091
2	7	88	14	-325	-9	330	.102
2	8	89	12	-325	-9	330	.101
2	9	80	9	-325	-9	330	.089
2	10	63	7	-325	-9	330	.07
2	11	40	4	-325	-9	330	.044
2	12	14	1	-325	-9	330	.015
3	1	14	-1	-444	-4	330	.119
3	2	15	-4	-444	-4	330	.118
3	3	20	-7	-444	-4	330	.119
3	4	30	-9	-444	-4	330	.12
3	5	49	-12	-444	-4	330	.124
3	6	74	17	-444	-4	330	.149
3	7	88	14	-444	-4	330	.156
3	8	89	12	-444	-4	330	.155
3	9	80	9	-444	-4	330	.148
3	10	63	7	-444	-4	330	.137
3	11	40	4	-444	-4	330	.126
3	12	14	1	-444	-4	330	.119
4	1	13	-1	-461	0	330	.066
4	2	14	-2	-461	0	330	.066
4	3	18	-3	-461	0	330	.066
4	4	27	-5	-461	0	330	.066
4	5	44	-6	-461	0	330	.068
4	6	67	0	-461	0	330	.075
4	7	80	7	-461	0	330	.078
4	8	81	6	-461	0	330	.078
4	9	73	5	-461	0	330	.076
4	10	57	3	-461	0	330	.072
4	11	36	2	-461	0	330	.068
4	12	12	1	-461	0	330	.066

MIRROR ELEMENT VECTOR-SUMMED SLOPE ERRORS - CONTINUED - RUN #60 GR+WINI

.....MICRO-RADIANS (RAD*1E-6)..... ...MRAD...

RIB #	NODE	(LONGITUDINAL)		(TRANSVERSE)			AREA-WEIGHTE VECTOR-SUM TOTAL
		STRINGER BENDING	DIRECTION SHEAR	CROSS BENDING	MEMBER SHEAR	DIRECTION ROTATION	
5	1	14	-1	325	9	330	.664
5	2	15	-4	325	9	330	.664
5	3	20	-7	325	9	330	.664
5	4	30	-9	325	9	330	.664
5	5	49	-12	325	9	330	.665
5	6	74	17	325	9	330	.67
5	7	88	14	325	9	330	.671
5	8	89	12	325	9	330	.671
5	9	80	9	325	9	330	.67
5	10	63	7	325	9	330	.667
5	11	40	4	325	9	330	.665
5	12	14	1	325	9	330	.664
6	1	14	-1	444	4	330	.779
6	2	15	-4	444	4	330	.779
6	3	20	-7	444	4	330	.779
6	4	30	-9	444	4	330	.779
6	5	49	-12	444	4	330	.78
6	6	74	17	444	4	330	.784
6	7	88	14	444	4	330	.786
6	8	89	12	444	4	330	.785
6	9	80	9	444	4	330	.784
6	10	63	7	444	4	330	.782
6	11	40	4	444	4	330	.78
6	12	14	1	444	4	330	.779
7	1	13	-1	461	0	330	.396
7	2	14	-2	461	0	330	.396
7	3	18	-3	461	0	330	.396
7	4	27	-5	461	0	330	.396
7	5	44	-6	461	0	330	.396
7	6	67	8	461	0	330	.398
7	7	80	7	461	0	330	.398
7	8	81	6	461	0	330	.398
7	9	73	5	461	0	330	.398
7	10	57	3	461	0	330	.397
7	11	36	2	461	0	330	.396
7	12	12	1	461	0	330	.396

RMS AVERAGE441

9.5.2.2 Rack Structure Deflections

A computer code named "WINDBEND" was developed to evaluate the combined bending and torsion of the torque tube, and bending of the truss members. Both gravity and wind can be evaluated separately or can be combined to determine the total effect. This computer program includes a wind force subroutine in which the wind forces are distributed over the mirrored surface of the heliostat in accordance with the method outlined in appendix section 9.5.1 (see page E-7). The wind or gravity loads from the mirror modules are transmitted to the trusses through the discrete attachment points, and the resultant beam bending, torque tube bending, and torque tube torsion deflections are computed and vectorially combined. The program is general in that any wind speed or elevation angle case can be evaluated.

The following section presents the "WINDBEND" analysis output for heliostat elevation angles from 0° (vertical) to 90° (horizontal) for the following cases:

- a. Gravity only, no wind, pg. E-30 through E-41
- b. No Gravity, 27 mph wind, pg. E-42 through E-53
- c. Gravity plus 27 mph wind, pg. E-54 through E-65

WIND & GRAVITY MRAD ERROR ANALYSIS

INPUT WIND SPEED AT 30', MPH = 0

INPUT MIRROR MODULE WEIGHT, EACH, LB = 199.2

INPUT BEAM INERTIA, IN⁴ = 249

INPUT BEAM WEIGHT, LB/FT = 6.65

INPUT TORQUE TUBE LENGTH, INCHES = 110.38

INPUT TORQUE TUBE O.D., INCHES = 12.75

INPUT TORQUE TUBE WALL THICKNESS, INCHES = .25

TORQUE TUBE I.D., INCHES = 12.25

TORQUE TUBE BENDING INERTIA, INCHES⁴ = 191.82

TORQUE TUBE + FLANGE EQUIV BENDING INERTIA, INCHES⁴ = 168.43

TORQUE TUBE POLAR INERTIA, INCHES⁴ = 383.64

TORQUE TUBE WEIGHT LB/FT = 33.34

WIND ANGLE, = 0 DEG, WIND SPEED = 0 MPH

(1). BEAM BENDING EFFECT (GRAVITY & WIND):

MODULE	DEF1, IN*10 ¹⁴	DEF2, IN*10 ¹⁴	MRAD ERROR
#1	0	0	1E-03
#2	0	0	1E-03
#3	0	0	1E-03
#4	0	0	1E-03
#5	0	0	1E-03
#6	0	0	1E-03
HELIOSTAT-AVERAGE MRAD ERROR:			1E-03

(2). TORQUE TUBE - WIND AND GRAVITY TORSIONAL LOADING

TORSION FROM	END TORSION	MID TORSION	EFF MRAD TORSIO
WIND	0	0	0
GRAVITY	.501	.193	.193
ARITHMETIC-SUM MRAD TORSIONAL ERROR:			.193

(3). TORQUE TUBE + FLANGE - WIND AND GRAVITY LOAD BENDING:

TORQUE TUBE	DEF1, IN*10 ¹⁴	DEF2, IN*10 ¹⁴	MRAD BEND
WIND	0	0	0
GRAVITY	803	70	.873
VECTOR-SUM MRAD BENDING ERROR:			0

(4). VECTOR-COMBINED BEAM & TORQUE TUBE BENDING & TORSION EFFECTS:

MIRROR MODULE	BEAM DEFLECTION MRAD ERROR	TORQUE TUBE TORSIONAL MRAD ERROR	TORQUE TUBE BENDING MRAD ERROR	VECTOR-SUM MRAD ERROR
#1	1E-03	.193	0	.193
#2	1E-03	.193	0	.193
#3	1E-03	.193	0	.193
#4	1E-03	.193	0	.193
#5	1E-03	.193	0	.193
#6	1E-03	.193	0	.193
TOTAL HELIOSTAT RMS MRAD ERROR:				.193

WIND ANGLE, = 10 DEG, WIND SPEED = 0 MPH

(1). BEAM BENDING EFFECT (GRAVITY & WIND):

MODULE	DEF1, IN*10 ¹⁴	DEF2, IN*10 ¹⁴	MRAD ERROR
#1	24	19	.029
#2	16	11	.027
#3	4	1	.016
#4	4	1	.016
#5	16	11	.027
#6	24	19	.029
HELIOSTAT-AVERAGE MRAD ERROR:			.024

(2). TORQUE TUBE - WIND AND GRAVITY TORSIONAL LOADING

TORSION FROM	END TORSION	MID TORSION	EFF MRAD TORSION
WIND	0	0	0
GRAVITY	.493	.19	.19
ARITHMETIC-SUM MRAD TORSIONAL ERROR:			.19

(3). TORQUE TUBE + FLANGE - WIND AND GRAVITY LOAD BENDING:

TORQUE TUBE	DEF1, IN*10 ¹⁴	DEF2, IN*10 ¹⁴	MRAD BEND
WIND	0	0	0
GRAVITY	803	70	.873
VECTOR-SUM MRAD BENDING ERROR:			.151

(4). VECTOR-COMBINED BEAM & TORQUE TUBE BENDING & TORSION EFFECTS:

MIRROR MODULE	BEAM DEFLECTION MRAD ERROR	TORQUE TUBE TORSIONAL MRAD ERROR	TORQUE TUBE BENDING MRAD ERROR	VECTOR-SUM MRAD ERROR
#1	.029	.19	.151	.266
#2	.027	.19	.151	.264
#3	.016	.19	.151	.255
#4	.016	.19	.151	.231
#5	.027	.19	.151	.222
#6	.029	.19	.151	.221
TOTAL HELIOSTAT RMS MRAD ERROR:				.243

WIND ANGLE, = 20 DEG, WIND SPEED = 0 MPH

(1). BEAM BENDING EFFECT (GRAVITY & WIND):

MODULE	DEF1, IN*10 ¹⁴	DEF2, IN*10 ¹⁴	MRAD ERROR
#1	48	37	.056
#2	32	22	.052
#3	9	3	.032
#4	9	3	.032
#5	32	22	.052
#6	48	37	.056
HELIOSTAT-AVERAGE MRAD ERROR:			.046

(2). TORQUE TUBE - WIND AND GRAVITY TORSIONAL LOADING

TORSION FROM	END TORSION	MID TORSION	EFF MRAD TORSION
WIND	0	0	0
GRAVITY	.47	.181	.181
ARITHMETIC-SUM MRAD TORSIONAL ERROR:			.181

(3). TORQUE TUBE + FLANGE - WIND AND GRAVITY LOAD BENDING:

TORQUE TUBE	DEF1, IN*10 ¹⁴	DEF2, IN*10 ¹⁴	MRAD BEND
WIND	0	0	0
GRAVITY	803	70	.873
VECTOR-SUM MRAD BENDING ERROR:			.298

(4). VECTOR-COMBINED BEAM & TORQUE TUBE BENDING & TORSION EFFECTS:

MIRROR MODULE	BEAM DEFLECTION MRAD ERROR	TORQUE TUBE TORSIONAL MRAD ERROR	TORQUE TUBE BENDING MRAD ERROR	VECTOR-SUM MRAD ERROR
#1	.056	.181	.298	.38
#2	.052	.181	.298	.378
#3	.032	.181	.298	.366
#4	.032	.181	.298	.333
#5	.052	.181	.298	.325
#6	.056	.181	.298	.323
TOTAL HELIOSTAT RMS MRAD ERROR:				.351

WIND ANGLE, = 30 DEG, WIND SPEED = 0 MPH

(1). BEAM BENDING EFFECT (GRAVITY & WIND):

MODULE	DEF1, IN*10 ¹⁴	DEF2, IN*10 ¹⁴	MRAD ERROR
#1	71	55	.081
#2	47	32	.076
#3	13	4	.047
#4	13	4	.047
#5	47	32	.076
#6	71	55	.081
HELIOSTAT-AVERAGE MRAD ERROR:			.068

(2). TORQUE TUBE - WIND AND GRAVITY TORSIONAL LOADING

TORSION FROM	END TORSION	MID TORSION	EFF MRAD TORSION
WIND	0	0	0
GRAVITY	.433	.167	.167
ARITHMETIC-SUM MRAD TORSIONAL ERROR:			.167

(3). TORQUE TUBE + FLANGE - WIND AND GRAVITY LOAD BENDING:

TORQUE TUBE	DEF1, IN*10 ¹⁴	DEF2, IN*10 ¹⁴	MRAD BEND
WIND	0	0	0
GRAVITY	803	70	.873
VECTOR-SUM MRAD BENDING ERROR:			.436

(4). VECTOR-COMBINED BEAM & TORQUE TUBE BENDING & TORSION EFFECTS:

MIRROR MODULE	BEAM DEFLECTION MRAD ERROR	TORQUE TUBE TORSIONAL MRAD ERROR	TORQUE TUBE BENDING MRAD ERROR	VECTOR-SUM MRAD ERROR
#1	.081	.167	.436	.501
#2	.076	.167	.436	.499
#3	.047	.167	.436	.485
#4	.047	.167	.436	.452
#5	.076	.167	.436	.445
#6	.081	.167	.436	.444
TOTAL HELIOSTAT RMS MRAD ERROR:				.471

WIND ANGLE, = 40 DEG, WIND SPEED = 0 MPH

(1). BEAM BENDING EFFECT (GRAVITY & WIND):

MODULE	DEF1, IN*10 ¹⁴	DEF2, IN*10 ¹⁴	MRAD ERROR
#1	91	70	.105
#2	61	42	.098
#3	17	5	.06
#4	17	5	.06
#5	61	42	.098
#6	91	70	.105
HELIOSTAT-AVERAGE MRAD ERROR:			.087

(2). TORQUE TUBE - WIND AND GRAVITY TORSIONAL LOADING

TORSION FROM	END TORSION	MID TORSION	EFF MRAD TORSION
WIND	0	0	0
GRAVITY	.383	.148	.148
ARITHMETIC-SUM MRAD TORSIONAL ERROR:			.148

(3). TORQUE TUBE + FLANGE - WIND AND GRAVITY LOAD BENDING:

TORQUE TUBE	DEF1, IN*10 ¹⁴	DEF2, IN*10 ¹⁴	MRAD BEND
WIND	0	0	0
GRAVITY	803	70	.873
VECTOR-SUM MRAD BENDING ERROR:			.561

(4). VECTOR-COMBINED BEAM & TORQUE TUBE BENDING & TORSION EFFECTS:

MIRROR MODULE	BEAM DEFLECTION MRAD ERROR	TORQUE TUBE TORSIONAL MRAD ERROR	TORQUE TUBE BENDING MRAD ERROR	VECTOR-SUM MRAD ERROR
#1	.105	.148	.561	.615
#2	.098	.148	.561	.612
#3	.06	.148	.561	.598
#4	.06	.148	.561	.568
#5	.098	.148	.561	.563
#6	.105	.148	.561	.562
TOTAL HELIOSTAT RMS MRAD ERROR:				.586

WIND ANGLE, = 50 DEG, WIND SPEED = 0 MPH

(1). BEAM BENDING EFFECT (GRAVITY & WIND):

MODULE	DEF1, IN*10 ¹⁴	DEF2, IN*10 ¹⁴	MRAD ERROR
#1	109	84	.124
#2	73	50	.117
#3	21	7	.071
#4	21	7	.071
#5	73	50	.117
#6	109	84	.124

HELIOSTAT-AVERAGE MRAD ERROR: .104

(2). TORQUE TUBE - WIND AND GRAVITY TORSIONAL LOADING

TORSION FROM	END TORSION	MID TORSION	EFF MRAD TORSION
WIND	0	0	0
GRAVITY	.322	.124	.124

ARITHMETIC-SUM MRAD TORSIONAL ERROR: .124

(3). TORQUE TUBE + FLANGE - WIND AND GRAVITY LOAD BENDING:

TORQUE TUBE	DEF1, IN*10 ¹⁴	DEF2, IN*10 ¹⁴	MRAD BEND
WIND	0	0	0
GRAVITY	803	70	.873

VECTOR-SUM MRAD BENDING ERROR: .669

(4). VECTOR-COMBINED BEAM & TORQUE TUBE BENDING & TORSION EFFECTS:

MIRROR MODULE	BEAM DEFLECTION MRAD ERROR	TORQUE TUBE TORSIONAL MRAD ERROR	TORQUE TUBE BENDING MRAD ERROR	VECTOR-SUM MRAD ERROR
#1	.124	.124	.669	.713
#2	.117	.124	.669	.711
#3	.071	.124	.669	.696
#4	.071	.124	.669	.671
#5	.117	.124	.669	.669
#6	.124	.124	.669	.669

TOTAL HELIOSTAT RMS MRAD ERROR: .688

WIND ANGLE, = 60 DEG, WIND SPEED = 0 MPH

(1). BEAM BENDING EFFECT (GRAVITY & WIND):

MODULE	DEF1, IN*10 ¹⁴	DEF2, IN*10 ¹⁴	MRAD ERROR
#1	123	95	.141
#2	82	56	.132
#3	24	8	.08
#4	24	8	.08
#5	82	56	.132
#6	123	95	.141
HELIOSTAT-AVERAGE MRAD ERROR:			.117

(2). TORQUE TUBE - WIND AND GRAVITY TORSIONAL LOADING

TORSION FROM	END TORSION	MID TORSION	EFF MRAD TORSION
WIND	0	0	0
GRAVITY	.25	.096	.096
ARITHMETIC-SUM MRAD TORSIONAL ERROR:			.096

(3). TORQUE TUBE + FLANGE - WIND AND GRAVITY LOAD BENDING:

TORQUE TUBE	DEF1, IN*10 ¹⁴	DEF2, IN*10 ¹⁴	MRAD BEND
WIND	0	0	0
GRAVITY	803	70	.873
VECTOR-SUM MRAD BENDING ERROR:			.756

(4). VECTOR-COMBINED BEAM & TORQUE TUBE BENDING & TORSION EFFECTS:

MIRROR MODULE	BEAM DEFLECTION MRAD ERROR	TORQUE TUBE TORSIONAL MRAD ERROR	TORQUE TUBE BENDING MRAD ERROR	VECTOR-SUM MRAD ERROR
#1	.141	.096	.756	.792
#2	.132	.096	.756	.789
#3	.08	.096	.756	.776
#4	.08	.096	.756	.756
#5	.132	.096	.756	.756
#6	.141	.096	.756	.757
TOTAL HELIOSTAT RMS MRAD ERROR:				.771

WIND ANGLE, = 70 DEG, WIND SPEED = 0 MPH

(1). BEAM BENDING EFFECT (GRAVITY & WIND):

MODULE	DEF1, IN*10 ⁴	DEF2, IN*10 ⁴	MRAD ERROR
#1	133	103	.153
#2	90	61	.143
#3	26	8	.087
#4	26	8	.087
#5	90	61	.143
#6	133	103	.153
HELIOSTAT-AVERAGE MRAD ERROR:			.127

(2). TORQUE TUBE - WIND AND GRAVITY TORSIONAL LOADING

TORSION FROM	END TORSION	MID TORSION	EFF MRAD TORSION
WIND	0	0	0
GRAVITY	.171	.066	.066
ARITHMETIC-SUM MRAD TORSIONAL ERROR:			.066

(3). TORQUE TUBE + FLANGE - WIND AND GRAVITY LOAD BENDING:

TORQUE TUBE	DEF1, IN*10 ⁴	DEF2, IN*10 ⁴	MRAD BEND
WIND	0	0	0
GRAVITY	803	70	.873
VECTOR-SUM MRAD BENDING ERROR:			.82

(4). VECTOR-COMBINED BEAM & TORQUE TUBE BENDING & TORSION EFFECTS:

MIRROR MODULE	BEAM DEFLECTION MRAD ERROR	TORQUE TUBE TORSIONAL MRAD ERROR	TORQUE TUBE BENDING MRAD ERROR	VECTOR-SUM MRAD ERROR
#1	.153	.066	.82	.848
#2	.143	.066	.82	.846
#3	.087	.066	.82	.834
#4	.087	.066	.82	.82
#5	.143	.066	.82	.823
#6	.153	.066	.82	.824
TOTAL HELIOSTAT RMS MRAD ERROR:				.832

WIND ANGLE, = 80 DEG, WIND SPEED = 0 MPH

(1). BEAM BENDING EFFECT (GRAVITY & WIND):

MODULE	DEF1, IN*10 ⁴	DEF2, IN*10 ⁴	MRAD ERROR
#1	140	108	.16
#2	94	64	.15
#3	27	9	.091
#4	27	9	.091
#5	94	64	.15
#6	140	108	.16
HELIOSTAT-AVERAGE MRAD ERROR:			.133

(2). TORQUE TUBE - WIND AND GRAVITY TORSIONAL LOADING

TORSION FROM	END TORSION	MID TORSION	EFF MRAD TORSION
WIND	0	0	0
GRAVITY	.087	.033	.033
ARITHMETIC-SUM MRAD TORSIONAL ERROR:			.033

(3). TORQUE TUBE + FLANGE - WIND AND GRAVITY LOAD BENDING:

TORQUE TUBE	DEF1, IN*10 ⁴	DEF2, IN*10 ⁴	MRAD BEND
WIND	0	0	0
GRAVITY	.803	.70	.873
VECTOR-SUM MRAD BENDING ERROR:			.86

(4). VECTOR-COMBINED BEAM & TORQUE TUBE BENDING & TORSION EFFECTS:

MIRROR MODULE	BEAM DEFLECTION MRAD ERROR	TORQUE TUBE TORSIONAL MRAD ERROR	TORQUE TUBE BENDING MRAD ERROR	VECTOR-SUM MRAD ERROR
#1	.16	.033	.86	.881
#2	.15	.033	.86	.879
#3	.091	.033	.86	.868
#4	.091	.033	.86	.861
#5	.15	.033	.86	.867
#6	.16	.033	.86	.869
TOTAL HELIOSTAT RMS MRAD ERROR:				.87

WIND ANGLE, = 90 DEG, WIND SPEED = 0 MPH

(1). BEAM BENDING EFFECT (GRAVITY & WIND):

MODULE	DEF1, IN*10 ¹⁴	DEF2, IN*10 ¹⁴	MRAD ERROR
#1	142	110	.162
#2	95	65	.152
#3	27	9	.093
#4	27	9	.093
#5	95	65	.152
#6	142	110	.162
HELIOSTAT-AVERAGE MRAD ERROR:			.135

(2). TORQUE TUBE - WIND AND GRAVITY TORSIONAL LOADING

TORSION FROM	END TORSION	MID TORSION	EFF MRAD TORSION
WIND	0	0	0
GRAVITY	-1E-03	-1E-03	-1E-03
ARITHMETIC-SUM MRAD TORSIONAL ERROR:			-1E-03

(3). TORQUE TUBE + FLANGE - WIND AND GRAVITY LOAD BENDING:

TORQUE TUBE	DEF1, IN*10 ¹⁴	DEF2, IN*10 ¹⁴	MRAD BEND
WIND	0	0	0
GRAVITY	803	70	.873
VECTOR-SUM MRAD BENDING ERROR:			.873

(4). VECTOR-COMBINED BEAM & TORQUE TUBE BENDING & TORSION EFFECTS:

MIRROR MODULE	BEAM DEFLECTION MRAD ERROR	TORQUE TUBE TORSIONAL MRAD ERROR	TORQUE TUBE BENDING MRAD ERROR	VECTOR-SUM MRAD ERROR
#1	.162	-1E-03	.873	.887
#2	.152	-1E-03	.873	.885
#3	.093	-1E-03	.873	.877
#4	.093	-1E-03	.873	.877
#5	.152	-1E-03	.873	.886
#6	.162	-1E-03	.873	.887
TOTAL HELIOSTAT RMS MRAD ERROR:				.883

TOTAL FIELD STATISTICAL SUMMARY:

FIELD RMS MRAD ERROR = .638

WIND ONLY (ZERO GRAVITY) MRAD ERROR ANALYSIS

INPUT WIND SPEED AT 30', MPH = 27

INPUT MIRROR MODULE WEIGHT, EACH, LB = 0

INPUT BEAM INERTIA, IN⁴ = 249

INPUT BEAM WEIGHT, LB/FT = 0

INPUT TORQUE TUBE LENGTH, INCHES = 110.38

INPUT TORQUE TUBE O.D., INCHES = 12.75

INPUT TORQUE TUBE WALL THICKNESS, INCHES = .25

TORQUE TUBE I.D., INCHES = 12.25

TORQUE TUBE BENDING INERTIA, INCHES⁴ = 191.82

TORQUE TUBE + FLANGE EQUIV BENDING INERTIA, INCHES⁴ = 168.43

TORQUE TUBE POLAR INERTIA, INCHES⁴ = 383.64

TORQUE TUBE WEIGHT LB/FT = 0

GRAVITY LOAD = 0, WIND ANGLE, = 0 DEG, WIND SPEED = 27 MPH

(1). BEAM BENDING EFFECT (GRAVITY & WIND):

MODULE	DEF1, IN*10 ⁴	DEF2, IN*10 ⁴	MRAD ERROR
#1	43	33	.049
#2	29	19	.046
#3	8	2	.029
#4	8	2	.029
#5	29	19	.046
#6	43	33	.049
HELIOSTAT-AVERAGE MRAD ERROR:			.041

(2). TORQUE TUBE - WIND AND GRAVITY TORSIONAL LOADING

TORSION FROM	END TORSION	MID TORSION	EFF MRAD TORSION
WIND	0	0	0
GRAVITY	0	0	0
ARITHMETIC-SUM MRAD TORSIONAL ERROR:			0

(3). TORQUE TUBE + FLANGE - WIND AND GRAVITY LOAD BENDING:

TORQUE TUBE	DEF1, IN*10 ⁴	DEF2, IN*10 ⁴	MRAD BEND
WIND	228	19	.248
GRAVITY	0	0	0
VECTOR-SUM MRAD BENDING ERROR:			.248

(4). VECTOR-COMBINED BEAM & TORQUE TUBE BENDING & TORSION EFFECTS:

MIRROR MODULE	BEAM DEFLECTION MRAD ERROR	TORQUE TUBE TORSIONAL MRAD ERROR	TORQUE TUBE BENDING MRAD ERROR	VECTOR-SUM MRAD ERROR
#1	.049	0	.248	.252
#2	.046	0	.248	.252
#3	.029	0	.248	.249
#4	.029	0	.248	.249
#5	.046	0	.248	.252
#6	.049	0	.248	.252
TOTAL HELIOSTAT RMS MRAD ERROR:				.251

GRAVITY LOAD = 0, WIND ANGLE, = 10 DEG, WIND SPEED = 27 MPH

(1). BEAM BENDING EFFECT (GRAVITY & WIND):

MODULE	DEF1, IN*10 ¹⁴	DEF2, IN*10 ¹⁴	MRAD ERROR
#1	49	38	.056
#2	33	22	.053
#3	9	3	.032
#4	7	2	.025
#5	25	17	.04
#6	37	28	.043
HELIOSTAT-AVERAGE MRAD ERROR:			.041

(2). TORQUE TUBE - WIND AND GRAVITY TORSIONAL LOADING

TORSION FROM	END TORSION	MID TORSION	EFF MRAD TORSION
WIND	.062	.024	.024
GRAVITY	0	0	0
ARITHMETIC-SUM MRAD TORSIONAL ERROR:			.024

(3). TORQUE TUBE + FLANGE - WIND AND GRAVITY LOAD BENDING:

TORQUE TUBE	DEF1, IN*10 ¹⁴	DEF2, IN*10 ¹⁴	MRAD BEND
WIND	228	19	.248
GRAVITY	0	0	0
VECTOR-SUM MRAD BENDING ERROR:			.248

(4). VECTOR-COMBINED BEAM & TORQUE TUBE BENDING & TORSION EFFECTS:

MIRROR MODULE	BEAM DEFLECTION MRAD ERROR	TORQUE TUBE TORSIONAL MRAD ERROR	TORQUE TUBE BENDING MRAD ERROR	VECTOR-SUM MRAD ERROR
#1	.056	.024	.248	.26
#2	.053	.024	.248	.259
#3	.032	.024	.248	.254
#4	.025	.024	.248	.248
#5	.04	.024	.248	.248
#6	.043	.024	.248	.248
TOTAL HELIOSTAT RMS MRAD ERROR:				.252

GRAVITY LOAD = 0, WIND ANGLE, = 20 DEG, WIND SPEED = 27 MPH

(1). BEAM BENDING EFFECT (GRAVITY & WIND):

MODULE	DEF1, IN*10 ⁴	DEF2, IN*10 ⁴	MRAD ERROR
#1	53	41	.061
#2	36	24	.057
#3	10	3	.035
#4	6	2	.023
#5	22	15	.036
#6	33	25	.039
HELIOSTAT-AVERAGE MRAD ERROR:			.041

(2). TORQUE TUBE - WIND AND GRAVITY TORSIONAL LOADING

TORSION FROM	END TORSION	MID TORSION	EFF MRAD TORSION
WIND	.102	.039	.039
GRAVITY	0	0	0
ARITHMETIC-SUM MRAD TORSIONAL ERROR:			.039

(3). TORQUE TUBE + FLANGE - WIND AND GRAVITY LOAD BENDING:

TORQUE TUBE	DEF1, IN*10 ⁴	DEF2, IN*10 ⁴	MRAD BEND
WIND	230	19	.25
GRAVITY	0	0	0
VECTOR-SUM MRAD BENDING ERROR:			.25

(4). VECTOR-COMBINED BEAM & TORQUE TUBE BENDING & TORSION EFFECTS:

MIRROR MODULE	BEAM DEFLECTION MRAD ERROR	TORQUE TUBE TORSIONAL MRAD ERROR	TORQUE TUBE BENDING MRAD ERROR	VECTOR-SUM MRAD ERROR
#1	.061	.039	.25	.269
#2	.057	.039	.25	.267
#3	.035	.039	.25	.26
#4	.023	.039	.25	.25
#5	.036	.039	.25	.25
#6	.039	.039	.25	.25
TOTAL HELIOSTAT RMS MRAD ERROR:				.257

GRAVITY LOAD = 0, WIND ANGLE, = 30 DEG, WIND SPEED = 27 MPH

(1). BEAM BENDING EFFECT (GRAVITY & WIND):

MODULE	DEF1, IN*10 ¹⁴	DEF2, IN*10 ¹⁴	MRAD ERROR
#1	57	44	.066
#2	38	26	.061
#3	11	3	.038
#4	6	2	.021
#5	20	14	.033
#6	30	23	.035
HELIOSTAT-AVERAGE MRAD ERROR:			.042

(2). TORQUE TUBE - WIND AND GRAVITY TORSIONAL LOADING

TORSION FROM	END TORSION	MID TORSION	EFF MRAD TORSION
WIND	.132	.051	.051
GRAVITY	0	0	0
ARITHMETIC-SUM MRAD TORSIONAL ERROR:			.051

(3). TORQUE TUBE + FLANGE - WIND AND GRAVITY LOAD BENDING:

TORQUE TUBE	DEF1, IN*10 ¹⁴	DEF2, IN*10 ¹⁴	MRAD BEND
WIND	231	19	.252
GRAVITY	0	0	0
VECTOR-SUM MRAD BENDING ERROR:			.252

(4). VECTOR-COMBINED BEAM & TORQUE TUBE BENDING & TORSION EFFECTS:

MIRROR MODULE	BEAM DEFLECTION MRAD ERROR	TORQUE TUBE TORSIONAL MRAD ERROR	TORQUE TUBE BENDING MRAD ERROR	VECTOR-SUM MRAD ERROR
#1	.066	.051	.252	.277
#2	.061	.051	.252	.275
#3	.038	.051	.252	.267
#4	.021	.051	.252	.253
#5	.033	.051	.252	.252
#6	.035	.051	.252	.252
TOTAL HELIOSTAT RMS MRAD ERROR:				.262

GRAVITY LOAD = 0, WIND ANGLE, = 40 DEG, WIND SPEED = 27 MPH

(1). BEAM BENDING EFFECT (GRAVITY & WIND):

MODULE	DEF1, IN*10 ¹⁴	DEF2, IN*10 ¹⁴	MRAD ERROR
#1	59	45	.068
#2	39	27	.063
#3	11	3	.039
#4	5	2	.02
#5	20	13	.031
#6	29	22	.034
HELIOSTAT-AVERAGE MRAD ERROR:			.042

(2). TORQUE TUBE - WIND AND GRAVITY TORSIONAL LOADING

TORSION FROM	END TORSION	MID TORSION	EFF MRAD TORSION
WIND	.148	.057	.057
GRAVITY	0	0	0
ARITHMETIC-SUM MRAD TORSIONAL ERROR:			.057

(3). TORQUE TUBE + FLANGE - WIND AND GRAVITY LOAD BENDING:

TORQUE TUBE	DEF1, IN*10 ¹⁴	DEF2, IN*10 ¹⁴	MRAD BEND
WIND	233	20	.254
GRAVITY	0	0	0
VECTOR-SUM MRAD BENDING ERROR:			.254

(4). VECTOR-COMBINED BEAM & TORQUE TUBE BENDING & TORSION EFFECTS:

MIRROR MODULE	BEAM DEFLECTION MRAD ERROR	TORQUE TUBE TORSIONAL MRAD ERROR	TORQUE TUBE BENDING MRAD ERROR	VECTOR-SUM MRAD ERROR
#1	.068	.057	.254	.283
#2	.063	.057	.254	.28
#3	.039	.057	.254	.271
#4	.02	.057	.254	.256
#5	.031	.057	.254	.255
#6	.034	.057	.254	.255
TOTAL HELIOSTAT RMS MRAD ERROR:				.266

GRAVITY LOAD = 0, WIND ANGLE, = 50 DEG, WIND SPEED = 27 MPH

(1). BEAM BENDING EFFECT (GRAVITY & WIND):

MODULE	DEF1, IN*10 ¹⁴	DEF2, IN*10 ¹⁴	MRAD ERROR
#1	60	46	.069
#2	40	27	.065
#3	11	3	.04
#4	5	1	.018
#5	17	12	.028
#6	26	20	.031
HELIOSTAT-AVERAGE MRAD ERROR:			.041

(2). TORQUE TUBE - WIND AND GRAVITY TORSIONAL LOADING

TORSION FROM	END TORSION	MID TORSION	EFF MRAD TORSION
WIND	.169	.065	.065
GRAVITY	0	0	0
ARITHMETIC-SUM MRAD TORSIONAL ERROR:			.065

(3). TORQUE TUBE + FLANGE - WIND AND GRAVITY LOAD BENDING:

TORQUE TUBE	DEF1, IN*10 ¹⁴	DEF2, IN*10 ¹⁴	MRAD BEND
WIND	233	19	.253
GRAVITY	0	0	0
VECTOR-SUM MRAD BENDING ERROR:			.253

(4). VECTOR-COMBINED BEAM & TORQUE TUBE BENDING & TORSION EFFECTS:

MIRROR MODULE	BEAM DEFLECTION MRAD ERROR	TORQUE TUBE TORSIONAL MRAD ERROR	TORQUE TUBE BENDING MRAD ERROR	VECTOR-SUM MRAD ERROR
#1	.069	.065	.253	.286
#2	.065	.065	.253	.284
#3	.04	.065	.253	.273
#4	.018	.065	.253	.257
#5	.028	.065	.253	.255
#6	.031	.065	.253	.255
TOTAL HELIOSTAT RMS MRAD ERROR:				.268

GRAVITY LOAD = 0, WIND ANGLE, = 60 DEG, WIND SPEED = 27 MPH

(1). BEAM BENDING EFFECT (GRAVITY & WIND):

MODULE	DEF1, IN*10 ¹⁴	DEF2, IN*10 ¹⁴	MRAD ERROR
#1	60	46	.069
#2	40	27	.065
#3	11	3	.039
#4	4	1	.014
#5	13	9	.021
#6	19	15	.024
HELIOSTAT-AVERAGE MRAD ERROR:			.038

(2). TORQUE TUBE - WIND AND GRAVITY TORSIONAL LOADING

TORSION FROM	END TORSION	MID TORSION	EFF MRAD TORSION
WIND	.198	.076	.076
GRAVITY	0	0	0
ARITHMETIC-SUM MRAD TORSIONAL ERROR:			.076

(3). TORQUE TUBE + FLANGE - WIND AND GRAVITY LOAD BENDING:

TORQUE TUBE	DEF1, IN*10 ¹⁴	DEF2, IN*10 ¹⁴	MRAD BEND
WIND	218	18	.237
GRAVITY	0	0	0
VECTOR-SUM MRAD BENDING ERROR:			.237

(4). VECTOR-COMBINED BEAM & TORQUE TUBE BENDING & TORSION EFFECTS:

MIRROR MODULE	BEAM DEFLECTION MRAD ERROR	TORQUE TUBE TORSIONAL MRAD ERROR	TORQUE TUBE BENDING MRAD ERROR	VECTOR-SUM MRAD ERROR
#1	.069	.076	.237	.277
#2	.065	.076	.237	.275
#3	.039	.076	.237	.263
#4	.014	.076	.237	.245
#5	.021	.076	.237	.243
#6	.024	.076	.237	.242
TOTAL HELIOSTAT RMS MRAD ERROR:				.257

GRAVITY LOAD = 0, WIND ANGLE, = 70 DEG, WIND SPEED = 27 MPH

(1). BEAM BENDING EFFECT (GRAVITY & WIND):

MODULE	DEF1, IN*10 ¹⁴	DEF2, IN*10 ¹⁴	MRAD ERROR
#1	59	46	.069
#2	40	27	.065
#3	11	3	.039
#4	2	0	8E-03
#5	7	5	.012
#6	10	8	.014
HELIOSTAT-AVERAGE MRAD ERROR:			.034

(2). TORQUE TUBE - WIND AND GRAVITY TORSIONAL LOADING

TORSION FROM	END TORSION	MID TORSION	EFF MRAD TORSION
WIND	.245	.094	.094
GRAVITY	0	0	0
ARITHMETIC-SUM MRAD TORSIONAL ERROR:			.094

(3). TORQUE TUBE + FLANGE - WIND AND GRAVITY LOAD BENDING:

TORQUE TUBE	DEF1, IN*10 ¹⁴	DEF2, IN*10 ¹⁴	MRAD BEND
WIND	172	14	.187
GRAVITY	0	0	0
VECTOR-SUM MRAD BENDING ERROR:			.187

(4). VECTOR-COMBINED BEAM & TORQUE TUBE BENDING & TORSION EFFECTS:

MIRROR MODULE	BEAM DEFLECTION MRAD ERROR	TORQUE TUBE TORSIONAL MRAD ERROR	TORQUE TUBE BENDING MRAD ERROR	VECTOR-SUM MRAD ERROR
#1	.069	.094	.187	.248
#2	.065	.094	.187	.245
#3	.039	.094	.187	.229
#4	8E-03	.094	.187	.206
#5	.012	.094	.187	.204
#6	.014	.094	.187	.203
TOTAL HELIOSTAT RMS MRAD ERROR:				.223

GRAVITY LOAD = 0, WIND ANGLE, = 80 DEG, WIND SPEED = 27 MPH

(1). BEAM BENDING EFFECT (GRAVITY & WIND):

MODULE	DEF1, IN*10 ¹⁴	DEF2, IN*10 ¹⁴	MRAD ERROR
#1	34	26	.04
#2	23	15	.038
#3	6	2	.022
#4	0	0	2E-03
#5	1	0	3E-03
#6	2	1	3E-03
HELIOSTAT-AVERAGE MRAD ERROR:			.018

(2). TORQUE TUBE - WIND AND GRAVITY TORSIONAL LOADING

TORSION FROM	END TORSION	MID TORSION	EFF MRAD TORSION
WIND	.163	.063	.063
GRAVITY	0	0	0
ARITHMETIC-SUM MRAD TORSIONAL ERROR:			.063

(3). TORQUE TUBE + FLANGE - WIND AND GRAVITY LOAD BENDING:

TORQUE TUBE	DEF1, IN*10 ¹⁴	DEF2, IN*10 ¹⁴	MRAD BEND
WIND	75	6	.082
GRAVITY	0	0	0
VECTOR-SUM MRAD BENDING ERROR:			.082

(4). VECTOR-COMBINED BEAM & TORQUE TUBE BENDING & TORSION EFFECTS:

MIRROR MODULE	BEAM DEFLECTION MRAD ERROR	TORQUE TUBE TORSIONAL MRAD ERROR	TORQUE TUBE BENDING MRAD ERROR	VECTOR-SUM MRAD ERROR
#1	.04	.063	.082	.131
#2	.038	.063	.082	.13
#3	.022	.063	.082	.118
#4	2E-03	.063	.082	.102
#5	3E-03	.063	.082	.102
#6	3E-03	.063	.082	.102
TOTAL HELIOSTAT RMS MRAD ERROR:				.114

GRAVITY LOAD = 0, WIND ANGLE, = 90 DEG, WIND SPEED = 27 MPH

(1). BEAM BENDING EFFECT (GRAVITY & WIND):

MODULE	DEF1, IN*10 ¹⁴	DEF2, IN*10 ¹⁴	MRAD ERROR
#1	0	0	1E-03
#2	0	0	1E-03
#3	0	0	1E-03
#4	0	0	1E-03
#5	0	0	1E-03
#6	0	0	1E-03
HELIOSTAT-AVERAGE MRAD ERROR:			1E-03

(2). TORQUE TUBE - WIND AND GRAVITY TORSIONAL LOADING

TORSION FROM	END TORSION	MID TORSION	EFF MRAD TORSION
WIND	0	0	0
GRAVITY	0	0	0
ARITHMETIC-SUM MRAD TORSIONAL ERROR:			0

(3). TORQUE TUBE + FLANGE - WIND AND GRAVITY LOAD BENDING:

TORQUE TUBE	DEF1, IN*10 ¹⁴	DEF2, IN*10 ¹⁴	MRAD BEND
WIND	0	0	0
GRAVITY	0	0	0
VECTOR-SUM MRAD BENDING ERROR:			0

(4). VECTOR-COMBINED BEAM & TORQUE TUBE BENDING & TORSION EFFECTS:

MIRROR MODULE	BEAM DEFLECTION MRAD ERROR	TORQUE TUBE TORSIONAL MRAD ERROR	TORQUE TUBE BENDING MRAD ERROR	VECTOR-SUM MRAD ERROR
#1	1E-03	0	0	0
#2	1E-03	0	0	0
#3	1E-03	0	0	0
#4	1E-03	0	0	0
#5	1E-03	0	0	0
#6	1E-03	0	0	0
TOTAL HELIOSTAT RMS MRAD ERROR:				0

TOTAL FIELD STATISTICAL SUMMARY:

FIELD RMS MRAD ERROR = .23

WIND & GRAVITY MRAD ERROR ANALYSIS

INPUT WIND SPEED AT 30', MPH = 27

INPUT MIRROR MODULE WEIGHT, EACH, LB = 199.2

INPUT BEAM INERTIA, IN⁴ = 249

INPUT BEAM WEIGHT, LB/FT = 6.65

INPUT TORQUE TUBE LENGTH, INCHES = 110.38

INPUT TORQUE TUBE O.D., INCHES = 12.75

INPUT TORQUE TUBE WALL THICKNESS, INCHES = .25

TORQUE TUBE I.D., INCHES = 12.25

TORQUE TUBE BENDING INERTIA, INCHES⁴ = 191.82

TORQUE TUBE + FLANGE EQUIV BENDING INERTIA, INCHES⁴ = 168.43

TORQUE TUBE POLAR INERTIA, INCHES⁴ = 383.64

TORQUE TUBE WEIGHT LB/FT = 33.34

WIND ANGLE, = 0 DEG, WIND SPEED = 27 MPH

(1). BEAM BENDING EFFECT (GRAVITY & WIND):

MODULE	DEF1, IN*10 ⁴	DEF2, IN*10 ⁴	MRAD ERROR
#1	43	33	.049
#2	29	19	.046
#3	8	2	.029
#4	8	2	.029
#5	29	19	.046
#6	43	33	.049
HELIOSTAT-AVERAGE MRAD ERROR:			.041

(2). TORQUE TUBE - WIND AND GRAVITY TORSIONAL LOADING

TORSION FROM	END TORSION	MID TORSION	EFF MRAD TORSION
WIND	0	0	0
GRAVITY	.501	.193	.193
ARITHMETIC-SUM MRAD TORSIONAL ERROR:			.193

(3). TORQUE TUBE + FLANGE - WIND AND GRAVITY LOAD BENDING:

TORQUE TUBE	DEF1, IN*10 ⁴	DEF2, IN*10 ⁴	MRAD BEND
WIND	228	19	.248
GRAVITY	803	70	.873
VECTOR-SUM MRAD BENDING ERROR:			.248

(4). VECTOR-COMBINED BEAM & TORQUE TUBE BENDING & TORSION EFFECTS:

MIRROR MODULE	BEAM DEFLECTION MRAD ERROR	TORQUE TUBE TORSIONAL MRAD ERROR	TORQUE TUBE BENDING MRAD ERROR	VECTOR-SUM MRAD ERROR
#1	.049	.193	.248	.346
#2	.046	.193	.248	.344
#3	.029	.193	.248	.332
#4	.029	.193	.248	.297
#5	.046	.193	.248	.288
#6	.049	.193	.248	.287
TOTAL HELIOSTAT RMS MRAD ERROR:				.316

WIND ANGLE, = 10 DEG, WIND SPEED = 27 MPH

(1). BEAM BENDING EFFECT (GRAVITY & WIND):

MODULE	DEF1, IN*10 ⁴	DEF2, IN*10 ⁴	MRAD ERROR
#1	73	57	.064
#2	49	34	.079
#3	14	4	.048
#4	12	4	.041
#5	41	28	.066
#6	61	47	.071
HELIOSTAT-AVERAGE MRAD ERROR:			.064

(2). TORQUE TUBE - WIND AND GRAVITY TORSIONAL LOADING

TORSION FROM	END TORSION	MID TORSION	EFF MRAD TORSION
WIND	.062	.024	.024
GRAVITY	.493	.19	.19
ARITHMETIC-SUM MRAD TORSIONAL ERROR:			.214

(3). TORQUE TUBE + FLANGE - WIND AND GRAVITY LOAD BENDING:

TORQUE TUBE	DEF1, IN*10 ⁴	DEF2, IN*10 ⁴	MRAD BEND
WIND	228	19	.248
GRAVITY	803	70	.873
VECTOR-SUM MRAD BENDING ERROR:			.4

(4). VECTOR-COMBINED BEAM & TORQUE TUBE BENDING & TORSION EFFECTS:

MIRROR MODULE	BEAM DEFLECTION MRAD ERROR	TORQUE TUBE TORSIONAL MRAD ERROR	TORQUE TUBE BENDING MRAD ERROR	VECTOR-SUM MRAD ERROR
#1	.084	.214	.4	.498
#2	.079	.214	.4	.495
#3	.048	.214	.4	.478
#4	.041	.214	.4	.436
#5	.066	.214	.4	.426
#6	.071	.214	.4	.425
TOTAL HELIOSTAT RMS MRAD ERROR:				.46

WIND ANGLE, = 20 DEG, WIND SPEED = 27 MPH

(1). BEAM BENDING EFFECT (GRAVITY & WIND):

MODULE	DEF1, IN*10 ⁴	DEF2, IN*10 ⁴	MRAD ERROR
#1	102	79	.117
#2	68	47	.109
#3	19	6	.067
#4	16	5	.054
#5	55	38	.088
#6	82	63	.094

HELIOSTAT-AVERAGE MRAD ERROR: .088

(2). TORQUE TUBE - WIND AND GRAVITY TORSIONAL LOADING

TORSION FROM	END TORSION	MID TORSION	EFF MRAD TORSION
WIND	.102	.039	.039
GRAVITY	.47	.181	.181

ARITHMETIC-SUM MRAD TORSIONAL ERROR: .221

(3). TORQUE TUBE + FLANGE - WIND AND GRAVITY LOAD BENDING:

TORQUE TUBE	DEF1, IN*10 ⁴	DEF2, IN*10 ⁴	MRAD BEND
WIND	230	19	.25
GRAVITY	803	70	.873

VECTOR-SUM MRAD BENDING ERROR: .549

(4). VECTOR-COMBINED BEAM & TORQUE TUBE BENDING & TORSION EFFECTS:

MIRROR MODULE	BEAM DEFLECTION MRAD ERROR	TORQUE TUBE TORSIONAL MRAD ERROR	TORQUE TUBE BENDING MRAD ERROR	VECTOR-SUM MRAD ERROR
#1	.117	.221	.549	.644
#2	.109	.221	.549	.64
#3	.067	.221	.549	.619
#4	.054	.221	.549	.574
#5	.088	.221	.549	.565
#6	.094	.221	.549	.563

TOTAL HELIOSTAT RMS MRAD ERROR: .601

WIND ANGLE, = 30 DEG, WIND SPEED = 27 MPH

(1). BEAM BENDING EFFECT (GRAVITY & WIND):

MODULE	DEF1, IN*10 ¹⁴	DEF2, IN*10 ¹⁴	MRAD ERROR
#1	128	99	.147
#2	86	59	.137
#3	25	8	.084
#4	20	6	.067
#5	68	47	.109
#6	101	78	.116
HELIOSTAT-AVERAGE MRAD ERROR:			.11

(2). TORQUE TUBE - WIND AND GRAVITY TORSIONAL LOADING

TORSION FROM	END TORSION	MID TORSION	EFF MRAD TORSION
WIND	.132	.051	.051
GRAVITY	.433	.167	.167
ARITHMETIC-SUM MRAD TORSIONAL ERROR:			.218

(3). TORQUE TUBE + FLANGE - WIND AND GRAVITY LOAD BENDING:

TORQUE TUBE	DEF1, IN*10 ¹⁴	DEF2, IN*10 ¹⁴	MRAD BEND
WIND	231	19	.252
GRAVITY	803	70	.873
VECTOR-SUM MRAD BENDING ERROR:			.689

(4). VECTOR-COMBINED BEAM & TORQUE TUBE BENDING & TORSION EFFECTS:

MIRROR MODULE	BEAM DEFLECTION MRAD ERROR	TORQUE TUBE TORSIONAL MRAD ERROR	TORQUE TUBE BENDING MRAD ERROR	VECTOR-SUM MRAD ERROR
#1	.147	.218	.689	.779
#2	.137	.218	.689	.775
#3	.084	.218	.689	.752
#4	.067	.218	.689	.705
#5	.109	.218	.689	.697
#6	.116	.218	.689	.696
TOTAL HELIOSTAT RMS MRAD ERROR:				.734

WIND ANGLE, = 40 DEG, WIND SPEED = 27 MPH

(1). BEAM BENDING EFFECT (GRAVITY & WIND):

MODULE	DEF1, IN*10 ⁴	DEF2, IN*10 ⁴	MRAD ERROR
#1	150	116	.172
#2	101	69	.161
#3	29	9	.098
#4	23	8	.079
#5	81	55	.129
#6	121	93	.138
HELIOSTAT-AVERAGE MRAD ERROR:			.129

(2). TORQUE TUBE - WIND AND GRAVITY TORSIONAL LOADING

TORSION FROM	END TORSION	MID TORSION	EFF MRAD TORSION
WIND	.148	.057	.057
GRAVITY	.383	.148	.148
ARITHMETIC-SUM MRAD TORSIONAL ERROR:			.205

(3). TORQUE TUBE + FLANGE - WIND AND GRAVITY LOAD BENDING:

TORQUE TUBE	DEF1, IN*10 ⁴	DEF2, IN*10 ⁴	MRAD BEND
WIND	233	20	.254
GRAVITY	803	70	.873
VECTOR-SUM MRAD BENDING ERROR:			.815

(4). VECTOR-COMBINED BEAM & TORQUE TUBE BENDING & TORSION EFFECTS:

MIRROR MODULE	BEAM DEFLECTION MRAD ERROR	TORQUE TUBE TORSIONAL MRAD ERROR	TORQUE TUBE BENDING MRAD ERROR	VECTOR-SUM MRAD ERROR
#1	.172	.205	.815	.897
#2	.161	.205	.815	.893
#3	.098	.205	.815	.869
#4	.079	.205	.815	.824
#5	.129	.205	.815	.818
#6	.138	.205	.815	.817
TOTAL HELIOSTAT RMS MRAD ERROR:				.853

WIND ANGLE, = 50 DEG, WIND SPEED = 27 MPH

(1). BEAM BENDING EFFECT (GRAVITY & WIND):

MODULE	DEF1, IN*10 ⁴	DEF2, IN*10 ⁴	MRAD ERROR
#1	169	131	.193
#2	114	78	.181
#3	33	11	.11
#4	26	8	.089
#5	91	62	.144
#6	135	104	.155
HELIOSTAT-AVERAGE MRAD ERROR:			.145

(2). TORQUE TUBE - WIND AND GRAVITY TORSIONAL LOADING

TORSION FROM	END TORSION	MID TORSION	EFF MRAD TORSION
WIND	.169	.065	.065
GRAVITY	.322	.124	.124
ARITHMETIC-SUM MRAD TORSIONAL ERROR:			.189

(3). TORQUE TUBE + FLANGE - WIND AND GRAVITY LOAD BENDING:

TORQUE TUBE	DEF1, IN*10 ⁴	DEF2, IN*10 ⁴	MRAD BEND
WIND	233	19	.253
GRAVITY	803	70	.873
VECTOR-SUM MRAD BENDING ERROR:			.922

(4). VECTOR-COMBINED BEAM & TORQUE TUBE BENDING & TORSION EFFECTS:

MIRROR MODULE	BEAM DEFLECTION MRAD ERROR	TORQUE TUBE TORSIONAL MRAD ERROR	TORQUE TUBE BENDING MRAD ERROR	VECTOR-SUM MRAD ERROR
#1	.193	.189	.922	.998
#2	.181	.189	.922	.993
#3	.11	.189	.922	.969
#4	.089	.189	.922	.927
#5	.144	.189	.922	.923
#6	.155	.189	.922	.922
TOTAL HELIOSTAT RMS MRAD ERROR:				.955

WIND ANGLE, = 60 DEG, WIND SPEED = 27 MPH

(1). BEAM BENDING EFFECT (GRAVITY & WIND):

MODULE	DEF1, IN*10 ¹⁴	DEF2, IN*10 ¹⁴	MRAD ERROR
#1	183	141	.209
#2	123	84	.196
#3	35	11	.119
#4	28	9	.094
#5	96	66	.152
#6	143	110	.164
HELIOSTAT-AVERAGE MRAD ERROR:			.155

(2). TORQUE TUBE - WIND AND GRAVITY TORSIONAL LOADING

TORSION FROM	END TORSION	MID TORSION	EFF MRAD TORSION
WIND	.198	.076	.076
GRAVITY	.25	.096	.096
ARITHMETIC-SUM MRAD TORSIONAL ERROR:			.173

(3). TORQUE TUBE + FLANGE - WIND AND GRAVITY LOAD BENDING:

TORQUE TUBE	DEF1, IN*10 ¹⁴	DEF2, IN*10 ¹⁴	MRAD BEND
WIND	218	18	.237
GRAVITY	803	70	.873
VECTOR-SUM MRAD BENDING ERROR:			.993

(4). VECTOR-COMBINED BEAM & TORQUE TUBE BENDING & TORSION EFFECTS:

MIRROR MODULE	BEAM DEFLECTION MRAD ERROR	TORQUE TUBE TORSIONAL MRAD ERROR	TORQUE TUBE BENDING MRAD ERROR	VECTOR-SUM MRAD ERROR
#1	.209	.173	.993	1.063
#2	.196	.173	.993	1.059
#3	.119	.173	.993	1.035
#4	.094	.173	.993	.996
#5	.152	.173	.993	.993
#6	.164	.173	.993	.993
TOTAL HELIOSTAT RMS MRAD ERROR:				1.023

WIND ANGLE, = 70 DEG, WIND SPEED = 27 MPH

(1). BEAM BENDING EFFECT (GRAVITY & WIND):

MODULE	DEF1, IN*10 ⁴	DEF2, IN*10 ⁴	MRAD ERROR
#1	193	149	.221
#2	130	88	.207
#3	37	12	.125
#4	28	9	.094
#5	97	66	.154
#6	144	111	.166
HELIOSTAT-AVERAGE MRAD ERROR:			.161

(2). TORQUE TUBE - WIND AND GRAVITY TORSIONAL LOADING

TORSION FROM	END TORSION	MID TORSION	EFF MRAD TORSION
WIND	.245	.094	.094
GRAVITY	.171	.066	.066
ARITHMETIC-SUM MRAD TORSIONAL ERROR:			.16

(3). TORQUE TUBE + FLANGE - WIND AND GRAVITY LOAD BENDING:

TORQUE TUBE	DEF1, IN*10 ⁴	DEF2, IN*10 ⁴	MRAD BEND
WIND	172	14	.187
GRAVITY	803	70	.873
VECTOR-SUM MRAD BENDING ERROR:			1.008

(4). VECTOR-COMBINED BEAM & TORQUE TUBE BENDING & TORSION EFFECTS:

MIRROR MODULE	BEAM DEFLECTION MRAD ERROR	TORQUE TUBE TORSIONAL MRAD ERROR	TORQUE TUBE BENDING MRAD ERROR	VECTOR-SUM MRAD ERROR
#1	.221	.16	1.008	1.077
#2	.207	.16	1.008	1.072
#3	.125	.16	1.008	1.047
#4	.094	.16	1.008	1.01
#5	.154	.16	1.008	1.008
#6	.166	.16	1.008	1.008
TOTAL HELIOSTAT RMS MRAD ERROR:				1.037

WIND ANGLE, = 80 DEG, WIND SPEED = 27 MPH

(1). BEAM BENDING EFFECT (GRAVITY & WIND):

MODULE	DEF1, IN*10 ¹⁴	DEF2, IN*10 ¹⁴	MRAD ERROR
#1	174	134	.2
#2	117	80	.187
#3	33	11	.113
#4	27	9	.093
#5	95	65	.152
#6	142	109	.163
HELIOSTAT-AVERAGE MRAD ERROR:			.151

(2). TORQUE TUBE - WIND AND GRAVITY TORSIONAL LOADING

TORSION FROM	END TORSION	MID TORSION	EFF MRAD TORSION
WIND	.163	.063	.063
GRAVITY	.087	.033	.033
ARITHMETIC-SUM MRAD TORSIONAL ERROR:			.096

(3). TORQUE TUBE + FLANGE - WIND AND GRAVITY LOAD BENDING:

TORQUE TUBE	DEF1, IN*10 ¹⁴	DEF2, IN*10 ¹⁴	MRAD BEND
WIND	75	6	.082
GRAVITY	803	70	.873
VECTOR-SUM MRAD BENDING ERROR:			.943

(4). VECTOR-COMBINED BEAM & TORQUE TUBE BENDING & TORSION EFFECTS:

MIRROR MODULE	BEAM DEFLECTION MRAD ERROR	TORQUE TUBE TORSIONAL MRAD ERROR	TORQUE TUBE BENDING MRAD ERROR	VECTOR-SUM MRAD ERROR
#1	.2	.096	.943	.988
#2	.187	.096	.943	.984
#3	.113	.096	.943	.965
#4	.093	.096	.943	.943
#5	.152	.096	.943	.944
#6	.163	.096	.943	.945
TOTAL HELIOSTAT RMS MRAD ERROR:				.961

WIND ANGLE, = 90 DEG, WIND SPEED = 27 MPH

(1). BEAM BENDING EFFECT (GRAVITY & WIND):

MODULE	DEF1, IN*10 ⁴	DEF2, IN*10 ⁴	MRAD ERROR
#1	142	110	.162
#2	95	65	.152
#3	27	9	.093
#4	27	9	.093
#5	95	65	.152
#6	142	110	.162
HELIOSTAT-AVERAGE MRAD ERROR:			.135

(2). TORQUE TUBE - WIND AND GRAVITY TORSIONAL LOADING

TORSION FROM	END TORSION	MID TORSION	EFF MRAD TORSION
WIND	0	0	0
GRAVITY	-1E-03	-1E-03	-1E-03
ARITHMETIC-SUM MRAD TORSIONAL ERROR:			-1E-03

(3). TORQUE TUBE + FLANGE - WIND AND GRAVITY LOAD BENDING:

TORQUE TUBE	DEF1, IN*10 ⁴	DEF2, IN*10 ⁴	MRAD BEND
WIND	0	0	0
GRAVITY	803	70	.873
VECTOR-SUM MRAD BENDING ERROR:			.873

(4). VECTOR-COMBINED BEAM & TORQUE TUBE BENDING & TORSION EFFECTS:

MIRROR MODULE	BEAM DEFLECTION MRAD ERROR	TORQUE TUBE TORSIONAL MRAD ERROR	TORQUE TUBE BENDING MRAD ERROR	VECTOR-SUM MRAD ERROR
#1	.162	-1E-03	.873	.887
#2	.152	-1E-03	.873	.885
#3	.093	-1E-03	.873	.877
#4	.093	-1E-03	.873	.877
#5	.152	-1E-03	.873	.886
#6	.162	-1E-03	.873	.887
TOTAL HELIOSTAT RMS MRAD ERROR:				.883

TOTAL FIELD STATISTICAL SUMMARY:

FIELD RMS MRAD ERROR = .817

9.5.2.3 Drive Unit Deflections

The attached analysis provides the drive unit deflections for the gravity-only case, the 27 mph wind-only case, and the combined gravity plus 27 mph wind case. A large portion of this analysis deals with the deflection of the ball bearings because it is believed that the bearings are the key to a stiff drive unit. The table on the following page summarizes the worst-case bearing deflections for both the azimuth and elevation axes. It should be noted that the design philosophy on treating gravity deflections such as the bearing deflections is to utilize the software and the mirror module canting/alignment fixture to remove these predictable deflections from the error category. The only error that would result is the error associated with the prediction, and with the correction technique.

ANALYSIS OF POINTING MISALIGNMENT DUE TO ELEVATION AND AZIMUTH BEARINGS

MISALIGNMENT SUMMARY - 27 MPH WIND AND GRAVITY

<u>CONDITION</u>	<u>BEARING</u>	<u>DIRECTION</u>	<u>MISALIGNMENT - RADIAN</u>		
			<u>TOTAL</u>	<u>GRAVITY</u>	<u>WIND</u>
(1E) HEL. 60° FROM VERT WIND 27 MPH $\alpha = 0$ (FRONTWIND)	ELEV	ELEV.	.00017	.00012	.00005
		AZIM.	.00078	.00069	.00010
(2E) HEL. 0° (VERT) WIND 27 MPH $\alpha = 70^\circ$ AZ. ELEV (FRONT OR BACKWIND)	ELEV	ELEV	.00015	.00015	0
		AZIM.	.00073	0	.00073
(1A) HEL. 60° FROM VERT 27 MPH WIND $\alpha = 0^\circ$ AZIM (BACKWIND)	AZIM	ELEV	.00091	.00075	.00016
		AZIM	0	0	0
(2A) HEL. 0° (VERT) 27 MPH $\alpha = 0^\circ$ AZIM (BACKWIND)	AZIM	ELEV	.00096	.00089	.00007
		AZIM	0	0	0
<u>COMBINED ELEV & AZIM BEARINGS *</u>					
(1) HEL. 60° FROM VERT 27 MPH $\alpha = 0^\circ$ AZIM (BACKWIND)	ELEV/AZIM	ELEV	.00108	.00087	.00021
		AZIM	.00078	.00069	.00010
(2) HEL. 0° (VERT) 27 MPH $\alpha = 70^\circ$ (BACKWIND)	ELEV/AZIM	ELEV	.00111	.00104	.00007
		AZIM	.00073	0	.00073

* CONDITIONS 1E & 1A WERE ENVELOPED - ALSO 2E AND 2A
E - 67

POINTING MISALIGNMENT DUE TO ELEVATION BEARING

CURVE DEVELOPMENT - ROTATION $\frac{1}{2}$ MOMENT AND
RADIAL LOAD FOR ELEVATION BEARING

ANGULAR MISALIGNMENT (DUE TO MOMENT ONLY)

USE METHOD ON PG 87, NEW DEPARTURE ENGG DATA,
ANALYSIS OF STRESSES AND DEFL., VOLUME 1, 1946.

ANGULAR CONTACT BEARING:

$$96 - \frac{1}{2}'' \text{ BALLS, } E = 17 \text{ IN, } f_o = f_i = .53, \beta_o' = \beta_o = 30^\circ, P_o = 0$$

$$B = .53 + .53 - 1 = .06$$

$$K = 180,000 \quad \text{CHART 57 VOL II}$$

$$Bd = .06(.5) = .03$$

$$\begin{aligned} R_i &= \frac{E}{2} + (f_i - .5)d \cos \beta_o' && \text{EQN 243} \\ &= \frac{17}{2} + (.53 - .5)(.5) \cos 30^\circ \\ &= 8.513 \end{aligned}$$

$$\left(\frac{\Sigma M}{E n d^2 K} \right) = \frac{M}{17 \times 96 \times .5^2 \times 180,000} = .0136 \times 10^{-6} \text{ M}$$

$$\frac{P_o}{Bd} = \frac{0}{.03} = 0$$

OBTAIN $\frac{\alpha R_i}{Bd}$ FROM CHART 70 VOL II

$$\alpha = \left(\frac{\alpha R_i}{Bd} \right) \frac{Bd}{R_i} = \left(\frac{\alpha R_i}{Bd} \right) \frac{.03}{8.513}$$

$$\alpha = .00352 \left(\frac{\alpha R_i}{Bd} \right)$$

ELEVATION BEARING (CONT)

<u>M</u>	$\left(\frac{\Sigma M}{E n d^2 K}\right)$	$\left(\frac{\alpha R_i}{B d}\right)$	<u>α</u>
20,000	.000272	.22	.000774
40,000	.000544	.264	.000929
60,000	.000816	.292	.001028
100,000	.00136	.333	.001172
200,000	.00272	.400	.001408

RADIAL DISPLACEMENT (DUE TO RADIAL LOAD)

$$\left(\frac{\Sigma V}{n d^2 K}\right) = \frac{\frac{1}{2} V}{96 (.5)^2 (180,000)} = .1157 \times 10^{-6} V \quad \left(\frac{1}{2} V \text{ IS PER FACE}\right)$$

$$\frac{h}{B d} = \frac{0}{B d} = 0$$

OBTAIN $\left(\frac{k}{B d}\right)$ FOR $\beta_0 = 25^\circ$ & $\beta_0 = 35^\circ$ CHARTS 63 & 64

AVERAGE THE VALUES

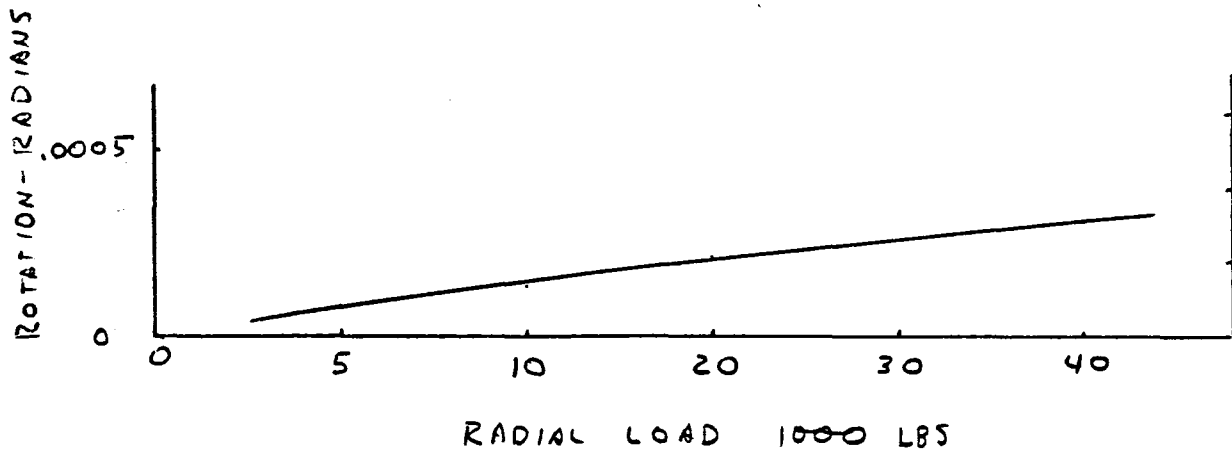
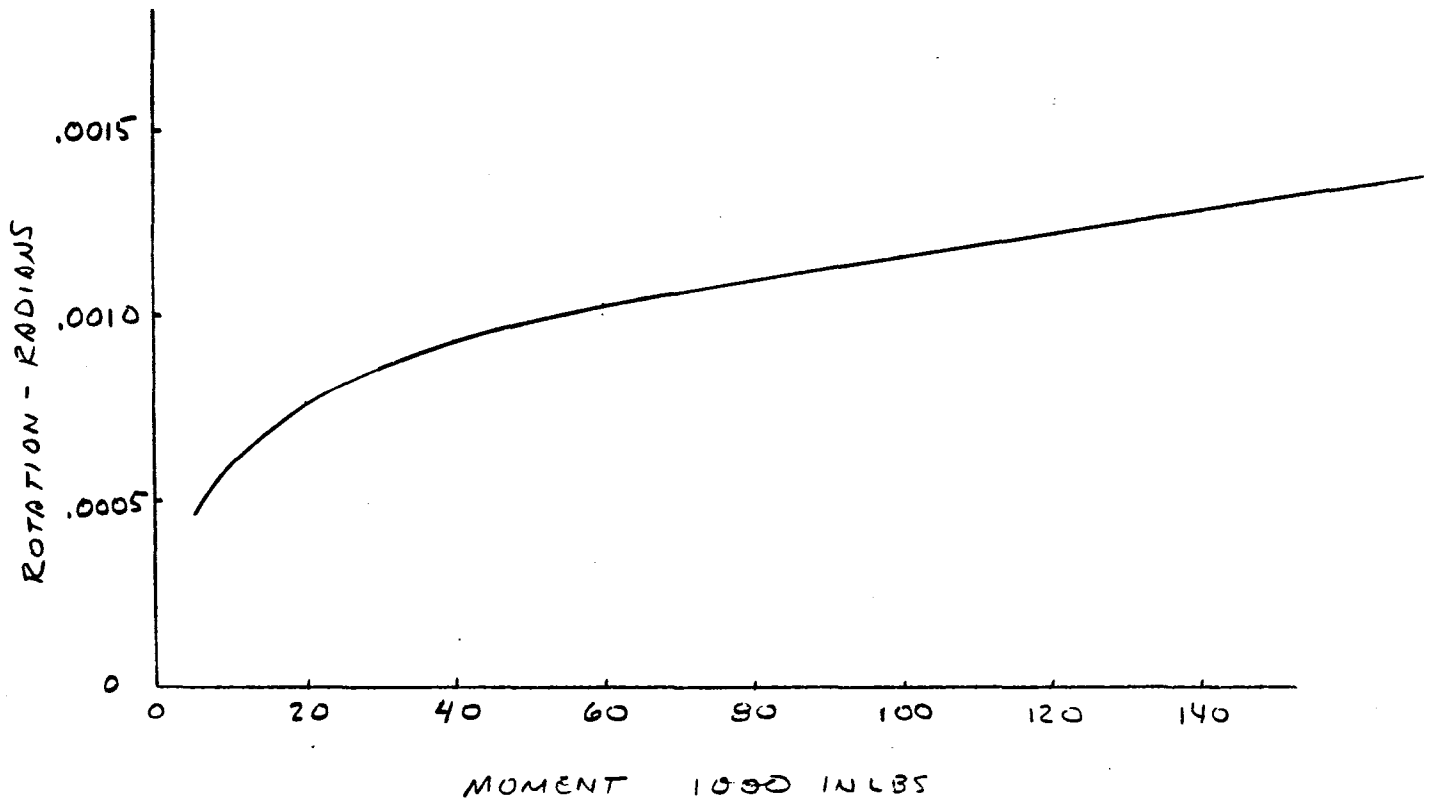
$$k = .03 \left(\frac{k}{B d}\right)_{\text{AVG}}$$

$$\alpha = \frac{k}{8.5}$$

ROTATION DUE TO BRG. RAD. DISPL.

<u>V</u>	$\left(\frac{\Sigma V}{n d^2 K}\right)$	$\left(\frac{k}{B d}\right)_{25^\circ}$	$\left(\frac{k}{B d}\right)_{35^\circ}$	$\left(\frac{k}{B d}\right)_{30^\circ}$	<u>k</u>	<u>α</u>
5,000	.00058	.0215	.026	.02375	.00071	.000084
10,000	.00116	.034	.040	.037	.00111	.00013
20,000	.00231	.055	.063	.059	.00177	.00021
40,000	.00463	.080	.098	.089	.00267	.00031

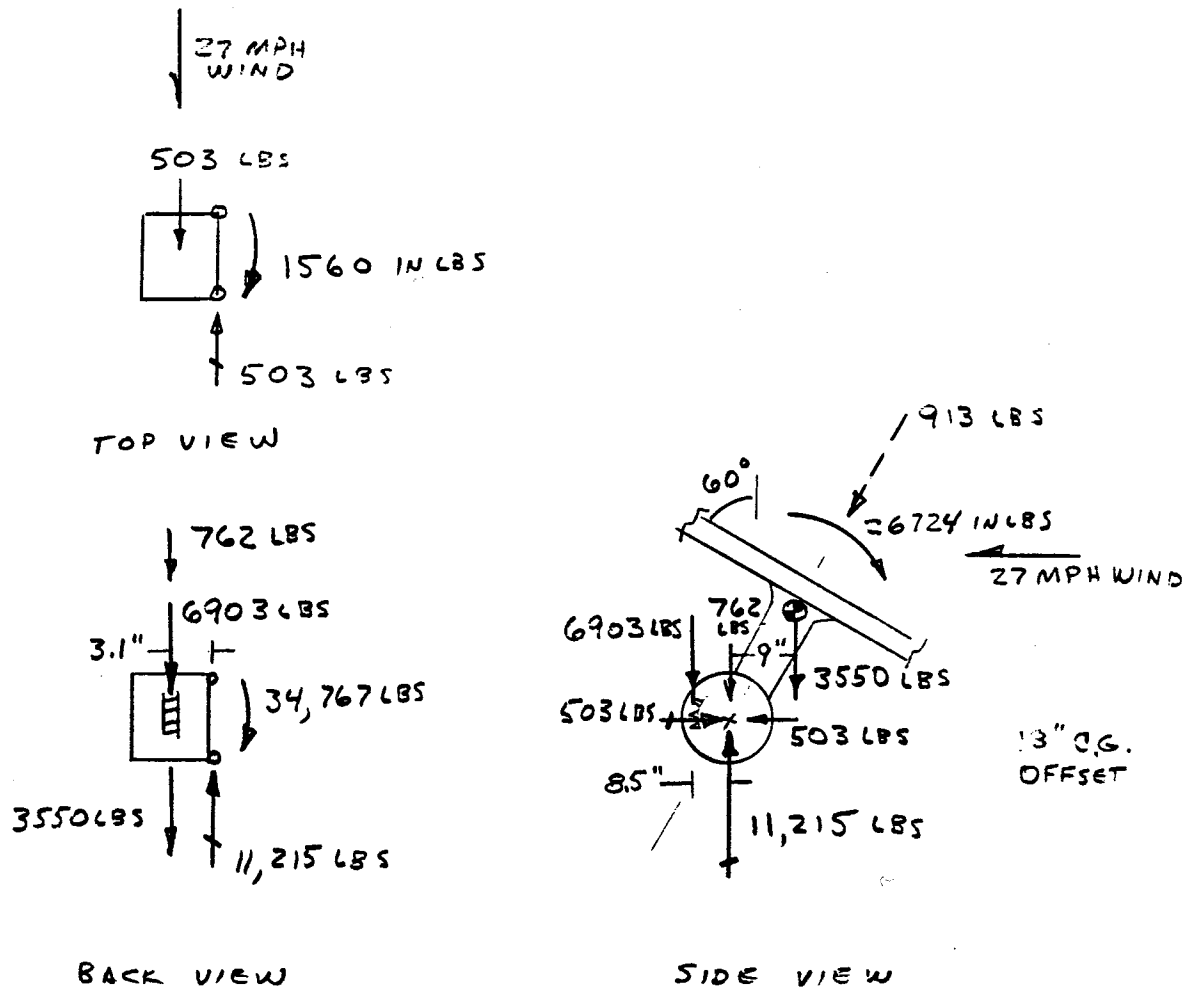
ELEVATION BEARING (CONT.)



POINTING MISALIGNMENT DUE TO ELEVATION BEARING

CONDITION 1E THE HELIOSTAT POSITIONED
 60° FROM VERTICAL AND A 27 MPH FRONT
 WIND AT 0° AZIMUTH ANGLE OF ATTACK

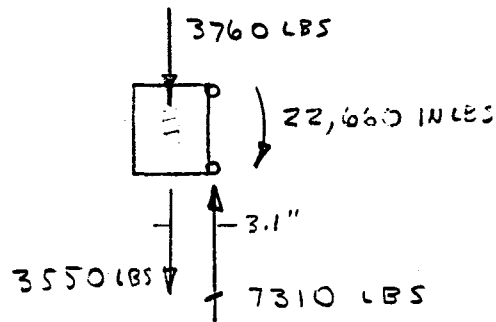
COMBINED WIND & GRAVITY LOADS



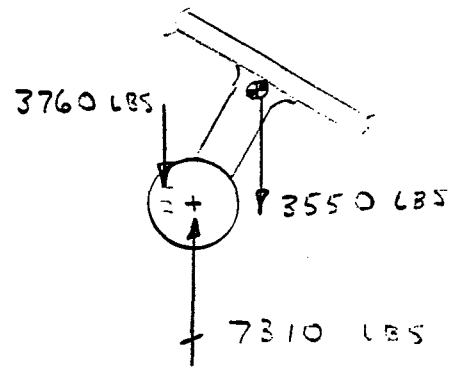
ELEVATION SKETCH (CONT)

THE MOMENT AND RADIAL REACTION
OF THE BEARINGS MAY BE NEGLECTED

GRAVITY ONLY LOADS



BACK VIEW



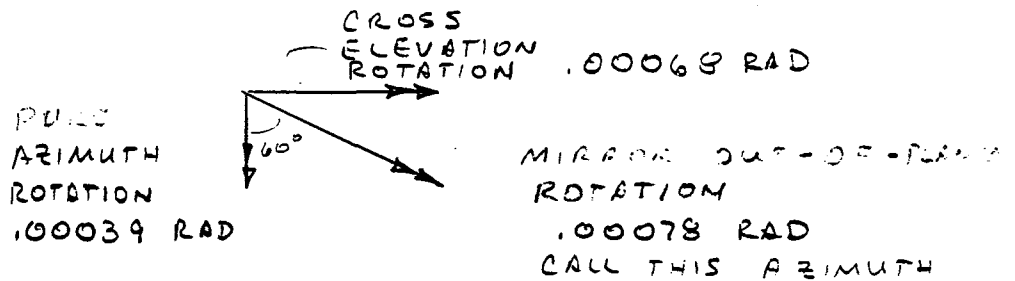
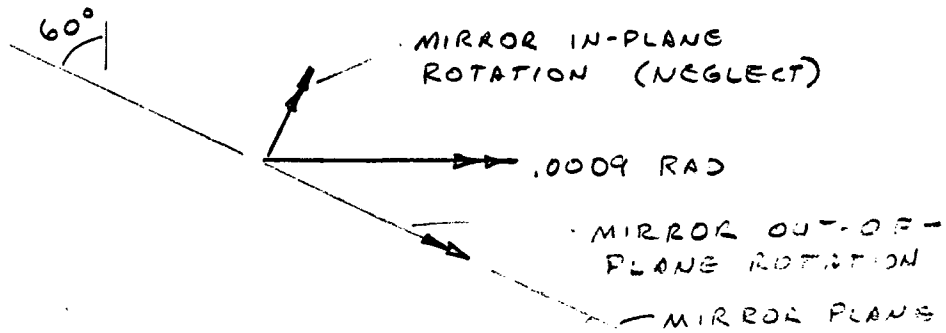
SIDE VIEW

ELEVATION BEARING (CONT.)

BEARING ROTATION DUE TO COMBINED WIND AND GRAVITY

$M = 34,767$ IN LBS

$\theta = .0009$ RAD. (ROTATION \propto MOMENT CURVE)



$R_{BV} = 11,215$ LBS

$\theta = .00017$ RAD (ROTATION \propto RADIAL LOAD CURVE)

ELEVATION ROTATION - PITCH FWD

ELEVATION BEARING (CONT.)

BEARING ROTATION DUE TO GRAVITY ONLY

$$M = 22,660 \text{ IN LBS}$$

$$\Theta = .00079 \text{ RAD}$$

ROTATION \propto MOMENT CURVE

$$\text{OUT-OF-PLANE ROTATION} = .00079 \sin 60^\circ = .00068 \text{ RAD}$$

CALL IT AZIMUTH

$$R_{BV} = 7310$$

$$\Theta = .00012 \text{ RAD}$$

POT. \propto FAL. LOAD CURVE

ELEV. ROT. - PITCH FWD

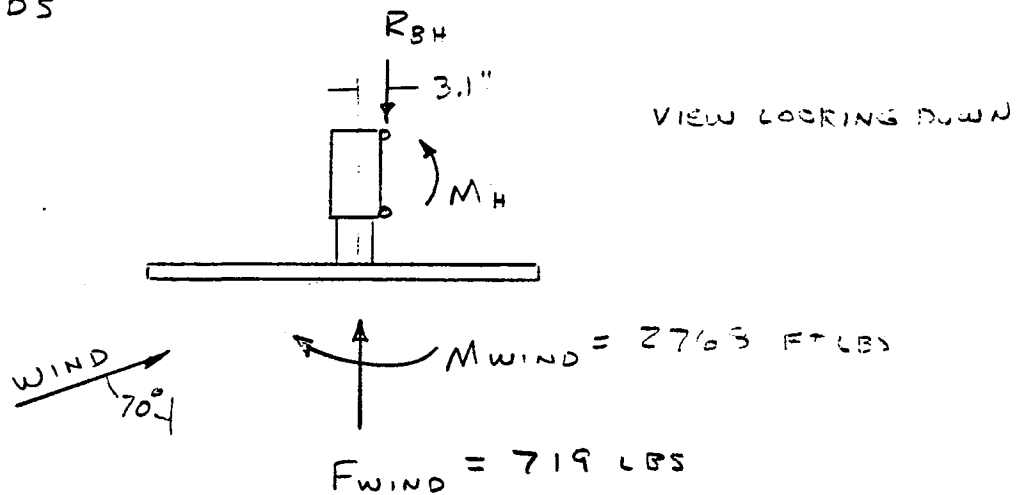
ELEVATION BEARING (CONT)

CONDITION 2E

THE HELIOSTAT

POSITIONED VERTICAL AND EXPERIENCING A 27 MPH WIND AT A 70° AZIMUTH ANGLE OF ATTACK.

WIND LOADS

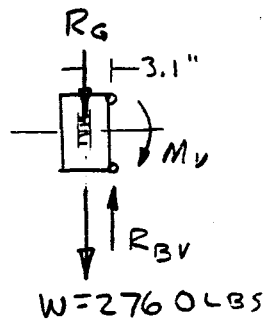


$$R_{BH} = 719 \text{ LBS}$$

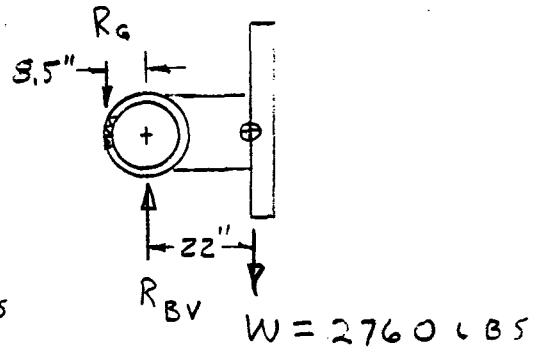
$$M_H = 2763 + \left(\frac{3.1}{12}\right) 719 = 2954 \text{ FT LBS}$$
$$= 35,445 \text{ IN LBS}$$

ELEVATION BEARING (CONT.)

GRAVITY LOADS



REAR VIEW



SIDE VIEW

$$R_G = \left(\frac{22}{8.5} \right) (2760) = 7144 \text{ LBS}$$

$$R_{BV} = 7144 + 2760 = 9904 \text{ LBS}$$

$$M_V = \left(\frac{3.1}{12} \right) (9904) = 2560 \text{ FT LBS}$$

$$= 30,720 \text{ IN LBS}$$

ELEVATION BEARING (CONT)

BEARING ROTATION DUE TO COMBINED WIND & GRAVITY

$$M = \sqrt{M_H^2 + M_V^2} = \sqrt{(35,445)^2 + (30,720)^2} = 46,900 \text{ IN LBS}$$

AT 41° FROM HORIZONTAL

$$\Theta = .00097 \text{ RAD} \quad \text{ROT. VS MOM CURVE}$$

ELEV. $\Theta = 0$ OUT-OF-PLANE

$$\text{AZIM } \Theta = .00097 \cos 41^\circ = .00073 \text{ RAD,}$$

$$R_{31} = 9904 \text{ LBS}$$

$$\Theta = .00015 \text{ RAD.} \quad \text{ROT VS RAD LOAD CURVE}$$

ELEV Θ - PITCH FWD

BEARING ROTATION DUE TO GRAVITY ONLY

WILL BE DUE ONLY TO RADIAL LOAD OF 9904 LBS

$$\Theta = .00015 \text{ RAD}$$

POINTING MISALIGNMENT DUE TO AZIMUTH BEARING

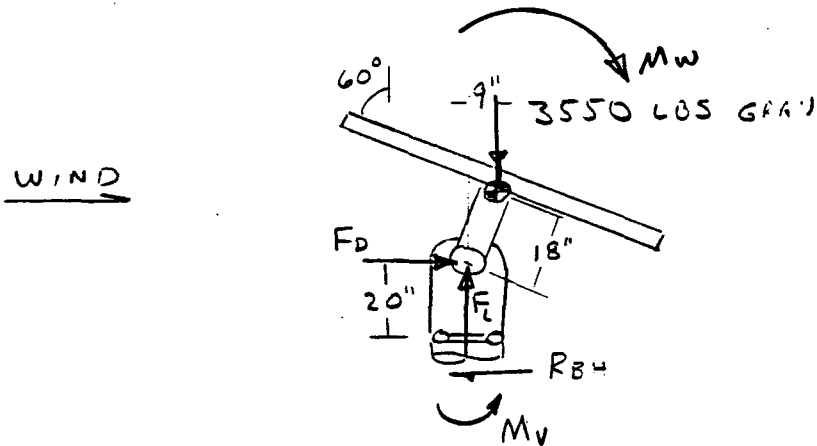
CONDITION 1A HELIOSTAT POSITION: 60° FROM VERTICAL.
27 MPH BACK WIND AT $\alpha = 0^\circ$ AZIM.

LOADS

$$F_D = 503 \text{ LBS}$$

$$F_L = 762 \text{ LBS}$$

$$M_{WIND} = 2227 \times 12 = 26724 \text{ IN LBS}$$



$$M_V = 20 \times 503 + 9 \times 3550 + 26724$$

$$= 68730 \text{ IN LBS} \quad \text{WIND \& GRAVITY}$$

$$M_V = 9 \times 3550 = 31950 \text{ IN LBS} \quad \text{GRAVITY}$$

AZIMUTH BEARING (CONT)

BEARING ROTATION DUE TO WIND & GRAVITY

BRG INFO (METHOD PG 97*):

106 - 1/2" BALLS, $f_o = f_i = .53$, $E = 18.8$, $\beta_o' = \beta_o = 30^\circ$, $P_o = 0$

$$B = .53 + .53 - 1 = .06$$

$$K = 180,000 \quad \text{CHART 57}$$

$$Bd = .06 (.5) = .03$$

$$\begin{aligned} R_i &= \frac{E}{2} + (f_i + .5)d \cos \beta_o' && \text{EQN 243} \\ &= \frac{18.8}{2} + (.53 + .5)(.5) \cos 30^\circ \\ &= 9.413 \end{aligned}$$

$$\frac{\Sigma M}{E n d^2 K} = \frac{63730}{18.8 \times 106 \times .5^2 \times 180000} = .000766$$

$$\frac{P_o}{Bd} = \frac{0}{.03} = 0$$

$$\frac{\alpha R_i}{Bd} = .287 \quad \text{CHART 70}$$

$$\alpha = \frac{.287 (.03)}{9.413} = .00091 \quad \text{RADIAN'S}$$

ELEV.

* NEW DEPARTURE

AZIMUTH BEARING (CONT)

BEARING ROTATION DUE TO GRAVITY

$$\frac{\Sigma M}{E n d^2 K} = .000766 \left(\frac{31950}{68730} \right) = .000356$$

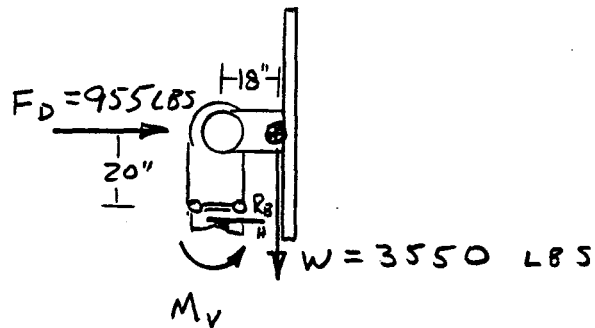
$$\frac{\alpha R_i}{B d} = .235 \quad \text{CHART 70}$$

$$\alpha = \frac{.235 (.03)}{7.414} = .00075 \quad \text{RAD. ELEV.}$$

AZIMUTH BEARING (CONT)

CONDITION 2A HELIOSTAT VERTICAL

27 MPH BACKWIND AT $\alpha = 0^\circ$ AZIM.



$$M_V = 18 \times 3550 + 20 \times 955$$

$$= 83,000 \text{ IN LBS} \quad \text{WIND \& GRAVITY}$$

$$M_V = 18 \times 3550$$

$$= 63,900 \text{ IN LBS} \quad \text{GRAVITY}$$

AZIMUTH BEARINGS (CONT.)

BEARING ROTATION DUE TO WIND & GRAVITY

$$\frac{\Sigma M}{E n d^2 K} = .000766 \left(\frac{83000}{68,730} \right) = .000925$$

$$\frac{\alpha R_i}{B d} = .3$$

$$\alpha = \frac{.3 (.03)}{9.413} = .00096 \text{ RAD}$$

ELEV

BEARING ROTATION DUE TO GRAVITY

$$\frac{\Sigma M}{E n d^2 K} = .000766 \left(\frac{68,730}{68,730} \right) = .000712$$

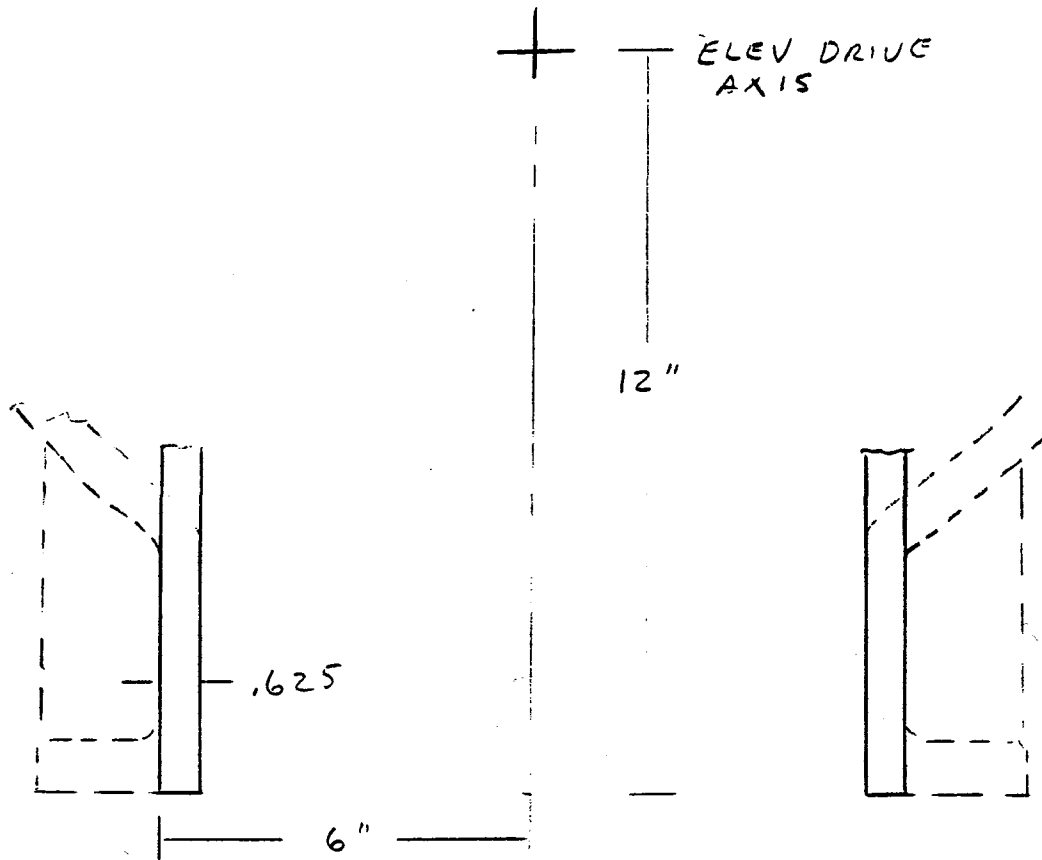
$$\frac{\alpha R_i}{B d} = .28$$

$$\alpha = \frac{.28 (.03)}{9.413} = .00089 \text{ RAD}$$

ELEV

DEFLECTION ANALYSIS - DRIVE HOUSINGS

ELEVATION DRIVE HOUSING BEAM PROPERTIES

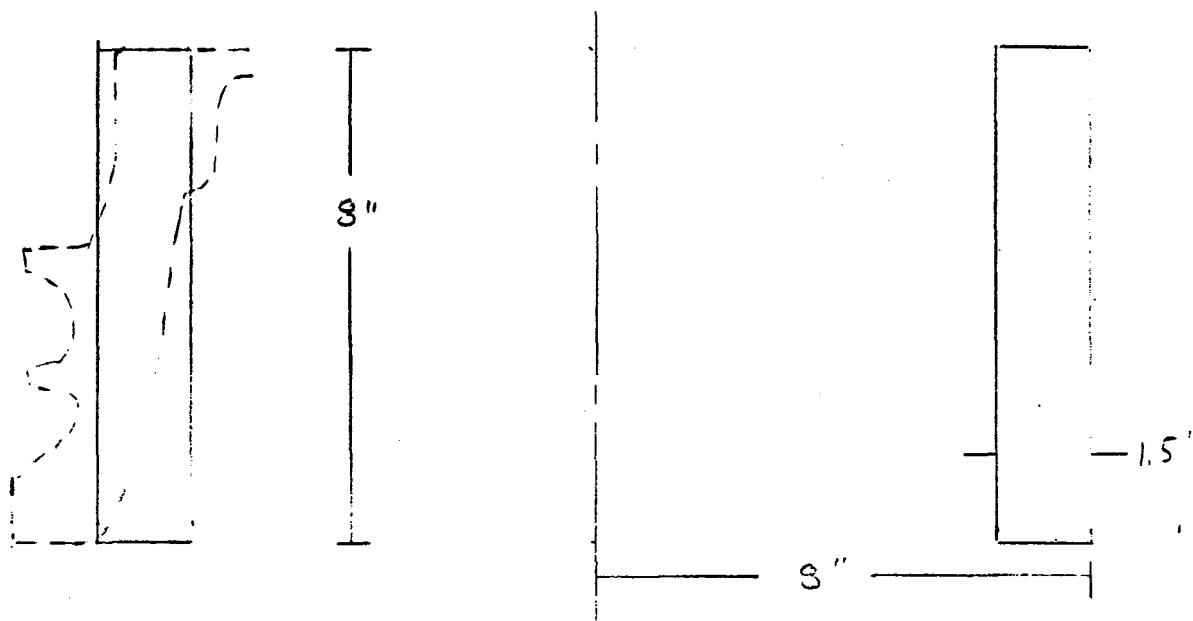


EQUIVALENT CYLINDER

$$A = \pi (6^2 - 5.375^2) = 22.3 \text{ IN}^2$$

$$I = \frac{\pi}{4} (6^4 - 5.375^4) = 362 \text{ IN}^4$$

AZIMUTH DRIVE GEAR HOUSING BEAM PROPERTIES

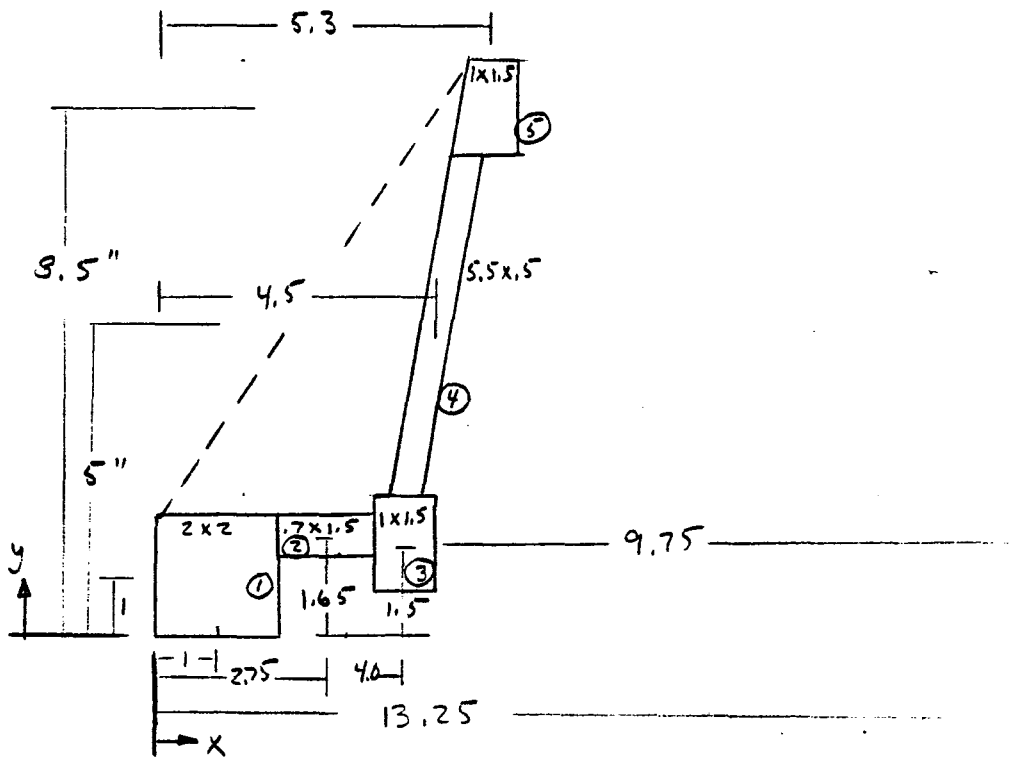


EQUIVALENT CYLINDER

$$A = \pi (8^2 - 6.5^2) = 68.3 \text{ in}^2$$

$$I = \frac{\pi}{4} (8^4 - 6.5^4) = 1815 \text{ in}^4$$

AZIMUTH DRIVE HOUSING RING PROPERTIES



	<u>A</u>	<u>y</u>	<u>Ay</u>	<u>Ay²</u>	<u>I_o</u>
1	4.0	1.0	4.0	4.0	1.333
2	1.05	1.65	1.733	2.859	.043
3	1.5	1.5	2.25	3.375	.281
4	2.75	5.0	13.75	68.75	6.932
5	1.5	8.5	12.75	108.375	.281
	<u>10.8</u>		<u>34.483</u>	<u>197.359</u>	<u>8.87</u>

$$\bar{y} = \frac{\sum Ay}{\sum A} = \frac{34.483}{10.8} = 3.2 \text{ IN}$$

$$I = \sum I_o + \sum Ay^2 - \frac{(\sum Ay)^2}{\sum A} = 8.87 + 197.359 - \frac{(34.483)^2}{10.8} = 96 \text{ IN}^4$$

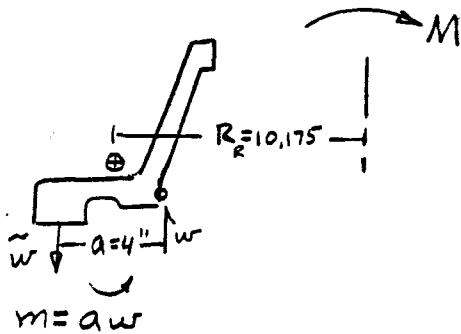
EFFECTIVE RADIUS

	<u>A</u>	<u>X</u>	<u>A X</u>
1	4.0	1.0	4.0
2	1.05	2.75	2.888
3	1.5	4.0	6.0
4	2.75	4.5	12.375
5	<u>1.5</u>	5.3	<u>7.95</u>
	10.8		33.213

$$\bar{X} = \frac{33.213}{10.8} = 3.075$$

$$R = 13.25 - 3.075 = 10.175$$

ROTATIONAL SPRING RATE (OF ARIMUTH DRIVE COUPLING)

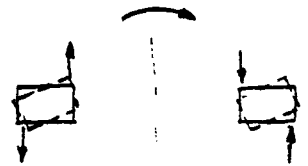


$$w = \frac{M}{\pi R^2}$$

$$m = a w = \frac{a M}{\pi R^2}$$

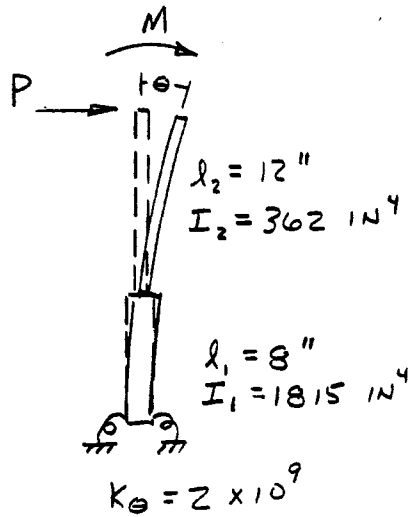
$$\theta = \frac{m R^2}{E I} = \frac{a M}{\pi E I}$$

$$K_{\theta} = \frac{M}{\theta} = \frac{\pi E I}{a}$$



$$K_{\theta} = \frac{\pi (30 \times 10^6) (86)}{4} = 2.03 \times 10^9 \frac{\text{IN LB}}{\text{RAD}}$$

INFLUENCE COEFFICIENTS - AZIMUTH & ELEVATION DRIVE



DUE TO M

$$\begin{aligned} \Theta &= \frac{M}{E} \left(\frac{l_1}{I_1} + \frac{l_2}{I_2} \right) + \frac{M}{K_\theta} \\ &= \frac{M}{30 \times 10^6} \left(\frac{8}{1815} + \frac{12}{362} \right) + \frac{M}{2 \times 10^9} \\ &= 1.75 \times 10^{-9} M \end{aligned}$$

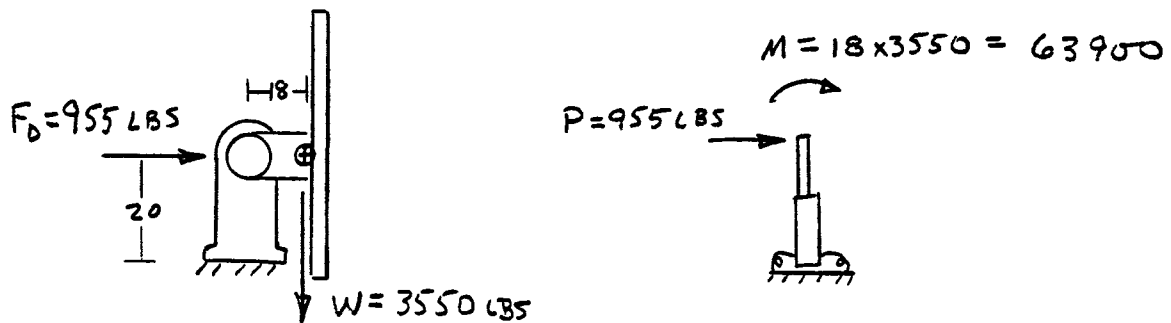
DUE TO P

$$\begin{aligned} \Theta &= \frac{P}{E} \left(\frac{l_1^2}{2I_1} + \frac{l_2 l_1}{I_1} + \frac{l_2^2}{2I_2} \right) + \frac{P(l_1 + l_2)}{K_\theta} \\ &= \frac{P}{30 \times 10^6} \left(\frac{8^2}{2 \times 1815} + \frac{12 \times 8}{1815} + \frac{12^2}{2 \times 362} \right) + \frac{P(12+8)}{2 \times 10^9} \\ &= (9 + 10) \times 10^{-9} P \\ &= 19 \times 10^{-9} P \end{aligned}$$

DRIVE DEFLECTIONS

CRITICAL DEFLECTION CONDITION

- o VERTICAL HELIOSTAT
- o 27 MPH BACK WIND



ROTATION DUE TO WIND & GRAVITY

$$\begin{aligned}\theta &= (1.75M + 19P)10^{-9} \\ &= (1.75 \times 63900 + 19 \times 955)10^{-9} \\ &= .00013 \text{ RADIAN}\end{aligned}$$

ROTATION DUE TO GRAVITY

$$\theta = 1.75 \times 10^{-9} (63900) = .00011 \text{ RADIAN}$$

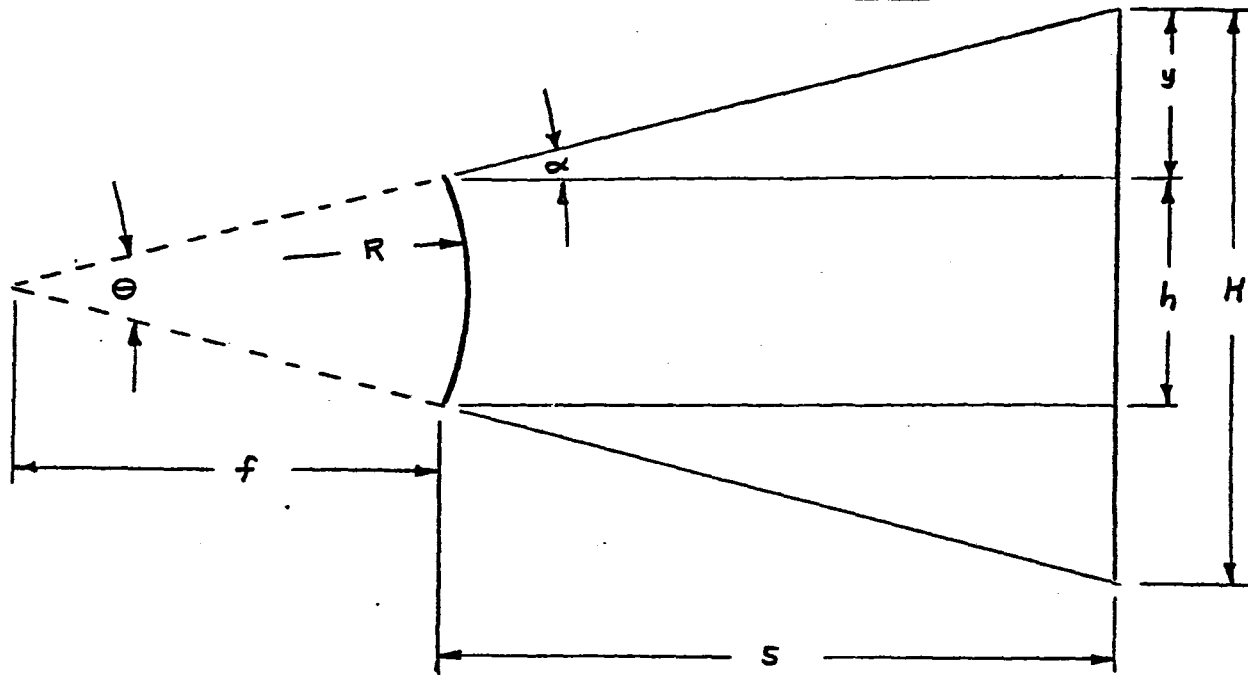
9.5.3 THERMAL CURVATURE AND STRESS

The subsection presents the derivation of mirror curvature effects. The first topic deals with the fringe angle effects for spherically curved convex and concave mirrors. The second topic is the thermal curvature and stress of a mirror module or mirror module substrate which is composed of three, layered materials; i.e., a tri-composite.

9.5.3.1 Beam Quality, Convex and Concave Mirrors

The following subsection presents the derivation of the appropriate equations for determining the fringe angle resulting from a mirror shape which is spherically convex or concave. The equations derived relate the fringe angle to the radius of curvature, slant range, and mirror size. The analysis method is based on the parallel-ray technique, and does not include the divergent real-sun effects, nor does it include any non-uniform or non-linear energy distributions within the reflected image.

BEAM QUALITY - CONVEX MIRROR



R = mirror radius of curvature

f = mirror focal length

s = slant range to target

h = mirror size

H = image size

y = fringe size

θ = focal angle

α = fringe angle

$$\alpha = \tan^{-1}(y/s) \approx y/s \text{ for small angles}$$

$$\alpha = \theta/2$$

$$\theta = 2 \tan^{-1}(h/2f) \approx h/f \text{ for small angles}$$

$$\text{But } f = R/2$$

$$\theta = 2h/f$$

$$\underline{\underline{\alpha = h/R}}$$

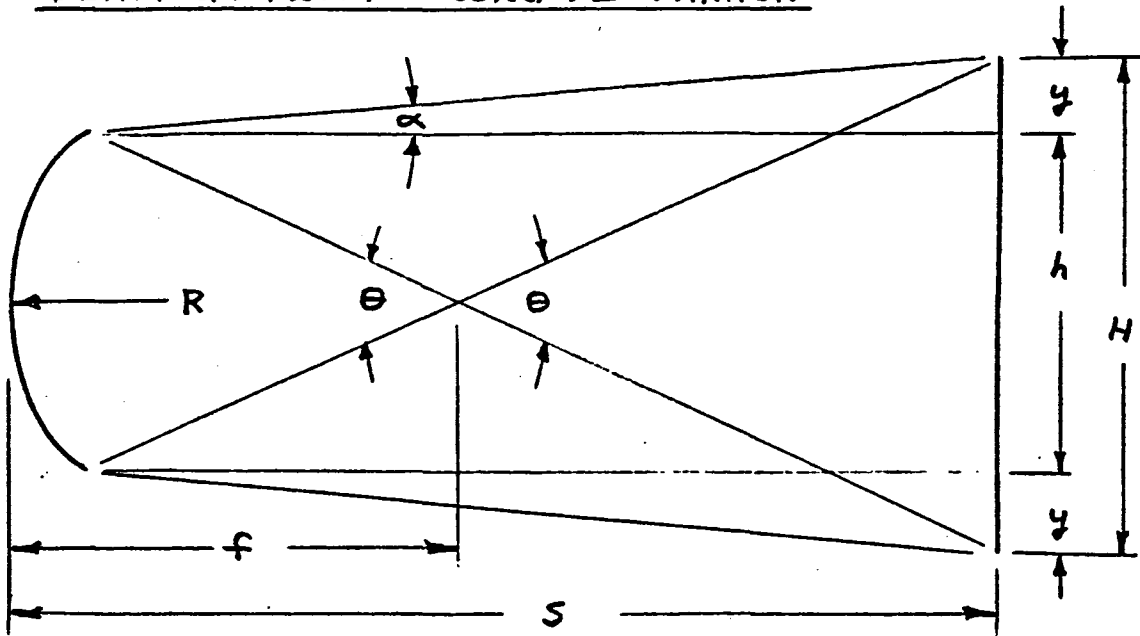
If $h = 12 \text{ ft}$, and the maximum α allowable is 1.4 mrad , the minimum permissible convex radius of curvature is :

$$R = h/\alpha$$

$$R = 12 / .0014$$

$$\underline{\underline{R = 8571 \text{ ft (convex)}}}$$

BEAM QUALITY - CONCAVE MIRROR



R = mirror radius of curvature

f = mirror focal length

s = slant range to target

h = mirror size

H = image size

y = fringe size

Θ = focal angle

α = fringe angle

$$1). \alpha = \tan^{-1}(y/s) \approx y/s \text{ for small angles}$$

$$2). \theta = 2 \tan^{-1}(h/2f) \approx h/f \text{ for small angles}$$

$$3). \theta = 2 \tan^{-1}[H/2(s-f)] \approx H/(s-f) \text{ for small angles}$$

Combining 2). and 3).

$$4). H = \frac{s-f}{f} \cdot h$$

$$5). y = \frac{H-h}{2} = \frac{h}{2} \left(\frac{s-f}{f} - 1 \right)$$

$$6). \alpha = y/s = \frac{h}{2s} \left(\frac{s-f-f}{f} \right) = \frac{h}{2s} \left(\frac{s}{f} - 2 \right)$$

$$\text{Since } f = R/2$$

$$7). \alpha = \frac{h}{2s} \left(\frac{2s}{R} - 2 \right)$$

$$\underline{\underline{\alpha = h \left(\frac{1}{R} - \frac{1}{s} \right)}} \quad \text{for } R < s$$

If $h = 12$ ft and the maximum slant range is 2500 ft, the minimum allowable convex curvature for a 1.4 mrad fringe angle is:

$$R = 1 / \left(\frac{\alpha}{h} + 1/s \right)$$

$$R = 1 / (.0014/12 + 1/2500)$$

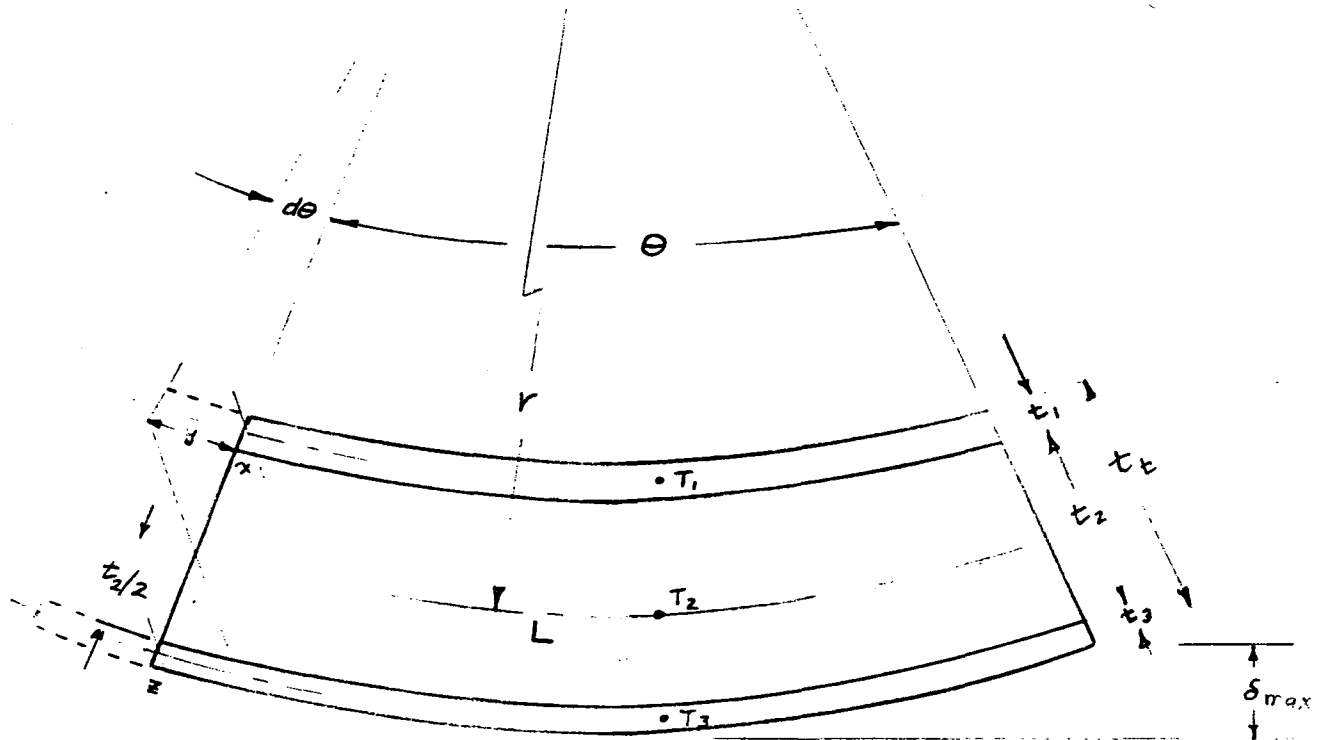
$$\underline{\underline{R = 1935 \text{ ft (concave)}}}$$

9.5.3.2 Thermal Curvature for Tri-Composites

In this subsection the thermally-induced curvature and stress analyses are presented for a mirror module or mirror module substrate which is composed of three, layered materials; i.e., a tri-composite. The equations derived herein have been incorporated into a Northrup computer code known as "MMOD". A thermal analyzer routine is also included in this program, so a complete temperature, curvature, and stress analysis can be performed for essentially any mirror module design, and any combination of ambient temperature, convective wind, solar heat flux, and mirror absorptance conditions.

TPI-COMPOSITE THERMAL CURVATURE

FIGURE 1



L = length, inches

t = layer thickness, inches

T = layer average temperature, $^{\circ}\text{F}$

I = moment of inertia about own neutral axis per unit of width, in^4/in

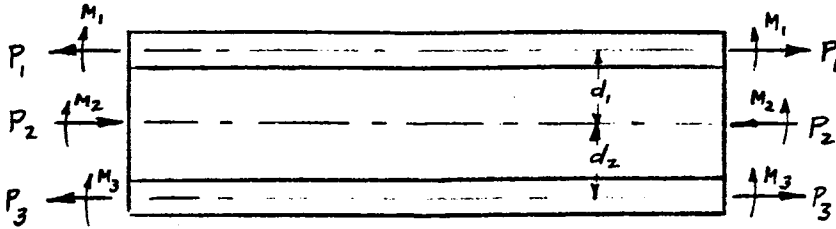
α = coefficient of thermal expansion, $\text{in}/\text{in}-^{\circ}\text{F}$

ΔT = temperature change referenced from the assembly temperature, $^{\circ}\text{F}$

A = cross section area per unit width, in^2/in

E = modulus of elasticity, lb/in^2

FIGURE 2



$$\sum F_x = 0, \quad (1). \quad P_1 + P_3 = P_2$$

$$\sum M_{P_2} = 0, \quad (2). \quad M_1 + M_2 + M_3 + P_3 \cdot d_2 - P_1 \cdot d_1 = 0$$

The bending moments required to produce the curvature of radius, r , shown in Figure 1 are :

$$(3). \quad M_1 = E_1 I_1 / r$$

$$(4). \quad M_2 = E_2 I_2 / r$$

$$(5). \quad M_3 = E_3 I_3 / r$$

Combining these moment equations with eq. (2) gives :

$$(6). \quad E_1 I_1 + E_2 I_2 + E_3 I_3 = r (P_1 \cdot d_1 - P_3 \cdot d_2)$$

At the bond lines, the elongation of the three layers due to thermal expansion are :

$$(7). \quad \epsilon_{T_1} = + \alpha_1 (T_1 - T_{ref}) = + \alpha_1 \Delta T_1$$

$$(8). \quad \epsilon_{T_2} = + \alpha_2 (T_2 - T_{ref}) = + \alpha_2 \Delta T_2$$

$$(9). \quad \epsilon_{T_3} = + \alpha_3 (T_3 - T_{ref}) = + \alpha_3 \Delta T_3$$

where T_{ref} is the reference assembly temperature, and the (+) sign denotes thermal growth if $T > T_{ref}$.

The elongation (+ or -) of the layers due to the induced compressive (-) or tensile (+) forces are given by the following :

$$\epsilon = \frac{\text{stress}}{E} = \frac{P}{A \cdot E}$$

But since we are working with a unit width, $A = t$

$$(10) \epsilon_{P_1} = +P_1 / t_1 \cdot E_1$$

$$(11) \epsilon_{P_2} = -P_2 / t_2 \cdot E_2$$

$$(12) \epsilon_{P_3} = +P_3 / t_3 \cdot E_3$$

The elongation due to bending (refer to Figure 1) at each of the bond line interfaces is given by :

Bending at the Bond Line 1-2

$$L = r \cdot \theta$$

$$L + y = (r - t_2/2) \cdot \theta$$

$$L + y = r \cdot \theta - (t_2/2) \cdot \theta$$

$$\text{Since } L = r \cdot \theta, \text{ or } \theta = L/r$$

$$L + y = L - (t_2/2) \cdot (L/r)$$

$$y = - (t_2/2) \cdot (L/r)$$

$$\text{But } \epsilon = y/L, \text{ so}$$

$$(13) \epsilon_{B_2} = -t_2/2 \cdot r \text{ at bond line 1-2}$$

similarly, the elongation of layer 2 at bond line 2-3 is

$$(14) \epsilon'_{B_2} = +t_2/2 \cdot r \text{ at bond line 2-3}$$

A similar analysis for bending deflections x and z gives

$$(15) \quad \epsilon_{B_1} = + t_1 / 2 \cdot r \quad \text{at bond line 1-2}$$

$$(16) \quad \epsilon_{B_3} = - t_3 / 2 \cdot r \quad \text{at bond line 2-3}$$

The combined elongations can now be determined for the layers at each bond line by adding together the elongations due to thermal expansion, induced tensile or compressive loads, and bending.

At Bond Line 1-2 Interface

$$\epsilon_1 = \epsilon_{T_1} + \epsilon_{P_1} + \epsilon_{B_1}$$

$$\epsilon_1 = \alpha_1 \Delta T_1 + P_1 / t_1 \cdot E_1 + t_1 / 2 \cdot r$$

$$\epsilon_2 = \epsilon_{T_2} + \epsilon_{P_2} + \epsilon_{B_2}$$

$$\epsilon_2 = \alpha_2 \Delta T_2 - P_2 / t_2 \cdot E_2 - t_2 / 2 \cdot r$$

Since $\epsilon_1 = \epsilon_2$ at the bond line

$$(17) \quad \alpha_1 \Delta T_1 + P_1 / t_1 \cdot E_1 + t_1 / 2 \cdot r = \alpha_2 \Delta T_2 - P_2 / t_2 E_2 - t_2 / 2 \cdot r$$

Similarly, for the bond line at the 2-3 interface

$$(18) \quad \alpha_3 \Delta T_3 + P_3 / t_3 E_3 - t_3 / 2 \cdot r = \alpha_2 \Delta T_2 - P_2 / t_2 E_2 + t_2 / 2r$$

Summarizing the independent equations thus far, it will be found we now have 4 equations and 4 unknowns; P_1 , P_2 , P_3 , and r (note that $d_1 = (t_1 + t_2)/2$ and $d_2 = (t_2 + t_3)/2$ which are known).

$$(19). \quad P_1 + P_3 = P_2$$

$$(20). \quad E_1 I_1 + E_2 I_2 + E_3 I_3 = r(P_1 \cdot d_1 - P_3 \cdot d_3)$$

$$(21). \quad \alpha_1 \Delta T_1 + P_1/t_1 \cdot E_1 + t_1/2r = \\ \alpha_2 \Delta T_2 - P_2/t_2 \cdot E_2 - t_2/2r$$

$$(22). \quad \alpha_3 \Delta T_3 + P_3/t_3 \cdot E_3 - t_3/2r = \\ \alpha_2 \Delta T_2 - P_2/t_2 \cdot E_2 + t_2/2r$$

The manipulation method is to eliminate P_1 , P_2 , and P_3 ; and to solve for the radius of curvature, r . The resulting equation is presented on the following page.

$$(23). \quad r = \frac{B \cdot \left[\left(\frac{1}{t_1 E_1} + \frac{1}{t_2 E_2} \right) \cdot d_2 + \frac{d_1}{t_2 E_2} \right] - A \cdot \left[d_2 - C \cdot \left(\frac{1}{t_2 E_2} d_1 \right) \right]}{A \cdot (\alpha_2 \Delta T_2 - \alpha_3 \Delta T_3) + B \cdot \left[\left(\frac{1}{t_2 E_2} \right) (\alpha_2 \Delta T_2 - \alpha_1 \Delta T_1) - \left(\frac{1}{t_2 E_2} + \frac{1}{t_1 E_1} \right) (\alpha_2 \Delta T_2 - \alpha_3 \Delta T_3) \right]}$$

$$(24). \quad A = \left[\left(\frac{1}{t_1 E_1} + \frac{1}{t_2 E_2} \right) \cdot \left(\frac{1}{t_2 E_2} + \frac{1}{t_3 E_3} \right) - \left(\frac{1}{t_2 E_2} \right)^2 \right]$$

$$(25). \quad B = \left[\frac{d_2}{d_1 \cdot (t_2 E_2)} + \left(\frac{1}{t_2 E_2} + \frac{1}{t_3 E_3} \right) \right]$$

$$(26). \quad C = E_1 I_1 + E_2 I_2 + E_3 I_3$$

$$(27). \quad d_1 = (t_1 + t_2) / 2$$

$$(28). \quad d_2 = (t_2 + t_3) / 2$$

$$(29). \quad I = \text{width} \cdot t^3 / 12 = t^3 / 12 \text{ for unit width}$$

Once the radius of curvature, r , is determined, the load P_3 can be computed from the following equation:

$$(30). \quad P_3 = \left[\left(\frac{1}{t_1 E_1} + \frac{1}{t_2 E_2} \right) \cdot (\alpha_2 \Delta T_2 - \alpha_3 \Delta T_3 + \frac{t_2}{2r} + \frac{t_3}{2r}) - \left(\frac{1}{t_2 E_2} \right) (\alpha_2 \Delta T_2 - \alpha_1 \Delta T_1 - \frac{t_2}{2r} - \frac{t_1}{2r}) \right] / \left[\left(\frac{1}{t_1 E_1} + \frac{1}{t_2 E_2} \right) \left(\frac{1}{t_2 E_2} + \frac{1}{t_3 E_3} \right) - \left(\frac{1}{t_2 E_2} \right)^2 \right]$$

Knowing r and P_3 , the load P_1 can now be computed from the following equation:

$$(31). \quad P_1 = \left[(E_1 I_1 + E_2 I_2 + E_3 I_3) / r + P_3 \cdot d_3 \right] / d_1$$

And the load P_2 computed from the following:

$$(32). \quad P_2 = P_1 + P_3$$

And the moments computed from the following:

$$(33). \quad M_1 = E_1 I_1 / r$$

$$(34). \quad M_2 = E_2 I_2 / r$$

$$(35). \quad M_3 = E_3 I_3 / r$$

And the stresses from the following:

$$(36). \quad S_1 = P_1 / t_1 \pm E_1 t_1 / 2r$$

$$(37). \quad S_2 = -P_2 / t_2 \pm E_2 t_2 / 2r$$

$$(38). \quad S_3 = P_3 / t_3 \pm E_3 t_3 / 2r$$

The maximum deflection, δ_{max} , can now be determined:

$$(39). \quad \theta = L/r$$

$$(40). \quad \delta_{max} = \frac{L}{2} \cdot \tan\left(\frac{\theta}{4}\right)$$

If a pre-curvature is fabricated into the mirror module creating an initial maximum deflection of δ_i , then the resultant curvature is modified as follows:

$$(41) \quad \delta_{tot} = \delta_i + \delta_{max}$$

$$(42) \quad \theta' = 4 \cdot \tan^{-1}\left(\frac{2 \cdot \delta_{tot}}{L}\right), \text{ radians}$$

$$(43) \quad r' = L/\theta'$$

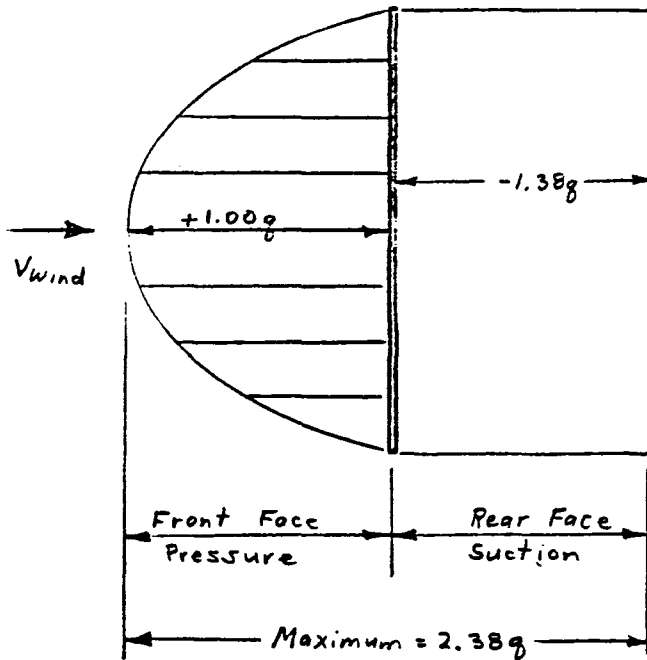
9.5.4 STRESS ANALYSIS - 90 MPH WIND

This subsection presents the stress analysis for the 90 mph wind condition. The Northrup philosophy is to stow in the vertical position normally, and to stow horizontally if high winds are forecast. However, from a stress standpoint, the goal is to show that the design is adequate for a 90 mph wind with the heliostat stowed either horizontally or vertically. Included in this section are stress analyses for the mirror modules, rack structure, and drive unit.

9.5.4.1 Mirror Module Stress Analysis

The following analysis presents the equations, assumptions, and calculations for the mirror module stress analysis. The aspects analyzed include stringer bending stress, stringer-flange buckling, stringer web shear stress, cross-member bending, local adhesive bond strength, local clip bending, local attachment effects, and glass bending stress.

90 mph Wind Analysis
LOADS



$$q = \frac{1}{2} \rho V^2 / g_c$$

$$\text{Heliostat Midpoint} = 12.75'$$

$$90 \text{ mph} = 132 \text{ ft/sec} @ 30'$$

$$V = 132 (12.75/30)^{0.15}$$

$$\underline{\underline{V = 116.1 \text{ ft/sec}}}$$

$$q = 0.075 \times 116.1^2 / 2 \times 32.2$$

$$\underline{\underline{q = 15.70 \text{ lb}_f/\text{ft}^2}}$$

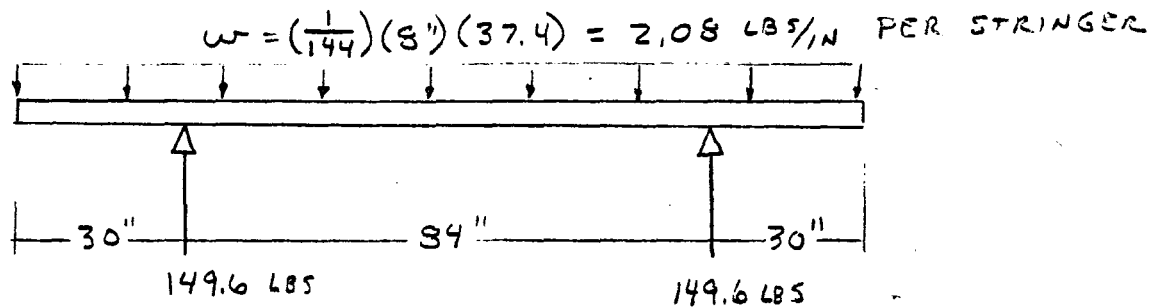
The maximum force on a central facet is $F_{max} =$

$$F_{max} = C_D q A$$

$$F_{max}/A = 2.38 \times 15.7$$

$$\underline{\underline{F_{max}/A = 37.4 \text{ lb}_f/\text{ft}^2}}$$

STRINGER BENDING ANALYSIS



MOMENT AT SUPPORTS

$$M_s = (2.08)(30)(15) = 936 \text{ IN LBS}$$

MOMENT AT CENTER

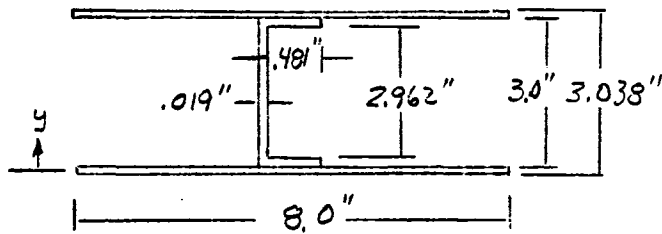
$$\begin{aligned} M_c &= \frac{wl^2}{8} - M_s \\ &= \frac{2.08(84)^2}{8} - 936 = 400 \text{ IN LBS} \end{aligned}$$

MAX SHEAR LOAD

$$V = \frac{1}{2}(2.08)(84) = 87.4 \text{ LBS IN BD OF SUPPORT}$$

STRINGER BENDING ANALYSIS (CONT)

STRINGER SECTION PROPERTIES



$$\begin{aligned} \text{TOTAL } I &= \frac{1}{12} (8 \times 3.039^3 - 7.5 \times 3.0^3 - .481 \times 2.962^3) \\ &= .776 \text{ FOR FULLY EFFECTIVE SKIN} \end{aligned}$$

$$A_s = 3.0 \times .019 = .057 \text{ IN}^2$$

COMPLETE MOMENT OF INERTIA FOR PARTIALLY EFFECTIVE SKIN

CHANNEL ONLY

$$I = \frac{1}{12} (.5 \times 3.0^3 - .481 \times 2.962^3) = .083 \text{ IN}^4$$

$$A = .5 \times 3.0 - .481 \times 2.962 = .0753 \text{ IN}^2$$

CHANNEL PLUS TOP SKIN

$$\Sigma a = .0753 + 3 \times .019 = .0753 + .152 = .2273$$

$$\Sigma ay = .0753 \times 1.510 + .152 \times 3.019 = .5726$$

$$\Sigma ay^2 = .0753 \times 1.51^2 + .152 \times 3.019^2 = 1.557$$

$$\Sigma I_0 = .083$$

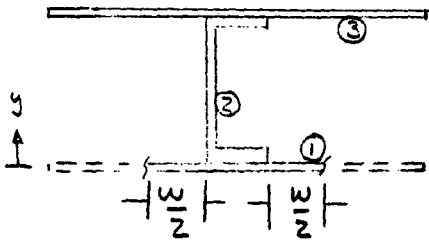
$$\bar{y} = \frac{\Sigma ay}{\Sigma a} = \frac{.5726}{.2273} = 2.52 \text{ IN}$$

$$\begin{aligned} I &= \Sigma I_0 + \Sigma ay^2 - \frac{(\Sigma ay)^2}{\Sigma a} \\ &= .083 + 1.557 - \frac{(.5726)^2}{.2273} = .1975 \end{aligned}$$

STRINGER BENDING ANALYSIS (CONT)

COMPUTE EFFECTIVE SKIN

$$f_b = \frac{M C}{I} = \frac{936(2.52)}{.1975} = 11,940 \text{ PSI}$$



$$\frac{w}{2t} = C \sqrt{\frac{E}{\sigma_{cr}}} \quad C = .85 *$$

$$\frac{w}{2} = .85 (.019) \sqrt{\frac{30 \times 10^6}{11,940}}$$

$$= .8 \text{ IN}$$

SECTION PROP.

	$\frac{a}{t}$	$\frac{y}{t}$	$\frac{a y}{t}$	$\frac{a y^2}{t}$	$\frac{I_0}{t^3}$
1	.04	0	0	0	-
2	.0753	1.51	.1137	.1717	.093
3	.152	3.019	.4539	1.3357	-
	.2673		.5726	1.5571	.083

$$\bar{y} = \frac{.5726}{.2673} = 2.14 \text{ IN}$$

$$I = .083 + 1.5571 - \frac{(.5726)^2}{.2673} = .413 \text{ IN}^4$$

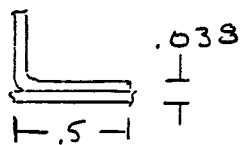
* YOUNGER, "MECHANICS OF AIRCRAFT STRUCTURES" PG 232

STRINGER BENDING ANALYSIS (CONT)

BENDING STRESS (BUCKLED LOWER PANEL)

$$f_b = \frac{M^c}{I} = \frac{936(2.14)}{.413} = 4850 \text{ PSI}$$

CHECK BUCKLING STRESS OF LOWER PLANGE/SKIN



$$F_{CR}^* = \frac{E}{\left(\frac{a}{\sqrt{K}}\right)^2}$$

$$\sqrt{K} = 1.08 \quad \text{Unrestrained edges}$$

$$= \frac{30 \times 10^6}{\left(\frac{.5}{.038 \times 1.08}\right)^2}$$

$$= 202,000 \text{ PSI}$$

$$F_{Ly} = 36,000 \text{ PSI}$$

$$M.S. = \frac{36,000}{4850} - 1 = \text{LARGE}$$

STRINGER WEB SHEAR ANALYSIS

SHEAR STRESS

$$f_s = \frac{V}{A_s} = \frac{37.4}{.057} = 1530 \text{ PSI.}$$

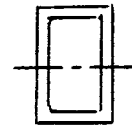
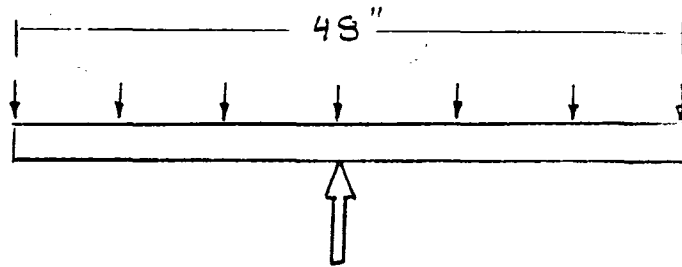
CHECK LOCAL BUCKLING

$$\begin{aligned} F_{scr}^* &= \frac{E}{\left(\frac{b}{t\sqrt{k_s}}\right)^2} & \sqrt{k} &= 2.85 \\ &= \frac{30 \times 10^6}{\left(\frac{3.0}{.019 \times 2.85}\right)^2} \\ &= 9770 \text{ PSI} \end{aligned}$$

$$M.S. = \frac{9770}{1530} = 6.38$$

* STRUCT DESIGN DATA, CVA, DEC. 1955, PG 47

CROSS MEMBER BENDING ANALYSIS



2 x 1/2 x .12
RECT. TUBE

$$I = .43 \text{ IN}^4$$

$$A = .78 \text{ IN}^2$$

897.6 LBS

DUE TO 90 MPH
WIND DRAG

$$M_{\text{max}} = \frac{897.6}{2} (12) = 5386 \text{ IN LBS}$$

$$f_b = \frac{M c}{I} = \frac{5386 (1.0)}{.43} = 12,500 \text{ PSI}$$

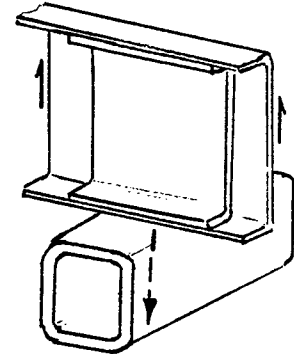
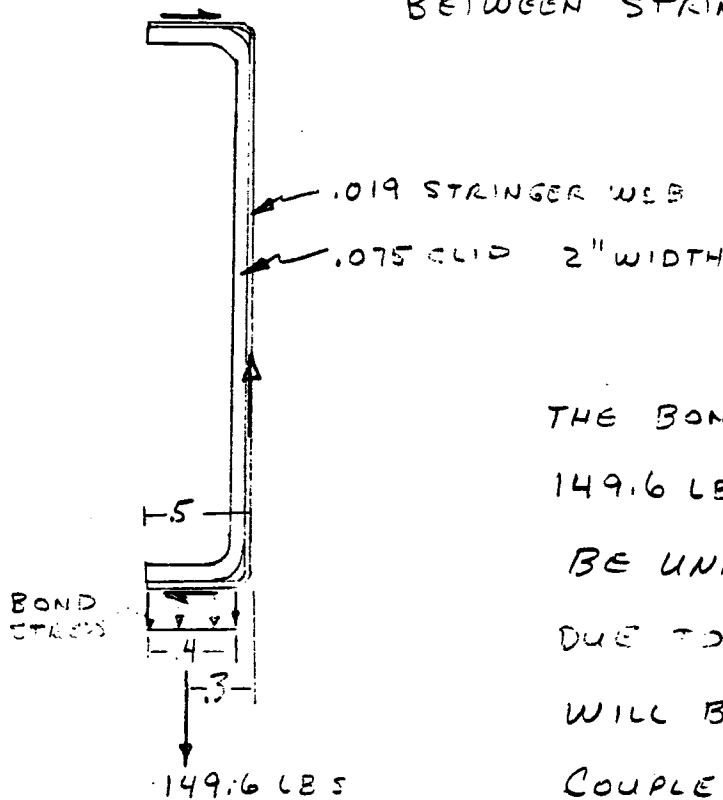
$$F_{ty} = 36,000 \text{ PSI}$$

NOT CRITICAL FOR BUCKLING

$$M.S. = \frac{36,000}{12,500} - 1 = \text{LARGE}$$

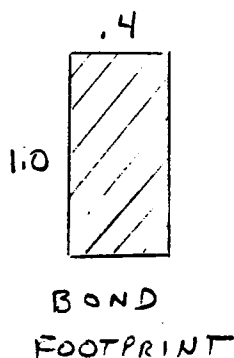
LOCAL STRINGER TO CROSS MEMBER BOND ANALYSIS

CHECK BOND FOR LOAD TRANSFER
BETWEEN STRINGER AND CROSS MEMBER



THE BOND STRESS DUE TO THE 149.6 LB LOAD WILL THEORETICALLY BE UNIFORM AS THE MOMENT DUE TO BENTHATIC LOADING WILL BE REACTED BY A COUPLE AT THE FLANGES,

HOWEVER SOME PEAKING WILL PROBABLY OCCUR DUE TO FLANGE BENDING AND OTHER STIFFNESS VARIATIONS. TO COMPENSATE FOR THIS EFFECT, THE BOND STRESS WILL BE AMPLIFIED BY A FACTOR OF 2. THE .019 FACE SHEET IS ASSUMED INEFFECTIVE.



$$f_t = \frac{P}{A} = \frac{149.6}{(1.0)(.4)} (2) = 748 \text{ PSI}$$

$$F_t = 1000 \text{ PSI}$$

$$M.S. = \frac{1000}{748} - 1 = +.34$$

LOCAL STRINGER CLIP BENDING ANALYSIS

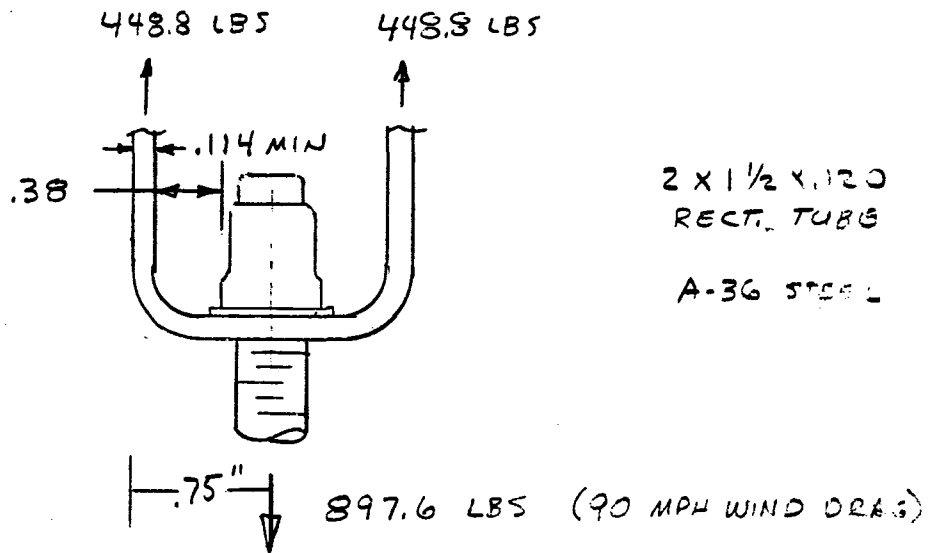
CLIP BENDING STRESS

$$\begin{aligned} f_b &= \frac{6 M}{b t^2} \\ &= \frac{6 (149.6 \times 25)}{2 (.075)^2} \\ &= 19,950 \text{ PSI} \end{aligned}$$

$$F_{ty} = 36 \text{ KSI}$$

$$M.S. = \frac{36,000}{19,950} - 1 = +.80$$

MIRROR MODULE MAIN ATTACHMENT POINT ANALYSIS



USE TENSION CLIP ALLOWABLE FOR L104-T4 ANGLE
WHICH HAS APPROXIMATELY THE SAME YIELD
STRENGTH AS A36 STEEL.

USE CURVES PG 95 OF "STRUCTURAL DESIGN DATA,
CHANCE VOUGHT AIRCRAFT, DEC 1955". USE MAX VALUE
ON CURVES FOR "2" AND OVER" SPACING, WHICH IS
 $t = .094$, AND ADJUST ALLOWABLE FOR THICKNESS
AND YIELD ALLOWABLE.

BOLT SPACING = 2 IN AND OVER

ANGLE THICKNESS = .094 IN

BOLT HEAD CLEARANCE = .38

YIELD LOAD PER BOLT = 430 LBS

MIRROR MODULE MAIN ATTACHMENT POINT ANALYSIS (CONT)

ADJUSTING FOR THICKNESS AND F_{ty}

SINGLE CLIP ALLOWABLE

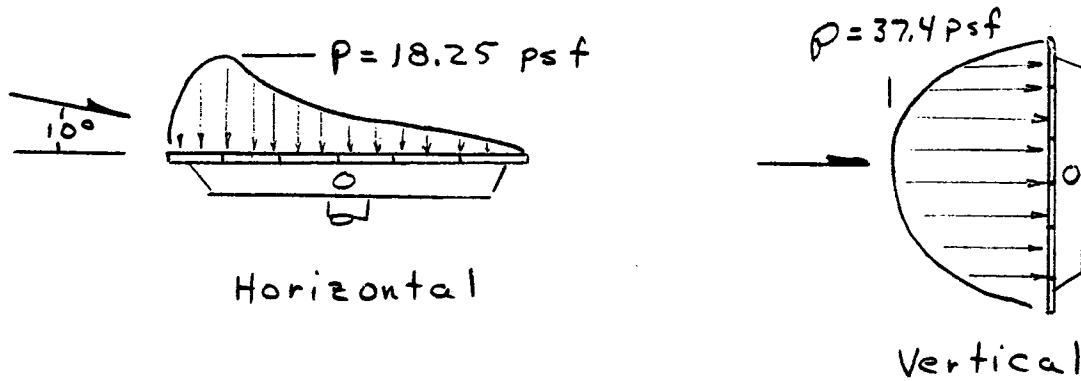
$$P_T = (430) \left(\frac{.114}{.094} \right)^2 \left(\frac{39,000}{49,000} \right)$$
$$= 600 \text{ LBS}$$

TOTAL ATTACH ALLOWABLE = $2(600) = 1200 \text{ LBS}$

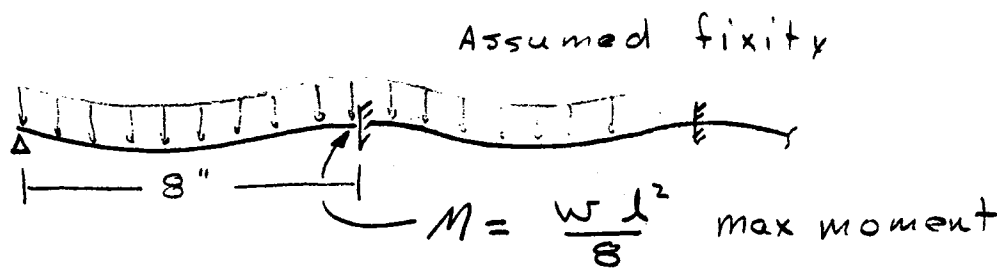
$$M.S. = \frac{1200}{3526} - 1 = +.34$$

Glass Bending Stress - 90 mph Wind

Pressure Loading



Highest stress occurs at edge span of mirror



Glass/steel composite stiffness

$$\text{Glass } D = \frac{E t^3}{12(1-\mu^2)} = \frac{10 \times 10^6 \times 0.094^3}{12(0.91)} = 760 \text{ lb in}^2$$

$$\text{Steel } D = \frac{E t^3}{12(1-\mu^2)} = \frac{30 \times 10^6 \times 0.022^3}{12(0.91)} = 30 \text{ lb in}^2$$

Glass Bending Stress (cont)

Bending moment in total composite (1" strip)

$$M = \frac{wl^2}{8} = \frac{\left(\frac{18.25}{144}\right)(8)^2}{8} = 1.01 \text{ in lbs Horiz. Hel.}$$

$$= \frac{\left(\frac{37.4}{144}\right)(8)^2}{8} = 2.08 \text{ in lbs Vert. Hel.}$$

Bending moment in glass

$$M_{\text{glass}} = M_{\text{Total}} \left(\frac{D_{\text{glass}}}{D_{\text{glass}} + D_{\text{steel}}} \right) = M_{\text{Total}} \left(\frac{760}{760+30} \right) = .962 M_{\text{Total}}$$

$$= .962 (1.01) = .97 \text{ in lbs Horiz. Hel.}$$

$$= .962 (2.08) = 2.00 \text{ in lbs Vert. Hel.}$$

Stress in glass

$$f_b = \frac{6M}{t^2} = \frac{6(.97)}{(.094)^2} = 660 \text{ psi Horiz. Hel.}$$

$$= \frac{6(2.00)}{(.094)^2} = 1360 \text{ psi Vert. Hel.}$$

$$F_b = 1000 \text{ psi (for high reliability)}$$

$$M.S. = \frac{1000}{660} - 1 = +.52 \text{ Horiz. H}$$

9.5.4.2 Rack Structure Stress Analysis

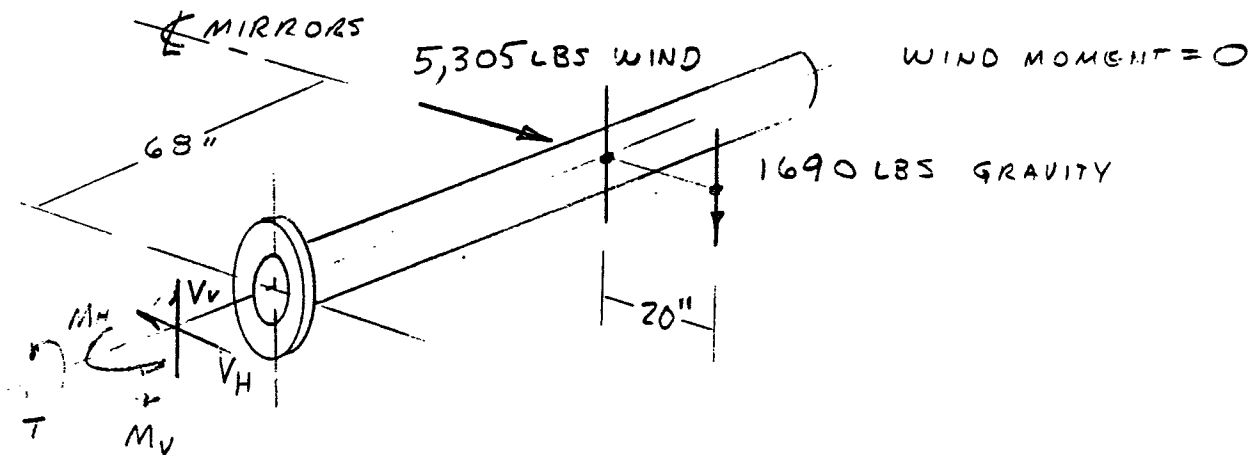
The following analysis presents the equations, assumptions, and calculations for the rack structure stress analysis. Included are calculations for the torque tube and flange bending stress, the torque tube bolt limit loads, the truss chord flexure stresses, the truss web critical buckling loads, and the truss-to-torque tube plate stresses (in plane, out-of-plane, weld shear, buckling, and lateral load cases).

TORQUE TUBE ANALYSIS (90 MPH WIND)

THE TORQUE TUBE IS CRITICAL FOR BENDING,
SHEAR, AND TORQUE AT ITS ROOT (BOLTED FLANGE)

THREE LOADING CONDITIONS ARE INVESTIGATED, 0° , 40° , AND
 70° FROM VERTICAL.

0° (VERTICAL) HELIOSTAT CONDITION (MAX GRAVITY MOMENT)



$$M_H = 68 \times 5305 = 360,740 \text{ IN LBS}$$

$$M_V = 68 \times 1690 = 114,920 \text{ IN LBS}$$

$$T = 20 \times 1690 = 33,800 \text{ IN LBS}$$

$$V_H = 5305 \text{ LBS}$$

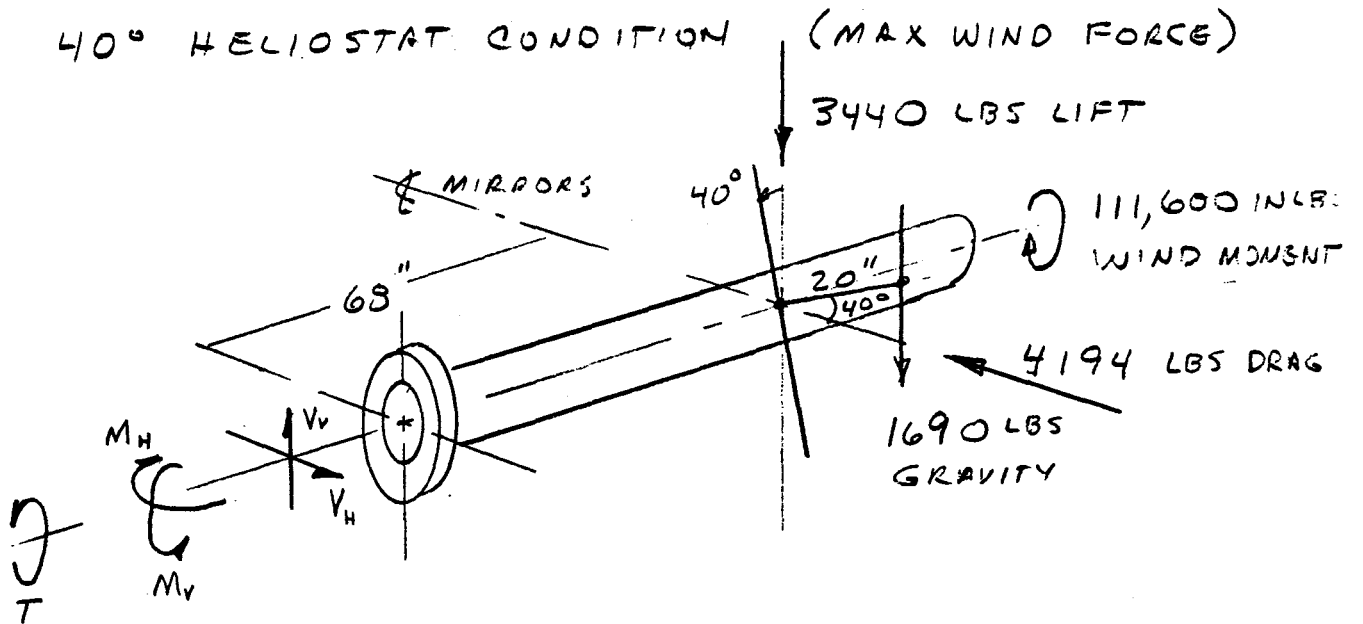
$$V_V = 1690 \text{ LBS}$$

$$M_{\text{MAX}} = 378,600 \text{ IN LBS}$$

AT 17.7° FROM HORIZ.

$$V_{\text{MAX}} = 5570 \text{ LBS}$$

AT 17.7° " " "



$$M_H = 68 (4194) = 285,190 \text{ IN LBS}$$

$$M_V = 68 (3440 + 1690) = 348,840 \text{ IN LBS}$$

$$V_H = 4194 \text{ LBS}$$

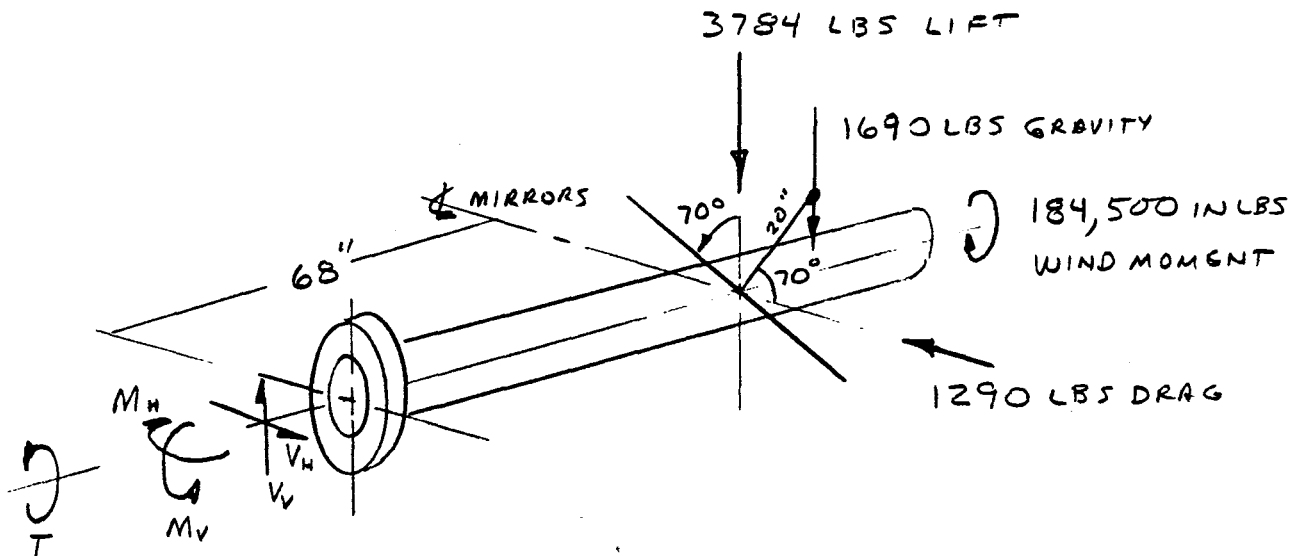
$$V_V = 3440 + 1690 = 5130 \text{ LBS}$$

$$T = 1690 (20 \cos 40^\circ) + 111,600 = 137,500 \text{ IN LBS}$$

$$M_{MAX} = 450,580 \text{ IN LBS AT } 50.7^\circ \text{ FROM HORIZ}$$

$$V_{MAX} = 6,630 \text{ LBS " } 50.7^\circ \text{ " "}$$

70° HELIOSTAT CONDITION (MAX WIND MOMENT)



$$M_H = 68 \times 1290 = 87,720 \text{ IN LBS}$$

$$M_V = 68(3784 + 1690) = 372,230 \text{ IN LBS}$$

$$V_H = 1290 \text{ LBS}$$

$$V_V = 3784 + 1690 = 5474 \text{ LBS}$$

$$T = 1690(20 \text{ cos } 70^\circ) + 184,500 = 196,060 \text{ IN LBS}$$

$$M_{\text{MAX}} = 382,430 \text{ IN LBS AT } 76.7^\circ \text{ FROM HORIZ.}$$

$$V_{\text{MAX}} = 5,620 \text{ LBS " } 76.7^\circ \text{ "}$$

TORQUE TUBE & WELD BENDING ANALYSIS

$$M_{\max} = 450,580 \text{ IN LBS} \quad 40^\circ \text{ COND}$$

$$T = 137,500 \text{ IN LBS}$$

$$I_{\text{TUBE}} = \frac{\pi}{64} (D_o^4 - D_i^4)$$

$$= \frac{\pi}{64} (12.75^4 - 12.25^4)$$

$$= 192 \text{ IN}^4$$

$$f_b = \frac{MC}{I} = \frac{450,580(6.25)}{192}$$

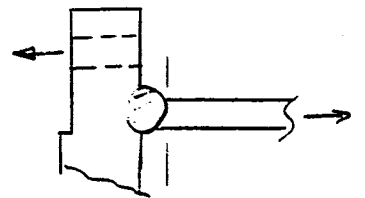
$$= 14,670 \text{ PSI}$$

$$f_{S(\text{TORS})} = \frac{TC}{J} = \frac{137,500(6.25)}{2(192)}$$

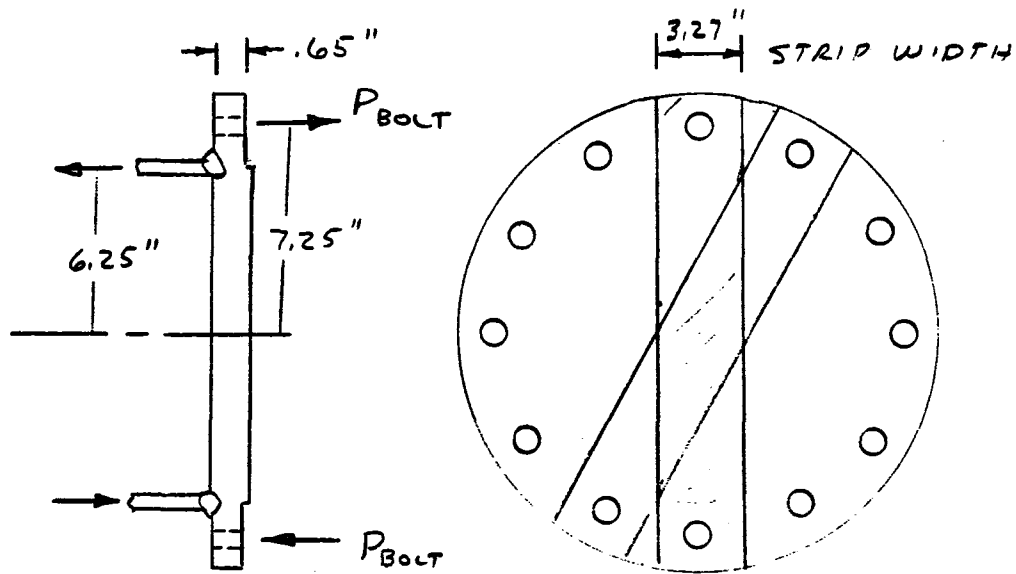
$$= 2,240 \text{ PSI} \quad \text{NOT SIGNIFICANT}$$

$$F_{ty} = 36,000 \text{ PSI}$$

$$M.S. = \frac{36,000}{14,670} - 1 = +1.45$$



TORQUE TUBE FLANGE PLATS ANALYSIS



BOLT LOAD (40° CONDITION)

$$P_{\text{REQUIR}} = \frac{2M}{R} = \frac{2(450,580)}{7.25} = 124,300 \text{ LBS}$$

$$P/\text{BOLT} = \frac{124,300}{12} = 10,360 \text{ LBS/BOLT}$$

$$M \text{ AT TUBE JCF} = 10,360 \times 1.0 = 10,360 \text{ IN LBS}$$

$$f_b = \frac{6M}{bt^2} = \frac{6(10,360)}{3.27(.65)^2} = 44,990 \text{ PSI}$$

$$F_{by} = 1.3 \times F_{ty} = 1.3 \times 36,000 = 46,800 \text{ PSI}$$

$$M.S. = \frac{46,800}{44,990} - 1 = +.04$$

TORQUE TUBE BOLT ANALYSIS

TENSION LOAD PER BOLT = 10,360 LBS

5/8 SAE GR 5 BOLTS

ULT TENSILE STRENGTH = 26,500 LBS

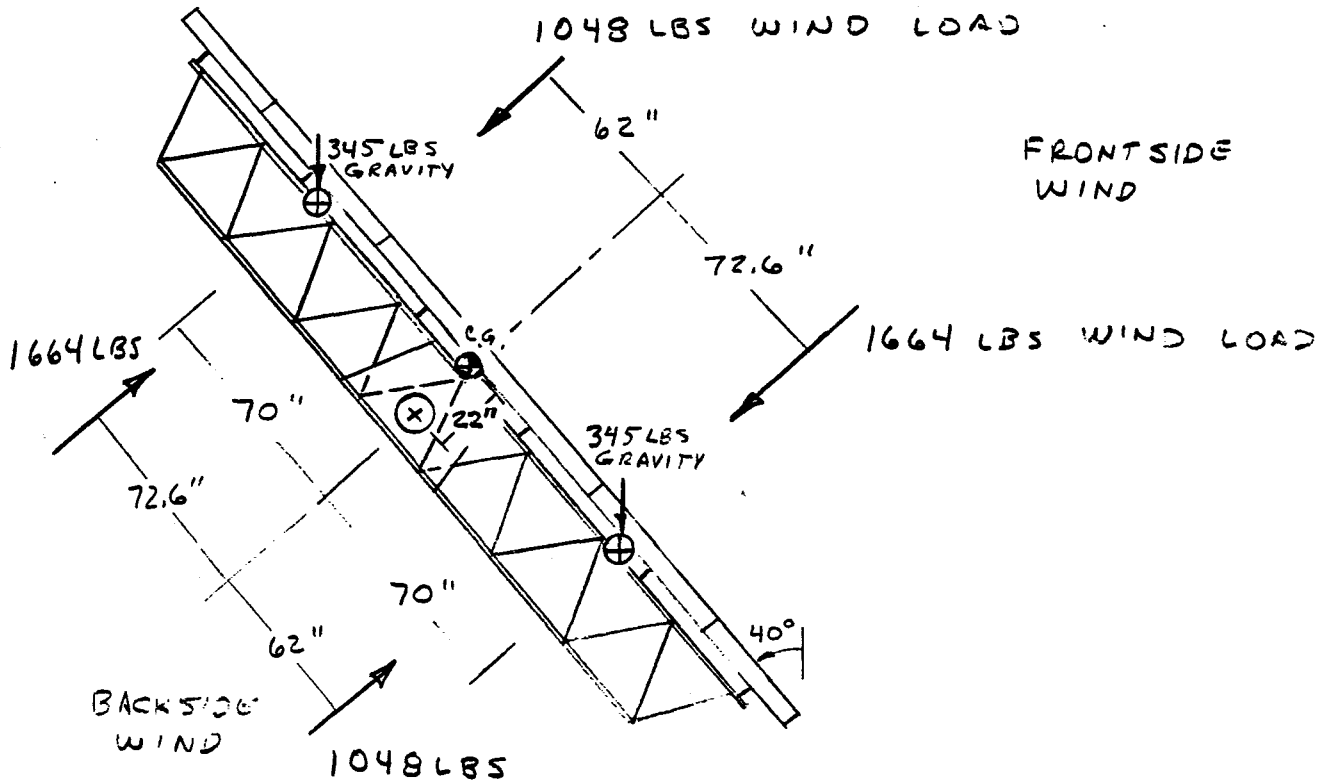
YIELD STRENGTH \approx 16,000 LBS

$$M.S. = \frac{16,000}{10,360} - 1 = +.54$$

4-3-80
RJT

TRUSS ANALYSIS — CHORD & WEB MEMBERS
(90 MPH WIND)

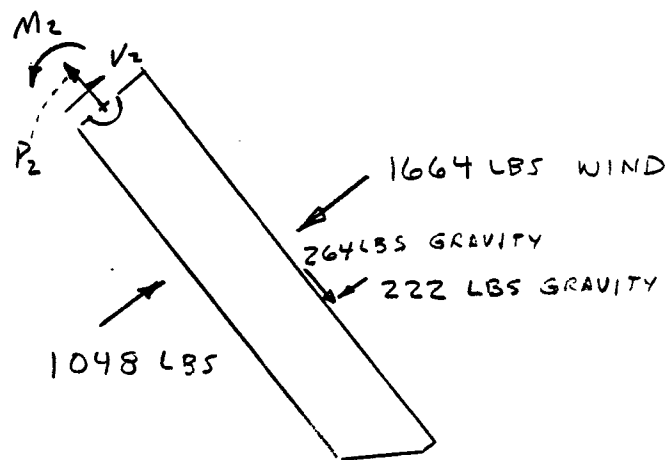
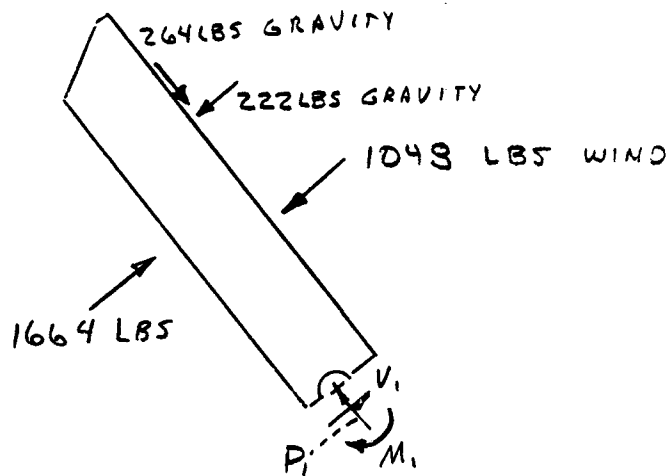
LOADS



40° FROM VERTICAL CONDITION (MAX WIND FORCE)

LOADS SHOWN ARE "PER TRUSS"

LOADS (CONT)



FRONT SIDE WIND

$$M_1 = 1048 \times 62 + 222 \times 70 - 264 \times 22 = 74,700 \text{ IN LBS}$$

$$V_1 = 1048 + 222 = 1270 \text{ LBS}$$

$$P_1 = 264 \text{ LBS}$$

$$M_2 = 1664 \times 72.6 + 222 \times 70 + 264 \times 22 = 142,150 \text{ IN LBS}$$

$$V_2 = 1664 + 222 = 1886 \text{ LBS}$$

$$P_2 = 264 \text{ LBS}$$

LOADS (CONT.)

BACKSIDE WIND

$$M_1 = 222 \times 70 - 264 \times 22 - 1664 \times 72.6 = -111,070 \text{ IN LBS}$$

$$V_1 = 222 - 1664 = -1442 \text{ LBS}$$

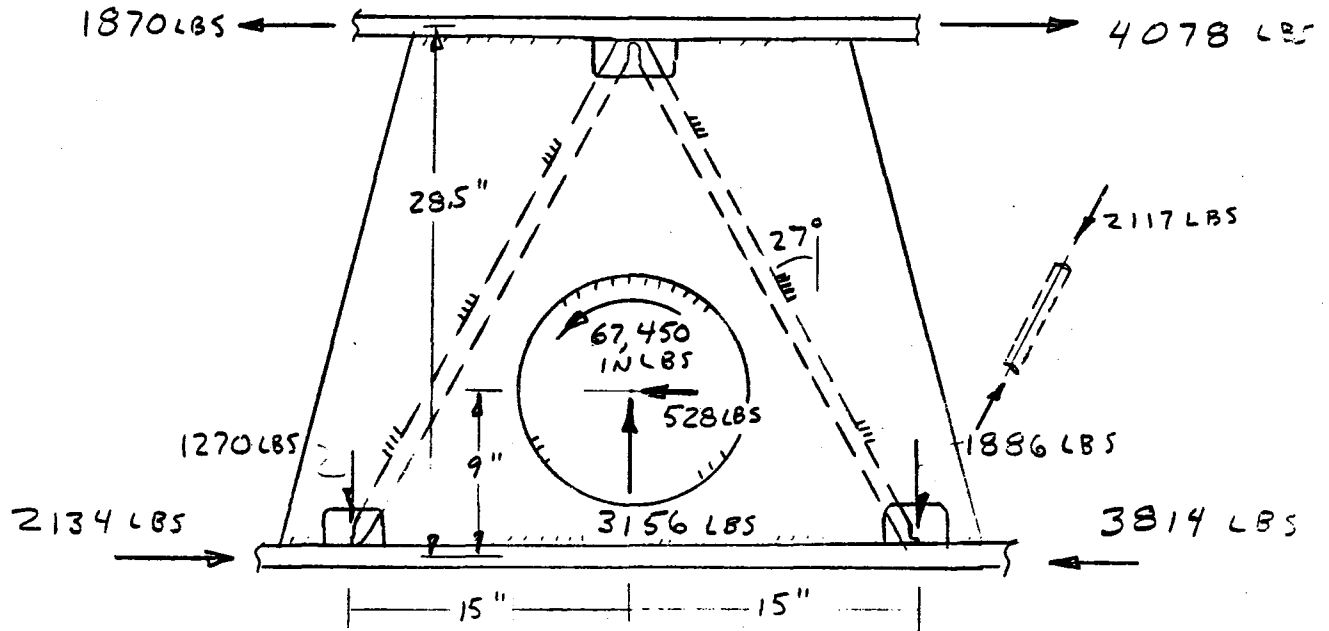
$$P_1 = 264 \text{ LBS}$$

$$M_2 = 222 \times 70 + 264 \times 22 - 1048 \times 62 = -43,630 \text{ IN LBS}$$

$$V_2 = 222 - 1048 = -826 \text{ LBS}$$

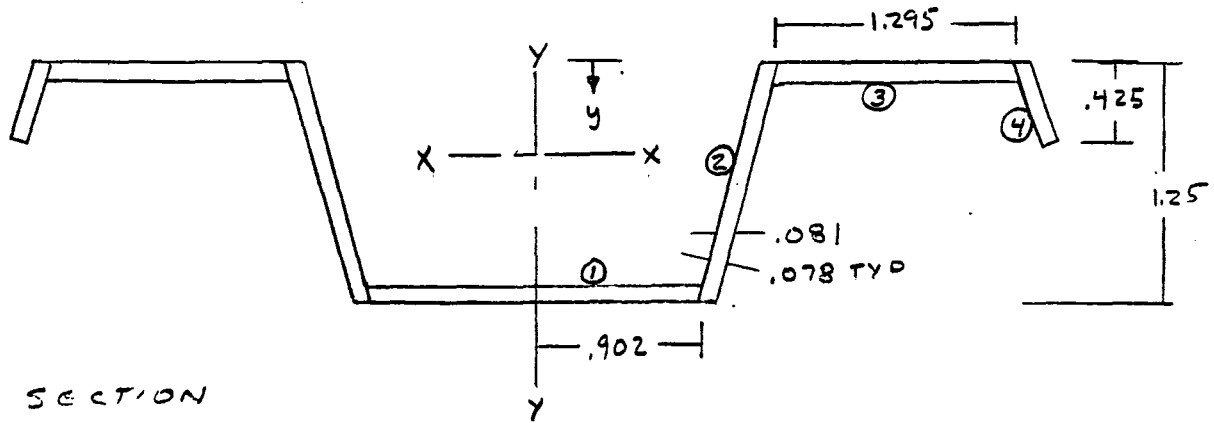
$$P_2 = 264 \text{ LBS}$$

LOADS (CONT.)



FRONTIER WIND SUBJECT TO HIGHEST LOAD
 & WEB LOAD AS SHOWN IN EQUILIBRIUM
 DIAGRAM ABOVE.

BUTLER CAP SECTION PROPERTIES



HALF SECTION

ELE	a	y	ay	ay ²	I _o
1	.070	1.211	.085	.103	—
2	.101	.625	.063	.039	.0132
3	.101	.039	.004	—	—
4	.034	.212	.007	.002	.0005
	<u>.306</u>		<u>.159</u>	<u>.144</u>	<u>.0127</u>

$$\bar{y} = \frac{\sum ay}{\sum a} = \frac{.159}{.306} = .52$$

$$I_{xx} = \sum (I_o + Ay^2) - \frac{(\sum ay)^2}{\sum a}$$

$$= .0137 + .144 - \frac{(.159)^2}{.306}$$

$$= .075$$

$$\text{TOTAL AREA} = 2 (.306) = .612 \text{ IN}^2$$

$$\text{TOTAL INERTIA} = 2 (.075) = .15 \text{ IN}^4$$

TRUSS CHORD ANALYSIS

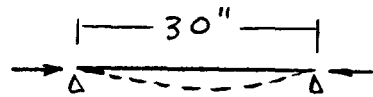
COMPRESSION

$$\text{MAX COMPRESSION } P = 3814 \text{ LBS}$$

$$I = .15 \text{ IN}^4 \quad A = .612 \text{ IN}^2$$

$$L' \approx .7 L \quad (\text{PARTIAL FIXITY})$$

$$P_{cr} = \frac{\pi^2 EI}{(L')^2}$$



$$= \frac{\pi^2 (30 \times 10^6) (.15)}{(.7 \times 30)^2}$$

$$= 100,700 \text{ LBS} \quad \text{NOT CRITICAL}$$

$$f_c = \frac{P}{A} = \frac{3814}{.612} = 6230 \text{ PSI}$$

$$F_{cy} = 36,000 \text{ PSI}$$

$$M.S. = \frac{36,000}{6230} - 1 = \text{LARGE}$$

TRUSS CHORD ANALYSIS

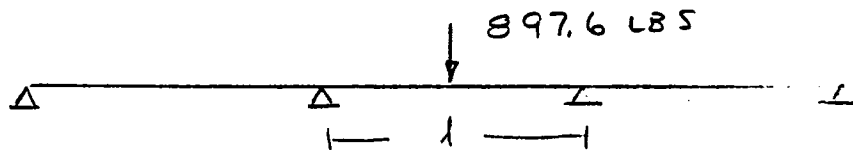
BENDING

CRITICAL BENDING IS DUE TO MIRROR
MODULE ATTACHMENT LOAD AT 2nd
MODULE FROM TOP OR BOTTOM.

CONSERVATIVELY USE 897.6 LBS

ATTACHMENT LOAD FROM MIRROR MODULE

ANALYSIS. NEGLECT BEAM COLUMN EFFECT.



$$I = .15 \text{ IN}^4 \quad l = 30'' \quad c = .73''$$

$$M = \frac{7}{40} P l = \frac{7}{40} (897.6 \times 30) = 4710 \text{ IN LBS}$$

$$f_b = \frac{M c}{I} = \frac{4710 (.73)}{.15} = 22,900 \text{ PSI}$$

$$F_{ty} = 36,000 \text{ PSI} \quad (\text{NOT CRIPPLING CRITICAL})$$

$$M.S. = \frac{36,000}{22,900} - 1 = 1.57$$

TRUSS WEB ANALYSIS

CHECK SECOND DIAGONAL OVER FROM TORQUE
TUBE FOR BUCKLING DUE TO COMPRESSION LOAD.

$$P = \frac{1886}{\sin 27^\circ} = 2117 \text{ LBS}$$

UNSUPPORTED LENGTH = 30 IN

$$I = .023 \text{ IN}^4$$

$$P_{cr} = \frac{\pi^2 EI}{L^2} = \frac{\pi^2 (30 \times 10^6) (.023)}{(30)^2} = 7570 \text{ LBS}$$

$$M.S. = \frac{7570}{2117} - 1 = 2.56$$

TRUSS WEB ANALYSIS

CHECK 1" WELDS (TUBULAR DIAGONALS-TO-PLATE)

$$\text{LOAD IN DIAGONAL} = \frac{1896}{\cos 27^\circ} = 2117 \text{ LBS}$$

3" OF WELD .075 THROAT THICKNESS

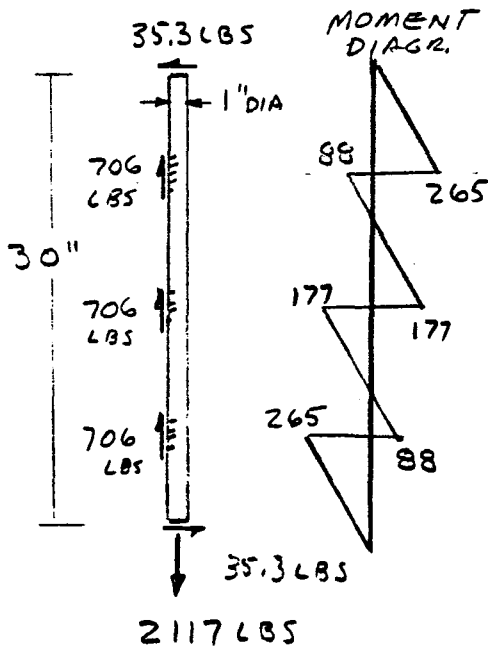
$$A = 3 \times .075 = .225 \text{ IN}^2$$

$$f_s = \frac{2117}{.225} = 9408 \text{ PSI}$$

$$F_{sy} = 20,000 \text{ PSI}$$

$$M.S. = \frac{20,000}{9408} - 1 = +1.13$$

CHECK TUBE STRESS (1" O.D. X .075 DIAG. MEMBER)



$$I_{\text{TUBE}} = .023 \text{ IN}^4$$

$$A_{\text{TUBE}} = .218 \text{ IN}^2$$

$$f = \frac{P}{A} + \frac{M C}{I}$$

$$= \frac{2117}{.218} + \frac{265(1.5)}{.023} = 15,470 \text{ PSI}$$

$$F_{ty} = 36,000 \text{ PSI}$$

$$M.S. = \frac{36,000}{15,470} - 1 = +1.32$$

TRUSS-TORQUE TUBE PLATE ANALYSIS
(90 MPH WIND)

LOADS (IN-PLANE)

THE CRITICAL IN-PLANE LOAD CONDITION IS THE 70° FROM VERTICAL CONDITION, PRODUCING MAXIMUM SHEAR STRESS IN THE PLATE AND WELD, DUE TO THE MAX WIND TORQUE CONDITION.

$$\text{MAX WIND TORQUE (PER TRUSS)} = \frac{184,500^*}{2} = 92,250 \text{ IN LBS}$$

$$\begin{aligned} \text{GRAVITY TORQUE (PER TRUSS)} &= \frac{1380 \text{ LBS}}{2} \times 22 \text{ IN} \times \sin 70^\circ \\ &= 5,190 \text{ IN LBS} \end{aligned}$$

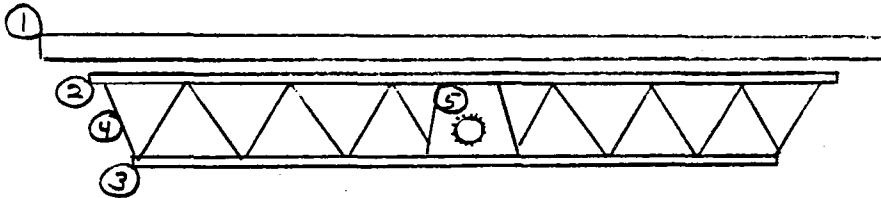
$$\text{TOTAL TORQUE} = 97,440 \text{ IN LBS}$$

$$\text{SHEAR} = \frac{1}{2} \times \sqrt{(3784 + 1380)^2 + (1290)^2} = 2660 \text{ LBS}$$

* REF TORQUE TUBE LOADS

LOADS (OUT-OF-PLANE)

SIDE LOAD ON RACK AND MIRROR MODULE STRUCTURE
DUE TO 40 MPH WIND



PROJECTED AREA

①	$293 \text{ IN} \times 3.1 \text{ IN} / 144$	=	6.3	FT ²
②	$252 \text{ IN} \times 1.25 \text{ IN} \times 2 / 144$	=	4.4	
③	$210 \text{ IN} \times 1.25 \text{ IN} \times 2 / 144$	=	3.6	
④	$500 \text{ IN} \times 1.0 \text{ IN} \times 2 / 144$	=	6.9	
⑤	$\left(\frac{27.5 + 39}{2} \times 27 - \frac{\pi}{4} \times 12.75^2 \right) \times 2 / 144$	=	9.8	
			<u>31.0</u>	FT ²

$$q_f = 15.7 \text{ PSF}$$

$$C_D = 1.13$$

$$F = q_f C_D A = 15.7 \times 1.13 \times 31.0 = 550 \text{ LBS}$$

$$\text{LOAD PER TRUSS} = \frac{550}{2} = 275 \text{ LBS}$$

CHECK SHEAR STRESS IN TORQUE TUBE - TO - PLATE
WELD

$$DIA = 12.75''$$

$$T = 97,440 \text{ IN LBS}$$

$$V = 2660 \text{ LBS}$$

WELD LOAD (LBS/IN)

$$W = \frac{T}{2\pi R^2} + (2) \frac{V}{2\pi R}$$

$$= \frac{97,440}{2\pi(6.375)^2} + (2) \frac{2660}{2\pi(6.375)}$$

$$= 382 + 133 = 515 \text{ LBS/IN}$$

SHEAR STRESS (.090 THroat THICKNESS)

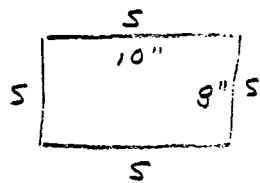
$$f_s = \frac{515}{.090} = 5720 \text{ PSI.}$$

$$F_{sy} = 20,000 \text{ PSI}$$

$$M.S. = \frac{20000}{5720} - 1 = \text{LARGE}$$

CHECK PLATE BUCKLING OF THE 1090
 PLATE ATTACHING THE TORQUE TUBE TO
 THE TRUSS ASSY.

USE EQUIV SIMPLY SUPPORTED PLATE (METHOD
 IN "STRUCTURAL DESIGN DATA", CHANCE VUGHT
 AIRCRAFT, DEC. 1955) WITH MAX CALCULATED
 WELD STRESS OF 5,720 PSI.



$$t = .09 \text{ IN}$$

$$\frac{a}{b} = \frac{10}{8} = 1.25$$

$$\frac{1}{K_s} = 2.7$$

$$F_{s_{cr}} = \frac{E}{\left(\frac{b}{t\sqrt{K_s}}\right)^2}$$

$$= \frac{30 \times 10^6}{\left(\frac{8}{.09 \times 2.7}\right)^2}$$

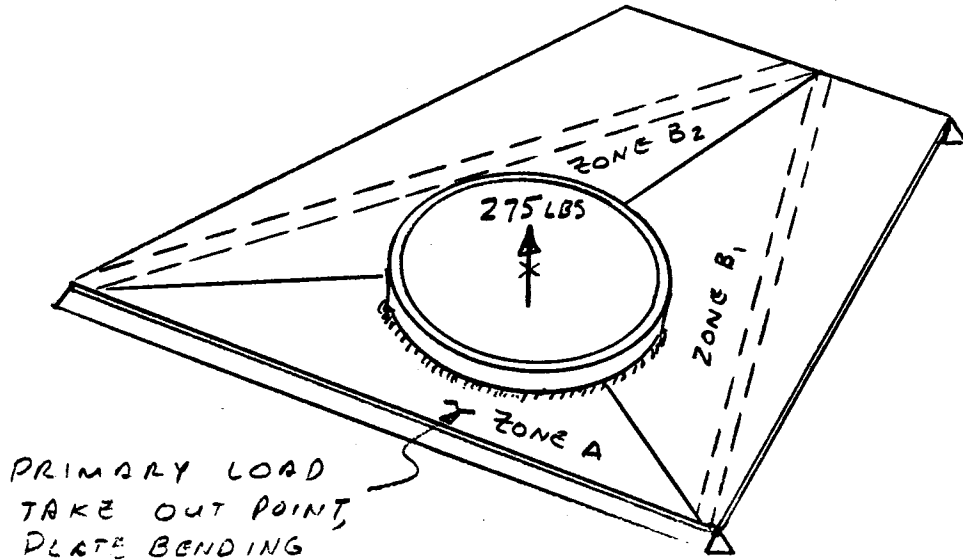
$$= 27,700 \text{ PSI.} \quad > F_{sy}$$

$$F_{sy} = 20,000 \text{ PSI}$$

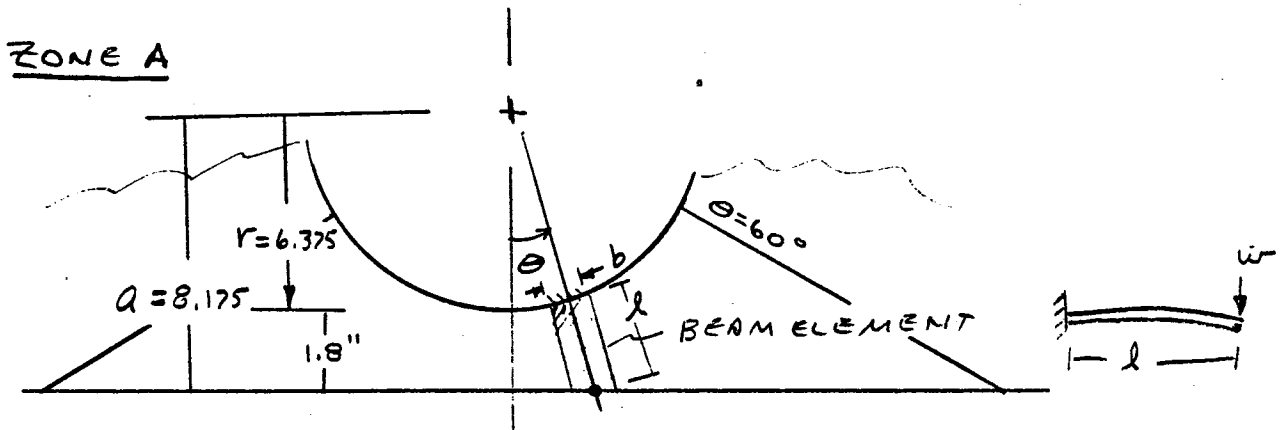
$$M.S. = \frac{20,000}{5,720} - 1 = \text{LARGE}$$

TRUSS-TORQUE TUBE PLATE LATERAL LOAD ANALYSIS.

NEGLECT GRAVITY LOAD



LOAD WILL BE DISTRIBUTED ACCORDING TO STIFFNESSES TO BE DETERMINED AS FOLLOWS



$$l = \frac{a}{\cos \theta} - r$$

$$k = \frac{Et^3b}{4(1-\mu^2)l^3} \quad \left(\frac{\text{LBS}}{\text{IN}}\right)$$

SPRING CONSTANT OF ELEMENT

$$= \frac{30 \times 10^6 (1.09)^3 (1.1'')}{4(1-.3^2) l^3}$$

FOR 10° INCREMENTS
(b = 1.1'')

$$= \frac{6610}{l^3}$$

<u>θ</u>	<u>l</u>	<u>k_s</u>
5°	1.93 IN	1079 LBS/IN
15°	2.09	724
25°	2.65	355
35°	3.6	142
45°	5.19	47
55°	7.88	14

TOTAL STIFFNESS (TWO
HALVES) K = 2(2361)

$$= 4722 \frac{\text{LBS}}{\text{IN}}$$

$$\Sigma = 2361$$

FOR ZONE B (B₁ & B₂)

LET $a = 9.0$ EQUIV TO ZERO MOMENT POINT

<u>θ</u>	<u>l</u>	<u>k</u>	
5°	2.66 IN	351	LBS/IN
15°	2.94	260	
25°	3.55	147	TOTAL STIFFNESS
35°	4.61	67	(4 HALVES)
45°	6.35	26	$K = 4(859) = 3436$ LBS/IN
55°	9.32	9	
		<hr/>	
		859	

TOTAL PLATE STIFFNESS (ZONES A, B₁ & B₂)

$$K = 4722 + 3436 = 8158 \text{ LBS/IN}$$

A 1" ELEMENT AT ZONE A ($\theta = 5^\circ$) WILL CARRY

$$\left(\frac{1.0}{1.1}\right) \frac{1079}{8158} = 12\% \text{ OF THE TOTAL PLATE LOAD}$$

CHECK BENDING IN 1" ELEMENT AT $\theta = 5^\circ$ (ZONE A)

$$F = (.121)(275 \text{ LBS}) = 33 \text{ LBS}$$

$$M = Pl = 33 \times 1.83 = 60.4 \text{ IN LBS}$$

$$f_b = \frac{6M}{bt^2} = \frac{6(60.4)}{(1.0)(.09)^2} = 44,740 \text{ PSI.}$$

F_{by} (YIELD BENDING MODULUS) $\approx 1.3 F_{ey}$

$$F_{by} = 1.3 (36,000) = 46,800 \text{ PSI}$$

$$M.S. = \frac{46,800}{44,740} - 1 = +.05$$

9.5.4.3 Drive Unit Stress Analysis

The primary concerns in the drive unit for the 90 mph wind case are the worm thread bending stress, the gear tooth shear stress, the gear tooth bending stress, and the main bearing loads (radial, thrust, and moment) versus the bearing ratings.

The analysis method for the main bearings is to determine the radial loads, thrust loads, and moments, and to compare these to the manufacturer's catalog rating. It will be noted that the catalog rating capacity is exceeded for the expected wind moments accompanying either the horizontal or vertical stow position with a 90 mph wind. However, the ratings contain a margin of safety, and the 90 mph wind is not a normal, every-day load condition. Hence, the bearing selected is currently considered acceptable, and a substantiating analysis is being performed by the bearing manufacturer.

Because of the variable conditions existing at the mesh of worm and worm gear, the analysis method is to use a unit value of the load; i.e., the load per inch of face. With the average unit load across the face the maximum intensity of this unit load will then be computed. This maximum-intensity load will then be used to compute the strength of the worm threads and the worm-gear teeth.

BEAM STRENGTH OF TEETH

The following analysis was performed in accordance with the "Design of Worm and Spiral Gears" by Earle Buckingham and Henry Ryffel.

$$w = W_{dn} \cos \lambda_1 / F$$

where w = the average or unit load per inch of face width of the worm gear, lb/in

W_{dn} = the normal dynamic load, lb (note: for low speeds, this is equal to the normal tooth load; $90 \text{ mph moment} / \text{gear pitch radius}$)

λ_1 = the lead angle of the worm at the pitch plane.

F = the face width of the gear

Having found the average or unit load, w , the next step is to find the maximum load, w_m , from Table 1 (interpolating if required):

Table 1

Maximum Unit Load, w_m

	$\frac{F/D_o_1}{0.5}$	$\frac{F/D_o_1}{0.4}$	$\frac{F/D_o_1}{0.3}$	$\frac{F/D_o_1}{0.2}$	$\frac{F/D_o_1}{0.1}$
$w_m =$	1.60w	1.37w	1.20w	1.09w	1.01w

Where w_m = the maximum unit load per inch
of face of worm gear, lb/inch
 D_o_1 = outside diameter of worm, in

WORM THREAD BENDING STRESS

$$s_b = w_m / p_n y_1$$

where s_b = the maximum bending stress at the
root of the worm thread, psi

p_n = the normal pitch of the worm threads, in.

$$p_n = p_x \cos \lambda_1$$

p_x = axial pitch of the worm threads, in.

y_1 = the tooth form factor for the
worm threads (see Table 2)

ϕ_n = the normal thread angle

Table 2

Worm Tooth Form Factors, y_1

	$\phi_n = 14.5^\circ$	$\phi_n = 20^\circ$	$\phi_n = 25^\circ$	$\phi_n = 30^\circ$
$y_1 =$	0.124	0.154	0.190	0.220

GEAR TOOTH SHEAR STRESS AT ROOT

$$s_s = w_m / A$$

where s_s = shear stress at tooth root, psi

w_m = max. unit load per inch of face of worm gear, lb/in.

A = unit area at root of worm gear tooth, in²/in (see Table 3)

Table 3

Unit Area at Root of Gear Tooth, A

	$\phi_n = 14.5^\circ$	$\phi_n = 20^\circ$	$\phi_n = 25^\circ$	$\phi_n = 30^\circ$
$A =$	$0.5 p_n$	$0.55 p_n$	$0.60 p_n$	$0.65 p_n$

These equations and tables have been incorporated into a computer code known as "TOOTH". For the Winsmith worm gear design used on the Northrup drive unit, an analysis was performed to determine the worm thread bending stress and the gear tooth shear stress. The following page presents the results for both a 90 mph and 50 mph wind speed for a vertical stow orientation.

The allowable worm thread bending stress (yield) is 190,000 psi, and the tooth shear stress allowable (yield) is 80,000 psi so the values shown on the computer tab have ample margin.

An additional area of concern on the gear tooth is the bending stress. The analysis of this stress for the vertical stow, 90 mph case was analyzed by Winsmith. The results of their analysis are provided on pages E-146 through E-149.

Winsmith Worm/Gear Stress

```
ENTER OUTPUT TORQUE, FT-LB 34758  
INPUT DIAM PITCH, D.P. 1.50000000  
ENTER WORM PITCH DIA 3.15000000  
ENTER WORM ANGLE, DEG 7.7  
ENTER GEAR PITCH DIA 18.07500000  
ENTER GEAR FACE WIDTH 2.362
```

90 mph

```
.....  
MAX WORM THREAD BENDING STRESS = 100708
```

```
MAX GEAR TOOTH SHEAR STRESS = 42089
```

```
.....
```

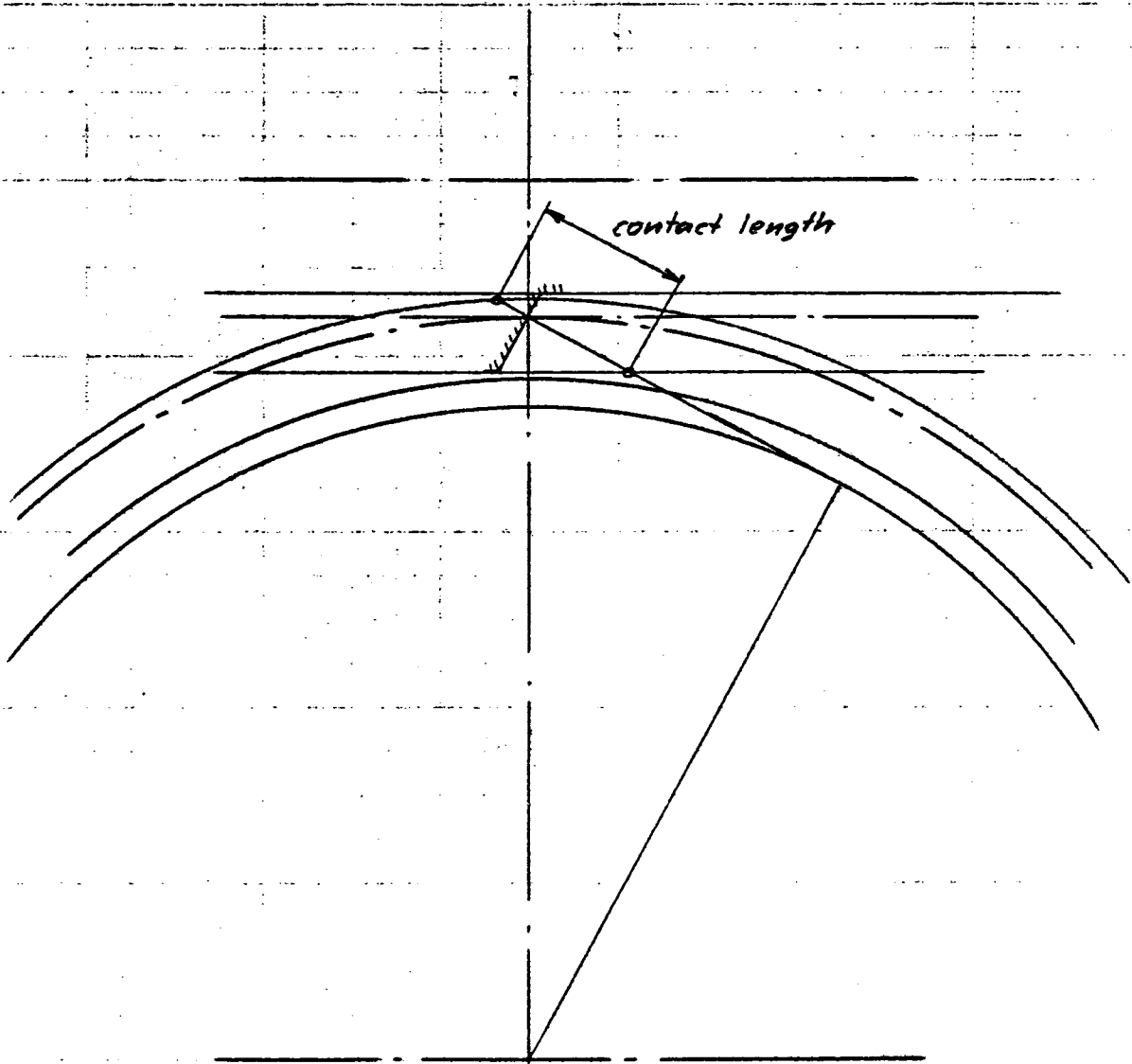
```
ENTER OUTPUT TORQUE, FT-LB 34758  
INPUT DIAM PITCH, D.P. 1.50000000  
ENTER WORM PITCH DIA 3.15000000  
ENTER WORM ANGLE, DEG 7.7  
ENTER GEAR PITCH DIA 18.07500000  
ENTER GEAR FACE WIDTH 2.362
```

50 mph

```
.....  
MAX WORM THREAD BENDING STRESS = 41326
```

```
MAX GEAR TOOTH SHEAR STRESS = 10006
```

```
.....
```



$$T.P.A. = \text{arc tg} (\text{tg} 28^\circ / \cos 7.7^\circ) = 28.2156^\circ$$

$$y = \sqrt{17.30097984^2 - 14.87334375^2} = 8.837847539''$$

$$x = \sqrt{16.87900472^2 - 14.87334375^2} = \frac{7.980253507''}{.4288''}$$

$$z = .632962677 / \sin 28.2156 = 1.3388''$$

$$\text{contact length} = 1.3388 + .4288 = \underline{\underline{1.7676''}}$$

$$E.P.D. \text{ gear} = 16.4570296''$$

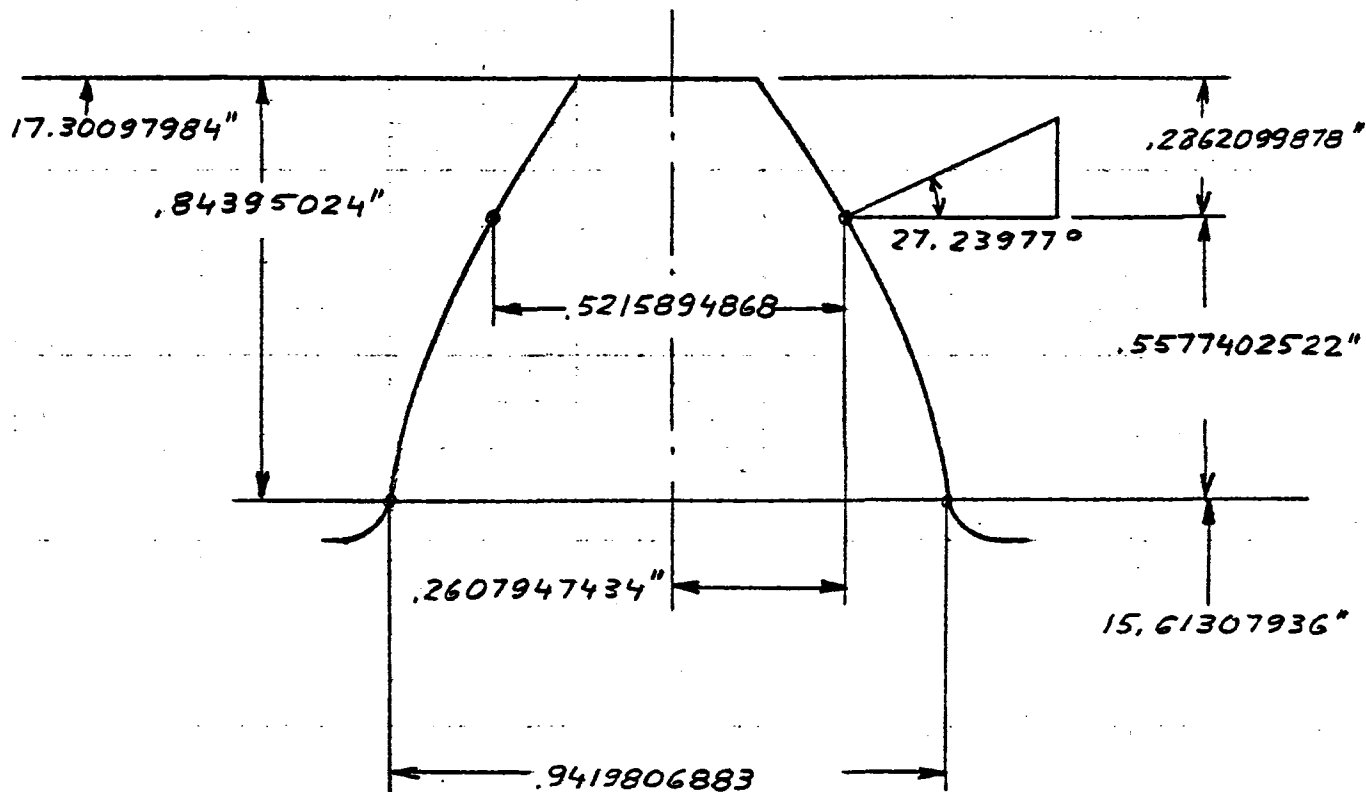
$$t \text{ at E.P.D} = .646266041''$$

$$T.P.A. \text{ at EPD} = \text{arc cos} (B.C. / E.P.D) = 25.34208171^\circ$$

$$D_2 = 15.61307936''$$

$$t_2 = .9419806883''$$

$$\text{cont. ratio} = 1.51316$$



position of highest point of single tooth contact is :

$$\frac{.84395024 (\text{cont ratio} - 1)}{\text{cont. ratio}} = .2862099878$$

$$\text{Tang. load} = \frac{30750 \times 12 \times 2}{16.72856013} = \underline{\underline{44116 \text{ lbs}}}$$

$$\text{Radial load} = 44116 \times \frac{1}{2} \times 27.23977 = \underline{\underline{22711 \text{ lbs}}}$$

$$\text{Section modulus} = \frac{b \times h^2}{6} = \frac{2.35 \times .9419806883^2}{6} = .34753665 \text{ in}^3$$

Bending stress due to tangential load :

$$\sigma = \frac{44\,116 \times .5577402522}{.34753665} = \underline{\underline{70\,799 \text{ psi}}}$$

Compressive stress due to radial load :

$$\sigma = \frac{22\,711}{2.35 \times .9419806883} = \underline{\underline{10\,259 \text{ psi}}}$$

Bending stress due to radial load :

$$\sigma = \frac{22\,711 \times .2607947434}{.34753665} = \underline{\underline{17\,042 \text{ psi}}}$$

Average stress concentration factor for bending stresses in the root of gear teeth is about 3.0 . For limit load conditions a stress concentration factor of 2.0 will allow for some stress redistribution without local yielding of a magnitude affecting the operating qualities of this gear drive.

Maximum tensile stresses are :

$$\begin{array}{rcl} + 2 \times 70\,799 & = & 141\,598 \\ - 10\,259 & = & 10\,259 \\ - 2 \times 17\,042 & = & \underline{34\,084} \\ & & \underline{\underline{97\,255 \text{ psi tensile}}} \end{array}$$

Maximum compressive stresses are :

$$\begin{array}{rcl} + 2 \times 70\,799 & = & 141\,598 \\ + 10\,259 & = & 10\,259 \\ - 2 \times 17\,042 & = & \underline{34\,084} \\ & & \underline{\underline{117\,773 \text{ psi compressive}}} \end{array}$$

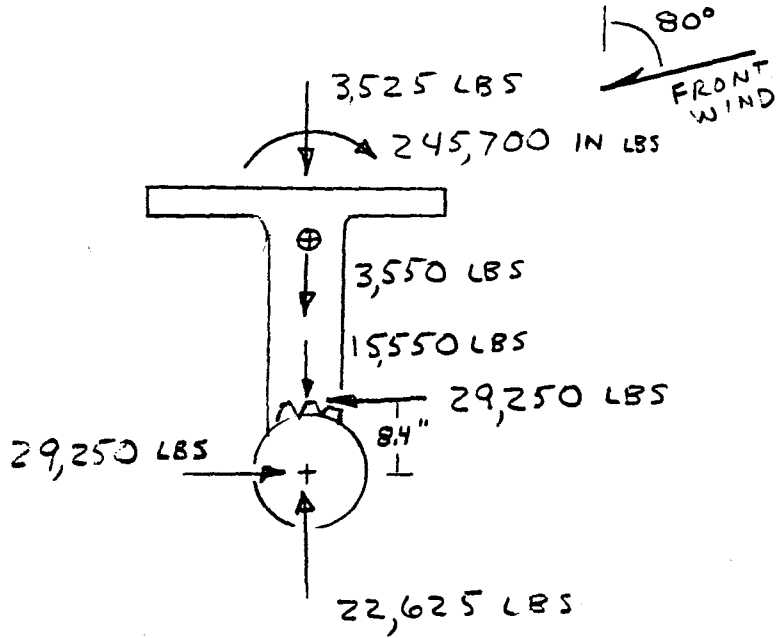
BEARING STATIC LOADS

90 MPH WIND

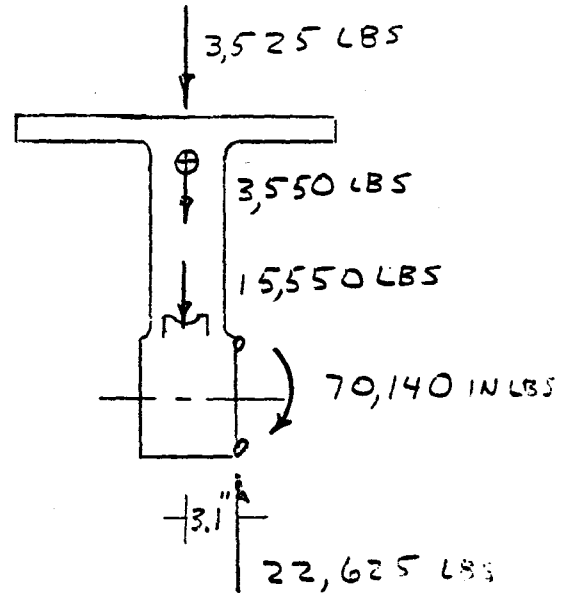
ELEVATION BEARING

HORIZONTAL HELIOSTAT

FRONT WIND COND



SIDE VIEW

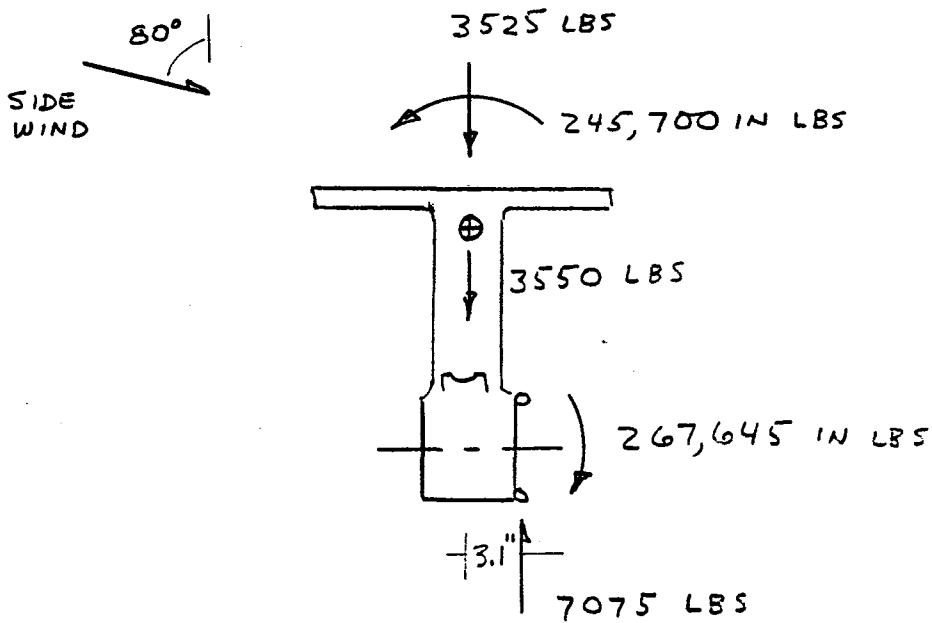


FRONT VIEW

$$\begin{aligned}
 \text{MAX MOMENT} &= 70,140 \text{ IN LBS} \\
 \text{MAX RADIAL LOAD} &= \sqrt{(22,625)^2 + (29,250)^2} = 36,980 \text{ LBS} \\
 \text{MAX THRUST LOAD} &= 0
 \end{aligned}$$

HORIZONTAL HELIOSTAT

SIDE WIND COND.



FRONT VIEW

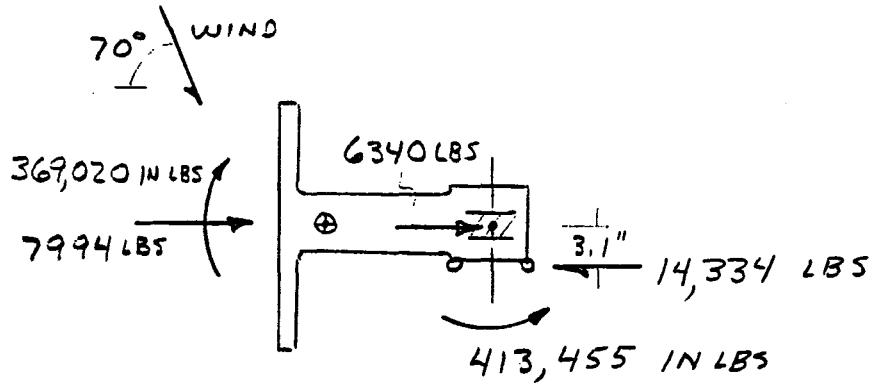
MOMENT = 267,645 IN LBS

RADIAL LOAD = 7,075 LBS

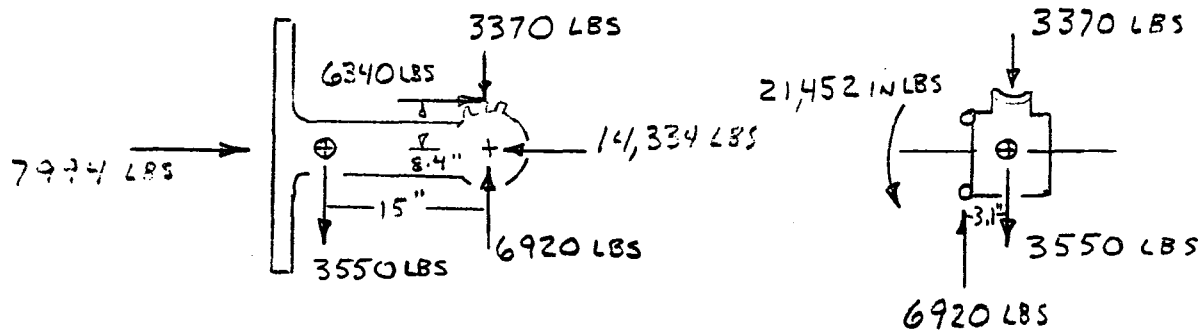
THRUST LOAD ≈ 0

VERTICAL HELIOSTAT

70° AZIMUTH WIND COND



TOP VIEW



SIDE VIEW

BACK VIEW

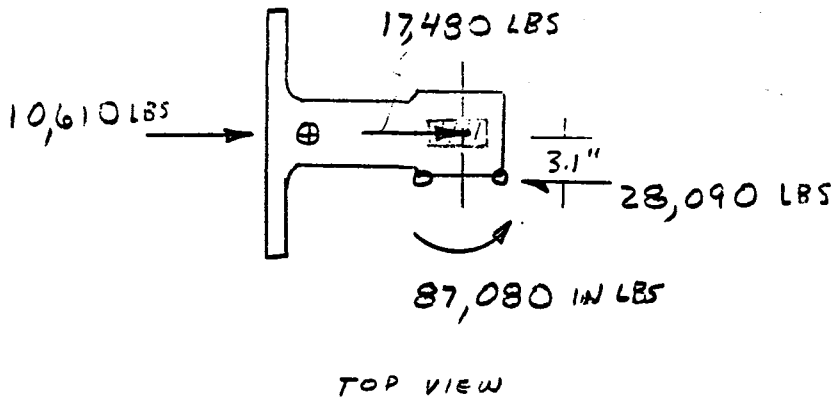
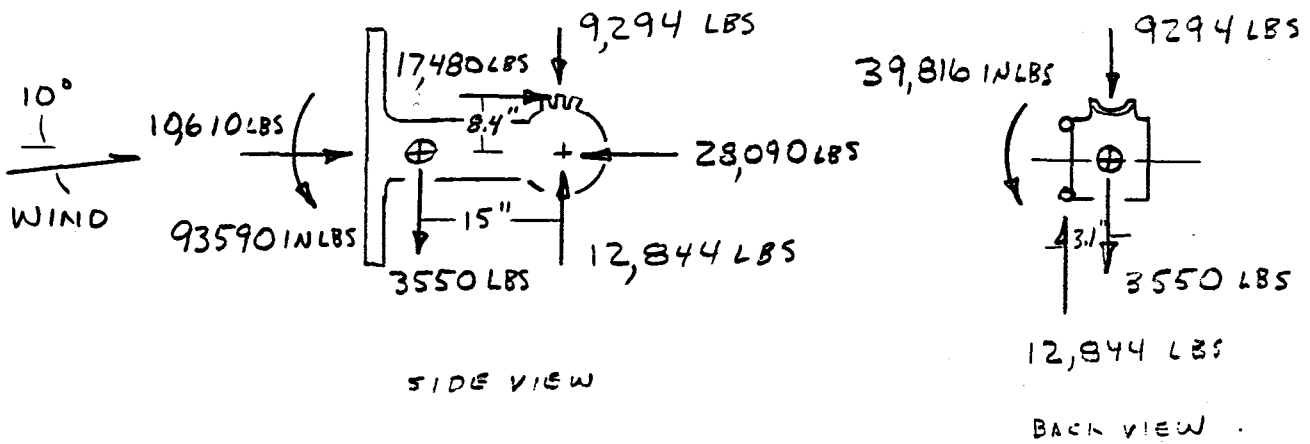
$$\text{MAX MOMENT} = \sqrt{(413,455)^2 + (21,452)^2} = 414,000 \text{ IN LBS}$$

$$\text{MAX RADIAL LOAD} = \sqrt{(14,334)^2 + (6920)^2} = 15,920 \text{ LBS}$$

$$\text{MAX THRUST LOAD} \approx 0$$

VERTICAL HELIOSTAT

FRONT WIND COND



$$\text{MAX MOMENT} = \sqrt{(39,816)^2 + (87,080)^2} = 95,750 \text{ IN LBS}$$

$$\text{MAX RADIAL LOAD} = \sqrt{(12,844)^2 + (28,090)^2} = 30,890 \text{ LBS}$$

$$\text{MAX THRUST LOAD} = 0$$

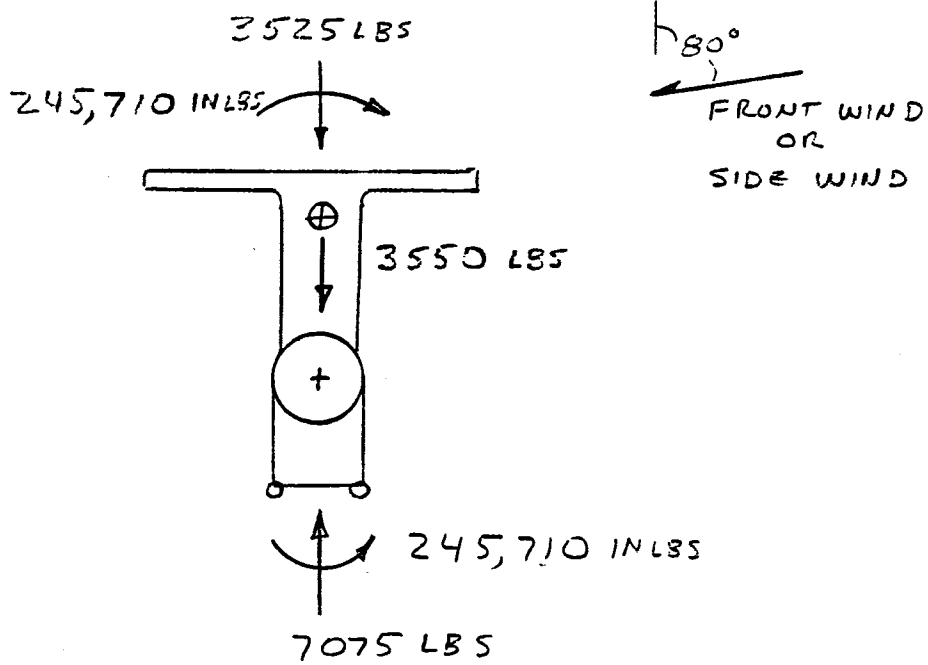
BEARING STATIC LOADS.

90 MPH WIND

AZIMUTH BEARING

HORIZONTAL HELIOSTAT

FRONT OR SIDE WIND COND



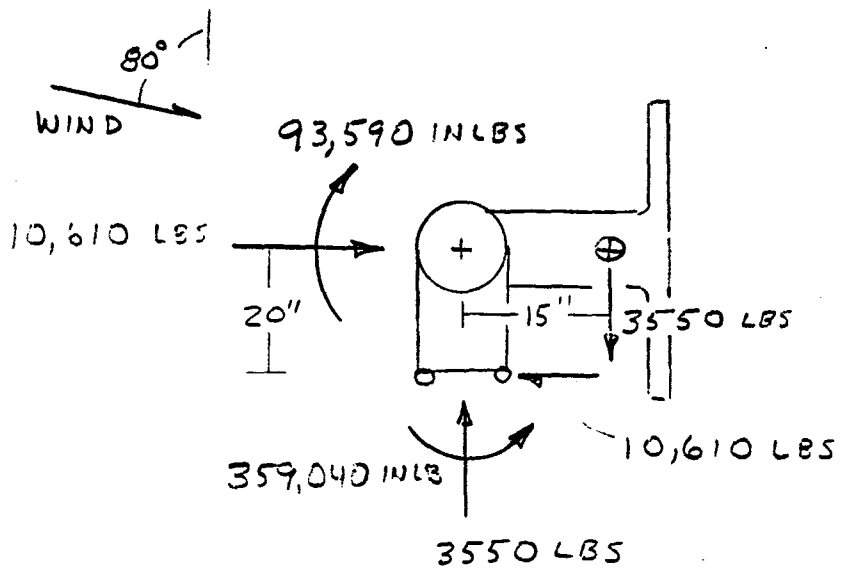
MOMENT = 245,710 IN LBS

RADIAL LOAD \approx 0

THRUST LOAD = 7075 LBS

VERTICAL HELIOSTAT

BACK WIND COND



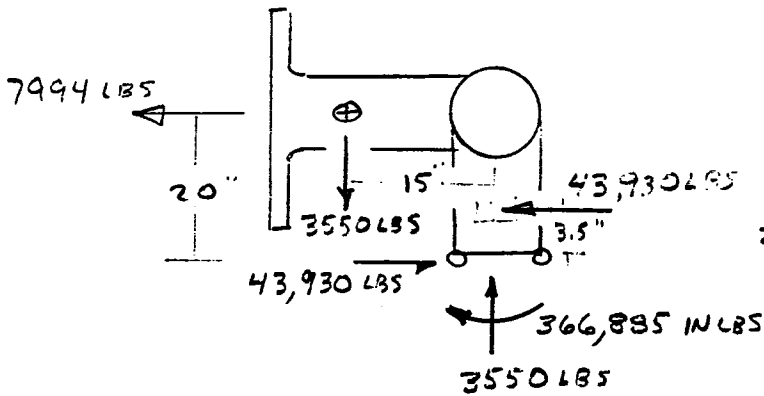
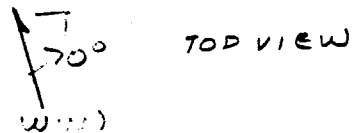
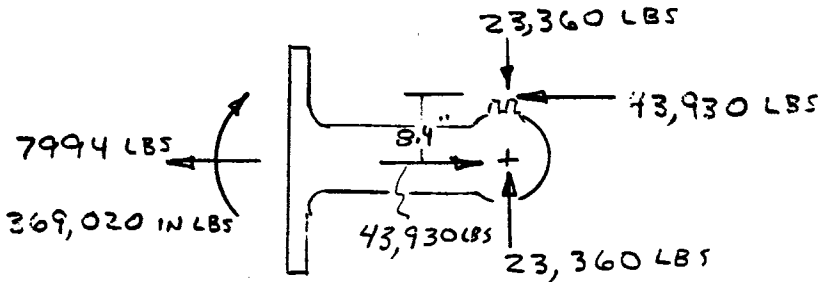
MOMENT = 359,040 IN LBS

RADIAL LOAD = 10,610 LBS

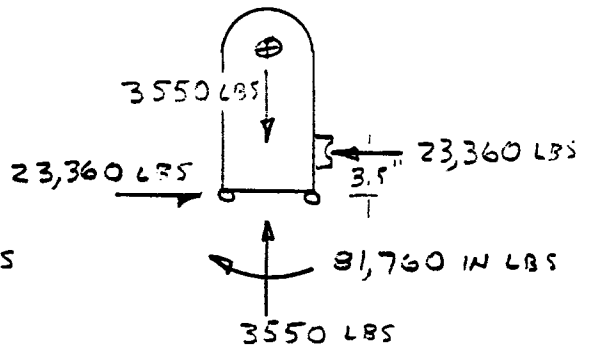
THRUST LOAD = 3,550 LBS

VERTICAL HELIOSTAT

70° SIDE WIND COND (WORM @ 90°)



SIDE VIEW



BACK VIEW

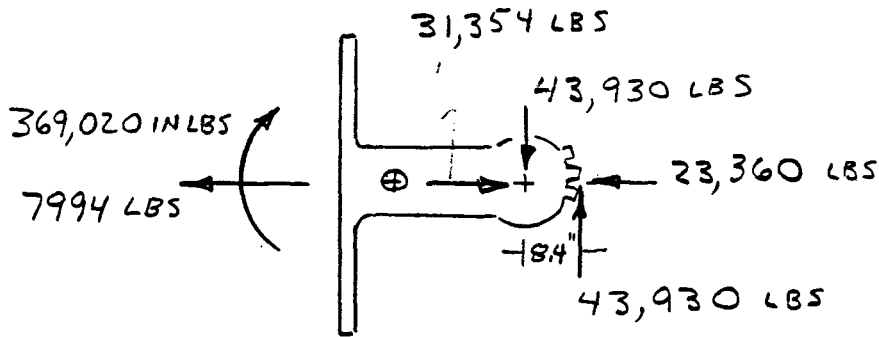
$$\text{MAX MOMENT} = \sqrt{(366,885)^2 + (31,760)^2} = 375,935 \text{ IN LBS}$$

$$\text{MAX RADIAL LOAD} = \sqrt{(23,360)^2 + (43,930)^2} = 49,755 \text{ IN LBS}$$

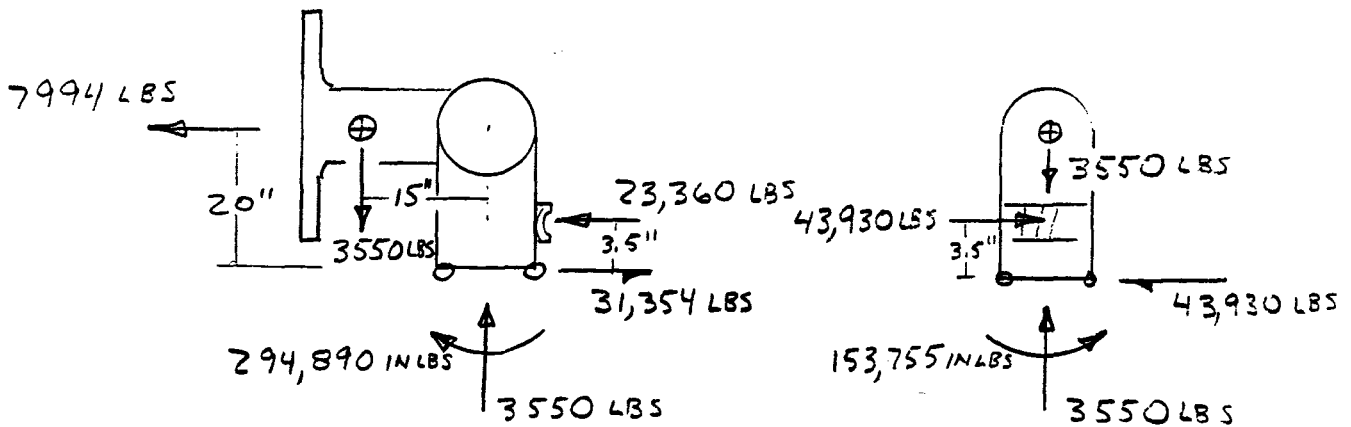
$$\text{MAX THRUST LOAD} = 3,550 \text{ LBS}$$

VERTICAL HELIOSTAT

70° SIDE WIND COND (WORM @ 180°)



TOP VIEW



SIDE VIEW

BACK VIEW

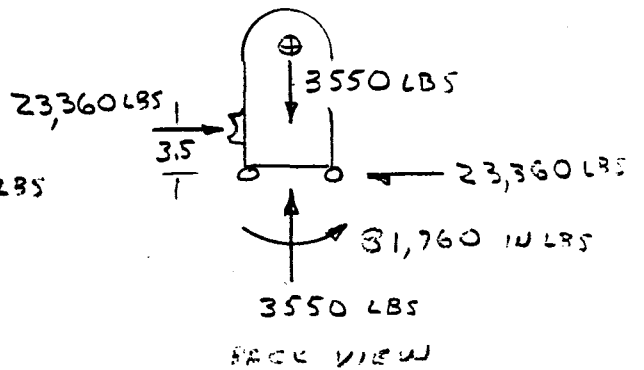
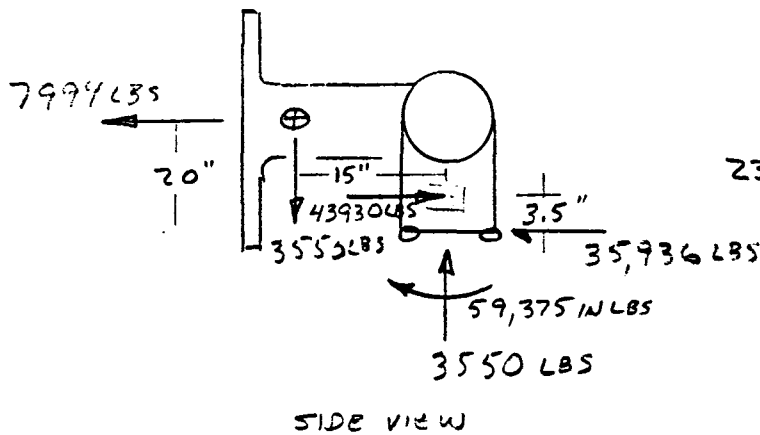
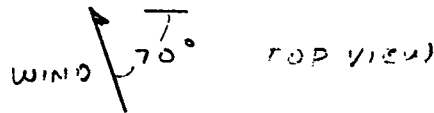
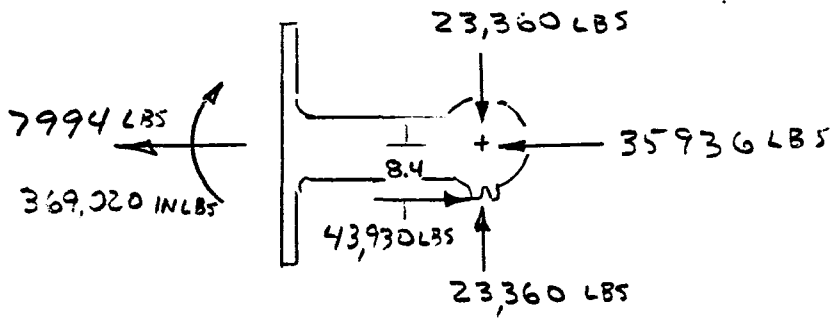
$$\text{MAX MOMENT} = \sqrt{(294,890)^2 + (153,755)^2} = 332,570 \text{ IN LBS}$$

$$\text{MAX RADIAL LOAD} = \sqrt{(31,354)^2 + (43,930)^2} = 53,970 \text{ LBS}$$

$$\text{MAX THRUST LOAD} = 3550 \text{ LBS}$$

VERTICAL HELIOSTAT

70° SIDE WIND COND (WORM @ 270°)



$$\text{MAX MOMENT} = \sqrt{(59,375)^2 + (31,760)^2} = 101,045 \text{ IN LBS}$$

$$\text{MAX RADIAL LOAD} = \sqrt{(35,936)^2 + (23,360)^2} = 42,860 \text{ IN LBS}$$

$$\text{MAX THRUST LOAD} = 3550$$

BEARING STATIC LOADS (90 MPH WIND)

<u>ELEVATION BEARING</u>		<u>RADIAL</u>	<u>THRUST</u>	<u>MOMENT</u>
HORIZONTAL HELIOSTAT	FRONT WIND	36,980 LBS	0 LBS	70,140 IN/LBS
	SIDE WIND	7,075	0	267,645
VERTICAL HELIOSTAT	70° AZIM WIND	15,920	0	414,000
	FRONT WIND	30,890	0	95,750
<u>AZIMUTH BEARING</u>				
HORIZONTAL HELIOSTAT	FRONT OR SIDE WIND	0	7075	245,710
VERTICAL HELIOSTAT	BACK WIND	10,610	3550	359,040
	70° AZIM WIND (90° worm)	49,755	3550	375,885
	(180° worm)	53,970	3550	332,570

E-161

9.5.5 DRIVE UNIT PERFORMANCE

The attached computer print-outs give the drive performance parameters for the Northrup - Winsmith drive unit as a function of the stepper motor pulse rate. The planetary gear box efficiency does not vary with motor speed, and is, therefore, an input constant. The worm and gear set efficiency is a function of speed, and is computed for every motor speed as follows:

$$\text{Efficiency} = \frac{\cos \phi_n \sin 2\lambda_e}{\cos \phi_n \sin 2\lambda_e + 2f}$$

where f = friction factor

ϕ_n = normal thread angle

λ_e = lead angle of worm at
effective radius of threaded worm

ϕ_x = axial thread angle

V = peripheral velocity of worm at
effective radius of threaded worm

R_e = effective radius of threaded worm

V_s = average sliding velocity

n = worm rpm

$$V_s = 0.5236 R_e \cdot n / \cos \lambda_e$$

f = function (V_s) from Table 1

FROM "DESIGN OF WORM AND SPIRAL GEARS" BY EARLE BUCKINGHAM AND HENRY RYFEL

$V_s, \text{ft/min}$	f	$V_s, \text{ft/min}$	f	$V_s, \text{ft/min}$	f
0	.2000	175	.0383	1750	.0545
10	.1209	200	.0365	2000	.0582
20	.0993	250	.0358	2500	.0650
30	.0859	300	.0330	3000	.0712
40	.0764	400	.0327	4000	.0822
50	.0693	500	.0335	5000	.0919
60	.0637	600	.0349	6000	.1007
70	.0591	700	.0366	7000	.1083
80	.0553	800	.0384	8000	.1163
90	.0522	900	.0402	9000	.1233
100	.0495	1000	.0420	10000	.1300
125	.0444	1250	.0465		
150	.0408	1500	.0506		

TABLE 1

The following computer print-outs are based on the theoretical planetary stage efficiency of 54.87%. The motor torque characteristic is for the M112-FJ327 motor and TBM 105-1218 translator combination which are installed on the heliostats delivered to the Sandia-Albuquerque Solar Thermal Test Facility. It should be noted that the drive efficiency goals based on this theoretical planetary efficiency were not attained during actual testing (see Appendix para. 9.7.2.5). A second set of computer print-outs is provided on pgs. E-171 through E-176 which are based on a planetary stage efficiency which closely matches the test data.

THEORETICAL DRIVE PERFORMANCE

NORTHROP-WINSMITH PLANETARY-WORM DRIVE UNIT

INPUT PLANETARY STAGE RATIO AT MOTOR 460
THEORETICAL PLANETARY STAGE EFFICIENCY,% 54.87
INPUT STEPPING RATE, STEPS/SEC 250
INPUT WORM/GEAR REDUCTION RATIO 40
INPUT WORM P.D. 3.121
INPUT WORM LEAD ANGLE 7.7

INPUT STAGE

MOTOR STEP RATE, STEPS/SEC = 250
MOTOR RPM = 75
MOTOR TORQUE, OZ-IN= 850
MOTOR OUTPUT HP = .06321875
PLANETARY OUTPUT TORQUE, IN-LB= 13408.8
PLANETARY EFFICIENCY,%= 54.87

OUTPUT STAGE

INPUT TORQUE, FT-LB= 1117.4
EFFICIENCY,%= 37.07
OUTPUT TORQUE, FT-LB= 16573.22
WORM RPM= .163

TOTAL DRIVE UNIT

INPUT TORQUE, OZ-IN= 850
EFFICIENCY,%= 20.34
OUTPUT TORQUE, FT-LB= 16573.22
DRIVE OUTPUT HP = .013
COMBINED RATIO= 18400
SLEW RATE, DEG/MIN = 1.467

THEORETICAL DRIVE PERFORMANCE

NORTHROP-WINSMITH PLANETARY-WORM DRIVE UNIT

INPUT PLANETARY STAGE RATIO AT MOTOR 460
THEORETICAL PLANETARY STAGE EFFICIENCY,% 54.87
INPUT STEPPING RATE, STEPS/SEC 500
INPUT WORM/GEAR REDUCTION RATIO 40
INPUT WORM P.D. 3.121
INPUT WORM LEAD ANGLE 7.7

INPUT STAGE

MOTOR STEP RATE, STEPS/SEC = 500
MOTOR RPM = 150
MOTOR TORQUE, OZ-IN= 860.297872
MOTOR OUTPUT HP = .127969309
PLANETARY OUTPUT TORQUE, IN-LB= 13571.3
PLANETARY EFFICIENCY,%= 54.87

OUTPUT STAGE

INPUT TORQUE, FT-LB= 1130.94
EFFICIENCY,%= 37.2
OUTPUT TORQUE, FT-LB= 16830.62
WORM RPM= .326

TOTAL DRIVE UNIT

INPUT TORQUE, OZ-IN= 860.29
EFFICIENCY,%= 20.41
OUTPUT TORQUE, FT-LB= 16830.62
DRIVE OUTPUT HP = .026
COMBINED RATIO= 18400
SLEW RATE, DEG/MIN = 2.934

THEORETICAL DRIVE PERFORMANCE

NORTHROP-WINSMITH PLANETARY-WORM DRIVE UNIT

INPUT PLANETARY STAGE RATIO AT MOTOR 460
THEORETICAL PLANETARY STAGE EFFICIENCY,% 54.87
INPUT STEPPING RATE, STEPS/SEC 750
INPUT WORM/GEAR REDUCTION RATIO 40
INPUT WORM P.D. 3.121
INPUT WORM LEAD ANGLE 7.7

INPUT STAGE

MOTOR STEP RATE, STEPS/SEC = 750
MOTOR RPM = 225
MOTOR TORQUE, OZ-IN= 700
MOTOR OUTPUT HP = .1561875
PLANETARY OUTPUT TORQUE, IN-LB= 11042.5
PLANETARY EFFICIENCY,%= 54.87

OUTPUT STAGE

INPUT TORQUE, FT-LB= 920.21
EFFICIENCY,%= 37.33
OUTPUT TORQUE, FT-LB= 13740.96
WORM RPM= .489

TOTAL DRIVE UNIT

INPUT TORQUE, OZ-IN= 700
EFFICIENCY,%= 20.48
OUTPUT TORQUE, FT-LB= 13740.96
DRIVE OUTPUT HP = .032
COMBINED RATIO= 18400
SLEW RATE, DEG/MIN = 4.402

THEORETICAL DRIVE PERFORMANCE

NORTHROP-WINSMITH PLANETARY-WORM DRIVE UNIT

INPUT PLANETARY STAGE RATIO AT MOTOR 460
THEORETICAL PLANETARY STAGE EFFICIENCY,% 54.87
INPUT STEPPING RATE, STEPS/SEC 1000
INPUT WORM/GEAR REDUCTION RATIO 40
INPUT WORM P.D. 3.121
INPUT WORM LEAD ANGLE 7.7

INPUT STAGE

MOTOR STEP RATE, STEPS/SEC = 1000
MOTOR RPM = 300
MOTOR TORQUE, OZ-IN = 525
MOTOR OUTPUT HP = .1561875
PLANETARY OUTPUT TORQUE, IN-LB = 8281.9
PLANETARY EFFICIENCY,% = 54.87

OUTPUT STAGE

INPUT TORQUE, FT-LB = 690.16
EFFICIENCY,% = 37.45
OUTPUT TORQUE, FT-LB = 10340.74
WORM RPM = .652

TOTAL DRIVE UNIT

INPUT TORQUE, OZ-IN = 525
EFFICIENCY,% = 20.55
OUTPUT TORQUE, FT-LB = 10340.74
DRIVE OUTPUT HP = .032
COMBINED RATIO = 18400
SLEW RATE, DEG/MIN = 5.869

THEORETICAL DRIVE PERFORMANCE

NORTHROP-WINSMITH PLANETARY-WORM DRIVE UNIT

INPUT PLANETARY STAGE RATIO AT MOTOR 460
THEORETICAL PLANETARY STAGE EFFICIENCY,% 54.87
INPUT STEPPING RATE, STEPS/SEC 1250
INPUT WORM/GEAR REDUCTION RATIO 40
INPUT WORM P.D. 3.121
INPUT WORM LEAD ANGLE 7.7

INPUT STAGE

MOTOR STEP RATE, STEPS/SEC = 1250
MOTOR RPM = 375
MOTOR TORQUE, OZ-IN= 425
MOTOR OUTPUT HP = .158046875
PLANETARY OUTPUT TORQUE, IN-LB= 6704.4
PLANETARY EFFICIENCY,%= 54.87

OUTPUT STAGE

INPUT TORQUE, FT-LB= 558.7
EFFICIENCY,%= 37.58
OUTPUT TORQUE, FT-LB= 8399.61
WORM RPM= .815

TOTAL DRIVE UNIT

INPUT TORQUE, OZ-IN= 425
EFFICIENCY,%= 20.62
OUTPUT TORQUE, FT-LB= 8399.61
DRIVE OUTPUT HP = .033
COMBINED RATIO= 18400
SLEW RATE, DEG/MIN = 7.336

THEORETICAL DRIVE PERFORMANCE

NORTHROP-WINSMITH PLANETARY-WORM DRIVE UNIT

INPUT PLANETARY STAGE RATIO AT MOTOR 460
THEORETICAL PLANETARY STAGE EFFICIENCY,% 54.87
INPUT STEPPING RATE, STEPS/SEC 1500
INPUT WORM/GEAR REDUCTION RATIO 40
INPUT WORM P. D. 3.121
INPUT WORM LEAD ANGLE 7.7

INPUT STAGE

MOTOR STEP RATE, STEPS/SEC = 1500
MOTOR RPM = 450
MOTOR TORQUE, OZ-IN = 370
MOTOR OUTPUT HP = .1651125
PLANETARY OUTPUT TORQUE, IN-LB = 5836.7
PLANETARY EFFICIENCY,% = 54.87

OUTPUT STAGE

INPUT TORQUE, FT-LB = 486.39
EFFICIENCY,% = 37.71
OUTPUT TORQUE, FT-LB = 7337.61
WORM RPM = .978

TOTAL DRIVE UNIT

INPUT TORQUE, OZ-IN = 370
EFFICIENCY,% = 20.69
OUTPUT TORQUE, FT-LB = 7337.61
DRIVE OUTPUT HP = .034
COMBINED RATIO = 18400
SLEW RATE, DEG/MIN = 8.804

TEST DATA MATCHED DRIVE PERFORMANCE

NORTHROP-WINSMITH PLANETARY-WORM DRIVE UNIT

INPUT PLANETARY STAGE RATIO AT MOTOR 460
PROBABLE ACTUAL PLANETARY STAGE EFFICIENCY,% 39
INPUT STEPPING RATE, STEPS/SEC 250
INPUT WORM/GEAR REDUCTION RATIO 40
INPUT WORM P.D. 3.121
INPUT WORM LEAD ANGLE 7.7

INPUT STAGE

MOTOR STEP RATE, STEPS/SEC = 250
MOTOR RPM = 75
MOTOR TORQUE, OZ-IN= 850
MOTOR OUTPUT HP = .06321875
PLANETARY OUTPUT TORQUE, IN-LB= 9530.6
PLANETARY EFFICIENCY,%= 39

OUTPUT STAGE

INPUT TORQUE, FT-LB= 794.21
EFFICIENCY,%= 37.07
OUTPUT TORQUE, FT-LB= 11779.76
WORM RPM= .163

TOTAL DRIVE UNIT

INPUT TORQUE, OZ-IN= 850
EFFICIENCY,%= 14.46
OUTPUT TORQUE, FT-LB= 11779.76
DRIVE OUTPUT HP = 9E-03
COMBINED RATIO= 18400
SLEW RATE, DEG/MIN = 1.467

TEST DATA MATCHED DRIVE PERFORMANCE

NORTHROP-WINSMITH PLANETARY-WORM DRIVE UNIT

INPUT PLANETARY STAGE RATIO AT MOTOR 460
PROBABLE ACTUAL PLANETARY STAGE EFFICIENCY,% 39
INPUT STEPPING RATE, STEPS/SEC 500
INPUT WORM/GEAR REDUCTION RATIO 40
INPUT WORM P.D. 3.121
INPUT WORM LEAD ANGLE 7.7

INPUT STAGE

MOTOR STEP RATE, STEPS/SEC = 500
MOTOR RPM = 150
MOTOR TORQUE, OZ-IN= 860.297872
MOTOR OUTPUT HP = .127969309
PLANETARY OUTPUT TORQUE, IN-LB= 9646
PLANETARY EFFICIENCY,%= 39

OUTPUT STAGE

INPUT TORQUE, FT-LB= 803.84
EFFICIENCY,%= 37.2
OUTPUT TORQUE, FT-LB= 11962.71
WORM RPM= .326

TOTAL DRIVE UNIT

INPUT TORQUE, OZ-IN= 860.29
EFFICIENCY,%= 14.5
OUTPUT TORQUE, FT-LB= 11962.71
DRIVE OUTPUT HP = .019
COMBINED RATIO= 18400
SLEW RATE, DEG/MIN = 2.934

TEST DATA MATCHED DRIVE PERFORMANCE

NORTHROP-WINSMITH PLANETARY-WORM DRIVE UNIT

INPUT PLANETARY STAGE RATIO AT MOTOR 460
PROBABLE ACTUAL PLANETARY STAGE EFFICIENCY,% 39
INPUT STEPPING RATE, STEPS/SEC 750
INPUT WORM/GEAR REDUCTION RATIO 40
INPUT WORM P.D. 3.121
INPUT WORM LEAD ANGLE 7.7

INPUT STAGE

MOTOR STEP RATE, STEPS/SEC = 750
MOTOR RPM = 225
MOTOR TORQUE, OZ-IN = 700
MOTOR OUTPUT HP = .1561875
PLANETARY OUTPUT TORQUE, IN-LB = 7848.7
PLANETARY EFFICIENCY,% = 39

OUTPUT STAGE

INPUT TORQUE, FT-LB = 654.06
EFFICIENCY,% = 37.33
OUTPUT TORQUE, FT-LB = 9766.68
WORM RPM = .489

TOTAL DRIVE UNIT

INPUT TORQUE, OZ-IN = 700
EFFICIENCY,% = 14.55
OUTPUT TORQUE, FT-LB = 9766.68
DRIVE OUTPUT HP = .023
COMBINED RATIO = 18400
SLEW RATE, DEG/MIN = 4.402

TEST DATA MATCHED DRIVE PERFORMANCE

NORTHROP-WINSMITH PLANETARY-WORM DRIVE UNIT

INPUT PLANETARY STAGE RATIO AT MOTOR 460
PROBABLE ACTUAL PLANETARY STAGE EFFICIENCY,% 39
INPUT STEPPING RATE, STEPS/SEC 1000
INPUT WORM/GEAR REDUCTION RATIO 40
INPUT WORM P.D. 3.121
INPUT WORM LEAD ANGLE 7.7

INPUT STAGE

MOTOR STEP RATE, STEPS/SEC = 1000
MOTOR RPM = 300
MOTOR TORQUE, OZ-IN= 525
MOTOR OUTPUT HP = .1561875
PLANETARY OUTPUT TORQUE, IN-LB= 5886.5
PLANETARY EFFICIENCY,%= 39

OUTPUT STAGE

INPUT TORQUE, FT-LB= 490.54
EFFICIENCY,%= 37.45
OUTPUT TORQUE, FT-LB= 7349.89
WORM RPM= .652

TOTAL DRIVE UNIT

INPUT TORQUE, OZ-IN= 525
EFFICIENCY,%= 14.6
OUTPUT TORQUE, FT-LB= 7349.89
DRIVE OUTPUT HP = .023
COMBINED RATIO= 18400
SLEW RATE, DEG/MIN = 5.869

TEST DATA MATCHED DRIVE PERFORMANCE

NORTHROP-WINSMITH PLANETARY-WORM DRIVE UNIT

INPUT PLANETARY STAGE RATIO AT MOTOR 460
PROBABLE ACTUAL PLANETARY STAGE EFFICIENCY,% 39
INPUT STEPPING RATE, STEPS/SEC 1250
INPUT WORM/GEAR REDUCTION RATIO 40
INPUT WORM P.D. 3.121
INPUT WORM LEAD ANGLE 7.7

INPUT STAGE

MOTOR STEP RATE, STEPS/SEC = 1250
MOTOR RPM = 375
MOTOR TORQUE, OZ-IN= 425
MOTOR OUTPUT HP = .158046875
PLANETARY OUTPUT TORQUE, IN-LB= 4765.3
PLANETARY EFFICIENCY,%= 39

OUTPUT STAGE

INPUT TORQUE, FT-LB= 397.1
EFFICIENCY,%= 37.58
OUTPUT TORQUE, FT-LB= 5970.2
WORM RPM= .815

TOTAL DRIVE UNIT

INPUT TORQUE, OZ-IN= 425
EFFICIENCY,%= 14.65
OUTPUT TORQUE, FT-LB= 5970.2
DRIVE OUTPUT HP = .023
COMBINED RATIO= 18400
SLEW RATE, DEG/MIN = 7.336

TEST DATA MATCHED DRIVE PERFORMANCE

NORTHROP-WINSMITH PLANETARY-WORM DRIVE UNIT

INPUT PLANETARY STAGE RATIO AT MOTOR 460
PROBABLE ACTUAL PLANETARY STAGE EFFICIENCY,% 39
INPUT STEPPING RATE, STEPS/SEC 1500
INPUT WORM/GEAR REDUCTION RATIO 40
INPUT WORM P.D. 3.121
INPUT WORM LEAD ANGLE 7.7

INPUT STAGE

MOTOR STEP RATE, STEPS/SEC = 1500
MOTOR RPM = 450
MOTOR TORQUE, OZ-IN= 370
MOTOR OUTPUT HP = .1651125
PLANETARY OUTPUT TORQUE, IN-LB= 4148.6
PLANETARY EFFICIENCY,%= 39

OUTPUT STAGE

INPUT TORQUE, FT-LB= 345.71
EFFICIENCY,%= 37.71
OUTPUT TORQUE, FT-LB= 5215.36
WORM RPM= .978

TOTAL DRIVE UNIT

INPUT TORQUE, OZ-IN= 370
EFFICIENCY,%= 14.7
OUTPUT TORQUE, FT-LB= 5215.36
DRIVE OUTPUT HP = .024
COMBINED RATIO= 18400
SLEW RATE, DEG/MIN = 8.804

UNLIMITED RELEASE
INITIAL DISTRIBUTION

UC-62d (350)

U.S. Department of Energy
600 E Street NW
Washington, D. C. 20585
Attn: W. W. Auer
G. W. Braun
K. Cherian
M. U. Gutstein
L. Melamed
J. E. Rannels

U.S. Department of Energy
San Francisco Operations Office
1333 Broadway
Oakland, CA 94612
Attn: S. D. Elliott
S. Fisk
R. W. Hughey
W. Nettleton

U.S. Department of Energy
Solar Ten Megawatt Project Office
P. O. Box 1449
Canoga Park, CA 91304
Attn: M. Slaminski

U.S. Department of Energy
Solar Ten Megawatt Project Office
5301 Bolsa Ave. MS14-1
Huntington Beach, CA 92649
Attn: R. N. Schweinberg

USAF Logistics Command
P. O. Box 33140
Wright-Patterson AFB
Ohio 45433
Attn: G. Kastanos

UCLA
900 Veteran Avenue
Los Angeles, CA 90024
Attn: F. Turner

Georgia Institute of Technology
Engineering Experiment St.
Atlanta, GA 30332
Attn: S. H. Bomar, Jr.

University of Houston
Houston
Solar Energy Laboratory
4800 Calhoun
Houston, TX 77004
Attn: A. F. Hildebrandt
L. L. Vant-Hull

U.S. Department of Interior
Water & Power Res. Service
P.O. Box 427
Boulder City, NV 89005
Attn: J. Sundberg

Acurex
485 Clyde Avenue
Mountain View, CA 94042
Attn: J. Hull

Aerospace Corporation
Solar Thermal Projects
Energy Systems Group, D-5
Room 1110
P.O. Box 92957
El Segundo, CA 90009
Attn: P. deRienzo
P. Mathur

Airesearch Manufacturing Co.
2525 West 190th Street
Torrance, CA 90509
Attn: M. G. Coombs
For: P. F. Connelly

AMFAC
700 Bishop Street
Honolulu, HI 96801
Attn: G. St. John

ARCO
911 Wilshire Blvd
Los Angeles, CA 90017
Attn: J. H. Caldwell, Jr.

Arizona Public Service
P. O. Box 21666
Phoenix, AZ 85036
Attn: D. L. Barnes
For: E. Weber

Arizona Solar Energy Commission
1700 W. Washington - 502
Phoenix, AZ 85007
Attn: R. Sears

Babcock & Wilcox
91 Stirling Avenue
Barberton, OH 44203
Attn: G. Grant
For: J. Pletcher
M. Seale

Babcock & Wilcox
P. O. Box 1260
Lynchburg, VA 24505
Attn: W. Smith

Babcock & Wilcox
20 S. VanBuren Avenue
Barberton, OH 44203
Attn: M. Wiener

Badger Energy, Inc.
One Broadway
Cambridge, MA 02142
Attn: F. D. Gardner

Battelle Pacific Northwest Labs
P. O. Box 999
Richland, WA 99352
Attn: M. A. Lind

Bechtel National, Inc.
P. O. Box 3965
San Francisco, CA 94119
Attn: E. Lam
For: J. B. Darnell
R. L. Lessley

Black & Veatch
P. O. Box 8405
Kansas City, MO 64114
Attn: C. Grosskreutz
For: J. E. Harder
S. Levy

Boeing Engineering & Construction
P. O. Box 3707
Seattle, WA 98124
Attn: R. L. Campbell
R. Gillette
J. R. Gintz

Booz, Allen & Hamilton, Inc.
8801 E. Pleasant Valley Road
Cleveland, OH 44131
Attn: W. Hahn

Brookhaven National Laboratory
Upton, NY 11973
Attn: G. Cottingham

Burns and Roe, Inc.
550 Kinderkamack Rd.
Oradell, NJ 07649
Attn: J. Willson

Burns and Roe, Inc.
185 Crossways Park Drive
Woodbury, NY 11797
Attn: R. Vondrasek

Busche Energy Systems
7288 Murdy Circle
Huntington Beach, CA 92647
Attn: K. Busche

California Public Utilities Commission
350 McAllister St., Room 5024
San Francisco, CA 94102
Attn: B. Barkovich
For: C. Waddell

Chevron Research
P. O. Box 1627
Richmond, CA 94804
Attn: L. Fraas

Chevron Oil Research
P. O. Box 446
La Habra, CA 90631
Attn: W. Peake
For: J. Ploeg
W. Stiles

Colt Industries
Trent Tube Division
East Troy, WI 53170
Attn: J. Thackray

Corning Glass Works
Advanced Products Dept.
M/S 25
Corning, NY 14830
Attn: W. M. Baldwin
A. Shoemaker

Custom Metals Enterprises, Inc.
3288 Main Street
Chula Vista, CA 92011
Attn: T. J. Bauer

Data Science Corp.
1189 Oddstad Drive
Redwood City, CA 94063
Attn: M. Liang

Electric Power Research Institute
P. O. Box 10412
Palo Alto, CA 93403
Attn: J. Bigger

El Paso Electric Company
P. O. Box 982
El Paso, TX 79946
Attn: J. E. Brown

Energy, Inc.
P. O. Box 736
Idaho Falls, ID 83401
Attn: G. Meredith

Exxon Enterprises-Solar Thermal Systems
P. O. Box 592
Florham Park, NJ 07932
Attn: P. Joy
For: D. Nelson
G. Yenetchi

Ford Aerospace
3939 Fabian Way, T33
Palo Alto, CA 94303
Attn: I. E. Lewis
For: H. Sund

Foster-Miller Associates
135 Second Avenue
Waltham, MA 02154
Attn: E. Poulin

Foster Wheeler Dev. Corp.
12 Peach Tree Hill Road
Livingston, NJ 07039
Attn: A. C. Gangadharan
For: R. Zoschak

GAI Consultants, Inc.
570 Beatty Rd.
Monroeville, PA 15146
Attn: H. Davidson

General Atomic Company
P. O. Box 81608
San Diego, CA 92138
Attn: H. A. Chiger

General Electric Company
Advanced Energy Programs
P. O. Box 8661
Philadelphia, PA 19101
Attn: A. A. Koenig

General Electric Company
1 River Road
Schenectady, NY 12345
tric Company
1 River Road
Schenectady, NY 12345
Attn: J. A. Elsner
For: R. N. Griffin
R. Horton

GM Transportation System Center
GM Technical Center
Warren, MI 48090
Attn: J. Britt

GM Corp. Harrison Rad. Division
A and E Building
Lockport, NY 14094
Attn: A. Stocker

Houston Lighting and Power
P. O. Box 1700
Houston, TX 77001
Attn: J. Ridgway

Institute of Gas Technology
Suite 218
1825 K Street, NW
Washington, D. C. 25006
Attn: D. R. Glenn

Jet Propulsion Laboratory
Building 520-201
4800 Oak Grove Drive
Pasadena, CA 91103
Attn: M. Adams
H. Bank
W. Carley
E. Cuddihy
J. Sheldon
J. Swan
V. Truscello

Kaiser Engineers, Inc.
300 Lakeside Drive
Oakland, CA 94612
Attn: I. Kornyey

Lawrence Berkeley National Laboratory
University of California
Berkeley, CA 94720
Attn: A. J. Hunt

Los Alamos National Laboratory
P. O. Box 1663
Los Alamos, NM 87545
Attn: S. W. Moore

Los Angeles Water and Power
111 North Hope Street
Los Angeles, CA 90051
Attn: B. M. Tuller
R. Radmacher

Martin Marietta Corporation
P. O. Box 179
Denver, CO 80201
Attn: P. R. Brown
A. E. Hawkins
T. Heaton
L. Oldham
H. C. Wroton

McDonnell Douglas Astronautics Co.
5301 Bolsa Avenue
Huntington Beach, CA 92647
Attn: P. Drummond
R. L. Gervais
D. A. Steinmeyer
L. Weinstein

Meridian Corporation
5515 Cherokee Avenue
Alexandria, VA 22312
Attn: B. S. Macazeer

Nielsen Engineering. & Research
510 Clyde Avenue
Mt. View, CA 94043
Attn: R. Schwind

Northrup, Inc.
302 Nichols Drive
Hutchins, TX 75141
Attn: J. A. Pietsch

ARCO Power Systems
Suite 301
7061 S. University Boulevard
Littleton, CO 80122
Attn: J. Anderson
F. Blake

Olin Corporation
275 Winchester Avenue
New Haven, CT 06511
Attn: S. L. Goldstein

OSC Department of Commerce
341 West 2d Street
San Bernardino, CA 92401
Attn: M. G. Heaviside

Pacific Gas and Electric Co.
77 Beale Street
San Francisco, CA 94105
Attn: P. D. Hindley
For: J. F. Doyle
A. Lam

Pacific Gas and Electric Co.
3400 Crow Canyon Road
San Ramon, CA 9426
Attn: H. Seielstad
For: J. Raggio

Phillips Chemical Co.
13-D2 Phillips Building
Bartlesville, OK 74004
Attn: M. Bowman

Pittsburgh Corning
800 Presque Isle Drive
Pittsburgh, PA 15239
Attn: W. F. Lynsavage

Pittsburgh Corning
723 N. Main Street
Port Allegany, PA 16743
Attn: W. J. Binder
For: R. Greene

PPG Industries, Inc.
One Gateway Center
Pittsburgh, PA 15222
Attn: C. R. Frownfelter

Public Service Co. of New Mexico
P. O. Box 2267
Albuquerque, NM 87103
Attn: A. Akhil

Research and Development
Public Service Co. of Oklahoma
P. O. Box 201
Tulsa, OK 74102
Attn: F. Meyer

Rockwell International
Energy Systems Group
8900 De Soto Avenue
Canoga Park, CA 91304
Attn: T. Springer

S. C. Plotkin & Associates
6451 West 83rd Street
Los Angeles, CA 90045
Attn: W. Raser

Safeguard Power Transmission Co.
Hub City Division
P. O. Box 1089
Aberdeen, SD 57401
Attn: R. E. Feldges

Sargent and Lundy
55 East Monroe
Chicago, IL 60603
Attn: N. Weber

Schumacher & Associates
2550 Fair Oaks Blvd., Suite 120
Sacramento, CA 95825
Attn: J. C. Schumacher

Sierra Pacific Power Co.
P. O. Box 10100
Reno, NV 89510
Attn: W. K. Branch

Solar Energy Research Institute
1617 Cole Boulevard
Golden, CO 80401
Attn: L. Duhham, TID
G. Gross
B. Gupta
D. W. Kearney
L. M. Murphy
R. Ortiz, SEIDB
J. Thornton

Solar Thermal Test Facility
User Association
Suite 1205
First National Bank East
Albuquerque, NM 87112
Attn: F. Smith

Solar Turbines International
P. O. Box 80966
San Diego, CA 92138
Attn: P. Roberts

Southern California Edison
2244 Walnut Grove Road
Rosemead, CA 91770
Attn: J. Reeves
For: C. Winarski

Southwestern Public Service Co.
P. O. Box 1261
Amarillo, TX 78170
Attn: A. Higgins

Standard Oil of California
555 Market Street
San Francisco, CA 94105
Attn: S. Kleespies

Stanford Research Institute
333 Ravenswood Avenue
Menlo Park, CA 94025
Attn: A. Slemmons

Stearns-Roger
P. O. Box 5888
Denver, CO 80217
Attn: W. Lang
For: J. Hopson

Stone & Webster Engineering Corp.
245 Summer Street
P. O. Box 2325
Boston, MA 02107
Attn: R. Kuhr

Townsend and Bottum
9550 Flair Drive
El Monte, CA 91731
Attn: R. Schwing

US Gypsum
101 S. Wacker Drive
Chicago, IL 60606
Attn: Ray McCleary

US Water & Power Resources Service
Bureau of Reclamation
Code 1500 E
Denver Federal Center
P. O. Box 25007
Denver, CO 80225
Attn: S. J. Hightower

Van Leer Plastics
15581 Computer Lane
Huntington Beach, CA 92649
Attn: Larry Nelson

Veda, Inc.
400 N. Mobile, Building D
Camarillo, CA 90310
Attn: L. E. Ehrhardt
For: W. Moore

Westinghouse Corporation
Box 10864
Pittsburgh, PA 15236
Attn: J. J. Buggy
For: R. W. Devlin
W. Parker

Winsmith
Division of UMC Industries
Springville, NY 14141
Attn: W. H. Heller

K. R. Miller, 3153
G. E. Brandvold, 4710; Attn: J. F. Banas, 4716
J. A. Leonard, 4717
B. W. Marshall, 4713; Attn: D. L. King
A. B. Maish, 4724
R. G. Kepler, 5810; Attn: L. A. Harrah, 5811
J. G. Curro, 5813
F. P. Gerstle, 5814
J. N. Sweet, 5824; Attn: R. B. Pettit and E. P. Roth
T. B. Cook, 8000; Attn: A. N. Blackwell, 8200
B. F. Murphey, 8300
C. S. Hoyle, 8122; Attn: V. D. Dunder
R. J. Gallagher, 8124; Attn: B. A. Meyer
D. M. Schuster, 8310; Attn: R. E. Stoltz, 8312, for M. D. Skibo
A. J. West, 8314
W. R. Even, 8315

R. L. Rinne, 8320
C. T. Yokomizo, 8326; Attn: L. D. Brandt
P. L. Mattern, 8342
L. Gutierrez, 8400; Attn: R. A. Baroody, 8410
D. E. Gregson, 8440
C. M. Tapp, 8460

C. S. Selvage, 8420
V. Burolla, 8424; Attn: C. B. Frost
R. C. Wayne, 8450
T. D. Brumleve, 8451
W. R. Delameter, 8451
P. J. Eicker, 8451 (5)
R. M. Houser, 8451
C. L. Mavis, 8451
W. L. Morehouse, 8451
H. F. Norris, Jr., 8451
W. S. Rorke, Jr., 8451
D. N. Tanner, 8451
S. S. White, 8451
A. C. Skinrod, 8452
W. G. Wilson, 8453
Publications Division, 8265/Technical Library Processes Division, 3141
Technical Library Processes Division, 3141 (2)
M. A. Pound, 8214, for Central Technical Files (3)